WADC TECHNICAL REPORT 56-51
PART V
ASTIA DOCUMENT NO. AD 161007

DETERMINING AIR REACTIONS ON MOVING VEHICLES

PART V. METHODS OF AERODYNAMICS—COMPOSITE BODIES

M. Z. Krzywoblocki

Institute for System Research
Laboratories for Applied Sciences
The University of Chicago

AUGUST 1960

Aeronautical Research Laboratory
Contract No. AF 33(616)-5689
Project No. 7060

WRIGHT AIR DEVELOPMENT DIVISION
AIR RESEARCH AND DEVELOPMENT COMMAND
UNITED STATES AIR FORCE
WRIGHT-PATTERSON AIR FORCE BASE, OHIO

400 – December 1960 – 13-578

FOREWORD

Contract AF 33(616)5689 between the United States Air Force and the University of Chicago provides for analytical studies of various flight systems under various flight situations for the purpose of determining dynamic factors and relationships involved and for the purpose of exploring design principles for such systems in the light of given performance requirements. The studies relate to problems of flight both within and beyond the earth's atmosphere. The contract is monitored by Wright Air Development Division, Directorate of Laboratories, Systems Dynamic Analysis Division Synthesis and Analysis Branch (WWDCS), Dr. Charles Goldman, Chief; Mr. Paul W. Nosker, Assistant Chief; and Mr. Richard Sudheimer, Task Scientist.

The work at the University under this contract has been conducted at the Laboratories for Applied Sciences, Institute for System Research, Dr. Bernard E. Howard, Associate Director. The institute for System Research, the Institute for Air Weapons Research, and Chicago Midway Laboratories comprise the Laboratories for Applied Sciences, Dr. Frank E. Bothwell, Director. Reports issued under this contract are prepared for publication by the Publications Branch, Mr. Burton P. Sauer, Chief.

Study 10, entitled "Aerodynamic Forces and Moments," under the above contract pertains to the determination of the aerodynamic forces and moments that will be exerted on a given vehicle during those portions of its flight that are within the sensible atmosphere--particularly those situations involving hypersonic speeds and highly rarefied atmosphere--and to the computation of short-period flight motions with application to the simulation of flight paths of weapons systems. Phase Two of this study calls for a unified set of technical documents comprising a comprehensive and authoritative treatment of the field of determining air reaction on air vehicles according to the state of knowledge now existing, such documents to be prepared for instructional and reference purposes. Phase Two is being conducted by Dr. M. Z. Krzywoblocki, professor of gasdynamics and theoretical aerodynamics at the University of Illinois, under a consulting agreement with the University of Chicago.

This WADC Technical Report 56-51, entitled Determining Air Reactions on Moving Vehicles, will review all the expressions for the components of forces and moments as functions of all parameters of flight known to affect these forces and moments. The treatment is intended to be as general as is practical and to include all terms known or anticipated to have an effect on flight.

The oldest theories concerned with the motion of a body through the air are ballistic theories: those concerned with the movement of a projectile launched from a gun or rifle. These are the classic and most fundamental theories and some of them recently have been extended to cover the trajectories of long-range rockets. It seems logical to begin this review with a description of ballistic theories.

Accordingly, the first volume, subtitled "Methods of Free Ballistics," describes the ballistic methods used in artillery to calculate the trajectory of a missile launched from a gun or rifle. It was the first of a series of successive parts to WADC TR 56-51.

Part II, "Methods of Rocketry," contains the expressions and methods which have been used to determine forces acting on a body in flight where the body has self-contained propulsion but no guidance.

Part III, "Methods of Hydrodynamics," contains classical methods of fluid dynamics and mathematical physics which have been used to determine the forces acting on a body moving within a fluid.

Part IV, "Methods of Aerodynamics--Elementary Bodies," contains both the analytical and test methods used by aerodynamicists to establish the quasi-static forces acting on elementary rigid bodies which are moving in an airstream.

The present and final volume, "Methods of Aerodynamics--Composite Bodies," is Part V and contains the methods used by aerodynamicists to determine the quasi-static forces acting on composite bodies moving in an airstream. Included in the volume are the methods for arriving at the quasi-static force picture for complex body shapes whose elements are subject to interaction, interference effects, and deformation (movable control surfaces).

ABSTRACT

The present volume, the fifth in the sequence, contains information concerning the following items: aerodynamics of composite bodies, effects of control flaps and ailerons, and nonsteady aerodynamics of composite elements including buffeting.

TABLE OF CONTENTS

Chapter 1

AERODYNAMIC METHODS REFERRING TO COMPOSITE BODIES

1.1 General Remarks on Interference Problems

In this chapter we shall briefly outline the methods referring to the aerodynamic interaction problems. Referring to a classical airplane, the following problems may be considered:

(i) Aerodynamic interference between the wing and the fuselage;

(ii) Aerodynamic interference of the wing on the tailplanes;

(iii) Aerodynamic interference of the propulsion system upon the lifting surfaces: the wings and/or the tailplanes.

The interferences mentioned in (i) and (iii) are mutual interferences since the aerodynamic phenomena on the wing affect the aerodynamic phenomena on the fuselage and vice versa. Similar situations exist with respect to the propulsion system and the wings or tailplanes. The interference phenomena to be included into (ii) are uni-directional phenomena, since the aerodynamic conditions on the wing affect the conditions on the tail surfaces but not vice versa.

Actually, the final purpose of the field of aerodynamics, known as interaction problems, is to derive the quantitative laws which may enable one to predict the aerodynamic behavior of a configuration composed of any combination of fundamental elements on the basis of knowledge of the aerodynamic action and properties of each of these elements (the wing, the fuselage, the tailplanes) when they operate alone and are not influenced by the rest of the elements in the ensemble in question. Obviously, the particular components can be tested and analyzed much earlier than the composite configuration. In the next step, one may attempt to explain clearly what kind of effect the juxtaposition of the particular components has upon the aerodynamic properties of the whole. This may supply us the ways in which the fundamental elements may be combined in order to produce the desired results.

Manuscript released by the author 24 June 1959 for publication as a WADC Technical Report.

1.2 Subsonic Range Wing-Tailplane Interference

Below, we shall briefly discuss the main results of the analysis of the wing-tailplane interference at subsonic speeds. The first aerodynamic phenomenon appearing in this problem is the induced velocity due to the wing. The magnitude of the induced velocity due to the bound vortex line is computed by means of the Biot-Savant formula

$$\frac{w_1}{U} = \frac{1}{2\pi} \int_{-1}^{+1} \frac{\gamma \xi_1 d\eta'}{[\xi_1^2 + (\eta-\eta')^2]^{3/2}} = \epsilon_1 \quad . \tag{1.1}$$

The system of trailing vortices induces a velocity w_2 at the same point, which is directed parallel to the z-axis (downward), and of a magnitude given by the relation

$$\frac{w_2}{U} = \frac{1}{2\pi} \int_{-1}^{+1} \frac{d\gamma}{d\eta'} \left[1 + \frac{\xi_1}{\sqrt{\xi_1^2 + (\eta-\eta')^2}} \right] \frac{d\eta'}{\eta-\eta'} = \epsilon_2 \quad . \tag{1.2}$$

The symbols, used above, denote;

w_1 = the induced velocity created at any point of the $\{x, y\}$ - horizontal plane;

$\xi_1 = \frac{2x_1}{b}$;

$\eta = \frac{2y}{b}$;

$\gamma = \frac{\Gamma}{bU}$;

b = the wing span;

Γ = circulation;

U = the velocity of the incoming undisturbed stream.

The ϵ_1 and ϵ_2 are the associated contributions to the downwash angle.

The total contribution to the downwash, $\epsilon = \epsilon_1 + \epsilon_2$, can be represented by means of the formula

$$\epsilon = \frac{1}{2\pi} \int_{-1}^{+1} \frac{d}{d\eta'} \left\{ \gamma \left[1 + \frac{\xi_1}{\sqrt{\xi_1^2 + (\eta-\eta')^2}} \right] \right\} \frac{d\eta'}{\eta-\eta'} \quad . \tag{1.3}$$

Using the notation

$$\widetilde{\gamma} = \gamma \quad 1 + \frac{\xi_1}{\sqrt{\xi_1^2 + (\eta - \eta')^2}} \quad , \tag{1.4}$$

the expression for the downwash may be given in the form

$$\epsilon = \frac{1}{2\pi} \int_{-1}^{+1} \frac{d\widetilde{\gamma}}{d\eta'} \frac{d\eta'}{\eta - \eta'} \quad . \tag{1.5}$$

Following Multhopp's method one may put down

$$\gamma = \frac{2}{m+1} \sum_{n=1}^{m} \gamma_n \sum_{\mu=1}^{m} \sin \mu\theta_n \sin \mu\theta \quad , \tag{1.6}$$

where γ_n is the value of γ when $\eta = \eta_n$, and the value of the latter being given by

$$\eta_n = \cos \frac{n\pi}{m+1} \quad . \tag{1.7}$$

The following solution also can be used:

$$\epsilon = b_{\nu\nu}\widetilde{\gamma}_\nu - \sum_{n=1}^{m}{}' b_{\nu n}\widetilde{\gamma}_n = 2b_{\nu\nu}\gamma_\nu - \sum_{n=1}^{m}{}' b_{\nu n} \left[1 + \frac{\xi_1}{\sqrt{\xi_1^2 + (\eta_n - \eta_\nu)^2}} \right] \gamma_n \quad , \tag{1.8}$$

or, using back the physical space coordinates

$$\epsilon(\xi, \eta_\nu) = 2b_{\nu\nu}\gamma_\nu - \sum_{n=1}^{m}{}' b_{\nu n} \left[1 + \frac{\xi}{\sqrt{\xi^2 + \beta^2(\eta_n - \eta_\nu)^2}} \right] \gamma_n \quad , \tag{1.9}$$

with

$$b_{\nu n} = \frac{\sin\theta_n}{(m+1)(\cos\theta_n - \cos\theta_\nu)^2} \quad , \qquad \text{for } |n - \nu| = 1, 3, 5, \ldots \; ; \tag{1.10}$$

$$b_{\nu n} = 0 \qquad \text{for } |n - \nu| = 2, 4, 6, \ldots \; ; \tag{1.11}$$

$$b_{\nu\nu} = \frac{m+1}{4 \sin\theta_\nu} \quad ; \quad \beta^2 = 1 - M_\infty^2 \quad . \tag{1.12}$$

This provides the means for determining the values of ϵ at the point $\{\xi, \eta_\nu\}$, when the pattern of variation of the circulation along the span of the wing is known. This is expressed in terms of the angle θ in Eq. (1.6). Employing a system of axes traveling with the impinging flow, one may derive the analytic expression for the discontinuity surface of the trailing vortices in the form

$$\xi_1 = \xi_0 + \int_{\xi_0}^{\xi} \epsilon \, d\xi \quad , \tag{1.13}$$

where ξ_0 is the vertical coordinate, measured at its trailing edge, of the wing located in an arbitrary vertical plane, η = constant.

The values of ϵ, obtained above, apply to the points which belong to the surface (wing). For points which are located outside this surface, one may use the Taylor series development

$$\epsilon(\xi,\eta,\zeta) = \epsilon(\xi,\eta,\zeta_1) + (\zeta-\zeta_1)\left(\frac{\partial\epsilon}{\partial\zeta}\right)_{\zeta=\zeta_1} + \dots \quad . \tag{1.14}$$

The *motion* in an arbitrary plane, ξ = constant, may be considered as two-dimensional, and the continuity equation may be written in the form

$$\frac{\partial\epsilon}{\partial\zeta} + \frac{\partial\sigma}{\partial\eta} = 0 \quad ; \quad \sigma = \frac{v}{U} \tag{1.15}$$

Using Eq. (1.14) and applying integration process to Eq. (1.15) one can find the downwash angle in the vicinity of the tail surfaces. Sometimes the value $(\zeta-\zeta_1)$, which corresponds to the point at which one wants to compute the value of the angle ϵ, is large; thus an application of the Taylor series is not justified. In such cases it is more convenient to calculate the value of $\epsilon(\xi,\eta,\zeta)$ by the use of the Biot-Savant rule

$$\epsilon(\xi,\eta,\zeta) = \frac{1}{2\pi}\int_{-1}^{+1} \frac{\gamma(\eta')[(\zeta-\zeta_1)^2 - (\eta-\eta')^2]}{[(\zeta-\zeta_1)^2 + (\eta-\eta')^2]^2}\left[1 + \frac{\xi}{\sqrt{\xi^2 + \beta^2[(\eta-\eta')^2 + (\zeta-\zeta_1)^2]}}\right]d\eta'$$
$$+ \frac{b^2\xi(\zeta-\zeta_1)^2}{2\pi}\int_{-1}^{+1} \frac{\gamma(\eta')\,d\eta'}{[(\zeta-\zeta_1)^2+(\eta-\eta')^2][\xi^2+\beta^2(\eta-\eta')^2+\beta^2(\zeta-\zeta_1)^2]^{3/2}} \; . \tag{1.16}$$

From the numerical calculations one can derive a conclusion that for a given angle of attack, α, an increase in the Mach number results in an increase of the downwash angle ϵ on the vortex sheet (denote it by Σ), Σ, as well as of the displacement ζ_1. The downwash angle ϵ for a given lift coefficient C_L decreases as M_∞ increases and the downward displacement $(\zeta_1 - \zeta_0)$ decreases as well. In the case of a wing of small aspect ratio or with a large amount of sweep, the downwash angle is given by the formula

$$\epsilon(\xi,\eta_\nu) = 2b_{\nu\nu}\gamma_\nu - \sum_{n=1}^{m}{}' b_{\nu n}\left[1 + \frac{\xi - |\eta_n|\tan\Lambda}{\sqrt{(\xi-|\eta_n|\tan\Lambda)^2 + \beta^2(\eta_n-\eta_\nu)^2}}\right]\gamma_n \; ; \qquad (1.17)$$

here Λ is the angle of sweep. The corresponding formula for the angle ϵ at some distance behind the wing may be found by using the Biot-Savant rule; the result is

$$\epsilon(\xi,\eta,\zeta) = \frac{1}{2\pi}\int_{-1}^{+1} \frac{(\zeta-\zeta_1)^2 - (\eta-\eta')^2}{[(\eta-\eta')^2(\zeta-\zeta_1)^2]^2}\left[1 + \frac{\xi-|\eta'|\tan\Lambda}{\sqrt{(\xi-|\eta'|\tan\Lambda)^2+\beta^2(\eta-\eta')^2+\beta^2(\zeta-\zeta_1)^2}}\right]\gamma d\eta'$$

$$+ \frac{\beta^2}{2\pi}(\zeta-\zeta_1)^2\int_{-1}^{+1} \frac{\xi-|\eta'|\tan\Lambda}{(\eta-\eta')^2+(\zeta-\zeta_1)^2}\,\frac{\gamma d\eta'}{[(\xi-|\eta'|\tan\Lambda)^2+\beta^2(\eta-\eta')^2+\beta^2(\zeta-\zeta_1)^2]^{3/2}} \; . \qquad (1.18)$$

The effect of the roll-up is not accounted for by this equation.

For small values of the aspect ratio, AR, and larger values of the wing lift coefficient C_L, one is confronted with the necessity of making better provision for the roll-up effects than is afforded by the relationships given above. Often the actual vortex system is replaced by a much simpler one made up of a single vortex. Along the single vortex Σ_w now being dealt with, the circulation is constant and has the value Γ_m which coincides with the value of the circulation found at the airfoil section located in the plane of symmetry. The two trailing vortices are assumed to have straight line axes lying parallel to the free stream velocity vector. The calculation of ϵ at any point P may be achieved by means of the Biot-Savant law. Let us consider a special case, when the point P lies in the plane of symmetry; then one obtains

$$\epsilon(\xi,0,\zeta) = \frac{\Gamma_m}{\pi}\left\{\frac{1}{\sqrt{\xi_1^2\cos^2\Lambda_1 + \zeta^2}}\left[\frac{\xi_1\sin\Lambda_1}{\sqrt{\xi_1^2+\zeta^2}} + \frac{1}{\cos\Lambda_1}\right.\right.$$

$$\left.\left.\frac{\eta_0 - \xi_1\sin\Lambda_1\cos\Lambda_1}{\sqrt{(\xi_1-\eta_0\tan\Lambda_1)^2 + \eta_0^2 + \zeta^2}}\right] + \frac{1}{\eta_0}\left[1 + \frac{\xi_1 - \eta_0\tan\Lambda_1}{\sqrt{(\xi_1-\eta_0\tan\Lambda_1)^2 + \eta_0^2+\zeta^2}}\right]\right\}, \qquad (1.19)$$

where the symbols used denote

$$\xi_1 = \frac{\xi}{\beta} \; ;$$

$$\tan\Lambda_1 = \frac{1}{\beta}\tan\Lambda \; ;$$

$$\eta_0 = \int_{-1}^{+1}\frac{\gamma}{\gamma_m}\,d\eta \; . \qquad (1.20)$$

The first step in the determination of the aerodynamic properties of the test when it is operating in the disturbed flow emanating from the wing is to compute the downwash values ϵ, all along the span of the stabilizer at the three-quarter chord locations of the airfoil sections constituting the surface. By applying Multhopp's procedure, the distribution of circulation due to the interference effect may be written down simply as

$$b_\nu \Delta \gamma_\nu = -\epsilon_\nu + \sum_{n=1}^{m}{}' b_{\nu n} \Delta\gamma_n \quad , \tag{1.21}$$

where

$$b_\nu = b_{\nu\nu} + \frac{b}{C_\nu (C_{\ell\alpha})_\nu} \quad ; \tag{1.22}$$

the meaning of the symbols is explained as follows:

> $b_{\nu\nu}$ and $b_{\nu n}$ are the Multhopp coefficients defined earlier; c_ν is the chord of the airfoil section of the tail at the spanwise position given by $\eta=\eta_\nu$, while $(c_{\ell\alpha})_\nu$ is the slope of the left curve of a two-dimensional wing possessing the same airfoil section.

The changes in the values of the local lift coefficient and local drag coefficient are furnished by the expressions given below, provided one has already obtained the results for the distribution of the incremental circulation $\Delta_{\gamma n}$ due to the interference

$$(\Delta C_L)_t = \frac{\pi (AR)_t}{m+1} \sum_{n=1}^{m} \Delta\gamma_n \sin\theta_n \quad ; \tag{1.23}$$

$$(\Delta C_{Di})_t = \frac{\pi (AR)_t}{m+1} \left[\sum_{n=1}^{m} \Delta\gamma_n (\epsilon_n + \alpha_i + \Delta\alpha_i) + \sum_{n=1}^{m} \gamma_n (\epsilon_n + \Delta\alpha_i) \sin\theta_n \right] , \tag{1.24}$$

where α_i is the self-induced angle of attack created by the circulation distribution γ_n. The changes in the tail-lift coefficient and of the tail drag coefficient due to interference effects may be expressed as

$$(\Delta C_L)_t = -\frac{\epsilon}{\alpha} (\overline{C}_L)_t \quad ; \tag{1.25}$$

$$(\Delta C_{Di})_t = (\overline{C}_L)_t \epsilon (1 - \frac{\epsilon}{\alpha}) - \frac{\epsilon}{\alpha} (\overline{C}_{Di})_t (2 - \frac{\epsilon}{\alpha}) \quad . \tag{1.26}$$

Thus the resultant lift coefficient for the tail in the presence of the wing, $(C_L)_t$, and also the resultant induced drag coefficient, $(C_{Di})_t$, are given by the relations

$$(C_L)_t = (\overline{C}_L)_t(1 - \frac{\epsilon}{\alpha}) \quad ; \tag{1.27}$$

$$(C_{Di})_t = \epsilon(C_L)_t + (1 - \frac{\epsilon}{\alpha})^2(\overline{C}_{Di})_t \quad , \tag{1.28}$$

where $(\overline{C}_L)_t$ and $(\overline{C}_{Di})_t$ are the coefficients of lift and induced drag, respectively, applying to the isolated tail surface.

The interference effect of the wing upon the tail is of a much more complicated character if the wing is provided with an extended high lift flap or if the flow is stalled over even the narrowest of spanwise regions. In both of these cases the lift distribution is altered from that produced at a small angle of attack. In the event the flow separation is present, it is necessary to distinguish between the cases of tip stalling and not stalling, i.e., whether the separation first takes place at the tips or over the central portions of the wing. In addition to the change in the form of the lift distribution, the separated flow conditions produce a wake whose thickness is of such magnitude that it can no longer be neglected. When the tail surface lies within the wake or in close proximity to its borders, it is necessary to add to the field of velocities directed normal to the free stream velocity (considered above) the field of interference velocities generated by the wake itself. This wake interference is characterized by a decrease of velocity within the wake and in a change in the induced angles of flow inclination compared to that which would have been found to hold true in the absence of the wake. A quantitative determination of such effects cannot be obtained from purely theoretical considerations. A satisfactory result may be obtained by using a procedure offered by Silverstein and Katzoff. The experimental investigations of Silverstein and Katzoff have led to two expressions for the correction to be applied to Eq. (1.13);

$$\Delta\xi_1 = \frac{1}{2} c_t \sin \delta_f + kc \,, \quad \text{for a flapped wing} \quad ; \tag{1.29}$$

here c_t denotes the chord length of the flap; δ_f is the angle through which the flap is deflected; c represents the wing chord; k = empirical factor;

$$\Delta\xi_1 = - \frac{1}{2} c_s \sin \alpha \,, \quad \text{for a stalled wing} \quad , \tag{1.30}$$

wherein c_s denotes the abscissa of the point from which the detachment takes place; this distance is measured back along the wing chord, starting at the trailing edge. The thickness of the wake may be found from the following formula:

$$\zeta_w = 0.68\, c_{do}^{1/2}(\xi_w + 0.15)^{1/2} \quad , \tag{1.31}$$

where the symbols used denote:

c_{do} - the profile drag coefficient applying to the airfoil section located at the spanwise position corresponding to the plane n = constant, in which the wake's behavior is investigated;

$$\zeta_w = \frac{1}{2} \frac{\text{wake thickness}}{\text{chord length of the airfoil}} \; ; \tag{1.32}$$

$$\xi_w = \frac{\text{distance downstream from the trailing edge of the airfoil}}{\text{chord length of the airfoil}} \; . \tag{1.33}$$

Similarly, one may calculate the velocity distribution in the wake from the formula

$$\frac{\mu'}{\mu} = \left[1 - \left(\frac{\zeta' w}{\zeta\, w}\right)^{1.75}\right]^2 ; \quad \mu' = 1 - \frac{\mu^2}{U^2} \; ; \quad \mu = 1 - \frac{u_0^2}{U^2} \; , \tag{1.34}$$

where u_0 denotes the velocity at the center of the wake, u stands for the value of the velocity at a point in the wake which lies at some vertical distance off the centerline. The vertical distance in question, when divided by the chord length of the wing, is represented by the symbol ζ'_w. Thus, one is able to determine whether the stabilizer lies within or outside of the wake. Whenever the tailplane lies within the wake it is essential to make allowance for the fact that the dynamic pressure applying to the region occupied by the tail is given by the formula

$$q = \frac{1}{1 + \frac{\gamma - 1}{2} M_\infty^2 \mu'} (1 - \mu') \frac{1}{2} \rho_\infty U^2 \quad , \tag{1.35}$$

with $\gamma = c_\rho / c_\nu$.

1.3 Subsonic Range Wing-Body Interference

The problem of wing-body interference at subsonic speeds may be solved by using the Multhopp method. In this method the idealized fuselage is assumed to be an infinitely long cylinder whose diameter is equal to that of the actual fuselage at the location corresponding to three-quarter chord position on the wing. The angle of attack of the fuselage with respect to the direction of the free stream velocity is denoted by α_f. The wing is substituted by a single bound vortex with its axis perpendicular to the plane of symmetry and passing through the aerodynamic center. The angle of attack of the wing with respect to the direction of the incoming flow is denoted by α_w. The trailing vortices are assumed to be straight lines parallel to the generatrices of the cylindrical fuselage. Let Γ represent the strength of the circulation about the airfoil section lying in any arbitrary plane y = constant. Then the potential function describing the flow created about the wing-body system, by the action of the impinging flow with a uniform velocity of U per upstream, has a discontinuity at the surface of the vortex sheet Σ_w of the amount

$$\Phi_{z=z_{\bar{w}}} - \Phi_{z=z_{\overset{+}{w}}} = \Gamma(y) \quad . \tag{1.36}$$

where $z = z_w$ is the equation of the horizontal plane in which Σ_w lies. This potential may be represented in the form

$$\Phi(x, y, z) = U[x - \alpha_f z - \alpha_f \Phi_1(y, z) + \Phi_2(x, y, z)] \quad . \tag{1.37}$$

Here $\Phi_1(y, z)$ is the additional potential which must be superimposed upon the body to counteract the cross-flow component. The $U\Phi_2$ denotes the harmonic function in the coordinates $\{x_1, y, z\}$ which represents the potential describing the flow due to the vortex system Σ_w in the presence of the fuselage. The coordinate x_1 is given by

$$x_1 = \frac{x}{\beta} \; ;$$
$$\beta^2 = 1 - M_\infty^2 \quad . \tag{1.38}$$

Due to the discontinuity relationship, given by Eq. (1.36), one can write

$$\Phi_2\Big|_{z=z_{\bar{w}}} - \Phi_2\Big|_{z=z_{\overset{+}{w}}} = \Gamma \frac{y}{U} \quad . \tag{1.39}$$

In the next part of the flow domain in question, the potential Φ_2 is continuous. Since the expression for the circulation can be given in the form

$$\Gamma(y) = \frac{1}{2} c_{\ell\alpha} (\alpha_w)_{eff} U c \quad , \tag{1.40}$$

where $(\alpha_w)_{eff}$ denotes the effective angle of incidence of the airfoil section measured with respect to the zero-lift line, c denotes the chord length and $c_{\ell\alpha}$ is the slope of the lift curve for a wing of this profile, having an infinite aspect ratio. The effective angle of attack is given by the formula

$$(\alpha_w)_{eff} = \alpha_w + \alpha_f\left(\frac{\partial \Phi_1}{\partial z}\right)_{z=z_w} - \epsilon , \quad (1.41)$$

where ϵ is the induced angle of attack due to the flow generated by the trailing vortices acting in the presence of the fuselage.

The flow approaching the fuselage in a direction perpendicular to the axis is called the crossflow. One has to apply a conformal transformation to the crossflow, so as to map the cross section of the body into a repeated segment of line located along the $\hat{z}$-axis. If the transformation function is symbolically represented in the form

$$\hat{t} = \hat{t}(t) , \quad (1.42)$$

where t and the transformed point $\hat{t}$ are expressed as complex variables

$$t = z + iy \ ; \quad \hat{t} = \hat{z} + i\hat{y} , \quad (1.43)$$

then one obtains the following expression for the derivative

$$\left(\frac{\partial \Phi_1}{\partial z}\right)_{z=z_w} = \left[\text{R.P.}\left(\frac{d\hat{t}}{dt}\right) - 1\right]_{t=z_w + iy} , \quad (1.44)$$

where the symbol R.P. denotes the real part. In an analogous way one may find the angle ϵ;

$$\epsilon = \frac{1}{2} \lim_{x \to \infty} \left(\frac{\partial \Phi_2}{\partial z}\right)_{z=z_w} = \frac{1}{2}\left(\frac{\partial \Phi_{2\infty}}{\partial z}\right)_{z=z_w} , \quad (1.45)$$

with

$$\Phi_{2\infty} = \lim_{x \to \infty} \Phi_2(x, y, z) . \quad (1.46)$$

It is possible to show that

$$\Phi_{2\infty}(\hat{z}, \hat{y}) = \frac{1}{2\pi U} \text{R.P.}\left[\oint \frac{d\Gamma}{d\hat{s}} \ln(\hat{t}-\hat{t}')d\hat{s}\right] , \quad (1.47)$$

where the symbol $\hat{t}'$ represents the complex coordinate, in the $\hat{t}$-plane, that gives the location of the element ds of the line corresponding to the segments $t = z_w + iy$, along which the free vortices in the t-plane are located. Since in the first approximation $d\hat{s}$ may be approximated by $d\hat{y}$, Eq. (1.47) becomes

$$\Phi_{2\infty}(\hat{z}, \hat{y}) = \frac{1}{2\pi U} \text{R.P.}\left[\int_{-\hat{b}/2}^{+\hat{b}/2} \frac{d\Gamma}{d\hat{y}'} \ln(\hat{t}-\hat{t}')d\hat{y}'\right] , \quad (1.48)$$

when $\hat{b}/2$ is the semispan of the wing in the $\hat{t}$-plane, which is related to the span of the physical wing by the expression

$$\hat{b} = 2\left\{\text{I.P.}\left[\hat{t}(z_w + i\,\frac{b}{2})\right]\right\} . \tag{1.49}$$

Further consideration gives

$$2\epsilon = \frac{1}{2\pi U}\,\text{R.P.}\left(\frac{d\hat{t}}{dt}\right)_{t=z_w+iy}\left[\int_{-\hat{b}/2}^{+\hat{b}/2} \frac{d\Gamma}{d\hat{y}'}\,\frac{d\hat{y}'}{\hat{y}-\hat{y}}\right] , \tag{1.50}$$

where

$$\Gamma(\hat{y}) = \frac{1}{2}\,c_{\ell\alpha}Uc\left\{\alpha_w + \alpha_f\left[\text{R.P.}\left(\frac{d\hat{t}}{dt} - 1\right)\right]\right.$$

$$\left. - \frac{1}{4\pi U}\left[\text{R.P.}\left(\frac{d\hat{t}}{dt}\right)\right]\int_{-\hat{b}/2}^{+\hat{b}/2} \frac{d\Gamma}{d\hat{y}'}\,\frac{d\hat{y}'}{\hat{y}-\hat{y}'}\right\} , \tag{1.51}$$

with the condition that $d\hat{t}/dt$ is evaluated at the location where $t = z_w + iy$. One can use the notations

$$\hat{\gamma} = \frac{\Gamma}{\hat{b}U} , \qquad \hat{\eta} = \frac{2\hat{y}}{\hat{b}} . \tag{1.52}$$

Let us decompose the quantity $\hat{\gamma}$ into two parts; one due to the incidence setting, $\alpha_w - \alpha_f$, and another one produced by the angle of attack α_f:

$$\hat{\gamma} = \gamma_0 + \alpha_f\hat{\gamma}_f , \tag{1.53}$$

then one gets

$$\hat{\gamma}_0 = \frac{1}{2}\,c_{\ell\alpha}\,\frac{c}{\hat{b}}\left[\text{R.P.}\left(\frac{d\hat{t}}{dt}\right)\right]\left\{\frac{\alpha_w - \alpha_f}{\text{R.P.}\left(\frac{d\hat{t}}{dt}\right)}\right.$$

$$\left. - \frac{1}{2\pi}\int_{-1}^{+1} \frac{d\hat{\gamma}_0}{d\hat{\eta}'}\,\frac{d\hat{\eta}'}{\hat{\eta}-\hat{\eta}'}\right\} ; \tag{1.54}$$

$$\hat{\gamma}_f = \frac{1}{2}\,c_{\ell\alpha}\,\frac{c}{\hat{b}}\left[\text{R.P.}\left(\frac{d\hat{t}}{dt}\right)\right]\left[1 - \frac{1}{2\pi}\int_{-1}^{+1} \frac{d\hat{\gamma}_f}{d\hat{\eta}'}\,\frac{d\hat{\eta}'}{\hat{\eta}-\hat{\eta}'}\right] . \tag{1.55}$$

When the values of γ are obtained, one may calculate the lift coefficient from the expression

$$(C_L)_w = AR\left[\int_{-1}^{-\ell_0} \gamma d\eta + \int_{\ell_0}^{+1} \gamma d\eta\right] , \tag{1.56}$$

where $\ell_0 = 2y_w/b$. In order to compute the total lift of the entire configuration it is necessary to add the lift acting on the fuselage to the above mentioned wing lift. It can be shown that this is given by

$$(C_L)_f = 2AR\,\frac{\hat{b}}{b}\left[-\int_{\hat{\xi}_1}^{\hat{\xi}_2} \hat{\Phi}_{2\infty}(\hat{\xi})\,\frac{d\eta}{d\hat{\xi}}\,d\hat{\xi}\right], \tag{1.57}$$

where

$$\hat{\Phi}_{2\infty} = \frac{\Phi_{2\infty}}{\hat{b}} .$$

$\hat{\xi}_1$, $\hat{\xi}_2$ represent the values of $\hat{\xi}$ that correspond to the end points of the slot into which the fuselage is transformed in the $\hat{t}$-plane. Eq. (1.57) can be transformed into the form

$$(C_L)_f = AR\left[2\gamma_0\hat{\ell}_0 - 2\,\frac{\hat{b}}{b}\,\hat{\epsilon}\int_{\hat{\xi}_1}^{\hat{\xi}_2}\frac{d\eta}{d\hat{\xi}}\,(\hat{\xi} - \hat{\xi}_w)\,d\hat{\xi}\right], \tag{1.58}$$

where

$$\gamma_0 = \frac{\Gamma y = 0}{bU} . \tag{1.59}$$

The moment coefficient of the fuselage in presence of the wing can be calculated in a similar way. The result is

$$(C_M)_f = -2\int_0^{L/c_{av}} \delta\,\frac{A^*}{A}\,d\left(\frac{x}{c_{av}}\right), \tag{1.60}$$

where c_{av} is the average chord of the wing $(c_{av} = A/b)$,

$$\delta = \alpha_f + \epsilon \quad , \quad L = \text{length of the body} \; ; \tag{1.61}$$

$$A^* = \pi h_1 b^2 . \tag{1.62}$$

The symbol A denotes the wing area; in the case of a body having an elliptic cross section with semihorizontal axis in the y-direction equal to $h_1 b$, the apparent area is given by Eq. (1.62).

The stability factor, or the derivative of the moment coefficient with respect to the angle of attack, which account for the effect of the wing upon the fuselage, is a factor of prime importance in determining the location of the aerodynamic center of the complete airplane. This is obtained from the formula

$$\frac{d(C_m)_f}{d\alpha} = -2\int_0^{L/c_{av}} \frac{d\delta}{d\alpha}\,\frac{A^*}{A}\,d\left(\frac{x}{c_{av}}\right) . \tag{1.63}$$

The influence of the Mach number upon the distribution of the circulation per unit span along the wing span and over the fuselage can be approximately estimated from the following formula:

$$\frac{(\gamma)_{M\infty}}{(\gamma)_{M\infty=0}} = \frac{0.965}{\sqrt{1 - M_\infty^2} + \frac{1}{\pi AR}(C_{L\alpha})_{M\infty=0}\left(1 - \sqrt{1 - M_\infty^2}\right)}, \qquad (1.64)$$

where the denominator of the right hand side represents the ratio of the slope of the lift curve in the incompressible case to that obtained for the Mach number in question, M_∞; i.e., the denominator is equivalent to the ratio $(C_{L\alpha})_{M=\infty}/(C_{L\alpha})_{M=\infty}$, provided the assumption of an elliptic lift distribution is postulated. The coefficient 0.965 is a correction factor that most likely arises because of the fact that the circulation distribution is not elliptic.

Although the correspondence between theory and experiment is satisfactory, it may be appropriate to point out why on the average, the theory can be expected to predict a larger amount of lift than that which is actually found from tests. First, the boundary layer exerts a pronounced effect on the actual result because in the first approximation it can be likened to a virtual increase in the body thickness parameter h_1. Moreover, the vorticity connected with the trailing vortices lying close to the fuselage is very strong. This introduces a certain amount of curvature into the part of the flow in which the central section of the wing operates.

The previous discussion refers to mid-wing configurations. In the case of a low-wing configuration the fuselage has a reduced influence on the spanwise lift distribution. If the free stream uniform flow that impinges upon the wing-body combination in question has a sidewind component producing the effect of an angle of incidence to the plane of symmetry, the problem of computing the mutual wing-body interference effects is much more complicated. An approximate way of handling the present problem concerning the effect of the fuselage upon the rolling moment has been suggested by Multhopp. He bases his analysis upon the assumption that the wing is elliptic, and then proceeds to find the rolling moment created by the asymmetric angle of attack distribution which is induced along the wing span due to the presence of the fuselage. The distribution of the induced angles of attack may be ascertained by following exactly the analysis discussed above. The free stream flow vector is now considered to impinge upon the plane of symmetry of the airplane at an angle of yaw, denoted by ψ. Thus, if at any point in the plane t the components of velocity in the directions of the y and z axes are denoted by v_y and v_z, then

$$\frac{d\hat{t}}{dt} = - \frac{v_y - iv_z}{U\psi} , \tag{1.65}$$

so that the induced angles of attack produced by the body upon the wing may be written as

$$(\alpha_i)_f = \frac{v_x}{U} = \psi \left[I.P.\left(\frac{d\hat{t}}{dt}\right) \right]_{t=y+iz_w} , \tag{1.66}$$

where I.P.( ) denotes the imaginary part of the quantity appearing in the parentheses. Under the hypothesis that the circulation along the wing has an elliptic distribution, the expression for the rolling moment then turns out to be

$$C_\ell = \frac{M_\ell}{\frac{1}{2}\rho_\infty U^2 A \frac{b}{2}} = - C\psi \int_{-1}^{+1} \left[I.P.\left(\frac{d\hat{t}}{dt}\right) \right]_{t=y+iz_w} \eta\sqrt{1-\eta^2}\, d\eta , \tag{1.67}$$

where M_ℓ is the rolling moment, C_ℓ is the rolling moment coefficient, and the constant C has been substituted for the factor

$$C = \frac{1}{\frac{\pi\beta}{(c_{\ell\alpha})_{m_w=0}} + \frac{2}{AR}} . \tag{1.68}$$

Using some approximations, Eq. (1.67) may be reduced to the form

$$C_\ell = - C\psi \int_{-2/\pi}^{+2/\pi} \left[I.P.\left(\frac{d\hat{t}}{dt}\right) \right]_{t=y+iz_w} \eta d\eta . \tag{1.69}$$

Suppose the fuselage cross section is of the shape of an ellipse having semi-axes $h_1 b$, and $h_2 b$. Then the rolling moment of such a configuration, calculated with the use of the above given technique, has the value

$$C_\ell = \frac{4}{\pi} C\psi h_2 (h_1 + h_2) \left[\frac{z_w}{h_2 b} \sqrt{1 - \frac{z_w}{h_2 b}^2} + \sin^{-1} \frac{z_w}{h_2 b} - \frac{2\pi z_w}{b} \right] . \tag{1.70}$$

This is valid for any value of z_w contained between the limits

$$- h_2 b \leq z_w \leq h_2 b . \tag{1.71}$$

Ward developed a different technique. Suppose a complex body is immersed in a uniform free stream flow of velocity U directed along the x-axis. The angle of attack is α. Let the symbol ϕ represent the perturbation potential governing the disturbances superimposed upon the uniform stream due to the presence of the wing-body combination. The aerodynamic force, normal to the x axis, created on the forward portion of the body is given by the formula

$$F_y + iF_z = \rho_\infty U \oint_{C_1} \Phi dt \quad , \tag{1.72}$$

where t denotes the complex variable, $t = y + iz$, and the line integral is to be taken around the complete contour C_1, produced by the intersection of the plane P with the body and wing surfaces. The plane P is perpendicular to the longitudinal axis of the body. For slender body configuration the equation of motion reduces to a two-dimensional Laplace equation

$$\frac{\partial^2\Phi}{\partial\eta^2} + \frac{\partial^2\Phi}{\partial\xi^2} = \frac{\partial^2\Phi}{\partial y^2} + \frac{\partial^2\Phi}{\partial z^2} = 0 \ . \tag{1.73}$$

The sought potential may be chosen to be of the form

$$\Phi(x, y, z) = \Phi_0(y, z;x) + \Phi_0^*(x) \quad , \tag{1.74}$$

with $\Phi_0(y, z;x)$ being a function satisfying Laplace equation

$$\nabla^2\Phi_0 = 0 \ . \tag{1.75}$$

The boundary conditions are of the form:

On the body: $$\frac{\partial\Phi_0}{\partial\eta} = - v_n \ ; \tag{1.76}$$

On the wake:

$$\nabla\left(\frac{\partial\Phi_0}{\partial y}\right)_0 = \left(\frac{\partial\Phi_0}{\partial y}\right)_{z=0^+} - \left(\frac{\partial\Phi_0}{\partial y}\right)_{z=0^-} = \frac{\partial\Gamma}{\partial y} = g(y) \quad , \tag{1.77}$$

where Γ is the circulation. When the fuselage is a body of revolution and the wing is a flat plate, the boundary conditions may be represented in the form:

On the body: $$v_n = - U\frac{dR_b}{dx} + \alpha_b U \sin\theta \quad , \tag{1.78}$$

and on the wing: $$v_n = \alpha_w U \ . \tag{1.79}$$

The symbols used denote:

v_n = the component of the free stream velocity $\vec{U}$, taken in the direction of the normal $\vec{n}$;

α_b = the angle of attack of the body's axis with respect to the free stream flow vector $\vec{U}$;

R_b = the radius of the section through the body at the axial location in question;

α_w = the angle of attack of the wing with respect to the free stream $\vec{U}$.

If the fuselage is not a body of revolution, then the component of the velocity, v_n, must satisfy the condition

$$v_n = - U \frac{dn}{dx} \quad . \tag{1.80}$$

The general law concerning v_n is

$$\oint_{C_1} v_n \frac{dS}{dx} = - U \oint_{C_1} \frac{dn}{dx} ds = - U \frac{dS}{dx} \quad , \tag{1.81}$$

where ds is the element of length along the contour C_1, and S is the cross-sectional area of the fuselage intercepted by the P-plane. Introduce a complex potential function $w_0 = \Phi_0 + i\psi_0$, where ψ_0 is the harmonic conjugate to Φ_0. Let it represent the function w_0 in terms of a power series of the form

$$w_0 = F + F_0 \ln t + \sum_{m=1}^{\infty} F_m t^{-m} \quad , \tag{1.83}$$

where F, F_0, and F_m are constants with respect to t, although, in general, they are functions of x. Also let

$$t_g = y_g + iz_g \quad , \tag{1.84}$$

represent the complex coordinate of the centroid of the area S. Then one can show that the complex force acting on the wing-body combination is given by the formula

$$F_y + iF_z = 2\pi\rho_\infty U F_1 + \rho_\infty U^2 \frac{d}{dx} (t_g S) \quad . \tag{1.85}$$

Likewise, the normal force per unit axial distance is given by

$$\frac{dF_y}{dx} + i\,\frac{dF_z}{dx} = 2\pi\rho_\infty U\left[\frac{dF_1}{dx} + \frac{U}{2\pi}\,\frac{d^2}{dx^2}\,(t_g S)\right] \quad . \tag{1.86}$$

The moment is given by

$$M_z + iM_y = \int_0^x x\left[\frac{dF_y}{dx} + i\,\frac{dF_z}{dx}\right]dx = x(F_y + iF_z) - 2\pi\rho_\infty U\left[\int_0^x F_1\,dx + \frac{U}{2\pi}\,t_g S\right] . \tag{1.87}$$

This method was applied to various wing-body combinations; flat plate-wing plus slender body, cruciform wing-body combination, wing-body combination having a cylindrical rump, etc.

The interference phenomena of the kind body-tail planes experience can be determined by the methods discussed above, provided that the aspect ratios pertaining to the stabilizing surfaces are not too large. If the aspect ratios pertaining to the stabilizing surfaces are too large then the determination of the effect of the fuselage on the tail may be difficult. In spite of that, in some instances the application of the methods discussed above proved to be valuable, and furnished a fair amount of good information.

1.4 Supersonic Range Wing-Tailplane Interference

In this section we shall briefly discuss the methods used in the supersonic range to evaluate the wing-tailplane interference. The following main points may be emphasized in this problem:

(i) evaluation of the field of induced angles of attack produced by the wing;

(ii) using the point (i), one has to evaluate the aerodynamic behavior of the stabilizer due to the perturbations introduced by the wing.

One may distinguish here certain types of the methods of attacking the problem:

(i) methods which treat the wing to be a lifting surface;

(ii) methods which treat the wing to be a lifting line.

Let us discuss as the first item the way of calculating the induced velocities produced by the wing using the concept of the lifting surface theory. Again in this respect one may distinguish several methods which can be used here, like the methods based on the conical flow theory and the so-called methods of singularities.

Let us begin with a semi-infinite trapezoidal wing subject to conical flow principles. Assume a ray t' having its origin at the tip of the leading edge. Let us make use of the following symbols:

τ_0 = the angle that the wing tip makes with the x-axis (in the direction of the motion);

$\beta = \sqrt{m_\infty^2 - 1}$ = cot (Mach angle);

$t_0 = \beta \tan \tau_0$;

$T = \dfrac{1 - \sqrt{1 - t'^2}}{t'}$;

$t' = \dfrac{\beta y}{x}$;

$C = \dfrac{1 - \sqrt{1 - t^2}}{t}$;

$t = \beta \tan \tau$;

τ = the angle that a ray makes with the x-axis.

Let us introduce a function $G(t, t')$ of the form

$$G(t, t') = \frac{1}{\pi}\left(\frac{1}{t} \ln|T| + 2 \tan^{-1} T + \frac{C^2 - 1}{2C} \ln\left|\frac{T - C}{1 - CT}\right| + \frac{\pi}{2}\right) , \tag{1.88}$$

then the induced downwash along a ray t' reduces to

$$\left(\frac{w}{U}\right)_{z=0} = \frac{2\alpha}{\pi} \int_{t_0}^{1} \frac{1}{\sqrt{1 - t}} \frac{1}{\sqrt{t - t_0}} G(t, t') dt . \tag{1.89}$$

The above formulas are valid in the region which falls within the Mach cone emanating from point A, i.e., from the tip of the leading edge. We have to consider also the region II, which is the region of the space lying downstream behind the Mach cone emanating from the point A.

The velocities induced in region II are given by

$$\left(\frac{w}{U}\right)_{z=0} = \frac{2\alpha}{\pi} \int_{t_0}^{1} \frac{1}{\sqrt{1 - t}} \frac{1}{\sqrt{t - t_0}} \left[G(t, t') - G(t, t'^*)\right] dt , \tag{1.90}$$

where the symbol used denotes:

$$t'^{*} = \frac{\frac{\beta y}{c_w} + 1}{\frac{x}{c_w} - 1} \quad ; \tag{1.91}$$

$$T^{*} = \frac{1 - \sqrt{1 - t'^{*2}}}{t'^{*}} \quad . \tag{1.92}$$

The expression for $G(t, t'^{*})$ may be obtained from the corresponding formula for $G(t, t')$ by merely substituting the quantity T^{*} for T in the latter formula. The symbol c_w represents the length of the wing chord located at a distance 0.75R from the root chord.

The above equations reduce to very simple formulae in two locations; at the trailing edge of the wing and at the Trefftz plane, i.e., for $x = \infty$. In the first case the result is

$$\frac{w}{U} = \alpha - \beta \frac{\mu t'}{U} \quad , \qquad \text{or} = 0 \quad , \tag{1.93}$$

depending upon the location of the point in question. In the case of the Trefftz plane the result is

$$\left(\frac{w}{U}\right)_{\substack{z=0 \\ x=\infty}} = \frac{2\alpha}{\pi^2} \int_{t_0}^{1} \frac{1}{t\sqrt{1 - t}} \frac{1}{\sqrt{t - t_0}} \ln\left|\frac{\beta \frac{y}{c_w}}{\frac{\beta y}{c_w} + t}\right| dt \quad . \tag{1.94}$$

In the special case of a rectangular wing the result is

$$\left(\frac{w}{U}\right)_{\substack{z=0 \\ x=\infty}} = \frac{2\alpha}{\pi}\left[1 - \sqrt{\frac{\beta \frac{y}{c_w} - 1}{\beta \frac{y}{c_w}}}\right] \quad \text{for } \beta \frac{y}{c_w} < 0 \quad , \tag{1.95}$$

or for

$$\frac{\beta_y}{c_w} > 1 \quad ; \qquad = \frac{2\alpha}{\pi} \quad \text{for } 0 \le \frac{\beta_y}{c_w} \le 1 \quad . \tag{1.96}$$

The method of singularities may be applied to the determination of the downwash behind a lifting surface in more than one manner. One may apply a distribution of pressure doublets over the wing; another way of achieving the same result is to distribute the velocity doublets over the wing and over the wake region; one may use vortices over both the wing and wake region. We may briefly discuss the method which employs the distribution of pressure doublets. The potential describing the perturbation field for the flow around the lifting surface is given in this case by the formula

$$\Phi = -\frac{z}{2\pi} \iint_{T} \frac{\Delta\Phi x_1 (x - x_1) dx_1 dy_1}{[(y - y_1)^2 + z^2] R(x)} \quad , \tag{1.97}$$

where the symbols used denote:

$$\Delta\Phi_{x_1} = \left(\frac{\partial\Phi}{\partial x}\right)_{z=0^-} - \left(\frac{\partial\Phi}{\partial x}\right)_{z=0^+} \; ; \tag{1.98}$$

$$R(x) = \sqrt{(x - x_1)^2 - \beta^2(y - y_1)^2 + z^2} \; ; \tag{1.99}$$

τ = region of integration on the wing; this is the intersection of the plane of the wing with the forward facing Mach cone issuing from the point $P(x, y, z)$. After some manipulations, the equation for the potential takes the form

$$\Phi = \frac{\beta^2 z}{2\pi} \iint_{\tau'} \frac{\Delta\Phi \, dx_1 \, dy_1}{[(x - x_1)^2 - \beta^2(y - y_1)^2 - \beta^2 z^2]^{3/2}} \; , \tag{1.100}$$

where the symbol τ' denotes that part of the region composed of the plane of the wing and the wake surface, which is restricted to that upstream portion for which $R > 0$. The formula for the downwash angles is of the form

$$\left(\frac{w}{U}\right) = \frac{1}{2\pi U} \iint_{\tau'} \Delta\Phi_{x_1 y_1} K dx_1 dy_1 + \frac{1}{2\pi U} \oint_S \Delta\Phi_{x_1} K^* dx_1 \tag{1.101}$$

where

$$K = \frac{(x - x_1)(y - y_1)(R^2 - \beta^2 z^2)}{[(x - x_1)^2 - \beta^2 z^2]\,[(y - y_1)^2 + z^2]R} \; . \tag{1.102}$$

The symbol $\Delta\Phi$ with the corresponding subscripts denotes the jump experienced by the potential. The symbol S on the line integral denotes the path of integration taken around the region τ_1 previously given. The symbol K^* is the same expression as K except that the values of x_1 and y_1 are restricted to those belonging to the boundary of the τ region. For points which lie in the wake $(z = 0)$, the previous equation reduces to a simpler form

$$\left(\frac{w}{U}\right)_{z=0} = \frac{1}{2\pi U} \iint_{\tau} \frac{\Delta\Phi_{x_1 y_1} R}{(x - x_1)(y - y_1)} dx, \, dy_1 + \frac{1}{2\pi U} \oint_S \Delta\Phi_{x_1} \frac{\sqrt{(x - x_1^*)^2 - \beta^2(y - y_1^*)^2}}{(x - x_1^*)(y - y_1^*)} dx_1^* \; . \tag{1.103}$$

In this equation the points confined to the contour line S have been distinguished from the general (x_1, y_1) coordinates by using the notations (x_1^*, y_1^*). This formula can be easily converted into the following one:

$$\left(\frac{w}{U}\right)_{z=0} = \frac{1}{2\pi U} \oint_S (\Delta\Phi_{y_1} dy_1^* + \Delta\Phi_{x_1} dx_1^*) \frac{R^*}{(x - x_1^*)(y - y_1^*)}$$

$$- \frac{1}{2\pi U} \iint_T \Delta\Phi_{y_1} \frac{\partial}{\partial x_1} \left[\frac{R}{(x - x_1)(y - y_1)}\right] dx_1 dy_1 \quad . \qquad (1.104)$$

For a semi-infinite trapezoidal wing the last equation gives

$$\left(\frac{w}{U}\right)_{z=0} = \frac{2\alpha}{\pi^2} \int_0^1 \frac{I(t, t')dt}{\sqrt{(t - t_0)(1 - t)}} \quad , \qquad (1.105)$$

with

$$I(t_1 t') = \frac{1}{\pi} \int_0^{c_w/x} \frac{\sqrt{(1 - \xi)^2 - (t' - t\xi)^2}}{(1 - \xi)(t' - t\xi)} d\xi \quad , \qquad (1.106)$$

and $\xi = x_1/x$. For a triangular wing with subsonic leading edges the formula gives the result

$$\left(\frac{w}{U}\right)_{z=0} = - \frac{\alpha\beta}{\pi E_0} \left\{ \oint_S \frac{y_1^* R^*}{\sqrt{\theta_0^2 x_1^{*2} - \beta^2 y_1^{*2}}} \frac{dy_1^*}{(x - x_1^*)(y - y_1^*)} \right.$$

$$\left. - \iint_T \frac{y_1}{\sqrt{\theta_0^2 x_1^2 - \beta^2 y_1^2}} \frac{\partial}{\partial x_1} \left[\frac{R}{(x - x_1)(y - y_1)}\right] dx_1 dy_1 \right\} , \qquad (1.107)$$

with E_0 denoting the complete elliptic integral of the second kind with the modulus $k = \sqrt{1 - \theta_0^2}$;

$$\theta_0 = \beta \tan \delta \quad , \qquad (1.108)$$

with δ denoting the half angle at the vertex of the triangular wing.

As the next theory, we shall discuss the lifting line theory. One may replace the concept of the lifting surface by the concept of a lifting line. Let the symbol Φ_s denote the potential for the flow when using the concept of a lifting surface and Φ_ℓ when using the concept of the lifting line. The difference of these two potentials is given by

$$\Phi_s - \Phi_\ell = \frac{\beta^2 z}{2\pi} \left[\iint_S \frac{\Delta\Phi(\xi_1 \eta) d\xi \, d\eta}{R^3} - \iint_{S_1} \frac{\Delta\Phi(\eta) d\xi \, d\eta}{R^3} \right] . \qquad (1.109)$$

In Eq. (1.109) the following symbols are used:

(i) the part of the lifting surface which is bounded by the forward-facing Mach cone having its vertex at the point $P(x, y, z)$, where one wishes to obtain the value of Φ, is denoted by S;

(ii) the part of the lifting surface which lies within the forward-facing Mach cone but is further restricted to just the region bounded upstream by the lifting line is denoted by S_1;

(iii) let ξ denote the abscissa value of the trailing edge location in any arbitrary one of the airfoil sections cut out by the general plane η = constant, then $\Delta\phi(\eta)$ is given by:

$$\Delta\Phi(\eta) = \Delta\Phi(\xi_2, \eta) \quad . \tag{1.110}$$

After some manipulations the difference expression becomes

$$\Phi_s - \Phi_\ell = \frac{z\beta^2}{2\pi} \int_{-b/2}^{b/2} \frac{d\eta}{\beta^2[(y-\eta)^2 + z^2]} \int_{\xi_1}^{\xi_2} \left[\frac{x - \xi'}{\sqrt{(x-\xi')^2 - \beta^2(y-\eta)^2 - \beta^2 z^2}} - \frac{x - \xi_0}{\sqrt{(x-\xi_0)^2 - \beta^2(y-\eta)^2 - \beta^2 z^2}} \right] m(\xi', \eta)\, d\xi' \quad , \tag{1.111}$$

with

$$m(\xi, \eta) = \frac{\partial}{\partial \xi} \Delta\Phi(\xi, \eta) \quad . \tag{1.112}$$

The downwash velocity at a point $P(x, y, z)$ lying downstream from the lifting line is equal to

$$\frac{W}{U} = \frac{\beta^2}{2\pi U} \int_{y_1}^{y_2} \frac{\Gamma[(y-\eta) - \nu(x - f)]d\eta}{\nu R^{3/2}} + \frac{1}{2\pi U} \int_{y_1}^{y_2} \frac{(x - f)(y - \eta)}{R[(y-\eta)^2 + z^2]} \frac{d\Gamma}{d\eta} d\eta \quad , \tag{1.113}$$

where the following notations are used:

(i) the equation defining the location in a fore-and-aft direction of the most representative lifting line is given by:

$$\xi_\nu = f(\eta) \quad ; \tag{1.114}$$

(ii) $\nu = \dfrac{d\eta}{d\xi}$;

(iii) the symbols y_1 and y_2 are the values of the spanwise coordinate η at which the forward-facing Mach cone emanating from the point P intersects the most advantageous lifting line (call it the line L);

$$\text{(iv)}\quad R = \sqrt{(x-f)^2 - \beta^2(y-\eta)^2 - \beta^2 z^2}\ . \tag{1.115}$$

In case of straight-line swept vortical axes, the equation for the downwash velocity reduces to

$$\frac{w}{U} = \frac{\Gamma(0)}{2\pi}\left[G(\nu_0^-) - G(\nu_0^+)\right]_{\eta=0} - \frac{1}{2\pi}\int_{y_1}^{y_2}\left[G(\nu) - G(0)\,\frac{d\Gamma}{d\eta}\right]d\eta\ , \tag{1.116}$$

where

$$G(\nu) = -\frac{[y-\eta-\nu(x-f)][\beta^2\nu(y-\eta)-(x-f)]}{R\{[(y-\eta)-\nu(x-f)]^2 + (1-\beta^2\nu^2)z^2\}}\ . \tag{1.117}$$

If the ultimate in simple wings is to be handled by this method, where the two swept lifting straight-line axes are now assumed to coalesce into one straight line which is parallel to the y-axis, then the equation for the induced velocity becomes

$$\frac{w}{U} = \frac{1}{2\pi U}\int_{y_1}^{y_2}\frac{x(y-\eta)(R^2-\beta^2z^2)}{R(x^2-\beta^2z^2)[(y-\eta)^2+z^2]}\,\frac{d\Gamma}{d\eta}\,d\eta\ . \tag{1.118}$$

For the calculation of the values of w/U which hold for points lying on the plane of the undisplaced wake behind the wing, Eq. (1.118) simplifies still further into

$$\left(\frac{w}{U}\right)_{z=0} = \frac{1}{2\pi U}\int_{y_1}^{y_2}\frac{R}{x(y-\eta)}\,\frac{d\Gamma}{d\eta}\,d\eta\ . \tag{1.119}$$

Now, if the point $P(x, y, z)$ at which the downwash is to be calculated, lies in the region II of the plane $z = 0$, which is defined as the region comprising all points which lie inside both Mach cones emanating from the extremities of the lifting straight-line axis under consideration, then the above equation may be written in the form

$$\frac{1}{2\pi U}\int_{-b/2}^{b/2}\frac{d\Gamma}{d\eta}\,\frac{R\,d\eta}{x(y-\eta)} = \frac{1}{2\pi U}\int_{-b/2}^{b/2}\frac{d\Gamma^*}{d\eta}\,\frac{d\eta}{y-\eta}\ , \tag{1.120}$$

where

$$\Gamma^* = \Gamma(\eta)\,\frac{x}{\sqrt{x^2-\beta^2(y-\eta)^2}}\ . \tag{1.121}$$

The circulation Γ is usually represented in the form

$$\Gamma = \frac{2}{m+1} \sum_{n=1}^{m} \Gamma_n \sum_{\mu=1}^{m} \sin(\mu\theta_n)\sin(\mu\theta) \quad , \qquad (1.122)$$

where Γ_n is the value of Γ at the location θ_n, and where the spanwise locations have been converted into angular measure according to scheme

$$\theta = \cos^{-1}\frac{2y}{b} \quad , \quad \text{so that } \theta_n = \cos^{-1}\frac{n\pi}{m+1} \quad . \qquad (1.123)$$

The downwash velocity is given by the formula

$$(\epsilon)_{z=0} = 2b_{\nu\nu}\frac{\Gamma(y_\nu)}{bU} - 2\sum_{n=1}^{m}{}' b_{n\nu}\frac{\Gamma(y_n)}{bU}\frac{x}{\sqrt{x^2 - \beta^2(y_\nu - y_n)^2}} \quad , \qquad (1.124)$$

where the symbols $b_{\nu\nu}$ and $b_{\nu n}$ are the well-known Multhopp coefficients and the prime superscript on the summation symbol denotes that the term with repeated subscripts, i.e., $n = \nu$, must be omitted. Applying a few additional manipulations the equation for the downwash angle in the plane of the wake can be put into the form

$$(\epsilon)_{z=0} = \left(\frac{\beta}{2\pi U}\right)\left(\frac{2}{m+1}\right) \sum_{n=1}^{m} \Gamma_n^* \sum_{\mu=1}^{m} \mu \sin(\mu\theta_n) \int_0^{\pi} \tan\theta \cos(\mu\theta)d\theta \quad . \qquad (1.125)$$

The evaluation of the remaining integrals in this expression for the induced vertical velocities comes about in a straight forward manner.

Eq. (1.125) was applied to various particular cases. The procedure expounded above may be utilized to determine the downwash induced in the region occupied by the horizontal tailplane, under the condition that the rolling-up of the trailing vortex sheet may be neglected at this stage of the computations. Let us use the following notation:

$Z_{t.e.}$, $x_{t.e.}$ are the vertical and horizontal coordinates of the trailing edge of the wing in question, respectively;

$(\epsilon)_{z=0}$ is the induced angle of downwash at the level of the wake.

Using these notations the actual displaced position of points lying on the trailing vortex sheet may be obtained from the relation

$$Z_1 = Z_{t.e.} + \int_{x_{t.e.}}^{x} (\epsilon)_{z=0} \, dx \quad . \tag{1.126}$$

The remaining part of the procedure requires some numerical methods. The results are usually presented in forms of diagrams.

If the trailing vortex sheet is considered completely rolled up, the induced velocity is given by the formula

$$\frac{w}{U} = \frac{x\Gamma_0}{2\pi U(x^2 - \beta^2 z^2)} \left[\frac{\left\{x^2 - \beta^2\left[(y-\frac{b'}{2})^2 + 2z^2\right]\right\}(y-\frac{b'}{2})}{\left[(y-\frac{b'}{2})^2 + z^2\right]\sqrt{x^2 - \beta^2\left[(y-\frac{b'}{2})^2 + z^2\right]}} \right.$$

$$\left. - \frac{\left\{x^2 - \beta^2\left[(y+\frac{b'}{2})^2 + 2z^2\right]\right\}(y+\frac{b'}{2})}{\left[(y+\frac{b'}{2})^2 + z^2\right]\sqrt{x^2 - \beta^2 \; (y+\frac{b'}{2})^2 + z^2}} \right] , \tag{1.127}$$

wherein the circulation at the plain of symmetry is denoted by Γ_0, i.e.,

$$\Gamma_0 = (\Gamma)_{y=0} \quad . \tag{1.128}$$

For $x \to \infty$, i.e., at the Trefftz plane, Eq. (1.128) reduces to

$$\left(\frac{w}{U}\right)_{x=0} = \frac{\Gamma}{2\pi U} \left[\frac{y - \frac{b'}{2}}{(y-\frac{b'}{2})^2 + z^2} + \frac{y + \frac{b'}{2}}{(y+\frac{b^2}{2})^2 + z^2} \right] . \tag{1.129}$$

1.5 Supersonic Range Wing-Body Interaction

In this domain, they usually distinguish two cases:

(i) the leading and trailing edges of the wing are supersonic;

(ii) the leading edge is subsonic.

At first, we shall consider configurations having wings with supersonic leading and trailing edges. The flow about a wing-body configuration is described by means of the velocity potential described by the equation

$$\Phi = U \frac{b}{2}\left\{\xi + (\phi_b)_1 + \alpha_w[(\phi_b)^2 - \zeta + \phi_w + \phi^{(w)} + \phi^{(b)}]\right\} , \qquad (1.130)$$

where

$$\xi = \frac{2x}{b} ; \quad \zeta = \frac{2z}{b} . \qquad (1.131)$$

The coordinates $\{x, y, z\}$, are converted into the physical coordinates $\{x_1, y_1, z_1\}$ by use of the Prandtl-Glauert transformation

$$x = \frac{x_1}{b} ; \quad y = y_1 ; \quad z = z_1 ; \quad \beta = \sqrt{m_\infty^2 - 1} ; \qquad (1.132)$$

$$\xi = \frac{2x}{b} ; \quad \zeta = \frac{2z}{b} ; \qquad (1.133)$$

b = length of the span of the wing;

$U \frac{b}{2}(\xi - \alpha_w\zeta)$ denotes the potential which governs the free stream flow;

$U \frac{b}{2}[(\phi_b)_1 + \alpha_w(\phi_b)_2]$ denotes the incremental potential that corresponds to the flow perturbations produced by the body when it alone is inserted into the free stream;

$U \frac{b}{2}\alpha_w\phi_w$ denotes the similar incremental potential which corresponds to the flow perturbations produced by the presence of the isolated wing in the otherwise undisturbed stream; the wing meant in this case is that resulting from an extension of the real exposed planform across the area normally covered by the fuselage;

$U \frac{b}{2}\alpha_w\phi^{(w)}$ denotes the incremental potential representing the interference effect of the body upon the wing;

$U \frac{b}{2}\alpha_w\phi^{(b)}$ stands for the analogous incremental potential representing the interference effect of the wing upon the body.

The potentials referring to the isolated components are assumed to be readily available by use of standard treatments. The interference potentials must satisfy the following potentials:

$$\left(\frac{\partial\phi^{(w)}}{\partial\zeta}\right)_{\zeta=0} = -\left(\frac{\partial(\phi_b)_2}{\partial\zeta}\right)_{\zeta=0} - \left(\frac{\partial\phi^{(b)}}{\partial\zeta}\right)_{\zeta=0} , \qquad (1.134)$$

over that part of the $\zeta = 0$ plane which lies within the extended wing;

$$\left(\frac{\partial \phi^{(b)}}{\partial r}\right)_{r=r_b} = -\left(\frac{\partial \phi_w}{\partial r} + \frac{\partial \phi^{(w)}}{\partial r}\right)_{r=r_b} , \tag{1.135}$$

over the body. In the equations above the following symbols are used:

$$r = \frac{2R}{b} ; \quad r_b = \frac{2R_b}{b} , \tag{1.136}$$

where there are used the cylindrical coordinates (x, R, θ) and R_b denotes the radius of a circular cross section produced by a plane passed normal to the axis of the body at the generic axial location $x =$ constant.

The interference potentials may be determined independently of each other. Thus $\phi^{(b)}$ can be expressed in the form

$$\phi^{(b)} = \sum_n \phi_n^{(b)}(\xi, r) r^n \cos n\theta , \tag{1.137}$$

where only the even values of n should be considered; analogously, the function $\phi^{(w)}$ may be represented in the form

$$\phi^{(w)} = \sum_m \phi_m^{(w)}(\xi, \zeta) \cos\left(\frac{\pi m \eta}{2}\right) , \tag{1.138}$$

where each function $\phi^{(w)}$ must satisfy the equation

$$\frac{\partial^2 \phi_m^{(w)}}{\partial \zeta^2} - \frac{\partial^2 \phi_m^{(w)}}{\partial \xi^2} = k^2 \phi_m^{(w)} , \tag{1.139}$$

$$k = \frac{\pi m}{2} . \tag{1.140}$$

The boundary conditions are

$$\left(\frac{\partial \phi_m^{(w)}}{\partial \zeta}\right)_{\zeta=0} = - G_m(\xi) , \tag{1.141}$$

where the functions G_m originate from the representation of the relative angle of attack in the form

$$\frac{(w_b^*)_2}{\alpha_w U} = \sum_m G_m(\xi)\cos\left(\frac{\pi m \eta}{2}\right) , \quad m = 1, 3, 5, \ldots . \tag{1.142}$$

The solution of Eq. (1.139) with the corresponding boundary conditions is

$$\phi_m^{(w)} = -\pi h_m(\xi^* - \zeta) + \pi k \zeta \int_0^{\xi^*-\zeta} h_m(\xi^{*\prime}) J_1\left[k\sqrt{(\xi^* - \xi^{*\prime})^2 - \zeta^2}\right] \frac{d\xi^{*\prime}}{\sqrt{(\xi^* - \xi^{*\prime})^2 - \zeta^2}} , \tag{1.143}$$

where a shift in the origin of coordinates has been introduced by means of $\xi^* = \xi - r_b$. The symbol J_n denoted the cylindrical Bessel function of nth order. The function h_m is given by the formula

$$h_m = -\frac{1}{\pi}\int_0^{\xi^*} G_m(\xi^{*\prime}) J_0[k(\xi^* - \xi^{*\prime})] d\xi^{*\prime} . \tag{1.144}$$

The formula for $\phi_m^{(w)}$ may be given in the form

$$\phi_m^{(w)} = \frac{2}{k}\int_0^{\xi^*-\zeta} L_m(\xi^*, \zeta; \xi^{*\prime}) dG_m , \tag{1.145}$$

where the integral in question is of the Stieltjes type and the function L_m is

$$L_m(\xi^*, \zeta; \xi^{*\prime}) = \sum_{j=1,3,5} \left(\frac{\xi^* - \xi^{*\prime} - \zeta}{\xi^* - \xi^{*\prime} + \zeta}\right) J_j\left[k\sqrt{(\xi^* - \xi^{*\prime})^2 - \zeta^2}\right] . \tag{1.146}$$

The component of velocity normal to the surface of the body of revolution, which is induced by action of the wing interference potential $\phi^{(w)}$ is

$$\left(\frac{v_{rb}^{(w)}}{\alpha_w U}\right)_{r = r_b} = \left(\frac{\partial\phi^{(w)}}{\partial r}\right)_{r = r_b} = -2\cos\theta\left(\sum_m \sin k\eta \int_0^{\xi^*} L_m dG_m\right)_{\substack{\eta = r_b\cos\theta \\ \zeta = r_b\sin\theta}}$$

$$-\sin\theta\left(\sum_m \cos k\eta \int_0^{\xi^*} L_m' dG_m\right)_{\substack{\eta = r_b\cos\theta \\ \zeta = r_b\sin\theta}} . \tag{1.147}$$

As the next item one should determine the potential corresponding to the interference effect of the wing upon the body in the portion of the space not influenced by the wing tips. Each function $\phi_n^{(b)}$ in Eq. (1.137) must satisfy the equation

$$\frac{\partial^2 \phi_n^{(b)}}{\partial r^2} + \frac{1 + 2n}{r} \frac{\partial \phi^{(b)}}{\partial r} = \frac{\partial^2 \phi_n^{(b)}}{\partial \xi^2} \quad . \tag{1.148}$$

The solution of this equation is of the form

$$\phi_n^{(b)} = \frac{(-1)^n}{r^n} \int_{\cosh^{-1}\xi/r}^{0} \mathscr{F}_n(\xi - r\cosh u)\cosh nu\, du \quad , \tag{1.149}$$

where the functions $\mathscr{F}_n$ may be determined from the relation

$$\left[\frac{\partial(r^n \phi_n^{(b)})}{\partial r}\right]_{r=r_b} = - \int_{\cosh^{-1}\xi/r_b}^{0} \dot{\mathscr{F}}_n(\xi - r_b \cosh u) \cosh nu \cosh u\, du = - F_n^*(\xi) \quad , \tag{1.150}$$

where

$$\dot{\mathscr{F}}_n(\xi) = \frac{d\mathscr{F}_n}{\partial \xi} \quad . \tag{1.151}$$

The function F_n^* may be also determined from the relation

$$- \frac{v_{rb}}{\alpha_w U} = \sum_n F_n^*(\xi) \cos n\theta \quad . \tag{1.152}$$

In the case of a cylindrical body one may use the substitution

$$\dot{\mathscr{F}}_n(\xi') = U_n(t') \quad ; \tag{1.153}$$

the solution for $U_n(t)$ is given in the form

$$U_n(t) = H_n(t) - \int_0^t S_n(t - t')H_n(t')dt' \quad , \tag{1.154}$$

and

$$H_n = - \frac{\sqrt{2}}{\pi} \int_0^t \frac{dF_n^*}{\sqrt{t - t'}} \quad ; \tag{1.155}$$

$$S_n(z) = Q_n^*(z) - \int_0^z Q_n^*(z - y)Q_n^*(y)\,dy$$

$$+ \int_0^z Q_n^*(z - y_1)\,dy_1 \int_0^{y_1} Q_n^*(y_1 - y_2)Q_n^*(y_2)\,dy_2 + \dots \quad , \qquad (1.156)$$

$$\frac{\sqrt{2}}{\pi} \dot{Q}_n(z) = Q_n^*(z) \quad , \qquad (1.157)$$

$$\frac{dQ_n}{dz} = \frac{\pi}{2\sqrt{2}} (1 - x^2)\Bigg\{[\Gamma(n - \tfrac{1}{2})]^{-2}\Bigg[x^{-1/2}(1 - x)^{n-3/2}(\tfrac{1}{2} - nx)B_{n-1}$$

$$+ x^{\frac{1}{2}}(1 - x)^{n-1/2}\frac{dB_{n-1}}{dx}\Bigg] + [\Gamma(n + \tfrac{3}{2})]^{-2}\Bigg[x^{-1/2}(1 - x)^{n+1/2}(\tfrac{1}{2} - nx - 2x)B_{n+1}$$

$$+ x^{1/2}(1 - x)^{n+3/2}\frac{dB_{n+1}}{dx}\Bigg]\Bigg\} \ ; \qquad (1.158)$$

$$Q_n(z) = \frac{\pi}{\sqrt{2}} x^{1/2}\Big\{[\Gamma(n - \tfrac{1}{2})]^{-2}(1 - x)^{n-1/2}B_{n-1}$$

$$+ [\Gamma(n + \tfrac{3}{2})]^{-2}(1 - x)^{n+3/2}B_{n+1}\Big\} \quad \text{for } n > 0; \qquad (1.159)$$

$$B_m = \frac{d^m}{dx^m}\left[x^m \frac{d^m}{dx^m}(x^{m-1/2}K)\right], \qquad (1.160)$$

where K is the complete elliptic integral of the first kind with modulus $\sqrt{x}$.

After the incremental interference potentials $\phi^{(w)}$ and $\phi^{(b)}$ have been determined, one may find the pressure coefficients on the wing and on the body, respectively:

$$(\Delta C_p)_w = -2\left[\frac{\partial\phi^{(w)}}{\partial\xi} + \frac{\partial\phi^{(b)}}{\partial\xi}\right]_{\zeta=0^+} \ ; \qquad (1.161)$$

$$(\Delta C_p)_b = -2\left[\frac{\partial\phi^{(b)}}{\partial\xi} + \frac{\partial\phi^{(w)}}{\partial\xi}\right]_{r=r_b} \qquad (1.162)$$

in the region where $\zeta > 0$.

From the equations given above, one gets

$$\left[\frac{\partial \phi^{(w)}}{\partial \xi}\,_{\zeta=0^+} + \sum_m \frac{\partial \phi_m^{(w)}}{\partial \xi}\right]_{\zeta=0^+} \cos\frac{(\pi m \eta)}{2} = \sum_k \cos k\eta \int_0^{\xi^*} J_0[k(\xi^* - \xi^{*\prime})]dG_m \quad . (1.163)$$

The second part of the contribution to the incremental wing pressures, arising from the body flow potential, is given by the formula

$$\left[\frac{\partial(r^n \phi_n^{(b)})}{\partial \xi}\right]_{\zeta=0^+} = (-1)^n \int_{\cosh^{-1}(\xi/\eta)}^{0} \dot{\mathscr{F}}_n(\xi - \eta \cosh u)\cosh nu\, du \quad . \qquad (1.164)$$

After all the substitutions and manipulations the formula for the sought pressures becomes

$$\left[\frac{\partial(r^n \phi_n^{(b)}}{\partial \xi}\right]_{\zeta=0^+} = (-1)^{n+2}\sqrt{\tau}\, F_n^*(t - \tau_1) + (-1)^{n+2}\int_0^{t-\tau_1} F_n^*(t'')\dot{\Omega}_n(t - t'')dt'', \quad (1.165)$$

where

$$\Omega_n(z) = \int_0^{z-\tau_1} \frac{\Phi_n(t^*)\cosh[n\cosh^{-1}\tau(z + 1 - t^*)]}{(z - \tau_1 - t^*)(z + \tau_2 - t^*)}\, dt^* \quad , \qquad (1.166)$$

$$\tau = \frac{r_b}{\eta} \; ; \quad \tau_1 = \frac{\eta}{r_b} - 1 \; ; \quad \tau_2 = \frac{\eta}{r_b} + 1 \quad . \qquad (1.167)$$

The complete expression for the wing incremental pressures due to the total of all interference has the value

$$(\Delta C_p)_w = -2\frac{(w_b^*)_2}{\alpha_w U} - 2\sqrt{\tau}\left(\frac{\bar{v}_{rb}}{\alpha_w U}\right)_{\theta=0} + 2\sum_m \cos k\eta \int_0^{\xi^*}\left\{1 - J_0[k(\xi^* - \xi^{*\prime})]\right\}dG_m$$

$$- 2\sum_n \int_0^{t-t_1} F_n^*(t'')\Omega_n(t - t'')dt'' \quad . \qquad (1.168)$$

In a similar manner one may calculate the pressures produced by interference effects on the body; the required formula for the derivative gives

$$\left(\frac{\partial \phi^{(w)}}{\partial \xi}\right)_{r=r_b} = \sum_m \cos(kr_b \cos\theta)\left[\frac{\partial \phi_m^{(w)}}{\partial \xi}\right]_{\zeta=r_b \sin\theta}$$

$$= \sum_m \cos(kr_b \cos\theta) \int_0^{\xi^* - r_b \sin\theta} J_0 \left[k\sqrt{(\xi^* - \xi^{*\prime})^2 - r_b^2 \sin^2\theta} \right] dG_m \quad , \qquad (1.169)$$

$$(\Delta C_p)_b = \frac{-2v_{rb}}{\alpha_w U} - 2 \sum_n \cos n\theta \int_0^t F^*(t'')\Omega_n(t - t'')dt''$$

$$+ 2 \sum_k \cos(kr_b \cos\theta) \int_0^{\xi^* - r_b \sin\theta} J_0 \left[k\sqrt{(\xi^* - \xi^{*\prime})^2 - r_b^2 \sin^2\theta} \right] dG_m \, . \qquad (1.170)$$

A similar procedure can be applied to the region located downstream of the trailing edge. The following conditions must be satisfied:

(i) $\Delta\Phi = (\Phi)_{\zeta=0^+} - (\Phi)_{\zeta=0^-} = \Delta\Phi(\xi_w, \eta)$ on the plane $\zeta = 0$; here the symbol ξ_w denotes the axial location of any one of the points located on the trailing edge of the wing;

(ii) the total induced velocity on the body itself is zero;

(iii) the function Φ must be continuous on the surface of the Mach plane $\xi - |\zeta| = \xi_w$ that originates on the trailing edge of the wing; a discontinuity of grad Φ is normal to this Mach plane.

The potential we seek is taken in the form

$$\phi_m^{\prime(w)} = \sum_m [\phi_m^{(w)} + \phi_m^{*(w)}] \cos\left(\frac{\pi m \eta}{2}\right) \quad , \qquad (1.171)$$

where

$$\phi_m^{(w)} = \pm \pi h_m(\xi_w^*) + \pi k \zeta \int_0^{\xi_w^*} h(\xi^{*\prime}) J_1 \left[k\sqrt{(\xi^* - \xi^{*\prime})^2 - \zeta^2} \right] \frac{d\xi^{*\prime}}{\sqrt{(\xi - \xi^{*\prime})^2 - \zeta^2}} \quad , \qquad (1.172)$$

in which $\xi_w^* = \xi_w - r_b$, and the function $h_m(\xi^*)$ represents the source strength given by Eq. (1.144). The function $\phi_m^{*(w)}$ must be evaluated in such a manner, that it should cancel the discontinuity in the component $u^{(b)}/(\alpha_w U)$ of the velocity along the x-axis. The analysis gives the following expression for this function

$$\phi_m^{*(w)} = \pm h_m^*(\xi - |\zeta|) + \pi k \zeta \int_{\xi_w}^{\xi - |\zeta|} h_m^*(\xi') J_1 \; k\sqrt{(\xi - \xi')^2 - \zeta^2} \frac{d\xi'}{\sqrt{(\xi - \xi')^2 - \zeta^2}} \quad . \qquad (1.173)$$

The second condition below Eq. (1.170) requires special attention. The potential $\phi^{(b)}$ may be chosen in the form

$$\phi^{(b)} = \sum_n \phi_n^{(b)} \cos n\theta \quad , \quad \text{for } 0 \leq \theta \leq \pi \quad , \tag{1.174}$$

$$= - \sum_n \phi_n^{(b)} \cos n\theta \quad , \quad \text{for } 0 \geq \theta \geq -\pi \quad . \tag{1.175}$$

The total radial derivative, evaluated at the surface of the body, originated from both interference contributions is chosen to be of the form

$$\left[\frac{\partial(\phi'^{(w)} + \phi^{(b)})}{\partial r}\right]_{r=r_b} = \sum_n T_n(\xi, r_b) \sin n\theta \quad . \tag{1.176}$$

Similarly, the induced velocity normal to the body originating from the wing-alone potential, ϕ_w, can be represented in the form

$$\left(\frac{\partial \phi^{(w)}}{\partial r}\right)_{r=r_b} = \sum_n T_n'(\xi, r_b) \sin n\theta \quad . \tag{1.177}$$

This implies that the total of the induced radial velocities normal to the fuselage behind the wing are given by the formula

$$\frac{v_r}{\alpha_w U} = \sum_n (T_n + T_n') \sin n\theta = \sum_n T_n^*(\xi, r_b) \sin n\theta \quad . \tag{1.178}$$

A counteracting potential, $\phi^{*(b)}$, has to be constructed having such a form that the following condition is satisfied on the surface of the body:

$$\left(\frac{\partial \phi^{*(b)}}{\partial r}\right)_{r=r_b} = - \sum_n T_n^*(\xi, r_b) \sin n\theta \quad . \tag{1.179}$$

This potential may have the form

$$\phi^{*(b)} = \sum_n \phi_n^{*(b)} \sin n\theta \quad , \quad n = 1, 3, 5 \ldots \quad , \tag{1.180}$$

with

$$\phi_n^{*(b)} = \frac{(-1)^n}{r^n} \int_{\cosh^{-1}\{[\xi - \xi_w + (r_b)_w/r\}}^{0} \mathscr{F}_n^*(\xi - r\cosh u)\cosh nu \, du \quad . \tag{1.181}$$

The symbol $(r_b)_w$ denotes the value of the body radius at the wing's trailing edge, located at $\xi = \xi_w$. One can verify that the functions $\mathscr{F}_n^*$ can be calculated from the equation

$$- T_n^*(\xi, r_b) = (-1)^{n+1} \int_{\cosh^{-1}\{[\xi - \xi_w + (r_b)_w]/r_b\}}^{0} \dot{\mathscr{F}}_n^*(\xi - r_b \cosh u) \cosh nu \cosh u \, du$$
$$+ (-1)^{n+2} \mathscr{F}_n^*[\xi_w - (r_b)_w] \cosh\left[n \cosh^{-1}\left(\frac{\xi - \xi_w + (r_b)_w}{r_b}\right)\right]$$
$$\left[\frac{\xi - \xi_w + (r_b)_w}{r_b\sqrt{[\xi - \xi_w + (r_b)_w]^2 - r_b^2}}\right]. \tag{1.182}$$

The determination of the harmonic components T_n^* presents a separate problem which is discussed and solved in some of the references cited in the List of References at the end of the present chapter.

In the case of the wings of high aspect ratio, the analysis given above may be simplified. We shall put down below the most significant formulae which differ from those derived above. These are

$$\left(\frac{\partial \phi_w}{\partial r}\right)_{r=r_b} = \sum_n F_n^*(\xi) \sin n\theta \quad , \qquad \text{for } n = 1, 3, 5, \ldots \quad , \tag{1.183}$$

in the whole interval $0 \leq \theta \leq 2\pi$. The potential $\phi^{(b)}$ is expressed in the form

$$\phi^{(b)} = \sum_n \phi_n^{(b)} \sin n\theta \quad , \tag{1.184}$$

with the value of the induced velocity given by

$$\left[\frac{1}{r} \frac{\partial \phi^{(b)}}{\partial \theta}\right]_{\theta=0} = \sum_n n \frac{(-1)^n}{r} \int_{\cosh^{-1}(\xi/r)}^{0} \mathscr{F}_n(\xi - r\cosh u)\cosh nu \, du = \frac{w^{(b)}}{\alpha_w U} \quad . \tag{1.185}$$

The boundary conditions reduce to

$$\left[\frac{\partial \phi^{(b)}}{\partial \zeta}\right]_{\zeta=0} = -\left[\frac{\alpha(\phi_b)_2}{\partial \zeta}\right]_{\zeta=0} \quad ; \tag{1.186}$$

$$\left[\frac{\partial\phi^{(b)}}{\partial r}\right]_{r=r_b} = -\left[\frac{\partial\varphi_w}{\partial r}\right]_{r=r_b} . \tag{1.187}$$

Once the potentials have been determined, one can calculate the aerodynamic coefficients

$$[(\Delta C_p)_w]_{\zeta=0^+} - [(\Delta C_p)_w]_{\zeta=0^-} = -4\,\frac{(w_b^*)_2}{\alpha_w U} + 4\sum_m \cos k\eta \int_0^{\xi^*} \{1 - J_0[k(\xi^* - \xi^{*\prime})]\} dG_m \; ; \tag{1.188}$$

the integrated lift over a chordwise strip of the wing is given by the formula

$$(\Delta c_\ell)_w = (\overline{\Delta c_\ell})_w + \frac{4}{\lambda_w} + \sum_m \cos k\eta \int_0^{\xi_w^*} \{1 - J_0[k(\xi^* - \xi^{*\prime})]\} G_m(\xi^{*\prime})\, d\xi^{*\prime} \; , \tag{1.189}$$

where $(\overline{\Delta c_\ell})_w$ is the two-dimensional lift coefficient of the strip in question, when the lift is assumed to be distributed over the profile according to the Ackeret formula.

The interference action on the part of the body which is influenced by the wing, consists of various parts. These are listed below:

(i) the axial components of velocity, stemming from the wing-alone potential ϕ_w, contributes to the total the part $\Delta_1 L_b$;

(ii) the axial components of the velocity, stemming from the wing interference potential $\phi^{(w)}$ contribute the part $\Delta_2 L_b$;

(iii) the radial components of velocity, stemming from the wing interference potential contribute the part $\Delta_3 L_b$;

Briefly, one can put down the equality

$$\Delta L_b = \Delta_1 L_b + \Delta_2 L_b + \Delta_3 L_b \; . \tag{1.190}$$

The formulae for $\Delta_2 L_b$ and $\Delta_3 L_b$ are

$$(\Delta_2 C_\ell)_b = \frac{8}{b^2}\,\frac{1}{\rho_\infty U^2}\,\frac{1}{\lambda_{w_0}}\left(\frac{d}{d\eta}\,\Delta_2 L_b\right) , \tag{1.191}$$

with

$\lambda_{w_0} = 2\,\dfrac{c_{w_0}}{b}$; c_{w_0} = the length of the wing chord at the wing-body juncture ;

$$(\Delta_2 C_\ell)_b = -\frac{4}{\lambda_{w_0}} \sum_m \cos(kr_b\cos\theta)\int_{r_b}^{\xi_w} G_m(\xi')J_0\left[k\sqrt{(\xi_w + r_b\sin\theta - \xi')^2 - r_b^2\sin^2\theta}\right]d\xi \quad ; (1.192)$$

$$\frac{1}{\frac{1}{2}\rho_\infty U^2}\frac{d}{d\xi}\Delta_3 L_b = -\frac{\pi b^2}{2}\left[\frac{\partial(r_b\phi_1^{(b)})}{\partial\xi}\right]_{r=r_b}$$

$$= \frac{\pi b^2}{2}\left[F_1'^{*}(t) + \int_0^t F_1'^{*}(t'')\Omega_1(t - t'')dt''\right] . \qquad (1.193)$$

Another procedure was proposed by Morikawa. His proposal may be described in the following manner. The interference effects are expressed by means of interference potentials $\phi^{(w)}$ and $\phi^{(b)}$. Usually, one attempts to calculate these potentials separately; Morikawa calculates the entire field of flow given by the sum $(\phi_w + \phi^{(w)} + \phi^{(b)})$. Formally, the Laplace transform is used. Let the potential describing the entire flow be denoted by ϕ. Then

$$\phi = \phi_w + \phi^{(w)} + \phi^{(b)} \quad . \qquad (1.194)$$

Assume that this potential satisfies the linearized equation of motion in cylindrical coordinates

$$\frac{\partial^2\phi}{\partial\xi^2} = \frac{\partial^2\phi}{\partial r^2} + \frac{1}{r}\frac{\partial\phi}{\partial r} + \frac{1}{r^2}\frac{\partial^2\phi}{\partial\theta^2} \quad , \qquad (1.195)$$

with the boundary conditions

$$\frac{1}{r}\left(\frac{\partial\phi}{\partial\theta}\right)_{\theta=0} = 1 + \frac{r_b^2}{r^2} \quad , \quad \text{for } x > 0 \text{ and } r \geq r_b \quad ; \qquad (1.196)$$

$$\left(\frac{\partial\phi}{\partial r}\right)_{r=r_b} = 0 \quad ; \qquad (1.197)$$

$$\phi(r,\theta,\theta) = \left(\frac{\partial\phi}{\partial x}\right)_{x\leq 0} = 0 \quad . \qquad (1.198)$$

Applying the Laplace transform to Eq. (1.195) transforms Eq. (1.195) onto the form

$$\nabla^2\bar{\phi} - s^2\bar{\phi} = 0 \quad , \qquad (1.199)$$

with the boundary conditions

$$\frac{1}{r}\left(\frac{\partial \overline{\phi}}{\partial \theta}\right)_{\theta=0} = \frac{1}{s}\left(1 + \frac{r_b^2}{r^2}\right), \quad \text{for } r \geq r_b \ ; \tag{1.200}$$

$$\left(\frac{\partial \overline{\phi}}{\partial r}\right)_{r=r_b} = 0 \ . \tag{1.201}$$

Using the notion of the Green function the solution of Eq. (1.199) is given in the form

$$\overline{\phi}(r,\theta;s) = \frac{1}{2\pi}\oint_C \mathscr{G}\,\frac{\partial\overline{\phi}}{\partial n}\,dc \ , \tag{1.202}$$

where the notation $\partial\overline{\phi}/\partial n$ stands for the directional derivative of $\overline{\phi}$ taken normal to the contour C; the symbol $\mathscr{G}$ denotes the Green function. Morikawa applied this process only to the semi-infinite plane where $z > 0$. In this case he succeeded to find the appropriate Green function in the form

$$\mathscr{G}\,(P;Q) = K_0(s\overline{\rho}) + K_0(s\overline{\rho}_1) - 2\,\frac{\dot{I}_0(s)}{\dot{K}_0(s)}\,K_0(sr)K_0(sr')$$

$$+ 4\sum_{n=1}^{\infty}\frac{\dot{I}_n(s)}{\dot{K}_n(s)}\,K_n(sr)K_n(sr')\cos n\theta\,\cos n\theta' \ , \tag{1.203}$$

where r, θ, and r', θ' are the polar coordinates of two points P and Q lying in the $\{y, z\}$-plane. The other symbols denote

$$\overline{\rho} = \sqrt{r^2 + r'^2 - 2rr'\cos(\theta - \theta')} \ ; \tag{1.204}$$

$$\overline{\rho} = \sqrt{r^2 + r'^2 - 2rr'\cos(\theta + \theta')} \ ; \tag{1.205}$$

$$P = P(r,\theta) \ ; \qquad Q = Q(r',\theta') \ ;$$

I_n and K_n are the modified cylindrical Bessel functions of the first and second kinds, respectively, with imaginary arguments, and of order n; $\dot{I}_n(s) = dI_n/ds$. The potential $\overline{\psi}$ may be given in the form

$$\overline{\phi}(r,\theta;s) = \frac{1}{2\pi s}\int_1^{\infty}\left(1 + \frac{r_b^2}{r'^2}\right)[\mathscr{G}(r,\theta;r',\pi) + \mathscr{G}\,(r,\theta;r'\theta)]dr'$$

$$= \frac{1}{\pi s}\int_1^\infty \left(1 + \frac{r_b}{r'^2}\right)\left\{K_0\left[s\sqrt{r^2 + r'^2 - 2rr'\cos\theta}\right]\right.$$

$$\left. + K_0\left[s\sqrt{r^2 + r'^2 + 2rr'\cos\theta}\right]\right\}dr'$$

$$- \frac{1}{\pi s}\int_1^\infty \left(1 + \frac{r_b^2}{r'^2}\right)\left[\frac{\dot{I}_0(s)}{\dot{K}_0(s)} K_0(sr)K_0(sr')\right.$$

$$\left. + 2\sum_{n=1}^{\infty} \frac{I_{2n}(s)}{K_{2n}(s)} K_{2n}(sr)K(sr')\cos 2n\theta \; dr'\right]. \quad (1.206)$$

The potential ϕ may be obtained upon reversing the transformation process

$$\phi = \alpha^{-1}[\overline{\phi}(r,\theta;s)] \;, \quad (1.207)$$

but this process presents insurmountable difficulty. Hence, Morikawa proposes another approximate form of the Green function

$$\mathscr{G}(r,\theta;r',\theta') = \left[K_0 \; s\sqrt{r^2 + r'^2 - 2rr'\cos(\theta - \theta')}\right] + K_0\left[s\sqrt{r^2 + r'^2 + 2rr'\cos(\theta + \theta')}\right]$$

$$- \frac{K_0(sr')}{I_0(\frac{s}{r'})} \frac{\dot{I}_0(s)}{\dot{K}(s)}\left\{K_0\left[s\sqrt{r^2 + \frac{1}{r'^2} - 2\frac{r}{r'}\cos(\theta - \theta')}\right]\right.$$

$$\left. + K_0\left[s\sqrt{r^2 + \frac{1}{r'^2} - 2\frac{r}{r'}\cos(\theta + \theta')}\right]\right\}. \quad (1.208)$$

With the use of Eq. (1.208) the inversion of the Laplace transform becomes feasible, but the solution is valid only for small values of $(\xi - r_b)$ at which the computations are made.

The above methods were applied to some particular cases with the following results:

(i) The predictions of the theoretical methods are confirmed by the experiments;

(ii) Morikawa's procedure gives fair answers but it can hardly be useful beyond $\xi_w^*/r_b > 1.5$.

In some cases it is possible to apply short-cut methods. Thus, for example, in a first approximation the lift on the wing induced by action of the fuselage is

$$\Delta L_w = \frac{1}{2}\rho_\infty U^2 b \frac{4\alpha_w}{\beta}\int_{r_b}^1 c_w \frac{r_b^2}{\eta^2}\, d\eta \;; \quad (1.209)$$

for a rectangular wing this reduces to

$$\Delta L_w = \frac{1}{2} \rho_\infty U^2 b \frac{4\alpha_w}{\beta} (1 - r_b) \quad . \tag{1.210}$$

The total lift coefficient on the wing may thus be reduced to the form

$$(C_L)_{w,\ total} = \frac{4\alpha_w}{\beta} (1 + r_b) \quad . \tag{1.211}$$

The lift induced on the body by the presence of the wing is equal to

$$\Delta L_b = \rho_\infty U b \int_{r_b}^{1} \Gamma(\eta) \frac{r_b^2}{\eta^2} d\eta_1 \quad , \tag{1.212}$$

where $\Gamma(\eta)$ is the circulation pertaining to the wing section at a spanwise location denoted by η; it may be expressed in the form

$$\Gamma(\eta) = \frac{1}{2} \frac{4\alpha_w}{\beta} c_w U \left(1 + \frac{r_b^2}{\eta^2}\right); \tag{1.213}$$

thus, the expression for the corresponding body lift is given by

$$\Delta L_b = \frac{1}{2} \rho_\infty U^2 \frac{4\alpha_w b}{\beta} \int_{r_b}^{1} c_w \left(1 + \frac{r_b^2}{\eta^2}\right) \frac{r_b^2}{\eta^2} d\eta \quad . \tag{1.214}$$

For a rectangular wing the above formula reduces to

$$\Delta L_b = \frac{1}{2} \rho_\infty U^2 c_w \frac{4\alpha_w}{\beta} r_b \left[1 - r_b + \frac{1}{3} (1 - r_b^3)\right] \quad . \tag{1.215}$$

The corresponding lift coefficient is devised, by referring this amount of lift to a reference area which is taken to be the exposed portion of both wing panels;

$$(\Delta C_L)_b = \frac{4\alpha_w}{\beta} \frac{r_b}{1 - r_b} \left[1 - r_b + \frac{1}{3} (1 - r_b^3)\right]. \tag{1.216}$$

The fractional part of the lift carried on the wing and body may be given in the form

$$\frac{(\Delta C_L)_b}{(C_L)_{w,\ total}} = r_b \frac{1 - r_b + \frac{1}{3} (1 - r_b^3)}{1 - r_b^2} \quad , \tag{1.217}$$

which is valid for a rectangular wing. The general formula for any planform is

$$\frac{(\Delta C_L)_b}{(C_L)_{w,\ total}} = \frac{\int_{r_b}^{1} c_w \left(1 + \frac{r_b^2}{\eta^2}\right) \frac{r_b^2}{\eta^2}\, d\eta}{\int_{r_b}^{1} c_w \left(1 + \frac{r_b^2}{\eta^2}\right) d\eta} . \tag{1.218}$$

Another useful formula for the incremental lift induced on the wing is

$$\begin{aligned}
\Delta L_w &= 2\rho_\infty U^2 b^2 \pi \sum_m h_m \left(\frac{2c_w}{b}\right) \int_{r_b}^{1} \cos k\eta\, d\eta \\
&= -2\rho_\infty U^2 \frac{b^2}{\beta} \sum_m \int_{r_b}^{1} d\eta \int_0^{2c_w/b} G_m(0) \cos\left(\frac{k\xi_1^*}{\sqrt{2}\beta}\right) \cos k\eta\, d\xi_1^* \\
&= -\rho_\infty U^2 \frac{b^2}{\beta} \int_0^{2c_w/b} d\xi_1^* \int_{r_b}^{1} \sum_m G_m(0) \cos k\left(\eta - \frac{\xi_1^*}{\sqrt{2}\beta}\right) d\eta \\
&\quad - \rho_\infty U^2 \frac{b^2}{\beta} \int_0^{2c_w/b} d\xi_1^* \int_{r_b}^{1} \sum_m G_m(0) \cos k\left(\eta + \frac{\xi_1^*}{\sqrt{2}\beta}\right) d\eta .
\end{aligned} \tag{1.219}$$

The expressions for the integrals are

$$\int_{r_b}^{1} \sum_m G_m(0) \cos k\left(\eta - \frac{\xi_1^*}{\sqrt{2}\beta}\right) d\eta = \sim -\alpha_w \int_{r_b}^{1} \frac{r_b^2}{\eta_1^2}\, d\eta_1 . \tag{1.220}$$

After some manipulations the above equation becomes

$$\Delta L_w = 2\rho_\infty U^2 \frac{b}{\beta} c_w \alpha_w r_b (1 - r_b) - \rho_\infty U^2 \frac{b^2}{\beta} \alpha_w \int_0^{2c_w/b} d\xi_1^* \int_{r_b}^{r_b + (\xi_1^*/\sqrt{2}\beta)} \frac{r_b^2}{\eta_1^2}\, d\eta_1 . \tag{1.221}$$

or

$$\Delta L_w = 2\rho_\infty U^2 \frac{b}{\beta} c_w \alpha_w r_b (1 - r_b) \left[1 - \frac{1 - \sqrt{2}\,\beta b \frac{r_b}{c_w} \ln\left(1 + \frac{c_w}{\sqrt{2}\,\beta b r_b}\right)}{2(r - r_b)}\right] . \tag{1.222}$$

The total lift of the wing is equal to

$$(C_L)_w = \frac{4\alpha_w}{\beta} \left(1 + f r_b - \frac{1}{2 AR \beta}\right) , \tag{1.223}$$

where

$$f = 1 - \frac{1 - \sqrt{2}\,\beta b \dfrac{r_b}{c_w} \ln\left(1 + \dfrac{c_w}{\sqrt{2}\,\beta b r_b}\right)}{2(1 - r_b)} \quad . \tag{1.224}$$

A few remarks will be given on configurations having a wing with subsonic leading edge. In particular, two cases are of interest:

(i) a triangular wing supported on a conical body;

(ii) a wing of any shape and sweep mounted on a cylindrical body.

Let us at first discuss a method for a triangular wing mounted on a cone with apexes coincident. Using the polar coordinates $\{\theta, w\}$, defined by

$$\theta = \tan^{-1}(z/y) \text{ and } \omega = \tan^{-1} \frac{\sqrt{\eta^2 + \zeta^2}}{\xi} \quad , \quad \text{for } 0 \leq \omega \leq \frac{\pi}{2} \; , \tag{1.225}$$

one can apply Chaplygin transformation

$$\tan \omega = t = \frac{2s}{1 + s^2} \quad ; \quad \text{for } 0 \leq s \leq 1 \quad ; \tag{1.226}$$

to transform the rays in the conical field of flow into points in the complex plane

$$\hat{\epsilon} = s \exp(i\theta) \quad ; \quad \hat{\epsilon} = \hat{\epsilon}_x + i\,\hat{\epsilon}_y \quad . \tag{1.227}$$

Using this transformation one can find the function describing the flow about an isolated extended wing which is located in the stream of a fluid at an angle of attack of γ radians. It is

$$f^{(w)} = \frac{\gamma t_1}{E(\sqrt{1 - t_1})} \frac{1}{\sqrt{1 - (\frac{\hat{\eta}}{t_1})^2}} \quad , \tag{1.228}$$

where:

E = complete elliptic integral of the second kind;

t_1 = the semispan of the wing;

the coordinates $\hat{\epsilon}$ and $\hat{\eta}$ are related by means of the equations

$$\frac{1}{\hat{\eta}} = \frac{1}{2}\left(\hat{\epsilon} + \frac{1}{\hat{\epsilon}}\right) \quad ; \quad \hat{\eta} = r \exp(i\sigma) = \hat{\eta}_x + i\hat{\eta} y \quad . \tag{1.229}$$

After all the manipulations the u component of velocity may be determined from the formulae:

on the wing,

$$u = \frac{\alpha_w t_1}{\Lambda E} \frac{1}{\sqrt{1 - \frac{t^2}{t_1^2}}} \left[1 - \frac{3}{2} \left(\frac{t_0}{t_1}\right)^4 \left(\frac{t_1^2}{t^2} - 1\right) - \frac{5}{16} \left(\frac{t_0}{t_1}\right)^8 \left(2 \frac{t_1^4}{t^4} - 3 \frac{t_1^2}{t^2} + 1\right) \right.$$

$$\left. - \frac{7}{256} \left(\frac{t_0}{t_1}\right)^{12} \left(16 \frac{t_1^6}{t^6} - 32 \frac{t_1^4}{t^4} + 19 \frac{t_1^2}{t^3} - 3\right) \right], \qquad (1.230)$$

with

$$\Lambda = 1 - (\tfrac{3}{2})(\frac{t_0}{t_1})^4 \frac{t_1}{E} I_2 - \frac{5}{16} (\frac{t_0}{t_1})^8 \frac{t_1}{E} I_4 - \dots ; \qquad (1.231)$$

$$I_2 = - \frac{t_1}{3} K - \frac{1 - 2t_1^2}{3t_1} E ; \qquad (1.232)$$

$$I_4 = \frac{16 t_1^3 - 16 t_1^2 + 1}{15 t_1} E + \frac{7 - 8 t_1^2}{15} K ; \qquad (1.233)$$

$$I_6 = \frac{- 256 t_1^6 + 384 t_1^4 - 134 t_1^2 + 3}{105 t_1} E + \frac{128 t_1^4 - 176 t_1^2 + 51}{105} t_1 K ; \qquad (1.234)$$

E = complete elliptic integral of the second kind and of the modulus $\sqrt{1 - t_1^2}$;

K = complete elliptic integral of the second kind and of the modulus $\sqrt{1 - t_1^2}$;

t_1 = the semispan of the wing;

$t_0 = \tan \omega_0$;

ω_0 = the semivertex angle of the conical body.

On the body one has

$$u = - \frac{\alpha_w t_1}{\Lambda E} \left[1 - (\frac{t_0}{t_1}) \cos 2\theta + \frac{1}{4} (\frac{t_0}{t_1})^4 (3 - \cos 4\theta) + (\frac{t_0}{t_1})^6 (\frac{13}{16}) \cos 2\theta - \frac{1}{8} \cos 6\theta \right]. \qquad (1.235)$$

The lift curve for the complete wing-body combination has the form

$$\frac{d(C_L)_{wb}}{d\alpha_w} = \frac{2\pi t_1}{\beta}\frac{1}{E}\frac{1 - \frac{8}{3\pi}\left(\frac{t_0}{t_1}\right)^3 + \frac{3}{2}\left(\frac{t_0}{t_1}\right)^4 - \frac{8}{15\pi}\left(\frac{t_0}{t_1}\right)^5 + \ldots}{\Lambda} \quad . \qquad (1.236)$$

As the last problem, consider a configuration composed of a cylindrical body and a wing of any shape of the leading edge. The complete interference potential is chosen in the form

$$\phi_i = \phi_I^{(w)} + \phi_{II}^{(w)} + \phi_{III}^{(w)} + \phi_I^{(b)} + \phi_{II}^{(b)} \quad . \qquad (1.237)$$

The following conditions should be satisfied:

$$\Delta\phi_I^{(b)} = \left(\phi_I^{(b)}\right)_{\zeta=0^+} - \left(\phi_I^{(b)}\right)_{\zeta=0^-} = 2\left(\phi_I^{(b)}\right)_{\zeta=0^+} \quad , \qquad (1.238)$$

where

$\Delta\phi_I^{(b)}$ = denotes the potential jump on the body.

The jump is defined by the function

$$\Delta\phi_I^{(b)} = -\ 2Q(\alpha,\beta) \quad , \qquad (1.239)$$

where $Q(\alpha,\beta)$ is a known function of the α,β location parameters. The potential $\phi_I^{(w)}$ which governs the perturbation flow about the wing should be found by one of the methods given above. The further conditions are

$$\left(\frac{\partial\phi_{II}^{(w)}}{\partial\zeta}\right)_{\zeta=0} = -\ 2\pi g(\alpha,\beta) \quad , \qquad (1.240)$$

1.6 Flight Investigation of a Tailless Triangular-Wing Airplane

Below, we shall briefly describe for illustrative purposes the results of flight investigation to determine the aerodynamic characteristics of models of a tailless triangular-wing airplane configuration following the report by Mitcham, Stevens, and Norris. The results refer to three successful flight tests for the Mach number range between 0.75 and 1.28.

The data showed that the models tended to tuck under slightly through the transonic region. The variation of lift coefficient with angle of attack was linear within the range of angles tested and the lift-curve slope increased gradually between Mach numbers of 0.88 and 1.00.

The hinge-moment coefficients increased rapidly between Mach numbers of 0.85 and 1.15 but showed a gradual decrease above a Mach number of 1.20. Elevator effectiveness decreased approximately 40 percent through the transonic region.

The models exhibited static and dynamic longitudinal stability throughout the test Mach number range with the center of gravity located at 20 and 25 percent mean aerodynamic chord. The aerodynamic center showed a gradual rearward movement of about 15 percent mean aerodynamic chord in the transonic region. All the models possessed directional stability throughout the angle-of-attack and speed ranges of the flight tests.

An analysis of the flying qualities of a full-scale configuration has been made from the data obtained from the three flight-test models. The analysis indicates adequate elevator control for trim in level flight over the speed range investigated. Through the transonic range there is a mild trim change with a slight tucking-under tendency. The elevator-control effectiveness in the supersonic range is reduced to about one-half the subsonic value, although sufficient control for maneuvering is available as indicated by the fact that 10° elevator deflection would produce 5g normal acceleration at a Mach number of 1.2, at an altitude of 40,000 feet. The elevator control forces are high and indicate the need of a control-boost system as well as the power required of such a system. The damping of the short-period oscillation is adequate at sea level and at 40,000 feet.

At first, we shall collect the symbols to be used in the text:

A = amplitude of a short-period oscillation,

a = velocity of sound, ft./sec.,

a_{ℓ} = longitudinal accelerometer reading, ft./sec.^{2},

a_n = normal accelerometer reading, ft./sec.^{2},

a_t = transverse accelerometer reading, ft./sec.^{2},

$C_{1/2}$ = cycles for short-period oscillation to damp to one-half amplitude,

C_c = chord-force coefficient, positive in a forward direction, $\frac{a_{\ell}}{g}\,\frac{W}{S}\,\frac{1}{q}$,

C_h = total hinge-moment coefficient,

$C_{h_{\alpha}}$ = rate of change of hinge-moment coefficient with angle-of-attack, per deg.,

$C_{h_{\delta}}$ = rate of change of hinge-moment coefficient with elevator deflection, per deg.,

C_{h_0} = basic hinge-moment coefficient at zero angle-of-attack and zero elevator deflection,

C_L = lift coefficient, $C_N \cos\alpha + C_c \sin\alpha$,

C_{L_α} = rate of change of lift coefficient with angle-of-attack, per deg.,

C_{L_δ} = rate of change of lift coefficient with elevator deflection for a constant angle-of-attack, per deg.,

$C_{L_{trim}}$ = trim lift coefficient,

$C_{L_{\delta_{trim}}}$ = rate of change of total lift coefficient between two trim conditions or elevator deflections, per deg.,

C_m = pitching moment coefficient,

C_{m_0} = basic untrimmed pitching-moment coefficient at zero angle-of-attack and zero elevator deflection,

$C_{m_{\delta\ \alpha=K}}$ = rate of change of pitching-moment coefficient with elevator deflection for constant angle-of-attack, per deg.,

C_{m_α} = rate of change of pitching-moment coefficient with angle-of-attack, per deg.,

$C_{m_{\frac{\dot{\alpha}\bar{c}}{2V}}}$ = $\dfrac{\partial C_m}{\partial(\dot{\alpha}\bar{c}/2V)}$, per radian,

C_{m_θ} = rate of change of pitching-moment coefficient with pitch angle,

$C_{m_{\frac{\dot{\theta}\bar{c}}{2V}}}$ = $\dfrac{\partial C_m}{\partial(\dot{\theta}\bar{c}/2V)}$, per radian,

C_N = normal-force coefficient, $\frac{a_n}{g} \frac{W}{S} \frac{1}{q}$,

$\bar{c}$ = mean aerodynamic chord, 2.19 ft.,

d = distance between center of pressure of angle-of-attack vane and center-of-gravity of model, ft.,

$\frac{d\delta}{d\alpha}$ = rate of change of elevator deflection with angle-of-attack (due to flexibility of control system),

$\frac{dC_m}{dc_L}$ = rate of change of pitching-moment coefficient with lift coefficient,

F	= stick force, lb.,
g	= acceleration due to gravity, 32.2 ft./sec.^{2},
H	= hinge-moment, in.-lb.; total impact pressure (Eqs. 1.232) and (1.233) lb./sq.fft.,
I_Y	= moment of inertia about pitch axis, slug-ft.^{2},
K	= constant,
M	= Mach number,
m	= mass of model, lb.-sec.^{2}/ft.,
P	= period of an oscillation, sec.,
p	= free-stream static pressure, lb./sq. ft.,
q	= dynamic pressure, $\frac{\gamma p M^2}{2}$, lb./sq. ft.,
R	= Reynolds number, $\frac{\rho V \bar{c}}{\mu}$,
S	= wing area, 6.25 sq. ft.,
$T_{1/2}$	= time to damp to one-half amplitude, sec.,
t	= time from launching, sec.,
V	= velocity, ft./sec.,
W	= weight of model, lb.,
x	= stick movement, in.,
α	= angle-of-attack corrected for flight-path curvature and angular velocity, deg.,
α_i	= angle-of-attack as measured during flight, deg.,
α_{trim}	= trim angle-of-attack, deg.,
$\frac{\dot{\alpha}\bar{c}}{2V}$	= nondimensional rate of change of angle-of-attack,
$(\frac{\Delta\alpha}{\Delta\delta})_{trim}$	= rate of change of angle-of-attack with elevator deflection between two trim conditions,
δ	= control deflection measured on chord line parallel to the plane of symmetry (positive with trailing edge down), deg.,

δ_{trim} = trim elevator deflection, deg.,

γ = specific-heat ratio (value taken as 1.40),

θ = pitch angle, deg.,

$\frac{\dot{\theta}\bar{c}}{2V}$ = nondimensional angular velocity of pitch,

μ = viscosity, slug/ft.-sec.,

ρ = mass density of air, slugs/cu. ft.

Subscripts:

1, 2 = conditions brought about by change in elevator deflection,

a = full-scale airplane,

m = model.

Dots over a quantity represent derivatives of the quantity with respect to time.

The models had a wing of triangular planform with 60° sweepback of the leading edge and an aspect ratio of 2.31, the profile at all spanwise stations being an NACA $65_{(06)}$-006.5 section. Longitudinal control was provided by a single set of constant-chord trailing-edge control surfaces on the wing called elevons. Deflecting the elevons together provides longitudinal controls and, in the assumed airplane, deflecting them differentially would give lateral control. The vertical fin of the models was of triangular planform with a leading-edge sweepback of 60°.

The model fuselage and components were constructed of duralumin, magnesium castings, and magnesium skin. The fuselage construction was of the monocoque type divided into three sections. The three sections were the nose section which held the telemeters, the center section which held the wings, vertical fin, compressed-air supply, and control-actuating system, and the tail section which contained the rocket motor and booster attachment.

The planned movement of the elevons called for abrupt pull-ups and push-downs operating at a frequency of about 1 cycle in 1.2 seconds and was accomplished by a compressed-air system. The controls surfaces, which were unsealed, moved together between stops in an approximately square-wave motion. On model 1 the surfaces were deflected down 5.3° and up 5.3°; on model 2 the deflection was down 4.7° and up 4.7°; and on model 3 the deflection was down 1.1° and up 5.2°. The controls were in operation during the entire flight.

The models were boosted to supersonic speeds by a solid-fuel, 6-inch-diameter Deacon rocket motor which is capable of producing an average thrust of 6,500 pounds for approximately

3.1 seconds. The rocket-sustainer motor for the model was a 5-inch solid-fuel high velocity aircraft rocket shortened to 17 inches and modified to give an average thrust of 900 pounds for 1.4 seconds. The small sustainer motor served a two-fold purpose: (1) during the power-on portion of the flight it prevented immediate deceleration after separation and allowed the controls to operate one complete cycle at approximately a constant Mach number, and (2) it assured a positive separation between model and booster at booster burnout. The sustain-motor nozzle served as the point of attachment of the booster to the model. This type of attachment also allowed a separation of the booster from the model if the ratio of drag to weight of the model and booster were favorable.

The booster-model combination was ground launched from a crutch-type launcher. The launching angle from the horizontal for model 1 was 43°40', for model 2 was 44°40', and for model 3 was 43°23'.

The data from the flights were obtained by the use of telemeters, CW Doppler velocimeter radar, photography, and radiosondes. The time histories of the data as the models traversed the Mach number range were transmitted and recorded by a telemeter system which gave eight channels of information. The data recorded were longitudinal, transverse, and normal acceleration; hinge moment; control position; angle of attack; total pressure; and a reference static pressure used to determine free-stream static pressure. Angles of attack were obtained by a vane-type angle-of-attack indicator located on a sting ahead of the nose of the model. The angle-of-attack range covered by the indicator with the vane located on the center line of the model was approximately ± 15°. On model 3 the angle-of-attack sting was deflected down 10° from the center line of the model in order to record higher positive values of angle-of-attack. Fixed wide-angle cameras and 16-millimeter motion picture cameras recorded the launchings. The motion picture cameras also tracked the flights.

The models were disturbed in pitch by the abrupt movement of elevons operated as elevators at preset time intervals which gave an approximately square-wave type of elevator motion. The desired aerodynamic coefficients and longitudinal-stability derivatives were obtained by analysis of the hinge moments, angle-of-attack, and acceleration responses resulting from these cyclic disturbances.

The aerodynamic coefficients, stability derivatives, and flying qualities presented in this paper were reduced from the model flight data. The results of the analysis are discussed below:

Lift. The lift data are presented in the form of lift-curve slope C_{L_α} for various Mach numbers as obtained from two models of the same configuration but having different center-of-gravity locations and different weights. The range of angle-of-attack in which data were considered for determining C_{L_α} was $\pm 15^\circ$. The lift coefficient varied linearly with angle-of-attack in this range. C_{L_α} increased approximately 25 percent from the lowest test Mach number (M = 0.88) to a Mach number of 1.00 and then decreased approximately 15 percent from M = 1.00 to M = 1.20. The increase in curve-lift slope in going through the transonic region was evident for both models.

Trim lift coefficient. Different elevator settings for models 2 and 3 confirmed the assumption that $C_{L_{trim}}$ varied linearly with elevator deflection. The plots show an inherent characteristic of the model configuration to trim at negative lift coefficients between Mach numbers of 0.90 and 1.08. This was due to a basic untrimmed pitching-moment coefficient C_{m_0} for the airplane at zero angle-of-attack and zero elevator deflection. The symmetry of the model configuration due to the vertical tail and the upswept rear of the body would indicate an expected positive C_{m_0} which was not in accord with test results.

Change of trim lift coefficient with respect to elevator deflection. As would be expected, the values of $C_{L_{\delta_{trim}}}$ for model 1 with the center of gravity at 25 percent mean aerodynamic chord were larger than those of models 2 and 3 with the center of gravity at 20 percent mean aerodynamic chord. Within the Mach number range covered by the tests, $C_{L_{\delta_{trim}}}$ remained fairly constant up to M = 0.86 at which point an abrupt reduction from 0.049 to 0.029 occurred between M = 0.86 and M = 1.00. A further decrease from 0.029 to 0.015 occurred in $C_{L_{\delta_{trim}}}$ between M = 1.00 and M = 1.28.

Hinge-moment coefficients. Calculations were made to determine the effect of elevon inertia on the hinge-moment coefficients. An extreme case showed the magnitude of the error to be negligible. Therefore, no such correction was applied to the data. Corrections were applied to eliminate the effect of phase lag between the hinge-moment coefficient and angle-of-attack curves and the effect of oscillations in elevon deflection due to angle-of-attack changes. Hinge-moment coefficients plotted as functions of angle-of-attack at a constant Mach number indicated that the variation was linear in the range covered by the tests ($\alpha = \pm 15^\circ$).

The tests show that C_{h_α} increases from - 0.008 at M = 0.85 to - 0.024 at M = 1.20. A corresponding increase from -0.015 to -0.037 is shown for C_{h_δ} between M = 0.85 and M = 1.05. Both curves indicate a gradual decrease in the low supersonic region.

The value of the basic hinge-moment coefficient at zero angle-of-attack and elevator deflection C_{h_0} is given as a function of Mach number. The basic hinge-moment coefficient C_{h_0} shows a reversal from positive to negative values at M = 0.95 and a tendency in the low supersonic region to return to positive values. The variation of hinge-moment coefficient with elevator deflection was assumed to be linear in the solution of C_{h_0}.

Control effectiveness. A characteristic of the elevator used on the models can be seen in the plot of change in lift coefficient per degree of elevator deflection C_{L_δ} as a function of Mach number. The parameter C_{L_δ} reaches a value of 0.022 at a Mach number of 0.96 and decreases to a value of 0.010 at M = 1.17, a reduction of about 55 percent through this speed range. Values of C_{L_δ} show good agreement with the flight-test values obtained in the high subsonic and low supersonic regions.

Two parameters of longitudinal control effectiveness for this configuration, change in trim angle-of-attack per degree of elevator deflection $(\frac{\Delta\alpha}{\Delta\delta})_{trim}$, and change in pitching-moment coefficient per degree of elevator deflection C_{m_δ}, are both given as functions of Mach number. The plots indicate an abrupt decrease in control effectiveness of the elevon between M = 0.90 and M = 1.00. This reduction is of the order of 25 percent for C_{m_δ} and 35 percent for $(\frac{\Delta\alpha}{\Delta\delta})_{trim}$. Above a Mach number of 1.00 the curves indicate a further gradual decrease in longitudinal control effectiveness to M = 1.28, the highest Mach number reached by the flight tests (-0.015 at M = 0.9 and -0.009 at M = 1.28). Values of C_{m_δ} were determined for the angle-of-attack range between 10° and -8°.

The effect of center-of-gravity location is apparent in plots by the relative displacement of results obtained from model 1 with the center-of-gravity at 25 percent mean aerodynamic chord and from models 2 and 3 with the center-of-gravity at 20 percent mean aerodynamic chord. The more rearward location of the center-of-gravity reduced the value of C_{m_δ} and increased the magnitude of $(\frac{\Delta\alpha}{\Delta\delta})_{trim}$.

Longitudinal stability. When the controls are moved up and down in a square-wave type of motion, corresponding changes are produced in angle-of-attack and normal acceleration. The stability of the configuration is indicated by the period and the rate of decay of the short-period longitudinal oscillation when the controls are held fixed between pulses.

The values of the period of the short-period oscillation induced by this abrupt control movement as determined from the time-history records show the variation of the period with Mach number for the models. The period decreased, a stability increase being indicated, from a Mach number of 0.75, the lower test limit, to approximately $M = 0.95$. Above this speed the period continued to decrease but at a much more gradual rate up to $M = 1.28$, the upper limit of the speed range covered by the flight tests. The period for model 1 was greater than that for models 2 and 3 throughout its test range as would be expected since the center-of-gravity of model 1 was 5 percent of the mean aerodynamic chord behind the center-of-gravity location for models 2 and 3.

The static-longitudinal-stability parameter in the form of the change in pitching-moment coefficient with respect to a change in angle-of-attack C_{m_α} is given as a function of Mach number for C_L values between ± 0.30. The determination of C_{m_α} involved the use of the period of the short-period oscillations as a primary factor. The value of C_{m_α} increased from a minimum of -0.0095 at $M = 0.85$ to a maximum of -0.0162 at $M = 1.15$ for models 2 and 3 with the center-of-gravity at 20 percent mean aerodynamic chord. An investigation of the change in C_{m_α} due to a 5-percent change in center-of-gravity location shows that C_{m_α} for model 1 is lower than would be expected from a comparison with models 2 and 3. Data concerning the evaluation of C_{m_α} were carefully rechecked and there were indications that the seemingly low values of C_{m_α} were due to accumulative errors within the accuracy of determining the physical characteristics used to calculate this parameter.

A plot of aerodynamic-center position against Mach number, also indicates the variation of the static longitudinal stability. The aerodynamic center moved very gradually from a minimum of 42 percent of the mean aerodynamic chord at a Mach number of 0.80 to a maximum of 54 percent of the mean aerodynamic chord at a Mach number of 1.15. The aerodynamic-center positions for model 1, however, were 2-1/2 percent of the mean aerodynamic chord ahead of models 2 and 3. The more forward aerodynamic-center locations for model 1 were a result of the low values of C_{m_α} obtained for this model. This difference, however, is within the accuracy of aerodynamic-center location usually obtained from flight and wind-tunnel data.

The three parameters discussed in the preceding paragraphs (period, C_{m_α}, and aerodynamic-center position) show that the static longitudinal stability of this configuration increased through the transonic region from a minimum value at about $M = 0.82$ to a maximum value at $M = 1.15$.

A qualitative evaluation of the dynamic stability may be made by inspection of the damping of the short-period oscillation induced by the abrupt control movement. Damping is represented by the parameter $T_{1/2}$, the time required to damp to one-half amplitude; it varies with Mach number. Since the flight-test models were not dynamic-scale models, the results are applicable to the full-scale airplane only after corrections are applied. Models 2 and 3 with the center of gravity at 20 percent mean aerodynamic chord showed more rapid damping characteristics than model 1 with its center of gravity at 25 percent mean aerodynamic chord.

The total damping factor $C_{m_{\frac{\dot{\theta}\bar{c}}{2V}}} + C_{m_{\frac{\dot{\alpha}\bar{c}}{2V}}}$, which is a measure of the dynamic stability of the configuration expressed nondimensionally, is given as a function of Mach number. Model 1 with the more rearward center-of-gravity location indicated less tendency to damp throughout the flight-test speed range than did models 2 and 3.

It will be noted that there is considerable scatter in the damping data. This type of scatter may also be expected for full-scale airplane conditions inasmuch as the present data were obtained in free flight and all the aerodynamic factors that affect damping were properly integrated into the motion of the models.

Directional stability. Only models 1 and 2 were instrumented to obtain transverse accelerations. Model 2 apparently had some directional asymmetry that caused it to develop a small positive side force throughout the flight. This effect approximately doubled at Mach numbers below 0.90. Model 1 did not exhibit any such consistent side-force variation; its side forces resulting from an occasional disturbance. Neither model showed divergence nor continuous oscillations; thus, positive directional stability was indicated.

Longitudinal trim characteristics. The longitudinal trim characteristics of the configuration are as follows:

Trim angle of attack: The angle of attack for trimmed level flight required for this configuration is given as a function of Mach number. Curves give center-of-gravity locations at 20 and 25 percent of the mean aerodynamic chord for both sea-level flight and flight at an altitude of 40,000 feet. The trim angle of attack shows a consistent small decrease with increasing speed except in the region between $M = 0.90$ and 0.95.

Control position for trim: The characteristics of the elevator control in level flight are given in the form of the variation of the elevator position required for trim with Mach number. Control-position trim change is manifested between a Mach number of 0.87 and 0.95 at sea level and 40,000 feet. The control-position trim change is a function of variation of out-of-trim pitching moment with Mach number, change in control effectiveness, and movement of the neutral point. The resultant change in trim, a tucking-under tendency, appears to be of moderate magnitude.

For example, at 40,000 feet a maximum up-elevator angle of about 5° is required for trim at a Mach number of 0.95.

An evaluation of the stick-fixed maneuver point in the Mach number range between 0.80 and 1.20 indicated that the point is well behind the most rearward center-of-gravity position and the requirements for maneuvering stability are met.

Longitudinal control forces: The stick forces are based on a conventional airplane configuration with 2° of elevator deflection for 1 inch of stick movement. The data indicate the power required of a control-boost system with no balancing and trimming devices. For example, with the center-of-gravity at 25 percent mean aerodynamic chord at a Mach number of 1.20 the stick force per g based on measured hinge-moments is about 900 pounds per g.

The variation of elevator control force for trim with Mach number indicate that pull forces were required at all speeds below the trim speed and push forces were required at all speeds above the trim speed within the range of Mach numbers from 0.95 to 1.20. The opposite is true for Mach numbers from 0.80 to 0.95, but the elevator angle for trim in this range of Mach number increases with increasing Mach number. Thus, the stick force would be in the correct sense with respect to stick movement throughout the transonic region.

The elevator hinge-moment data obtained for model 1 indicate a force reversal at high angles-of-attack ($\alpha \geq 15^{\circ}$) at Mach numbers below 0.90. Model 2, which flew at angles-of-attack of about 7° at $M = 0.90$, did not show a hinge-moment reversal but did indicate hinge-moments near zero.

Longitudinal control effectiveness. At sea level a large variation in elevator effectiveness was apparent from subsonic to low supersonic speeds with minimum effectiveness occurring at a Mach number of 1.06 for model 1 with the center-of-gravity location at 25 percent mean aerodynamic chord and at a Mach number of 0.98 for models 2 and 3 with the center-of-gravity location at 20 percent mean aerodynamic chord. Sufficient control for maneuvering is available as indicated by the fact that 10° elevator deflection will produce 5g acceleration at a Mach number of 1.20 at 40,000 feet with the center-of-gravity located at 25 percent mean aerodynamic chord.

Dynamic stability. Military specifications for stability-and-control characteristics of airplanes require that the short-period dynamic oscillation of normal acceleration produced by moving and quickly releasing the elevator shall be damped to 1/2 amplitude in one cycle (based on free controls). The damping characteristics for the full-scale configuration have been evaluated for the control-fixed condition although there is a slight oscillation in the control position due to hinge-moment effect. The fixed-control characteristics would probably dictate the behavior of this airplane since it would require some kind of control-boost system to aid the pilot in overcoming the extremely large stick forces encountered in maneuvering.

As can be deduced from tests, $T_{1/2a}$ decreases through the transonic region and reaches a relatively constant value at about M = 1.20. Both the time to damp to half amplitude and period indicate increasing stability for the configuration with increasing Mach number in the transonic and low supersonic speed range.

From the results of a flight investigation made to evaluate the aerodynamic characteristics and flying qualities of models of a tailless triangular-wing airplane configuration, the following general conclusions are indicated for the Mach number range between 0.75 and 1.28:

Aerodynamic Characteristics

1. The lift coefficients varied linearly in the angle-of-attack test range of $\pm 15^{\circ}$. The lift-curve slope C_{L_α} varied from 0.045 at a Mach number M of 0.88 to a maximum of 0.055 at a Mach number of 1.0 and then decreased to 0.0475 at a Mach number of 1.20.

2. The hinge-moment coefficient per degree of angle-of-attack increased 200 percent between M = 0.85 and M = 1.20; whereas the hinge-moment coefficient per degree of elevator showed a corresponding rise of 150 percent between M = 0.85 and M = 1.05. Both of these values showed a gradual decrease in the low supersonic region.

3. The elevator effectiveness decreased by approximately 40 percent from a Mach number of 0.9 to 1.25. For example, with the center-of-gravity at 20 percent mean aerodynamic chord, the rate of change of pitching-moment coefficient with elevator deflection C_{m_δ} at a Mach number of 0.9 was -0.015 and at a Mach number of 1.25 was -0.009.

4. The configuration tested possessed static longitudinal stability throughout the Mach number range covered by these flight tests. The value of C_{m_α} (rate of change of pitching-moment coefficient with angle-of-attack) increased from a minimum at M = 0.80 to a maximum at M = 1.15 with the center-of-gravity at 20 percent mean aerodynamic chord.

5. The aerodynamic center moved very gradually from a minimum of 42 percent of the mean aerodynamic chord at a Mach number of 0.80 to a maximum of 54 percent of the mean aerodynamic chord at a Mach number of 1.15.

6. The damping parameters and coefficients indicated that the configuration possessed dynamic longitudinal stability throughout the test speed range.

7. The models exhibited directional stability throughout the angle-of-attack and speed ranges of the tests.

Flying Qualities

1. There is ample control for trim in level flight at sea level or at altitude. At 40,000 feet a maximum up-elevator angle of about 5° is required for trim at a Mach number of 0.96. The transonic trim change, a tucking-under tendency, appears to be mild.

2. The elevator control remains effective in changing lift or angle-of-attack over the entire speed range. The effectiveness of the elevator in changing angle-of-attack, however, is reduced to about half of its subsonic value at supersonic speeds. This change of effectiveness occurs gradually.

3. With the center-of-gravity at 25 percent mean aerodynamic chord the normal acceleration produced per degree elevator deflection is such that about 10° up-elevator deflection is required to produce a 5g acceleration at 40,000 feet at a Mach number of 1.2. The corresponding stick force per g based on the measured hinge-moments is about 900 pounds per g, a figure which gives an indication of the power required of a control-boost system.

4. According to military requirements, the damping of the short-period longitudinal oscillation is adequate over the speed range for both sea-level conditions and at an altitude of 40,000 feet.

Below, we shall reproduce the equations which were used in the reduction of data.

Mach number. The total pressures obtained from the telemeter records were reduced to Mach number by use of the following equations:

Subsonic:

$$\frac{H}{p} = \left(1 + \frac{\gamma - 1}{2} M^2\right)^{\frac{\gamma}{\gamma - 1}}, \qquad (1.241)$$

Supersonic:

$$\frac{H}{p} = \frac{\left(\frac{\gamma + 1}{2} M^2\right)^{\frac{\gamma}{\gamma - 1}}}{\left(\frac{2\gamma}{\gamma + 1} M^2 - \frac{\gamma - 1}{\gamma + 1}\right)^{\frac{1}{\gamma - 1}}}, \qquad (1.242)$$

where p, free-stream static pressure, was obtained from the reference static-pressure record in conjunction with radiosonde data. Models 1 and 3 reached a maximum altitude of 4,000 feet while model 2 attained a maximum of 4,700 feet. The Doppler velocimeter radar unit served as an independent check of the Mach number obtained by reduction of the total and reference static pressures.

Angle-of-attack. Since angle-of-attack data were measured at a point some distance ahead of the center-of-gravity location, it was necessary to correct these data for flight-path curvature and angular velocity as described in reference 1. The following equation was used:

$$\alpha = \alpha_i + \frac{d}{V}\left(1{,}844\,\frac{a_n}{g}\,\frac{1}{V} + \frac{d\alpha_i}{dt}\right) . \tag{1.243}$$

Control position. Prior to the flight test of each model a static hinge-moment calibration of the control system was conducted to determine the amount of twist that would be encountered in the elevons and control linkage under aerodynamic loads. The elevons were loaded at two spanwise stations and readings were taken at five points to measure the amount of twist or deflection induced. Control-position data recorded during flight were corrected by the calibration obtained from the static test.

The methods of analysis used herein apply to the free oscillation resulting from a step function disturbance. The disturbance was created by an approximately square-wave type of motion of the elevators moved abruptly between limit stops. The complete derivation of the equations used will not be given herein but the basic equations of motion are as follows:

$$Vm(\dot{\theta} - \dot{\alpha}) = \left(C_{L_\alpha}\,\alpha + C_{L_\delta}\,\delta\right)57.3qS \ , \tag{1.244}$$

$$I_Y\ddot{\theta} = \left(C_{m_\alpha}\,\alpha + C_{m_{\dot{\alpha}}}\,\dot{\alpha} + C_{m_{\dot{\theta}}}\,\dot{\theta} + C_{m_\delta}\,\delta\right)57.3qS\bar{c} \ . \tag{1.245}$$

In order to simplify the analysis and to permit the determination of equations for the more important aerodynamic derivatives, a number of assumptions are necessary. It is assumed that, during the time interval over which each calculation is made, the forward velocity is constant and the aerodynamic forces and moments vary linearly with the variables α, δ, and θ.

Lift-curve slope. Several methods were tried for determining the lift-curve slope with respect to angle-of-attack. The most expeditious method found was to measure the instantaneous slopes $\frac{dC_L}{dt}$ and $\frac{d\alpha}{dt}$ at a given Mach number. Care was exercised in using only the portions of the lift coefficient and angle-of-attack time-history curves where the slopes could be accurately ascertained. The effect of lift due to the flexibility of the elevator was eliminated by correcting $\frac{dC_L}{dt}$ for the lift due to the deviation of the elevator deflection from a fixed value at an instantaneous time. The following relation exists:

$$C_{L_\alpha} = \frac{\Delta C_{L_{2-1}} - C_{L_\delta} \Delta\delta_{2-1}}{\Delta\alpha_{2-1}} , \qquad (1.246)$$

where $\Delta C_{L_{2-1}}$ is the change in C_L between C_{L_2} and C_{L_1} taken over a relatively straight portion of the lift time history, and $\Delta\delta_{2-1}$ and $\Delta\alpha_{2-1}$ are incremental changes in δ and α over the same time interval. The value of C_{L_δ} used in this equation was a first approximation. Successive approximations and evaluations were unnecessary.

After the corrected value of C_{L_α} was determined, it was then possible to determine an exact value for C_{L_δ}, the lift-curve slope due to the elevons, from the portions of the time histories where the controls were moving from one extreme position to the other. The following relation exists:

$$C_{L_\delta} = \frac{\left(\Delta C_{L_{2-1}}\right)_{trim} - C_{L_\alpha}\left(\Delta\alpha_{2-1}\right)_{trim}}{\left(\Delta\delta_{2-1}\right)_{trim}} . \qquad (1.247)$$

The variation of trim lift coefficient with respect to elevator deflection $C_{L_{\delta_{trim}}}$ was found by the same method used to find C_{L_δ}. The equation is

$$C_{L_{\delta_{trim}}} = \frac{\left(\Delta C_{L_{2-1}}\right)_{trim}}{\left(\Delta\delta_{2-1}\right)_{trim}} . \qquad (1.248)$$

Pitching-moments. The basic untrimmed pitching-moment coefficient C_{m_0} was calculated from the conventional moment-coefficient equation solved for C_{m_0} as follows:

$$C_{m_0} = - C_{m_\alpha}\alpha_{trim} - \left(C_{m_\delta}\right)_{\alpha=K}\delta_{trim} . \qquad (1.249)$$

The derivatives C_{m_α} and C_{m_δ} were considered linear in the range of the tests. The second term was eliminated by taking values of $C_{L_{trim}}$ for an elevator deflection of 0° and dividing the first term by C_{L_α} to make C_{m_0} a function of the trim lift coefficient, or

$$C_{m_0} = - C_{m_\alpha}\alpha_{trim_{\delta=0}} , \qquad (1.250)$$

and

$$C_{m_0} = - \frac{C_{m_\alpha}}{C_{L_\alpha}}\left(C_{L_{trim}}\right)_{\delta=0} , \qquad (1.251)$$

The values of C_{m_α} were obtained as described in the section on longitudinal stability.

Hinge-moments. Hinge-moment data were reduced to coefficient form and plotted directly against angle-of-attack for both up and down elevator deflection to obtain an approximate value of C_{h_δ}. This value was used in conjunction with the change in δ due to changes in α to correct the values of the total hinge-moment for constant elevator deflection as follows:

$$(C_h)_{\delta=K} = C_h + \Delta\delta C_{h_\delta} \quad . \tag{1.252}$$

A method was derived to eliminate the effect of phase lag between the two variables. Constant values of C_h were chosen on each side of an oscillation peak and a mean value of α corresponding to the constant value of C_h was determined analytically and graphically. Finally, the corrected values of C_h and α were plotted for up and down elevator to determine C_{h_α} and C_{h_δ}. There were indications that these values were linear and C_{h_0}, the hinge-moment coefficient at zero angle-of-attack and elevator, was determined by direct interpolation.

Control effectiveness. The variation of trim angle-of-attack with elevator deflection $(\Delta\alpha/\Delta\delta)_{trim}$ was found by using the found by using the following equation:

$$\left(\frac{\Delta\alpha}{\Delta\delta}\right)_{trim} = \frac{(\Delta\alpha_{2-1})_{trim}}{(\Delta\delta_{2-1})_{trim}} \quad . \tag{1.253}$$

The resulting values were used to obtain the control-effectiveness parameter C_{m_δ} at a constant angle-of-attack in the following manner:

$$\left(C_{M_\delta}\right)_{\alpha=K} = - C_{M_\alpha}\left(\frac{\Delta\alpha}{\Delta\delta}\right)_{trim} \quad . \tag{1.254}$$

The solution of C_{m_α} is presented in the discussion of longitudinal stability which follows.

Longitudinal stability. Evaluations of the longitudinal stability were obtained by analysis of the short-period oscillations induced by the abrupt control movements and shown in the angle-of-attack curves in the time-histories. The solution of C_{m_α}, the static longitudinal stability derivative, is obtained from the following equation as derived from the simultaneous solution of the two equations of motion:

$$C_{m_\alpha} = - \frac{I_Y}{qS\bar{c}}\left[\frac{4\pi^2}{P^2} + \left(\frac{0.693}{T_{1/2}}\right)^2\right]. \tag{1.255}$$

A correction was applied to C_{m_α} to eliminate the effect of elevon flexibility and the second-order effects from the two-degrees-of-freedom method of analysis were neglected since they constituted less than 0.5 percent of the results.

The periods of the short-period oscillation P were read from the time-history curves and the time to damp the amplitudes to one-half magnitude was determined by the use of the following formula:

$$T_{1/2} = \frac{0.693\,P}{2\log_e(A_1/A_2)} , \qquad (1.256)$$

where A_1 and A_2 were successive amplitudes above and below the neutral axis of the angle-of-attack time-history at the point where $T_{1/2}$ was sought.

The quantities C_{m_α} and C_{L_α}, corrected for the effect of elevator oscillations, were used in conjunction with the model center-of-gravity locations to determine the aerodynamic-center positions in percentages of the mean aerodynamic chord. The following relation was used:

$$\text{Aerodynamic center} = \text{Center-of-gravity} - \left(\frac{dC_{m_\alpha}}{dC_{L_\alpha}}\right)_{\text{corrected}} . \qquad (1.257)$$

The dynamic-longitudinal-stability data were reduced to the form of

$$C_{m_{\frac{\dot{\theta}\bar{c}}{2V}}} + C_{m_{\frac{\dot{\alpha}\bar{c}}{2V}}} ,$$

by the following equation derived from the simultaneous solution of the two equations of motion:

$$C_{m_{\frac{\dot{\theta}\bar{c}}{2V}}} + C_{m_{\frac{\dot{\alpha}\bar{c}}{2V}}} = -\frac{8I_Y}{\rho VS\bar{c}^2}\left(\frac{0.693}{T_{1/2}} - \frac{57.3C_{L_\alpha}\rho VS}{4m}\right) . \qquad (1.258)$$

Flying-Qualities Analysis

Variation with Mach number of the control position required for trim in level flight. The trim lift coefficient $C_{L_{trim}}$ for 0^o elevator deflection was obtained by plotting values of C_L corresponding to constant positive and negative elevator deflections against Mach number, and the variations were considered to be linear in the test range. These values were taken from the time-history data of the flight tests of the three models. The value of $C_{L_{trim}}$ for $\delta = 0^o$ was obtained by interpolation. Values of C_L for level flight for the full-scale airplane were obtained from the relation, $(C_L)_{1g} = \frac{W/S}{q}$. The difference between $(C_L)_{1g}$ for straight and level flight and $C_{L_{trim}}$ for $\delta = 0^o$ was divided by $C_{L_{\delta_{trim}}}$ to give δ for straight and level flight for various Mach numbers.

$$\delta_{trim} = \frac{(C_L)_{1g} - \left(C_{L_{trim}}\right)_{\delta=0^\circ}}{C_{L_{\delta_{trim}}}} \quad . \tag{1.259}$$

Elevator control force for trim against Mach number. A value of deflection of elevator per inch of stick movement for a high-speed fighter-type airplane was assumed to be

$$\frac{\delta}{x} = 2^\circ \text{ per inch} \quad .$$

Values of hinge-moment were obtained from the time-history plots of models for corresponding δ_{trim} values against Mach number. The value of $(\frac{\Delta H}{\Delta \delta})_{trim}$ was obtained from

$$(\frac{\Delta H}{\Delta \delta})_{trim} = \frac{(H_2 - H_1)_{trim}}{(\delta_2 - \delta_1)_{trim}} = \frac{(\Delta H_{2-1})_{trim}}{(\Delta \delta_{2-1})_{trim}} \quad . \tag{1.260}$$

At a given Mach number a value of hinge-moment was read at a given elevator deflection and corrected to the δ_{trim} for straight and level flight at sea-level conditions by

$$H_{\delta_{trim}} = H_1 - (\delta_1 - \delta_{trim})(\frac{\Delta H}{\Delta \delta})_{trim} \quad . \tag{1.261}$$

If the hinge-moment for δ_{trim} for straight and level flight at sea-level conditions is known, the elevator control force is obtained by

$$F = \frac{H}{57.3} \frac{\delta}{x} \quad , \tag{1.262}$$

where H has been corrected to full scale.

Change in normal acceleration for a corresponding change in elevator deflection $(\Delta a_n/\Delta\delta)_{trim}$ against Mach number. In order to obtain the change in normal accleration for a corresponding change in elevator deflection against Mach number, the values of C_L for level flight for various Mach numbers were divided by $C_{L_{\delta_{trim}}}$ (Eq. (1.248)) so that for 1g the reciprocal of $(\Delta a_n/\Delta\delta)_{trim}$, is

$$\Delta\delta = \frac{(C_L)_{1g}}{C_{L_{\delta_{trim}}}} \quad . \tag{1.263}$$

Stick force per g against Mach number. The change in elevator deflection required for a change in normal acceleration of 1g, reciprocal of $(\Delta a_n/\Delta\delta)_{trim}$, was multiplied by $(\Delta H/\Delta\delta)_{trim}$ (Eq. (1.260)) to obtain the change in hinge-moment required for a change in normal acceleration of 1g. Then, for $\Delta F/g$ in pounds per g,

$$\frac{\Delta F}{g} = \left(\frac{\Delta\delta}{g}\right)_{trim}\left(\frac{\Delta H}{\Delta\delta}\right)_{trim}\frac{\delta}{x}\,\frac{1}{57.3} \;. \qquad (1.264)$$

Dynamic stability. The dynamic stability of the airplane in terms of period and damping of the short-period longitudinal oscillations was determined from the oscillations of the model corrected to full-scale conditions.

The correction factors were determined from a two-degree-of-freedom method of analysis of the motion which assumes no changes in forward speed during the oscillation. The period of the oscillation for the airplane in terms of period for the model was obtained from a ratio of the C_{m_α} equations for the two as

$$P_a = P_m \frac{a_m}{a_a}\sqrt{\frac{I_{Y_a}}{S_a c_a}\,\frac{S_m c_m}{I_{Y_m}}\,\frac{m}{a}} \;. \qquad (1.265)$$

The time to damp to one-half amplitude for the airplane was determined by the following relationship:

$$C_{M_{\frac{\dot\theta \bar c}{2V}}} + C_{m_{\frac{\dot\alpha \bar c}{2V}}} = \frac{-8I_Y}{\rho a M S \bar c^2}\left(\frac{0.693}{T_{1/2}} - \frac{57.3 C_{L_\alpha}\rho a M S}{4m}\right), \qquad (1.266)$$

and equated for model and airplane as follows:

$$\frac{0.693}{T_{1/2a}} = -\frac{57.3 C_{L_\alpha}\rho_a a_a M S_a}{4}\left(-\frac{1}{m_a} + \frac{I_{Y_m}\bar c_a^{\,2}}{I_{Y_a} m_m c_m^{\,2}}\right) + \left(\frac{I_{Y_m} a_a \rho_a S_a \bar c_a^{\,2}}{I_{Y_a} a_m \rho_m S_m \bar c_m^{\,2}}\right)\frac{0.693}{T_{1/2m}} \;. \qquad (1.267)$$

Flying-qualities specifications require that the short-period oscillations damp to one-half amplitude in one complete cycle. This value was determined from the relation,

$$C_{1/2a} = \frac{T_{1/2a}}{P_a} \;, \qquad (1.268)$$

for the representative full-scale airplane.

1.7 List of References to Chapter 1

1. Ackeret, J.: Ueber die Druckverteilung an schraeg angestromten Rotationskoerpern bei Unterschallgeschweindigkeit. Anniversary Volume in honor of Prof. M. Panetti, published jointly by Assoc. Ital. di Aerotecrica, Assoc. Termotecnica Ital, and Assoc. Tecnica Automobile, 1950. Also: Aerotecnica, XXXI: 11-19, (1951).

2. Adams, M. C., and W. R. Sears: "Slender-Body Theory--Review and Extension." J. Aero. Sci., XX: 85-98, (1953).

3. Aiken, W. S., Jr., and B. Wiener: Analysis of the Horizontal-Tail Loads Measured in Flight on a Multiengine Jet Bomber. NACA TN 3479, Sept. 1955.

4. Alexander, S. R.: Flight Investigation to Determine the Aerodynamic Characteristics of Rocket-Powered Models Representative of a Fighter-Type Airplane Configuration Incorporating an Inverse-Taper Wing and a Vee Tail. NACA RM L8G29, 2 Nov. 1948.

5. Alford, W. J., Jr.: Theoretical and Experimental Investigation of the Subsonic-Flow Fields Beneath Swept and Unswept Wings with Tables of Vortex-Induced Velocities. Aug. 1956. NACA TN 3738.

6. Alford, W. J., Jr. and T. B. Pasteur, Jr.: The Effects of Changes in Aspect Ratio and Tail Height on the Longitudinal Stability Characteristics at High Subsonic Speeds on a Model with a Wing Having 32.6° Sweepback. Feb. 1954. NACA RM L53L09.

7. Alksne, A.: A Comparison of Two Methods for Computing the Wave Drag of Wing-Body Combinations. Apr. 1955. NACA RM A55A06a.

8. Allen, E. C.: Experimental Investigation of the Effects of Plan-Form Taper on the Aerodynamic Characteristics of Symmetrical Unswept Wings of Varying Aspect Ratio. May 1953. NACA RM A53C19.

9. Anderson, S. B., and R. S. Bray: A Flight Evaluation of the Longitudinal Stability Characteristics Associated with the Pitch-Up of a Swept-Wing Airplane in Maneuvering Flight at Transonic Speeds. 1955. NACA Rept. 1237. Supersedes RM A51I12.

10. Axelson, J. A.: Downwash Behind a Triangular Wing of Aspect Ratio 3-Transonic Bump Method. Dec. 1953. NACA RM A53I23.

11. Bamber, M. J., and R. O. House: Wind Tunnel Investigation of Effect of Yaw on Lateral Stability Characteristics. Part II: Rectangular NACA 23012 Wing with a Circular Fuselage and a Fin. NACA TN J30, 1939.

12. Bandettini, A., and R. Selan: The Effects of Horizontal-Tail Height and a Partial-Span Leading-Edge Extension on the Static Longitudinal Stability of a Wing-Fuselage-Tail Combination Having a Sweptback Wing. Mar. 1954. NACA RM A53J07.

13. Banner, R. D., R. D. Reed and W. L. Marcy: Wing-Load Measurements of the Bell X-5 Research Airplane at a Sweep Angle of 58.7°. Apr. 1955. NACA RM H55A11.

14. Becht, R. E., and A. L. Byrnes, Jr.: Investigation of the Low Speed Aerodynamic Characteristics of a Variable-Sweep Airplane Model with a Wing Having Partial-Span Cambered-Leading-Edge Modifications. Sept. 1952. NACA RM L52G08a.

15. Berler, I., and S. Nichols: Interference Between Wing and Body at Supersonic Speeds. Part VI: Data Report on Pressure Distribution Tests of Wing Body Interference Models at Mach Number 2.0, Phase Two Tests of June 1949. Cornell Aeron. Lab. Bumblebee Rep. CAL/CF-1569, May 1951.

16. Berler, I., and S. Nichols: Interference Between Wing and Body at Supersonic Speeds. Part VII: Data Report on Pressure Distribution Tests of Wing-Body Interference Models at Mach Number 2.0, Phase Three Tests of Aug. 1949. Cornell Aeron Lab. Bumblebee Rep. CAL/CF-1570, June 1951.

17. Betz, A.: "Verhalten von Wirbelsystemen." ZAMM, 12, 164-174, 1932.

18. Bielat, R. P., and G. S. Campbell: A Transonic Wind-Tunnel Investigation of the Longitudinal Stability and Control Characteristics of a 0.09-Scale Model of the Bell X-5 Research Airplane and Comparison with Flight. Oct. 1953. NACA RM L53H18.

19. Blackaby, J. R.: Wind-Tunnel Investigation at Low Speed of a Wing Having 63° Sweepback and a Drooped Tip. Apr. 1955. NACA RM A55B14.

20. Bland, W. M., Jr.: Effect of Fuselage Interference on the Damping in Roll of Delta Wings of Aspect Ratio 4 in the Mach Number Range Between 0.6 and 1.6 as Determined with Rocket-Propelled Vehicles. July 1952. NACA RM L52E13.

21. Bland, W. M., Jr.: Effect of Wing Flexibility on the Damping in Roll of a Notched Delta Wing-Body Combination Between Mach Numbers 0.6 and Approximately 2.2 as Determined with Rocket-Propelled Models. June 1954. NACA RM L54E04.

22. Bland, W. M., Jr., and A. E. Dietz: Some Effects of Fuselage Interference, Wing Interference and Sweepback on the Damping in Roll of Untapered Wings as Determined by Techniques Employing Rocket-Propelled Vehicles. Oct. 1951. NACA RM L51D25.

23. Bobbitt, P. J., and P. J. Macie, Jr.: Sidewash in the Vicinity of Lifting Swept Wings at Supersonic Speeds. February 1957. NACA TN 3938.

24. Boddy, L. E., and C. P. Morrill, Jr.: The High-Speed Aerodynamic Effects of Modifications to the Wing and Wing-Fuselage Intersection of an Airplane Model with the Wing Swept Back 35°. Feb. 18, 1948. NACA RM A7J02.

25. Boddy, L. E., and C. P. Morrill, Jr.: The Aerodynamic Effects of Rockets and Fuel Tanks Mounted Under the Swept-Back Wing of an Airplane Model. Apr. 23, 1948. NACA RM A7J03.

26. Boltz, F. W., and H. H. Shibata: Pressure Distribution at Mach Numbers Up to 0.90 on a Cambered and Twisted Wing Having 40° of Sweepback and an Aspect Ratio of 10, Including the Effects of Fences. Mar. 1953. NACA RM A52K20.

27. Boswinkle, R. W., Jr.: Comparison of Lift-Curve Slopes for a Model Tested in Two Slotted Tunnels of Different Sizes at High Subsonic Speeds. June 1953. NACA RM L53E20a.

28. Bray, R. S.: The Effects of Fences on the High-Speed Longitudinal Stability of a Swept-Wing Airplane. Aug. 1953. NACA RM A53F23.

29. Brown, C. E., and L. K. Hargrave: Investigation of Minimum Drag and Maximum Lift-Drag Ratios of Several Wing-Body Combinations Including a Cambered Triangular Wing at Low Reynolds Numbers and at Supersonic Speeds. Aug. 1951. NACA RM L51E11.

30. Browne, S. H., L. Friedman, and I. Hodes: "A Wing-Body Problem in a Supersonic Conical Flow." J. Aeron. Sci., 15, 443-452, 1948.

31. Buell, D. A., and B. E. Tinling: Ground Effects on the Longitudinal Characteristics of Two Models with Wings Having Low Aspect Ratio and Pointed Tips. July 1955. NACA RM A55E04.

32. Burrows, D. L., and W. E. Palmer: A Transonic Wind-Tunnel Investigation of the Longitudinal Force and Moment Characteristics of a Plane and a Cambered 3-Percent-Thick Delta Wing of Aspect Ratio 3 on a Slender Body. Nov. 1954. NACA RM L54H25.

33. Cahn, M. S., and C. R. Bryan: A Transonic-Wing Investigation in the Langley 8-Foot High-Speed Tunnel at High Subsonic Mach Numbers and at a Mach Number of 1.2. Wing-Fuselage Configuration Having a Wing of 0° Sweepback, Aspect Ratio 4.0, Taper Ratio 0.6, and NACA 65A006 Airfoil Section. 6 Mar. 1951. NACA RM L51A02.

34. Carner, H. A., and R. J. Knapp: Flight Measurements of the Pressure Distribution on the Wing of the X-1 Airplane (10-Percent-Thick Wing) Over a Chordwise Station Near the Midspan, in Level Flight at Mach Numbers From 0.79 to 1.00 and in a Pull-Up at a Mach Number of 0.96. Sept. 12, 1950. NACA RM L50H04.

35. Carner, H. A., and M. M. Payne: Tabulated Pressure Coefficients and Aerodynamic Characteristics Measured on the Wing of the Bell X-1 Airplane in Level Flight at Mach Numbers From 0.79 to 1.00 and in a Pull-Up at a Mach Number of 0.96. 18 Sept. 1950. NACA RM L50H25.

36. Chapman, R. Jr., and J. D. Morrow: Longitudinal Stability and Drag Characteristics at Mach Numbers From 0.70 to 1.37 of Rocket-Propelled Models Having a Modified Triangular Wing. May 1952. NACA RM L52A31.

37. Childs, J. M.: Flight Measurements of the Stability Characteristics of the Bell X-5 Research Airplane in Sideslips at 59° Sweepback. Feb. 1953. NACA RM L52K13b.

38. Cleary, J. W.: The Transonic Aerodynamic Characteristics of Structurally Related Wings of Low Aspect Ratio Having a Spanwise Variation in Thickness Ratio- Transonic Bump Technique. Apr. 1954. NACA RM A54B18.

39. Clevenson, S. A., and S. A. Leadbetter: Some Measurements of Aerodynamic Forces and Moments at Subsonic Speeds on a Wing-Tank Configuration Oscillating in Pitch About the Wing Midchord. Dec. 1956. NACA TN 3822.

40. Coe, C. F.: The Effects of Tip-Mounted Jet Nacelles on the Transonic Characteristics of Low-Aspect-Ratio Wings. Dec. 1952. NACA RM A52J21.

41. Coletti, D. E.: Investigation of the Effects of Model Scale and Stream Reynolds Number on the Aerodynamic Characteristics of Two Rectangular Wings at Supersonic Speeds in the Langley 9-Inch Supersonic Tunnel. Donald E. Coletti, June 1955. 32p. diagrs. NACA RM L55D29.

42. Connors, J. F., and R. R. Woollett: Experimental Investigation of a Two-Dimensional Split-Wing Ram-Jet Inlet at Mach Number of 3.85. Aug. 1952. NACA RM E52F04.

43. Conrard, D.: Lift, Drag, and Pitching Moment of Low-Aspect-Ratio Wings at Subsonic and Supersonic Speeds-Plane Triangular Wing of Aspect Ratio 3 with Air-to-Air Missile Models Mounted Externally. June 1952. NACA RM A52C10a.

44. Cramer, R. H.: Interference Between Wing and Body at Supersonic Speeds. Part V: Phase One Wind Tunnel Tests Correlated with the Linear Theory. Cornell Aer. Lab., Bumblebee Rept. CAL/CM-597, Dec. 1950.

45. Cramer, R. H.: "Interference Between Wing and Body at Supersonic Speeds. Theoretical and Experimental Determination of Pressures on the Body." J. Aeron. Sci., 18, 629-632, 1951.

46. Cramer, R. H.: Wing-Body Interference at Supersonic Speeds. Recent Experimental Results and Their Bearing on Advances in Theory. Proc. U. S. Navy Symposium on Aeroballistics, NAVORD Rept. 3146, May 1952.

47. Dods, J. B., Jr., and B. E. Tinling: Summary of Results of a Wind-Tunnel Investigation of Nine Related Horizontal Tails. July 1955. NACA TN 3497. Formerly RM A51G31a.

48. Drake, H. M., H. R. Goodman, and H. H. Hoover: Preliminary Results of NACA Transonic Flights of the XS-1 Airplane with 10-Percent-Thick Wing and 8-Percent-Thick Horizontal Tail. Oct. 13, 1948. NACA RM L8I29.

49. Dye, F. E., Jr.: Interference Between Wing and Body at Supersonic Speeds. Part IX: Data Report on Pressure Distribution Tests of Wing-Body Interference Models at Mach Number 2.0, Phase Five Tests of August 1951. Cornell Aeron. Lab. Bumblebee Rept. CAL/CF-1684, Dec. 1951.

50. Dye, F. E., Jr.: A Comparison of Pressure Predicted by Exact and Approximate Theories with Some Experimental Results on an Ogival-Nosed Body at a Mach Number of 2.0. Cornell Aeron. Lab. Bumblebee Rept. CAL/CF-1723, Dec. 1951.

51. Edwards, G. G., et al: Analysis of Wind-Tunnel Tests to a Mach Number of 0.90 of a Four-Engine Propeller-Driven Airplane Configuration Having a Wing with 40° of Sweepback and an Aspect Ratio of 10. Sept. 1956. NACA TN 3790. Supersedes RM A54F14.

52. Edwards, G. G., J. K. Dickson, F. B. Sutton, and F. A. Demele: The Results of Wind-Tunnel Tests to a Mach Number of 0.90 of a Four-Engine Propeller-Driven Airplane Configuration Having a Wing with 40° of Sweepback and an Aspect Ratio of 10. Sept. 1956. NACA TN 3789. Supersedes RM A53I28.

53. Edwards, G. G., B. E. Tinling, and A. C. Ackerman: The Longitudinal Characteristics at Mach Numbers Up to 0.92 of a Cambered and Twisted Wing Having 40° of Sweepback and an Aspect Ratio of 10. Sept. 1952. NACA RM A52F18.

54. Emerson, H. F.: Wind-Tunnel Investigation of the Effect of Clipping the Tips of Triangular Wings of Different Thickness, Camber, and Aspect Ratio-Transonic Bump Method. June 1956. NACA TN 3671. Supersedes RM A53L03.

55. English, R. D.: Some Effects of Aeroelasticity and Sweepback on the Rolling Effectiveness and Drag of a 1/11-Scale Model of the Bell X-5 Airplane Wing at Mach Numbers From 0.6 to 1.5. Nov. 1953. NACA RM L53I18b.

56. Estabrooks, B. B.: Transonic Wind-Tunnel Investigation of an Unswept Wing in Combination with a Systematic Series of Four Bodies. Jan. 1953. NACA RM L52K12a.

57. Estabrooks, B. B.: A Transonic Wind-Tunnel Investigation of an Unswept-Wing-Body Combination at Angles of Attack Up to 24°. Feb. 1953. NACA RM L52L19.

58. Evvard, J. C.: Use of Source Distribution for Evaluating Theoretical Aerodynamics of Thin Finite Wings at Supersonic Speeds. NACA Rept. 951, 1950.

59. Faber, S., and J. M. Eggleston: A Transonic Investigation by the Free-Fall Method of an Airplane Configuration Having 45° Sweptback Wing and Tail Surfaces. June 1953. NACA RM L53D10.

60. Ferrari, C.: "Sul Problema Dell' Elica con Vento Laterale." Atti Accad. Sci; Torino 68, 60-65, 1928. Also: Aerotecnica, 8, 171-176, 1928.

61. Ferrari, C.: "Determinazione dei nuclei vorticosi risultanti dall' arrotolamento della superficie di discontinuita dietro a un'ala, a calcolo della forza viva da essi indotta." Mem. reale acad. Italia, 1934, 249-267.

62. Ferrari, C.: "Some Experiments on the Slipstream Effect." Rendiconti Sperimentali del laboratorio di Aeronautica del Reale Instituto Superiore di Ingegneria di Torino. Seconde Serie: Tests on Models "Torino 30, 31, 32 and E1. 38-55, 1936. Also: Aerotecnica, 15, 979-1036, 1935.

63. Ferrari, C.: "Test Reports of the Aeronautical Laboratory of the R. Instituto Superiore di Ingegneria, of Turin." J. Roy. Aer. Soc. 40, 388-404, 1936. Also: NACA TM 820, 1937.

64. Ferrari, C.: "Il problema dell'elica con vento laterale." Atti. acad. sci. Torino 75, 2-31, 1940.

65. Ferrari, C.: "Interference Between Wing and Body at Supersonic Speeds. Theory and Numerical Applications." J. Aeron. Sci. 15, 317-336, 1948.

66. Ferrari, C.: "Interference Between Wing and Body at Supersonic Speeds. Note on Wind-Tunnel Results and Addendum to Calculations." J. Aeron. Sci. 16, 542-546, 1949.

67. Ferrari, C.: Interference Between Wing and Body at Supersonic Speeds. Part III: Numerical Applications of the Linear Theory. Cornell Aeron. Lab. Bumblebee Rept. CAL/CM-463, Apr. 1951.

68. Ferrari, C.: "Calcolo della velocita indotta da un'ala in corrente supersonica linearizzata." Encomium volume of Aerotecnica, in honor of Prof. G. A. Crocco, 33, 65-69, 1953. Trans.: Cornell Aeron. Lab., Rep. CAL-59, July 1953.

69. Ferrari, C.: "Sulla determinazione di alcuni tipi di campi di corrente ipersonora." Rend. reale. acad. nazl. Lincei, Rome, VII (6), Ser. VIII, 1949. Also: NACA TM 1381, Nov. 1954.

70. Ferrari, C.: Interaction Problems. Section C in: Aerodynamic Components of Aircraft at High Speeds, pp. 281-551. High Speed Aerodynamics and Jet Propulsion, Vol. VII, Princeton University Press, 1957.

71. Few, A.G., Jr., and T.J. King, Jr.: Some Effects of Tail Height and Wing Plan Form on the Static Longitudinal Stability Characteristics of a Small-Scale Model at High Subsonic Speeds. May 1957. NACA TN 3957. Supersedes RM L54G12.

72. Flax, A.H.: "Integral Relations in the Linearized Theory of Wing-Body Interference." J. Aeron. Sci., 20, 483-490, 1953.

73. Foster, G.V.: Longitudinal Stability and Wake-Flow Characteristics of a Twisted and Cambered Wing-Fuselage Combination of 45° Sweepback and Aspect Ratio 8 with a Horizontal Tail and Stall-Control Devices at a Reynolds Number of 4.0×10^{6}. June 1953. NACA RM L53D08.

74. Foster, G.V., and R.F. Griner: A Study of Several Factors Affecting the Stability Contributed by a Horizontal Tail at Various Vertical Positions on a Sweptback-Wing Airplane Model. 28 Oct. 1949. NACA RM L9H19.

75. Foster, G.V., and R.F. Griner: Low-Speed Longitudinal and Wake Airflow Characteristics at a Reynolds Number of 5.5×10^{6} of a Circular-Arc 52° Sweptback Wing with a Fuselage and a Horizontal Tail at Various Vertical Positions. June 19, 1951. NACA RM L51C30.

76. Foster, G.V., and R.F. Griner: A Study of Several Factors Affecting the Stability Contributed by a Horizontal Tail at Various Vertical Positions on a Sweptback-Wing Airplane Model. Nov. 1956. NACA TN 3848. Supersedes RM L9H19.

77. Fournier, P.G.: Wind-Tunnel Investigation of the Aerodynamic Characteristics in Pitch and Side-Slip at High Subsonic Speeds of a Wing-Fuselage Combination Having a Triangular Wing of Aspect Ratio 4. Aug. 1953. NACA RM L53G14a.

78. Fournier, P.G.: Effects of Spanwise Location of Sweep Discontinuity on the Low-Speed Static Lateral Stability Characteristics of a Complete Model with Wings of m and w Plan Form. May 1955. NACA RM L55D22.

79. Fournier, P. G.: Effects of Spanwise Location of Sweep Discontinuity on the Low-Speed Longitudinal Stability Characteristics of a Complete Model with Wings of M and W Planform. Jan. 1955. NACA RM L54K23.

80. Fournier, P. G.: Low-Speed Static Stability Characteristics of a Complete Model with an m-Wing in Mid and High Positions and with Three Horizontal-Tail Heights. Jan. 1956. NACA RM L55J06.

81. Fournier, P. G., and A. L. Byrnes, Jr.: Wind-Tunnel Investigation of the Static Lateral Stability Characteristics of Wing-Fuselage Combinations at High Subsonic Speeds. Aspect Ratio Series. Feb. 1953. NACA RM L52L18.

82. Franks, R. W.: Tests in the Ames 40-by 80-Foot Wind Tunnel of the Aerodynamic Characteristics of Airplane Models with Plain Spoiler Ailerons. Dec. 1954. NACA RM A54H26.

83. Gallagher, J. J., and J. N. Mueller: An Investigation of the Maximum Lift of Wings at Supersonic Speeds. 1955. NACA Rep. 1227. Supersedes RM L7J10.

84. Gammal, A. A., and T. L. Kennedy: Flight Investigation to Determine Lift and Drag Characteristics of a Canard Ram-Jet Missile Configuration in the Mach Number Range of 0.8 to 2.0. June 1954. NACA RM L54D28.

85. Glauert, H.: Wind-Tunnel Interference on Wings, Bodies and Airscrews. Gr. Brit. ARC, R&M No. 1566, 1933.

86. Goodman, T. R.: Some Simplications of Ferrari's Theory of Wing-Body Interference at Supersonic Speeds. Cornell Aeron. Lab., Bumblebee Rep. CAL/CM-687, Dec. 1954.

87. Goodson, K. W., and R. E. Becht: Wind-Tunnel Investigation at High Subsonic Speeds of the Stability Characteristics of a Complete Model Having Sweptback-, m-, w-, and Cranked-Wing Plan Forms and Several Horizontal-Tail Locations. May 1954. NACA RM L54C29.

88. Goodson, K. W., and R. E. Becht: Wind-Tunnel Investigation at High Subsonic Speeds of the Static Longitudinal Stability Characteristics of a Complete Model Having Cropped-Delta, Swept, and Unswept Wings and Several Horizontal-Tail Heights. Oct. 1954. NACA RM L54H12.

89. Graham, D., and D. G. Koenig: Tests in the Ames 40- by 80-Foot Wind Tunnel of an Airplane Configuration with an Aspect Ratio 2 Triangular Wing and an All-Movable Horizontal Tail-Longitudinal Characteristics. Apr. 23, 1951. NACA RM A51B21.

90. Graham, D., and D. G. Koenig: Tests in the Ames 40- by 80-Foot Wind Tunnel of an Airplane Configuration with an Aspect Ratio 4 Triangular Wing and an All-Movable Horizontal Tail-Longitudinal Characteristics. Oct. 1951. NACA RM A51H10a.

91. Grant, F. C.: The Proper Combination of Lift Loadings for Least Drag on a Supersonic Wing. 1956. NACA Rep. 1275. Supersedes TN 3533.

92. Griner, R. F.: Static Lateral Stability Characteristics of an Airplane Model Having a 47.7° Sweptback Wing of Aspect Ratio 6 and the Contribution of Various Model Components at a Reynolds Number of 4.45×10^{6}. Sept. 1953. NACA RM L53G09.

93. Habel, L. W., and D. R. Bowman: Measurements of Fluctuating Pressures on the Wings and Body of a Sweptback Wing-Body Combination in the Langley 16-Foot Transonic Tunnel. Sept. 1953. NACA RM L53G06a.

94. Hadaway, W. M., and P. A. Cancro: Low-Speed Longitudinal Characteristics of Two Unswept Wings of Hexagonal Airfoil Sections Having Aspect Ratios of 2.5 and 4.0 with Fuselage and with Horizontal Tail Located at Various Vertical Positions. Oct. 1953. NACA RM L53H14a.

95. Haefeli, R., H. Mirels, and J. Cummings: Charts for Estimating Downwash Behind Rectangular, Trapezoidal and Triangular Wings at Supersonic Speeds. NACA, Tech. N. 2141, 1950.

96. Hall, C. F., and J. C. Heitmeyer: Aerodynamic Study of a Wing-Fuselage Combination Employing a Wing Swept Back 63°. Characteristics at Supersonic Speeds of a Model with the Wing Twisted and Cambered for Uniform Load. Jan. 9, 1950. NACA RM A9J24.

97. Hallissy, J. M., and D. R. Bowman: Transonic Characteristics of a 45° Sweptback Wing-Fuselage Combination. Effect of Longitudinal Wing Position and Division of Wing and Fuselage Forces and Moments. Feb. 1953. NACA RM L52K04.

98. Harrison, D. E.: A Transonic Wing-Tunnel Investigation of the Characteristics of a Twisted and Cambered 45° Sweptback Wing-Fuselage Configuration. Dec. 1952. NACA RM L52K18.

99. Hayes, W. D.: Linearized Supersonic Flow. Thesis, CALTECH, 1947. Also: North Amer. Aerophys. Lab. Rep. 222, June 1947.

100. Heaslet, M. A., and J. R. Spreiter: Three-Dimensional Transonic Flow Theory Applied to Slender Wings and Bodies. July 1956. NACA TN 3717.

101. Hedgepeth, J. M., and R. J. Kell: Comparison Between Theoretical and Experimental Rates of Roll of Two Models with Flexible Rectangular Wings at Supersonic Speeds. Aug. 1954. NACA RM L54F23.

102. Heitmeyer, J. C.: Aerodynamic Study of a Wing-Fuselage Combination Employing a Wing Sweptback 63°-Effect of Reynolds Number at Supersonic Mach Numbers on the Longitudinal Characteristics of a Wing Twisted and Cambered for Uniform Load. 9 Oct. 1950. NACA RM A50G10.

103. Henry, B. Z., Jr.: High-Speed Wind-Tunnel Investigation of a Sweptback Wing with an Added Triangular Area at the Center. Jan. 14, 1949. NACA RM L8J12.

104. Henry, B. Z., Jr.: A Transonic Wing Investigation in the Langley 8-Foot High-Speed Tunnel at High Subsonic Mach Numbers and at a Mach Number of 1. 2. Wing-Fuselage Configuration Having a Wing of 35° Sweepback, Aspect Ratio 4, Taper Ratio 0. 6, and NACA 65A006 Airfoil Section. 15 Nov. 1950. NACA RM L50J09.

105. Hieser, G.: An Investigation at Transonic Speeds of the Effects of Fences, Drooped Nose, and Vortex Generators on the Aerodynamic Characteristics of a Wing-Fuselage Combination Having a 6-Percent-Thick, 45° Sweptback Wing. Mar. 1953. NACA RM L53B04.

106. Hopkins, E. J.: Aerodynamic Study of a Wing-Fuselage Combination Employing a Wing-Sweptback 63°.-Effects of Split Flaps, Elevons, and Leading-Edge Devices at Low Speed. 19 May 1949. NACA RM A9C21.

107. Jacobs, E. N., and K. E. Ward: Interference of Wing and Fuselage from Tests of 209 Combinations in the NACA Variable Density Tunnel. NACA, Rep. 540, 1935.

108. Jaquet, B. M.: Effects of Chord Discontinuities and Chordwise Fences on Low-Speed Static Longitudinal Stability of an Airplane Model Having a 35° Sweptback Wing. June 1952. NACA RM L52C25.

109. Jaquet, B. M.: Effects of Chord-Extension and Droop of Combined Leading-Edge-Flap and Chord-Extension on Low-Speed Static-Longitudinal Stability Characteristics of an Airplane Model Having a 35° Sweptback Wing with Plain Flaps Neutral or Deflected. Jan. 1953. NACA RM L52K21a.

110. Jaquet, B. M.: Some Low-Speed Wind-Tunnel Experiments Pertaining to the Longitudinal Stability Characteristics of a 35° Swept-Wing Model and an Unswept-Wing Model. Oct. 1953. NACA RM L53H31.

111. Jaquet, B. M.: Calculated Lateral Frequency Response and Lateral Oscillatory Characteristics for Several High-Speed Airplanes in Various Flight Conditions. Dec. 1953. NACA RM L53J01.

112. Jaquet, B. M., and H. S. Fletcher: Experimental Steady-State Yawing Derivatives of a 60° Delta-Wing Model as Affected by Changes in Vertical Position of the Wing and in Ratio of Fuselage Diameter to Wing Span. Oct. 1956. NACA TN 3843.

113. Jaquet, B. M., and H. S. Fletcher: Effects of Fuselage Nose Length and a Canopy on the Static Longitudinal and Lateral Stability Characteristics of 45° Sweptback Airplane Models Having Fuselages with Square Cross Sections. Apr. 1957. NACA TN 3961.

114. Johnson, B. H., Jr., and H. H. Shibata: Characteristics Throughout the Subsonic Speed Range of a Plane Wing and of a Cambered and Twisted Wing, Both Having 45° of Sweepback. July 1951. NACA RM A51D27.

115. Jones, J. L., and F. A. Demele: Aerodynamic Study of a Wing-Fuselage Combination Employing a Wing Sweptback 63°. -Characteristics Throughout the Subsonic Speed Range with the Wing Cambered and Twisted for a Uniform Load at a Lift Coefficient of 0.25. 15 Aug. 1949. NACA RM A9D25.

116. Jones, R. T.: Theory of Wing-Body Drag at Supersonic Speeds. Sept. 1953. NACA RM A53H18a.

117. Jones, R. T.: Theory of Wing-Body Drag at Supersonic Speeds. 1956. NACA Rep. 1284. Supersedes RM A53H18a.

118. Kaden, H.: "Aufwicklung Einer Unstabilen Unstetigkeitsflaeche." Ing. Arch. 2, 140-168, 1931. Also: Roy. Aircraft Establishment Library, Trans. 403, Farnborough, Eng., 1939.

119. Karman, von T., and E. Trefftz: "Potentialstroemung um Gegebene Tragflaechen Querschnitte." Z. Flugtech. Motorluftschiffahrt. q., 111, 1918.

120. Katzen, E. D., and G. E. Kaattari: Drag Interference Between a Pointed Cylindrical Body and Triangular Wings of Various Aspect Ratios at Mach Numbers of 1.50 and 2.02. Nov. 1956. NACA TN 3794. Supersedes RM A51C27.

121. Kelly, T. C.: Transonic Wind-Tunnel Investigation of the Aerodynamic Characteristics of a 60° Triangular Wing in Combination with a Systematic Series of Three Bodies. Apr. 1953. NACA RM L52L22a.

122. King, T. J., Jr., and T. B. Pasteur, Jr.: Wind-Tunnel Investigation of the Aerodynamic Characteristics in Pitch of Wing-Fuselage Combinations at High Subsonic Speeds. Taper-Ratio Series. June 1953. NACA RM L53E20.

123. King, T. J., Jr., and T. B. Pasteur, Jr.: Wind-Tunnel Investigation of the Aerodynamic Characteristics in Pitch of Wing-Fuselage Combinations at High Subsonic Speeds. Taper-Ratio Series. Dec. 1956. NACA TN 3867. Supersedes RM L53E20.

124. Kirby, R. H.: Flight Investigation of the Stability and Control Characteristics of a Vertically Rising Airplane Research Model with Swept or Unswept Wings and x- or +-Tails. Oct. 1956. NACA TN 3812.

125. Kirkby, S., and A. Robinson: Wing Body Interference at Supersonic Speeds. College of Aeronautics, Cranfield, Rep. 7, Apr. 1947.

126. Knapp, R. J.: Tabulated Pressure Coefficients and Aerodynamic Characteristics Measured on the Wing of the Bell X-1 Airplane in an Unaccelerated Low-Speed Stall, in Pushovers at Mach Numbers of 0.83 and 0.99, and in a Pull-Up at a Mach Number of 1.16. Sept. 1951. NACA RM L51F25.

127. Knapp, R. J., and G. H. Jordan: Flight-Determined Pressure Distribution Over the Wing of the Bell X-1 Research Airplane 10-Percent-Thick Wing at Subsonic and Transonic Speeds. June 1953. NACA RM L53D20.

128. Knapp, R. J., and G. H. Jordan: Wing Loads on the Bell X-1 Research Airplane 10 Percent Thick Wing as Determined by Pressure-Distribution Measurements in Flight at Subsonic and Transonic Speeds. Nov. 1953. NACA RM L53G14.

129. Knapp, R. J., and G. V. Wilken: Tabulated Pressure Coefficients and Aerodynamic Characteristics Measured on the Wing of the Bell X-1 Airplane in Pull-Ups at Mach Numbers from 0.53 to 0.99. 1 Nov. 1950. NACA RM L50H28.

130. Koenig, D. G.: Tests in the Ames 40- by 80-Foot Wind Tunnel of an Airplane Configuration with an Aspect Ratio 3 Triangular Wing and an All-Movable Horizontal Tail-Longitudinal and Lateral Characteristics. Apr. 1953. NACA RM A52L15.

131. Koenig, D. G.: Tests in the Ames 40- by 80- Foot Wind Tunnel of the Effects of Various Wing Modifications on the Longitudinal Characteristics of Two Triangular-Wing Airplane Models with and without Horizontal Tails. Apr. 1954. NACA RM A54B09.

132. Kolbe, C. D., and F. W. Boltz: Effects of Operating Propellers on the Wing-Surface Pressures of a Four-Engine Tractor Airplane Configuration Having a Wing with 40° of Sweepback. Apr. 1954. NACA RM A53L29.

133. Kolnick, J. J., and R. M. Kennedy: The Effects of Sweepback on Longitudinal Characteristics of a 1/30-Scale Semispan Model of the Bell X-5 Airplane as Determined from NACA Wing-Flow Tests at Transonic Speeds. Nov. 1952. NACA RM L52I23.

134. Krienes, K.: Die elliptische Tragflaeche auf potential theoreticscher grundlage. ZAMM 20, 65-88, 1940. Also: NACA TM 971, Mar. 1911.

135. Kuhl, A. E., and C. T. Johnson: Flight Measurements of Wing Loads on the Convair XF-92A Delta-Wing Airplane. May 1956. NACA RM H55D12.

136. Kuhn, R. E., and J. W. Draper: Wind-Tunnel Investigation of the Effects of Geometric Dihedral on the Aerodynamic Characteristics in Pitch and Sideslip of an Unswept- and a 45° Sweptback-Wing Fuselage Combination at High Subsonic Speeds. July 1953. NACA RM L53F09.

137. Kuhn, R. E., and J. W. Draper: Investigation of the Aerodynamic Characteristics of a Model Wing-Propeller Combination and of the Wing and Propeller Separately at Angles of Attack Up to 90°. 1956. NACA Rep. 1263. Supersedes TN 3304.

138. Kuhn, R. E., and P. G. Fournier: Wind-Tunnel Investigation of the Static Lateral Stability Characteristics of Wing-Fuselage Combinations at High Subsonic Speeds. Sweep Series. Sept. 1952. NACA RM L52G11a.

139. Kuhn, R. E., and J. W. Wiggins: Wind-Tunnel Investigation of the Aerodynamic Characteristics in Pitch of Wing-Fuselage Combinations at High Subsonic Speeds. Aspect-Ratio Series. Apr. 1952. NACA RM L52A29.

140. Kurbjum, M. C., and J. R. Thompson: Transonic Drag Characteristics and Pressure Distribution on the Body of a Wing-Body Combination Consisting of a Body of Revolution of Fineness Ratio 12 and a Wing Having Sweepback of 45°, Aspect Ratio 4, Taper Ratio 0.6, and NACA 65A006 Airfoil Sections. Apr. 1952. NACA RM L52B12.

141. Kurbjum, M. C., and J. R. Thompson: Free-Fall Measurements of the Effects of Wing-Body Interference on the Transonic Drag Characteristics of Swept-Wing-Slender-Body Configurations. May 1953. NACA RM L53C31.

142. Lagerstrom, P., and M. Graham: Downwash and Sidewash Induced by Three-Dimensional Lifting Wings in Supersonic Flow. Douglas Aircraft Co., Rep. SM-13007, Apr. 1947.

143. Lagerstrom, P. A., and M. E. Graham: Aerodynamic Interference in Supersonic Missiles. Douglas Aircraft, Inc., Rep. SM-13743, July 1950.

144. Lagerstrom, P. A., and M. Graham: "Methods for Calculating the Flow in the Trefftz-Plane Behind Supersonic Wings." J. Aeron. Sci. 18, 179-191, 1951.

145. Lagerstrom, P. A., and Van Dyke, M. D.: General Considerations about Planer and Nonplaner Lifting Systems. Douglas Aircraft Co. Rep. SM-13432. Santa Monica, June 1949.

146. Lawrence, H. R., and A. H. Flax: "Wing-Body Interference at Subsonic and Supersonic Speeds. Survey and New Developments." J. Aer. Sci., 21, 289-328, 1954.

147. Lawrence, L. F., and J. L. Summers: Wind-Tunnel Investigation of a Tailless Triangular-Wing Fighter Aircraft at Mach Numbers from 0.5 to 1.5. June 24, 1949. NACA RM A9B16.

148. Lennertz, J.: "Beitrag zur theoretischen Behandlung des gegenzeitigen Einflusses von Tragflaeche und Rumpf Abhandl." Aerodyn. Inst. Aachen, 8, 3-30, 1928. Also: Z. Flugtech. Motorluftschiflahrt, 8, 11-13, 1927.

149. Lessing, H. C.: Aerodynamic Study of a Wing-Fuselage Combination Employing a Wing Sweptback 63°-Effect of Sideslip on Aerodynamic Characteristics at a Mach Number of 1.4 with the Wing Twisted and Cambered. 29 Sept. 1950. NACA RM A50F09.

150. Letko, W.: Experimental Investigation at Low Speed of the Effects of Wing Position on the Static Stability of Models Having Fuselages of Various Cross Section and Unswept and 45° Sweptback Surfaces. Nov. 1956. NACA TN 3857.

151. Lindsey, W. F.: The Flow Past an Unswept- and a Swept-Wing-Body Combination and Their Equivalent Bodies of Revolution at Mach Numbers Near 1.0. June 1956. NACA TN 3703. Supersedes RM L54A28a.

152. Lomax, H., L. Sluder, and M. A. Heaslet: The Calculation of Downwash Behind Supersonic Wings with an Application to Triangular Plan Forms. NACA, Rep. 957, 1950.

153. Love, E. S.: Investigations at Supersonic Speeds of 22 Triangular Wings Representing Two Airfoil Sections for Each of 11 Apex Angles. 1955. NACA Rep. 1238. Supersedes RM L9D07.

154. Loving, D. L.: A Transonic Wind-Tunnel Investigation of the Effects of Longitudinal Wing Location and Varying Body Size on the Interference Characteristics of a 45° Sweptback Wing. Mar. 1953. NACA RM L52L16.

155. Loving, D. L., and B. B. Estabrooks: Transonic-Wing Investigation in the Langley 8-Foot High-Speed Tunnel at High Subsonic Mach Numbers and at a Mach Number of 1.2. Analysis of Pressure Distribution of Wing-Fuselage Configuration Having a Wing of 45° Sweepback, Aspect Ratio 4, Taper Ratio 0.6, and NACA 65A006 Airfoil Section. Sept. 1951. NACA RM L51F07.

156. Loving, D. L., and D. E. Wornom: Transonic Wind-Tunnel Investigation of the Interference Between a 45° Sweptback Wing and a Systematic Series of Four Bodies. Nov. 1952. NACA RM L52J01.

157. Luoma, A.A.: Aerodynamic Characteristics of Four Wings of Sweepback Angles 0°, 35°, 45°, and 60°, NACA 65A006 Airfoil Section, Aspect Ratio 4, and Taper Ratio 0.6 in Combination with a Fuselage at High Subsonic Mach Numbers and at a Mach Number of 1.2. June 6, 1951. NACA RM L51D13.

158. McDearmon, R.W., and H.S. Heinke, Jr.: Investigations of the Damping in Roll of Swept and Tapered Wings at Supersonic Speeds. Mar. 1953. NACA RM L53A13.

159. McDevitt, J.B.: A Correlation by Means of Transonic Similarity Rules of Experimentally Determined Characteristics of a Series of Symmetrical and Cambered Wings of Rectangular Plan Form. 1955. NACA Rep. 1253. Supersedes RM A51L17b; RM A53G31.

160. McDevitt, J.B.: The Linearized Subsonic Flow About Symmetrical Nonlifting Wing-Body Combinations. Apr. 1957. NACA TN 3964.

161. McDevitt, J.B., and W.M. Haire: Investigation at High Subsonic Speeds of a Body-Contouring Method for Alleviating the Adverse Interference at the Root of a Sweptback Wing. Apr. 1956. NACA TN 3672. Supersedes RM A54A22.

162. McFadden, N.M., G.A. Rathert, Jr., and R.S. Bray: The Effectiveness of Wing Vortex Generators in Improving the Maneuvering Characteristics of a Swept-Wing Airplane at Transonic Speeds. Sept. 1955. NACA TN 3523. Supersedes RM A51J18.

163. Madden, R.T.: Aerodynamic Study of a Wing-Fuselage Combination Employing a Wing Sweptback 63°.-Characteristics at a Mach Number of 1.53 Including Effect of Small Variations of Sweep. 26 January 1949. NACA RM A8J04.

164. Madden, R.T.: Aerodynamic Study of a Wing-Fuselage Combination Employing a Wing Sweptback 63°.-Investigation at a Mach Number of 1.53 to Determine the Effects of Cambering and Twisting the Wing for Uniform Load at a Lift Coefficient of 0.25. 6 May 1949. NACA RM A9C07.

165. Martin, J.: The Calculation of Downwash Behind Wings of Arbitrary Plan Form at Supersonic Speeds. NACA TN 2135, 1950.

166. Martina, A. P.: The Interference of a Body on the Spanwise Load Distribution of Two 45° Sweptback Wings of Aspect Ratio 8.02 from Low-Speed Tests. Aug. 1956. NACA TN 3730. Supersedes RM L51K23.

167. Mas, N. A.: Aerodynamic Study of a Wing-Fuselage Combination Employing a Wing Sweptback 63°. -Characteristics for Symmetrical Wing Sections at High Subsonic and Moderate Supersonic Mach Numbers. 7 July 1949. NACA RM A9E09.

168. Mirels, H., and R. Haefeli: Line Vortex Theory for Calculation of Supersonic Downwash. NACA Rep. 983, 1950.

169. Mitcham, G. L., J. E. Stevens, and H. P. Norris: Aerodynamic Characteristics and Flying Qualities of a Tailless Triangular-Wing Airplane Configuration as Obtained from Flights of Rocket-Propelled Models at Transonic and Low Supersonic Speeds. 9 Feb. 1950. NACA RM L9L07.

170. Mitcham, G. L., J. E. Stevens, and H. P. Norris: Aerodynamic Characteristics and Flying Qualities of a Tailless Triangular-Wing Airplane Configuration as Obtained from Flights of Rocket-Propelled Models at Transonic and Low Supersonic Speeds. Nov. 1956. NACA TN 3753. Supersedes RM L9L07.

171. Morgan, F. G., Jr.: Transonic Wind-Tunnel Investigation of the Effects of Wing Incidence Angle on the Characteristics of Two Wing-Body Combinations. Jan. 1953. NACA RM L52K06a.

172. Morikawa, G. K.: The Wing-Body Problem for Linearized Supersonic Flow. Calif. Inst. Tech., Jet Prop. Lab. Progress Rep. 4-116, ORDCIT Project, Dec. 1949.

173. Morikawa, G. K.: "A Non-Planar Boundary Problem for the Wave Equation." Quarterly App. Math. 10(2), 129-140, 1952.

174. Morrow, J. D.: Measurements of the Effect of Trailing-Edge Thickness on the Zero-Lift Drag of Thin Low-Aspect-Ratio Wings. Nov. 1955. NACA TN 3550. Supersedes RM L50F26.

175. Morrow, J. D., and E. Katz: Flight Investigation at Mach Numbers from 0.6 to 1.7 to Determine Drag and Base Pressures on a Blunt-Trailing-Edge Airfoil and Drag of Diamond and Circular-Arc Airfoils at Zero Lift. Nov. 1955. NACA TN 3548. Supersedes RM L50E19a.

176. Muggia, A.: "Sul Calcolo dell'interferenza elica-ala." Atti Acad. Nazl. Lincei, Rome, 11, 53-57, 1951.

177. Multhopp, H.: "Die Berechnung des Abwindes hinter Tragfluegeln." Luftfahrtforschung, 15, 463-467, 1938.

178. Multhopp, H.: "Die Berechnung der Auftriebsverteilung von Tragfluegeln." Luftfahrtforschung 15, 153-169, 1938. Also: Brit. R. T. P. Tran. 2392, 1938. Also: Consolidated Vultee Rep. 1277, 1938.

179. Multhopp, H.: "Zur Aerodynamik des Flugzeugrumpfes." Luftfahrtforschung, 18, 52-66, 1941.

180. Munk, M.: The Aerodynamic Forces on Airslip Hulls. NACA Rep. 184, 1923.

181. Nelson, W. H.: The Transonic Characteristics of Unswept Wings Having Aspect Ratios of 4, Spanwise Variations in Thickness Ratio, and Variations in Plan-Form Taper-Transonic Bump Technique. Mar. 1954. NACA RM A53L17.

182. Nelson, W. H., E. C. Allen, and W. J. Krumm: The Transonic Characteristics of 36 Symmetrical Wings of Varying Taper, Aspect Ratio, and Thickness as Determined by the Transonic-Bump Technique. Dec. 1955. NACA TN 3529. Supersedes RM A53I29.

183. Nelson, W. H., and W. J. Krumm: The Transonic Characteristics of 38 Cambered Rectangular Wings of Varying Aspect Ratio and Thickness as Determined by the Transonic-Bump Technique. June 1955. NACA TN 3502. Formerly RM A52D11.

184. Nelson, W. H., and J. B. McDevitt: The Transonic Characteristics of 22 Rectangular, Symmetrical Wing Models of Varying Aspect Ratio and Thickness. June 1955. NACA TN 3501. Formerly RM A51A12.

185. Nichols, S.: Interference Between Wing and Body at Supersonic Speeds. Part VIII: Data Report on Pressure Distribution Tests of Wing Body Interference Models at Mach Number 2.0, Phase Four Tests of March 1950. Cornell Aer. Lab. Bumblebee Rep. CAL/CF-1571, July 1951.

186. Nielsen, J. N., E. D. Katzen, and K. K. Tang: Lift and Pitching-Moment Interference Between a Pointed Cylindrical Body and Triangular Wings of Various Aspect Ratios at Mach Numbers of 1.50 and 2.02. Dec. 1956. NACA TN 3795. Supersedes RM A50F06.

187. Nielsen, J. N., and W. C. Pitts: Wing Body Interference at Supersonic Speeds with an Application to Combinations with Rectangular Wings. NACA TN 2677, 1952.

188. Olson, R. N., and M. H. Mead: Aerodynamic Study of a Wing-Fuselage Combination Employing a Wing Sweptback 63°. -Effectiveness of an Elevon as a Longitudinal Control and the Effects of Camber and Twist on the Maximum Lift-Drag Ratio at Supersonic Speeds. 8 May 1950. NACA RM A50A31a.

189. Osborne, R. S.: A Transonic-Wing Investigation in the Langley 8-Foot High-Speed Tunnel at High Subsonic Mach Numbers and at a Mach Number of 1.2 Wing-Fuselage Configuration with a Wing of 45° Sweepback, Aspect Ratio 4, Taper Ratio 0.6, and NACA 65A006 Airfoil Section. 10 Oct. 1950. NACA RM L50H08.

190. Osborne, R. S., and J. P. Mugler, Jr.: Aerodynamic Characteristics of a 45° Sweptback Wing-Fuselage Combination and the Fuselage Alone Obtained in the Langley 8-Foot Transonic Tunnel. Sept. 1952. NACA RM L52E14.

191. Palmer, W. E.: Effect of Reduction in Thickness from 6 to 2 Percent and Removal of the Pointed Tips on the Subsonic Static Longitudinal Stability Characteristics of a 60° Triangular Wing in Combination with a Fuselage. Aug. 1953. NACA RM L53F24.

192. Pasamanick, J., and W. I. Scallion: The Effects of Suction Through Porous Leading-Edge Surfaces on the Aerodynamic Characteristics of a 47.5° Sweptback Wing-Fuselage Combination at a Reynolds Number of 4.4×10^6. Mar. 1952. NACA RM L51K15.

193. Peck, R. F., and J. L. Mitchell: Rocket-Model Investigation of Longitudinal Stability and Drag Characteristics of an Airplane Configuration Having a 60° Delta Wing and a High Unswept Horizontal Tail. Jan. 1953. NACA RM L52K04a.

194. Pepper, W. B., Jr.: Free-Flight Tests at Math Numbers from 0.8 to 1.4 to Determine the Effect on Zero-Lift Drag of Increasing the Leading-Edge Bluntness of a 45° Sweptback Wing Having an NACA 65A009 Airfoil. Aug. 1952. NACA RM L52F30.

195. Pepper, W. B., Jr., and S. Hoffman: Transonic Flight Tests to Determine the Effect of Thickness Ratio and Plan-Form Modification on the Zero-Lift Drag of a 45° Sweptback Wing. Aug. 1952. NACA RM L52F02a.

196. Perkins, E. W., and T. N. Canning: Investigation of Downwash and Wake Characteristics at a Mach Number of 1.53. III - Swept Wings. 23 Feb. 1950. NACA RM A9K02.

197. Pittel, M.: Flight Tests at Supersonic Speeds to Determine the Effect of Taper on the Zero-Lift Drag of Sweptback Low-Aspect-Ratio Wings. June 1956. NACA TN 3697. Supersedes RM L50F30a.

198. Pitts, W. C., J. N. Nielsen, and M. P. Gionfriddo: Comparison Between Theory and Experiment for Interference Pressure Field Between Wing and Body at Supersonic Speeds. NACA TN 3128, 1954.

199. Polhamus, E. C.: Some Factors Affecting the Variation of Pitching Moment with Sideslip of Aircraft Configurations. July 1955. NACA RM L55E20b.

200. Polhamus, E. C.: Summary of Results Obtained by Transonic-Bump Method on Effects of Plan Form and Thickness on Lift and Drag Characteristics of Wings at Transonic Speeds. Nov. 1955. NACA TN 3469. Supersedes RM L51H30.

201. Polhamus, E. C., and A. G. Few, Jr.: Pressure Distribution at Low Speed on a Model Incorporating a Wing with Aspect Ratio 6, 45° Sweep Taper Ratio 0.6, and an NACA 65A009 Airfoil Section. Aug. 1952. NACA RM L52F11.

202. Polhamus, E. C., and K. P. Spreemann: Subsonic Wind-Tunnel Investigation of the Effect of Fuselage Afterbody on Directional Stability of Wing-Fuselage Combinations at High Angles of Attack. Dec. 1956. NACA TN 3896.

203. Possio, C.: "Ricerche sperimentali sull'interferenza elica-ala." Aerotecnica, 26, 73-77, 1946.

204. Racisz, S. F.: Wind-Tunnel Investigation at High and Low Subsonic Mach Numbers of Two Unswept Wings Having NACA 2-006 and NACA 65A006 Airfoil Sections. Dec. 1953. NACA RM L53J29.

205. Reed, W. H., III: An Analytical Study of the Effect of Airplane Wake on the Lateral Dispersion of Aerial Sprays. 1954. NACA Rep. 1196. Formerly TN 3032.

206. Robinson, A., and J. Hunter-Tod: Bound and Trailing Vortices in the Linearized Theory of Supersonic Flow, and the Downwash in the Wake of a Delta Wing. College of Aeronautics, Cranfield, Rep. 10, 1947.

207. Robinson, A., and A. D. Young: Note on the Application of the Linearized Theory for Compressible Flow to Transonic Speeds. College of Aer., Cranfield, Rep. 2, 1947.

208. Root, L. E.: "Empennage Design with Single and Multiple Vertical Surfaces." J. Aer. Sci. 6, p. 353, 1939.

209. Rossner, R.: "Die Ermittlung der Aufriebsverteilung am Elliptischen Tragfluegel bei beliebig gegebener Verwindung unter Zugrundelegung des Princips der Einflussfunktion." Jahrbuch deut. Luftfahrtforschung, 1940.

210. Ruden, P.: "Das NACA - Profil in der Nachbarschaft nechteckiger Strahl - und Windschatten - Profile." Jahrbuch deut. Luftfahrtforschung; 114--38, 1939.

211. Sadoff, M., F. M. Matteson, and R. D. Van Dyke, Jr.: The Effect of Blunt-Trailing-Edge Modifications on the High-Speed Stability and Control Characteristics of a Swept-Wing Fighter Airplane. May 1954. NACA RM A54C31.

212. Salmi, R. J.: Horizontal-Tail Effectiveness and Downwash Surveys for Two 47.7° Sweptback Wing-Fuselage Combinations with Aspect Ratios of 5.1 and 6.0 at a Reynolds Number of 6.0×10^6. 12 Jan. 1951. NACA RM L50K06.

213. Saltzman, E. J.: Flight Measurements of Lift and Drag for the Bell X-1 Research Airplane Having a 10-Percent-Thick Wing. Sept. 1953. NACA RM L53F08.

214. Sanders, E. C., Jr.: Damping in Roll of Straight and 45° Swept Wings of Various Taper Ratios Determined at High Subsonic, Transonic, and Supersonic Speeds with Rocket-Powered Models. Oct. 1951. NACA RM L51H14.

215. Sanders, E. C., Jr.: Damping in Roll of Models with 45°, 60°, and 70° Delta Wings Determined at High-Subsonic, Transonic, and Supersonic Speeds with Rocket-Powered Models. June 1952. NACA RM L52D22a.

216. Sanders, E. C., Jr., and J. L. Edmondson: Damping in Roll of Rocket-Powered Test Vehicles Having Swept, Tapered Wings of Low Aspect Ratio. Oct. 1951. NACA RM L51G06.

217. Scher, S. H., and L. J. Gale: An Investigation of the Spin and Recovery Characteristics of a 1/25-Scale Model of the Douglas D-558-II Airplane. 18 Jan. 1949. NACA RM L8K19a.

218. Schlichting, H.: Ueber das ebene Windschatten problem. Dissertation, Goettingen, 1930.

219. Selan, R., and A. Bandettini: The Effects of Leading-Edge Extensions, a Trailing-Edge Extension, and a Fence on the Static Longitudinal Stability of a Wing-Fuselage-Tail Combination Having a Wing with 35° of Sweepback and an Aspect Ratio of 4.5. Aug. 1953. NACA RM A53E12.

220. Shibata, H. H., A. Bandettini, and J. Cleary: An Investigation Throughout the Subsonic Speed Range of a Full-Span and a Semispan Model of a Plane Wing and of a Cambered and Twisted Wing, All Having 45° of Sweepback. June 1952. NACA RM A52D01.

221. Silvers, H. N., and T. J. King, Jr.: A Small-Scale Investigation of the Effect of Spanwise and Chordwise-Positioning of a Ogive-Cylinder Underwing Nacelle on the High-Speed Aerodynamic Characteristics of a 45° Sweptback Tapered-in-Thickness Wing of Aspect Ratio 6. Dec. 1952. NACA RM L52J22.

222. Silvers, H. N., and T. J. King, Jr.: Investigation of the Effect of Chordwise Positioning and Shape of an Underwing Nacelle on the High-Speed Aerodynamic Characteristics of a 45° Sweptback Tapered-in-Thickness-Ratio Wing of Aspect Ratio 6. Jan. 1953. NACA RM L52K25.

223. Silvers, H. N., T. J. King, Jr., and T. B. Pasteur, Jr.: Investigation of the Effect of a Nacelle at Various Chordwise and Vertical Positions on the Aerodynamic Characteristics at High Subsonic Speeds of a 45° Sweptback Wing with and without a Fuselage. Sept. 1951. NACA RM L51H16.

224. Silverstein, A., and S. Katzoff: Design Charts for Predicting Downwash Angles and Wake Characteristics Behind Plain and Flapped Wings. NACA Rep. 648, 1939.

225. Silverstein, A., S. Katzoff, and W. K. Bullivant: Downwash and Wake Behind Plain and Flapped Airfoils. NACA Rep. 651, 1939.

226. Sleeman, W. C., Jr.: Experimental Investigation at High Subsonic Speeds to Determine the Rolling-Stability Derivatives of Three Wing-Fuselage Configurations. Oct. 1954. NACA RM L54H11.

227. Smith, D. W., and J. C. Heitmeyer: Lift, Drag, and Pitching Moment of Low-Aspect-Ratio Wings at Subsonic and Supersonic Speeds-Plane Triangular Wing of Aspect Ratio 2 with NACA 0005-63 Section. 1 Feb. 1951. NACA RM A50K21.

228. Smith, D. W., and V. D. Reed: Subsonic Static Longitudinal Stability and Control Characteristics of a Wing-Body Combination Having a Pointed Wing of Aspect Ratio 2 with Constant-Percent-Chord Trailing-Edge Elevons. May 1953. NACA RM A53C20.

229. Smith, D. W., H. H. Shibata, and R. Selan: Lift, Drag, and Pitching Moment of Low-Aspect-Ratio Wings at Subsonic and Supersonic Speeds. -An Investigation at Large Reynolds Numbers of the Low-Speed Characteristics of Several Wing-Body Combinations. Feb. 1952. NACA RM A51K28.

230. Smith, L. A.: Tabulated Pressure Coefficients and Aerodynamic Characteristics Measured on the Wing of the Bell X-1 Airplane in an Unaccelerated Stall and in Pull-Ups at Mach Numbers of 0.74, 0.75, 0.94, and 0.97. 19 June 1951. NACA RM L51B23.

231. Spooner, S. H., and A. P. Martina: Longitudinal Stability Characteristics of a 42° Sweptback Wing and Tail Combination at a Reynolds Number of 6.8×10^6. 22 July 22 1948. NACA RM L8E12.

232. Spreemann, K. P.: Experimental Investigation at High Subsonic Speeds of the Effects of Leading-Edge Radius on the Aerodynamic Characteristics of a Sweptback-Wing-Fuselage Combination with Leading-Edge Flaps and Chord-Extensions. July 1955. NACA RM L55E25a.

233. Spreemann, K. P., and W. J. Alford, Jr.: Investigation of the Effects of Geometric Changes in an Underwing Pylon-Suspended External-Store Installation on the Aerodynamic Characteristics of a 45° Sweptback Wing at High Subsonic Speeds. 5 Mar. 1951. NACA RM L50L12.

234. Spreemann, K. P., and W. J. Alford, Jr.: Investigation of the Effects of Twist and Camber on the Aerodynamic Characteristics of a 50° 38' Sweptback Wing of Aspect Ratio 2.98. Transonic-Bump Method. Aug. 1951. NACA RM L51C16.

235. Spreemann, K. P., and H. N. Silvers: Experimental Investigation of Various Wing-Mounted External Stores on a Wing-Fuselage Combination Having a Sweptback Wing of Inverse Taper Ratio. 15 Sept. 1950. NACA RM L9J06.

236. Spreiter, J.R.: The Aerodynamic Forces on Slender Plane- and Cruciform-Wing and Body Combinations. NACA Rep. 962, 1950.

237. Spreiter, J.R.: Downwash and Sidewash Fields Behind Cruciform Wings. Jan. 1952. NACA RM A51L17.

238. Stewart, H.J.: "The Lift of Delta Wing at Supersonic Speeds." Quart. Appl. Math. 4(3), 246-254, 1946.

239. Stocker, P.M.: "Supersonic Flow Past Bodies of Revolution with Thin Wings of Small Aspect Ratio." Aer. Quart. 3, Part 1, May 1951, pp. 28-42.

240. Stone, D.G.: Flight-Test Evaluation of the Longitudinal Stability and Control Characteristics of 0.5-Scale Models of the Lark Pilotless-Aircraft Configuration. 6 Feb. 1948. NACA RM L7I26.

241. Stone, D.G.: Wing-Dropping Characteristics of Some Straight and Swept Wings at Transonic Speeds as Determined with Rocket-Powered Models. 26 May 1950. NACA RM L50C01.

242. Stone, D.G.: A Collection of Data for Zero-Lift Damping in Roll of Wing-Body Combinations as Determined with Rocket-Powered Models Equipped with Roll-Torque Nozzles. July 1953. NACA RM L53E26.

243. Stone, D.G.: A Collection of Data for Zero-Lift Damping in Roll of Wing-Body Combinations as Determined with Rocket-Powered Models Equipped with Roll-Torque Nozzles. Apr. 1957. NACA TN 3955. Supersedes RM L53E26.

244. Strass, H.K., and E.T. Marley: Rolling Effectiveness of All-Movable Wings at Small Angles of Incidence at Mach Numbers from 0.6 to 1.6. Oct. 1951. NACA RM L51H03.

245. Sutton, F.B., and A. Martin: Aerodynamic Characteristics Including Pressure Distributions of a Fuselage and Three Combinations of the Fuselage with Sweptback Wings at High Subsonic Speeds. 6 Feb. 1951. NACA RM A50J26a.

246. Tinling, B. E., and A. E. Lopez: The Effects of Reynolds Number at Mach Numbers Up to 0.94 on the Loading on a 35° Sweptback Wing Having NACA 651A012 Streamwise Sections. June 1952. NACA RM A52B20.

247. Tinling, B. E., and A. E. Lopez: The Effects of Horizontal-Tail Location and Size on the Subsonic Longitudinal Aerodynamic Characteristics of an Airplane Model Having a Triangular Wing of Aspect Ratio 3. Mar. 1954. NACA RM A53L15.

248. Tucker, W. A.: A Method for the Design of Sweptback Wings Warped to Produce Specified Flight Characteristics at Supersonic Speeds. 1955. NACA Rep. 1226. Supersedes RM L51F08.

249. Turner, T. R.: Effects of Sweep on the Maximum-Lift Characteristics of Four Aspect-Ratio-4 Wings at Transonic Speeds. July 1955. NACA TN 3468. Formerly RM L50H11.

250. Vandrey, F.: "Abschaetzung des Rump feinflusses auf das Laengsmoment eines Flugzeuges." Jahrbuch deut. Luftfahrtforschung, 367-370, 1940.

251. Vincenti, W. G.: Measurements of the Effects of Finite Span on the Pressure Distribution Over Double-Wedge Wings at Mach Numbers Near Shock Attachment. Sept. 1955. NACA TN 3522.

252. Vitale, A. J.: Effects of Wing Elasticity on the Aerodynamic Characteristics of an Airplane Configuration Having 45° Sweptback Wings as Obtained From Free-Flight Rocket-Model Tests at Transonic Speeds. Jan. 1953. NACA RM L52L30.

253. Walker, H. J., and W. C. Maillard: A Correlation of Airfoil Section Data with the Aerodynamic Loads Measured on a 45° Sweptback Wing Model at Subsonic Mach Numbers. May 1955. NACA RM A55C08.

254. Ward, G. N.: "Supersonic Flow Past Slender Pointed Bodies." Quart. J. Mech. and Appl. Math. 2, Part 1, March 1949, pp. 37-59.

255. Ward, G. N.: "Supersonic Flow Past Thin Wings. I. General Theory" Quart. J. Mech. and Appl. Math. 2, Part 2, 136-152, 1949.

256. Weil, J., and W. C. Sleeman, Jr.: Prediction of the Effects of Propeller Operation on the Static Longitudinal Stability of Single Engine Tractor Monoplanes with Flaps Retracted. NACA Rep. 941, 1949.

257. Weil, J., W. C. Sleeman, Jr., and A. L. Byrnes, Jr.: Investigation of the Effects of Wing and Tail Modifications on the Low-Speed Stability Characteristics of a Model Having a Thin 40° Swept Wing of Aspect Ratio 3.5. Apr. 1953. NACA RM L53C09.

258. Weinig, F.: Aerodynamik der Luftschraube. Springer Verlag, Berlin 1940. Also: Air Documents Division, Intelligence Department, U.S. Air Material Command, Dayton, 366-369, 1947.

259. Weissinger, S.: Ueber die Auftriebsverteilung von Pfeilfluegeln. Zentrale fuer wissenschaftliches Berichtwesen der Luftfahrtforschung des Generalluftzeugmeisters (ZWB), Berich 1553, Feb. 1942. Also: NACA TM 1120, Mar. 1947.

260. Well, J., G. S. Campbell, and M. S. Diederich: An Analysis of Estimated and Experimental Transonic Downwash Characteristics as Affected by Plan Form and Thickness for Wing and Wing-Fuselage Configurations. Apr. 1956. NACA TN 3628. Supersedes RM L52I22.

261. West, F. E., Jr., G. Liner, and G. S. Martz: Effect of Leading-Edge Chord-Extension on the Aerodynamic Characteristics of a 45° Sweptback Wing-Fuselage Combination at Mach Numbers of 0.40 to 1.03. Apr. 1953. NACA RM L53B02.

262. Whitcomb, R. T.: A Study of the Zero-Lift Drag-Rise Characteristics of Wing-Body Combinations Near the Speed of Sound. Sept. 1952. NACA RM L52H08.

263. Whitcomb, R. T.: A Study of the Zero-Lift Drag-Rise Characteristics of Wing-Body Combinations Near the Speed of Sound. 1956. NACA Rep. 1273. Supersedes RM L52H08.

264. Whitcomb, R. T., and T. C. Kelly: A Study of the Flow Over a 45° Sweptback Wing-Fuselage Combination at Transonic Mach Numbers. June 1952. NACA RM L52D01.

265. White, M. D.: Effect of Camber and Twist on the Stability Characteristics of Models Having a 45° Swept Wing as Determined by the Free-Fall Method at Transonic Speeds. Aug. 1952. NACA RM A62F16.

266. White, M. D.: A Flight Investigation at Transonic Speeds of a Model Having a Triangular Wing of Aspect Ratio 3. June 1955. NACA RM A55D18.

267. Wieselsberger, C.: Der Einfluss von eingebauten Motorgondeln auf die Luftkraefte eines Tragfluegels. Inter. Eng. Con. Paper 203, Tokyo, 1929.

268. Wiggins, J. W.: Wind-Tunnel-Investigation at High Subsonic Speeds of the Static Longitudinal and Static Lateral Stability Characteristics of a Wing-Fuselage Combination Having a Triangular Wing of Aspect Ratio 2.31 and an NACA 65A003 Airfoil. Aug. 1953. NACA RM L53G09a.

269. Wiggins, J. W.: Wind-Tunnel Investigation at High Subsonic Speeds to Determine the Rolling Derivatives of Two Wing-Fuselage Combinations Having Triangular Wings, Including a Semi-empirical Method of Estimating the Rolling Derivatives. Feb. 1954. NACA RM L53L18a.

270. Wiggins, J. W., and P. G. Fournier: Wind-Tunnel Investigation of the Static Lateral Stability Characteristics of Wing-Fuselage Combinations at High Subsonic Speeds. Taper-Ratio Series. Apr. 1953. NACA RM L53B25a.

271. Wiggins, J. W., and R. E. Kuhn: Wind-Tunnel Investigation of the Aerodynamic Characteristics in Pitch of Wing-Fuselage Combinations at High-Subsonic Speeds. July 1952. NACA RM L52D16.

272. Wiggins, J. W., and R. E. Kuhn: Wind-Tunnel Investigation of the Effects of Steady Rolling on the Aerodynamic Loading Characteristics of a 45° Sweptback Wing at High Subsonic Speeds. Nov. 1953. NACA RM L53J01a.

273. Wiley, H. G., and W. C. Moseley, Jr.: An Investigation at High Subsonic Speeds of the Pressure Distributions on a 45° Sweptback Vertical Tail in Sideslip with and without a 45° Sweptback Horizontal Tail Located on the Fuselage Center Line. Nov. 1954. NACA RM L54H23.

274. Wolhart, W. D.: Static Longitudinal Stability Characteristics of a Composite-Plan-Form Wing Model Including Some Comparisons with a 45° Sweptback Wing at Transonic Speeds. Aug. 1954. NACA RM L54F24.

275. Wood, R. B., and F. F. Fleming: A Transonic-Wing Investigation in the Langley 8-Foot High-Speed Tunnel at High Subsonic Mach Numbers and at a Mach Number of 1.2 Wing-Fuselage Configuration Having a Wing of 60°-Sweepback, Aspect Ratio 4, Taper Ratio 0.6, and NACA 65A006 Airfoil Section. 24 Jan. 1951. NACA RM L50J25.

276. Young, de, Jr., and C. W. Harper: Theoretical Symmetric Span Loading at Subsonic Speeds for Wings Having Arbitrary Planform. NACA Rep. 921, 1948.

277. Zahm, F.: Flow and Force Equations for a Body Revolving in a Fluid. NACA Rep. 323, 1928.

Chapter 2

EFFECTS OF CONTROL FLAPS AND AILERONS

2.1 General Remarks

The results of the control flaps upon the pressure distribution can be deduced from the tests in wind tunnels. At Mach numbers below the critical value changes of flap angle have considerable effects on the pressures in front of the hinge, but at high Mach numbers, when shock waves occur at or behind the hinge line, the pressures in front of the hinge are nearly independent of the flap angle. This result is to be expected, because at high Mach numbers there is a large supersonic region, extending forward from the shock wave towards the leading edge, and changes due to movements of the flap cannot be transmitted upstream through this supersonic region. The loss of control effectiveness due to this phenomenon is discussed below.

Another important phenomenon, which takes place over a fairly narrow range of Mach number around 0.85 is of the following nature. In general, when there is a well developed supersonic region on one surface of an airfoil with a control flap, this is terminated by a normal shock at the control hinge, with severe thickening (possibly separation of the boundary layer there). It appears that it may often happen that at a slightly higher Mach number the flow behind the hinge reattaches itself to the surface, the necessary turning of the flow at the hinge occurring through an oblique shock wave of suitable magnitude or even in some cases through a Prandtl-Meyer expansion.

A normal shock wave with thickening of the boundary layer then occurs farther back along the control and may even be delayed to the trailing edge. It has been verified that this effect is not dependent on the state of the boundary layer before the hinge, since very similar changes occurred in an experiment when the stream ahead of the airfoil was made turbulent by a wire. It seems necessary that the pressure distribution ahead of the hinge should be favorable (i.e., accelerating flow) and that a high local Mach number, about 1.4 for an oblique shock wave, 1.25 for a Prandtl-Meyer expansion, should be reached.

The effectiveness of the flap as a control decreases to zero at high Mach numbers. This loss of control is explained by the fact that, at high Mach numbers, the pressures on the part of the airfoil in front of the hinge are not affected by changes of flap angle. Thus, changes of flap angle at high Mach numbers can only affect the lift on the flap itself, and cannot affect the lift on the front part of the airfoil. The reversal of control effectiveness for Mach numbers above 0.8, is caused by fore and aft movements of the shock waves on the flap.

2.2 Airfoil with Flap or Aileron in Incompressible Flow

Assume a broken straight line as the mean line of the airfoil. This represents the idealized case of an airfoil with a flap like an aileron, or the case of a tail surface with a rudder. The chord of the mean wing may have the length C_1, the chord of the flap the length C_2. The value of the angle θ corresponding to the intersection between the two straight portions of the airfoil, at the hinge will be denoted by θ_0. The angle of attack of the main wing may be equal to α, the angle of attack of the flap $(\alpha - \delta)$, and the relative angle between flap and main wings δ. One can use Munk's formula to find the total lift acting on the system. The circulation Γ is given by the formula

$$\Gamma = -2aV\int_0^{2\pi} \frac{dy}{dx}(1 + \cos\tau)\,d\tau \quad , \tag{2.1}$$

where

V = the velocity of the incoming flow

$4a \approx$ length of the chord

$y = y(x)$ = the equation of the shape of the airfoil.

In the case under consideration, the formula (2.1) takes the form

$$\Gamma = 2Va\alpha\int_{\theta_0}^{2\pi-\theta_0} (1 + \cos\theta)\,d\theta + 2Va(\alpha - \delta)\int_{-\theta_0}^{\theta_0} (1 + \cos\theta)d\theta \quad , \tag{2.2}$$

or

$$\Gamma = 2Va\alpha\int_0^{2\pi} (1 + \cos\theta)d\theta - 2Va\,\delta\int_{-\theta_0}^{+\theta_0} (1 + \cos\theta)d\theta \quad ; \tag{2.3}$$

evaluating the integrals we obtain

$$\Gamma = 4\pi Va\left[\alpha - \delta\left(\frac{\theta_0}{\pi} + \frac{\sin\theta_0}{\pi}\right)\right] \quad , \tag{2.4}$$

$$L = 4\pi\rho a V^2\left[\alpha - \delta\left(\frac{\theta_0}{\pi} + \frac{\sin\theta_0}{\pi}\right)\right] \quad . \tag{2.5}$$

This equation shows that the inclination δ of the flap is equivalent to a decrease of the angle of attack by $\Delta\alpha = \delta(\theta_0 + \sin\theta_0)/\pi$. The angle θ_0 is given by $\cos\theta_0 \simeq 1 - 2c_2/c$. For small values of c_2/c one may write $\theta_0 \simeq \sin\theta_0 \simeq 2\sqrt{c_2/c}$, so that the change of the angle of attack amounts to $\Delta\alpha = 4\delta/\pi \sqrt{c_2/c}$. This is a simple rule for estimating the effect of the ailerons on the total lift of a wing section. The second point of interest is the hinge moment. This is the moment of the forces acting on the flap relative to the hinge. Let x_0 denote the abscissa of the hinge; then one has

$$M_h = \rho V \int_{x_0}^{c/2} \overline{\gamma}(x)(x - x_0)\, dx \quad , \tag{2.6}$$

or

$$M_h = \rho V \frac{c^2}{4} \int_0^{\theta_0} \overline{\gamma}(\theta)(\cos\theta - \cos\theta_0)\sin\theta\, d\theta \quad . \tag{2.7}$$

The quantity $\overline{\gamma}(\theta)$ is given by the formula

$$\overline{\gamma} = -\frac{V\alpha}{\pi\sin\theta} \int_0^{2\pi} \frac{dy}{dx} \cot\frac{\theta - \tau}{2} \sin\tau\, d\tau + \Gamma(2\pi a \sin\theta)^{-1} \quad ; \tag{2.8}$$

again putting $dy/dx = -\alpha$ for $\theta_0 < \theta < (2\pi - \theta_0)$, and $dy/dx = -(\alpha - \delta)$ for $-\theta_0 < \theta < \theta_0$, we have

$$\overline{\gamma} = \frac{V\alpha}{\pi\sin\theta} \int_0^{2\pi} \cot\frac{\theta - \tau}{2} \sin\tau\, d\tau - \frac{V\delta}{\pi\sin\theta} \int_{-\theta_0}^{\theta_0} \cot\frac{\theta - \tau}{2} \sin\tau\, d\tau$$

$$+ \Gamma(2\pi a \sin\theta)^{-1} \quad . \tag{2.9}$$

Thus the hinge moment has the value

$$M_h = 4\rho V^2 a^2 (\eta_1 \alpha + \eta_2 \delta) \quad , \tag{2.10}$$

where

$$\eta_1 = \frac{1}{\pi} \int_0^{\theta_0} (\cos\theta - \cos\theta_0) d\theta \int_0^{2\pi} \cot\frac{\theta - \tau}{2} \sin\tau\, d\tau + 2\int_0^{\theta_0} (\cos\theta - \cos\theta_0)\, d\theta \quad ; \tag{2.11a}$$

$$\eta_2 = -\frac{1}{\pi} \int_0^{\theta_0} (\cos\theta - \cos\theta_0) d\theta \int_{-\theta_0}^{\theta_0} \cot\frac{\theta - \tau}{2} \sin\tau\, d\tau$$

$$- \frac{2}{\pi}(\theta_0 + \sin\theta_0) \int_0^{\theta_0} (\cos\theta - \cos\theta_0) d\theta \quad . \tag{2.11b}$$

Now one has

$$\int_0^{2\pi} \cot \frac{\theta - \tau}{2} \sin \tau \, d\tau = -2\pi \cos \theta \quad ; \qquad (2.12)$$

thus one has

$$\eta_1 = -\theta_0 + \sin \theta_0 \cos \theta_0 + 2 \sin \theta_0 - 2\theta_0 \cos \theta_0 \; . \qquad (2.13)$$

To calculate η_2 we have to evaluate the integrals

$$T_1 = \int_0^{\theta_0} \int_0^{\theta_0} \cos \theta \sin \tau \cot \frac{\theta - \tau}{2} \, d\theta \, d\tau \quad ; \qquad (2.14)$$

$$T_2 = \int_0^{\theta_0} \int_{-\theta_0}^{0} \cos \theta \sin \tau \cot \frac{\theta - \tau}{2} \, d\theta \, d\tau \quad ; \qquad (2.15)$$

$$T_3 = \int_0^{\theta_0} \int_0^{\theta_0} \sin \tau \cot \frac{\theta - \tau}{2} \, d\theta \, d\tau \quad . \qquad (2.16)$$

Next one gets

$$T_1 = \frac{1}{2} \int_0^{\theta_0} \int_0^{\theta_0} (\cos \theta \sin \tau - \cos \tau \sin \theta) \cot \frac{\theta - \tau}{2} \, d\theta \, d\tau$$

$$= \frac{1}{2} \int_0^{\theta_0} \int_0^{\theta_0} \sin(\tau - \theta) \cot \frac{\theta - \tau}{2} \, d\theta \, d\tau \quad , \qquad (2.17)$$

or

$$T_1 = -\frac{1}{2} \int_0^{\theta_0} \int_0^{\theta_0} 1 + \cos(\theta - \tau) \, d\theta \, d\tau = -\frac{\theta_0^2}{2} - \frac{\sin^2 \theta_0}{2} - \frac{(1 - \cos \theta_0)^2}{2} \; . \qquad (2.18)$$

In a similar way we obtain

$$T_2 = -\frac{\theta_0^2}{2} - \frac{\sin^2 \theta_0}{2} + \frac{(1 - \cos \theta_0)^2}{2} \quad ; \qquad (2.19)$$

$$T_3 = \frac{1}{2} \int_0^{\theta_0} \int_0^{\theta_0} (\sin \tau - \theta) \cot \frac{\theta - \tau}{2} \, d\tau \, d\theta \quad ; \qquad (2.20)$$

since

$$\int_0^{\theta_0} \int_0^{\theta_0} \sin \tau \cot \frac{\tau - \theta}{2} \, d\tau \, d\theta = \int_0^{\theta_0} \int_0^{\theta_0} \sin \theta \cot \frac{\tau - \theta}{2} \, d\theta \, d\tau \quad ; \qquad (2.21)$$

$$\sin \tau - \sin \theta = 2 \cos \frac{\tau + \theta}{2} \sin \frac{\tau - \theta}{2} \quad ; \qquad (2.22)$$

thus

$$T_3 = \frac{1}{2}\int_0^{\theta_0}\int_0^{\theta_0} (\sin\tau - \sin\theta)\cot\frac{\theta-\tau}{2}\, d\tau\, d\theta$$

$$= -\int_0^{\theta_0}\int_0^{\theta_0} \cos\frac{\theta-\tau}{2}\cos\frac{\theta+\tau}{2}\, d\tau\, d\theta = -\frac{1}{2}\int_0^{\theta_0}\int_0^{\theta_0}(\cos\tau + \cos\theta)d\tau\, d\theta \; ; \quad (2.23)$$

or

$$T_3 = -\int_0^{\theta_0}\int_0^{\theta_0} \cos\tau\, d\tau\, d\theta = -\theta_0\int_0^{\theta_0}\cos\tau\, d\tau = -\theta_0 \sin\theta_0 \; . \quad (2.24)$$

The expression for η_2 takes the form

$$\eta_2 = \frac{1}{\pi}\left[\theta_0^2 + 2\theta_0^2\cos\theta_0 - 2\theta_0\sin\theta_0 - \sin^2\theta_0\right] \; . \quad (2.25)$$

For small values of θ_0, i.e., of c_2/c, we find

$$\eta_2\,\alpha + \eta_2\,\delta = \frac{\theta_0^5}{15}\,\alpha - \frac{\theta_0^4}{3}\,\frac{\delta}{\pi} \; . \quad (2.26)$$

Let

$$M_h = C_h c_1^2\,\frac{1}{2}\,\rho V^2 \; , \quad (2.27)$$

then the coefficient C_h is equal to

$$C_h \simeq \frac{4}{3}\sqrt{\frac{c}{c_1}}\;\alpha - \frac{8}{3\pi}\;\delta \; . \quad (2.28)$$

Below we shall present another way of calculating the changes in forces when the ailerons are moved out of their neutral position. When this happens, the characteristic properties of the airfoil profile show an abrupt change at particular values of y. Moreover, in the ordinary case, when the ailerons are moved in opposite directions, the lift distribution ceases to be symmetrical. The problem of determining the distribution of the lift in such cases has been attacked from various sides. We shall at first present a general method proposed by Trefftz.

Consider a two-dimensional field of motion, which is to be found in a section of the wake at a great distance behind the airfoil. This field is generated by the system of trailing vortices, which form a band along the y-axis, stretching from y = -b to y = +b. The general conditions, from which the integral equation can be obtained, may be expressed in the form of a boundary condition for the potential of this two-dimensional field. With the aid of conformal transformation the field is brought into relation with the field outside of a circle of unit radius; then the potential is approximated by a trigonometric expression and an approximate solution given by Trefftz have been the starting point for much of the further work on this subject.

A new variable ψ is substituted for y, defined by the relation

$$y = -b\cos\psi \quad ; \tag{2.29}$$

the connection between ψ and y is such that to y = -b corresponds the value $\psi = 0$; for y = 0, $\psi = \frac{\pi}{2}$ and for y = +b, $\psi = \pi$. It is then assumed that ℓ (lift per unit span) can be developed into a series proceeding according to sines of multiples of the angle ψ, of the form

$$\ell = 4\rho V^2 b \sum A_n \sin n\psi \quad , \tag{2.30}$$

where the A_n represents a set, finite or infinite, of numerical coefficients. This series belongs to the type of trigonometric series, and it is known that a great number of functions can be approximated in a satisfactory way by taking only a limited number of terms. The series written in Eq. (2.30) satisfies the condition that ρ becomes zero at the wing tips in a way mathematically equivalent to that assumed in Eq. (2.31);

$$\ell = \sqrt{b^2 - y^2}\,(\ell_0 + \ell_2 y^2 + \ell_4 y^4 + \dots) \quad . \tag{2.31}$$

Let us now substitute Eq. (2.30) into the formula

$$\phi = \frac{w}{V} = \frac{1}{\rho V^2} \int_{-b}^{+b} d\eta \, \frac{d\ell/d\eta}{4\pi(y-\eta)} \quad , \tag{2.32}$$

where w denotes the vertical velocity. Writing

$$-b\cos\psi' = \eta \quad ; \quad d\eta = b\sin\psi'\, d\psi \, , \tag{2.33}$$

one gets

$$\frac{d\ell}{d\eta} = 4\rho V^2 \, \frac{\sum nA_n \cos n\psi'}{\sin\psi'} \quad , \tag{2.34}$$

which furnishes

$$\phi = \int_0^\pi d\psi' \frac{\sum nA_n \cos n\psi'}{\pi(\cos\psi' - \cos\psi)} \quad . \tag{2.35}$$

Making use of the equation

$$\int_0^\pi d\psi' \frac{\cos n\psi}{\cos\psi' - \cos\psi} = \pi \frac{\sin n\psi}{\sin\psi} \quad , \tag{2.36}$$

the expression for ϕ takes the form

$$\phi = \sum nA_n \frac{\sin n\psi}{\sin\psi} \quad . \tag{2.37}$$

The expressions (2. 30) and (2. 37) are now inserted into the expression for the lift per unit span, ℓ, containing the effective angle of incidence $(\alpha - \phi)$;

$$\ell = \frac{1}{2}\rho V^2 c\; m(\alpha - \phi) \quad , \tag{2.38}$$

where the symbols used denote:

c = chord of the profile

m = constant, equal approximately to 2π.

After some manipulations one gets

$$\sum A_n \sin n\psi = \frac{mc}{8b}\left(\alpha - \sum nA_n \frac{\sin n\psi}{\sin\psi}\right) \quad , \tag{2.39}$$

Usually, c, m, α are known functions of y, and thus also of the auxiliary variable ψ. Writing

$$\mu = \frac{mc}{8b} \quad , \tag{2.40}$$

and further taking together the terms containing the A's , and multiplying by $\sin\psi$, we can transform Eq. (2. 39) into

$$\sum A_n \sin n\psi\,(n\mu + \sin\psi) = \mu\,\alpha \sin\psi \quad . \tag{2.41}$$

This equation is the basic relation considered in the theory of airfoils. The exact solution of the problem of the lift distribution would require that Eq. (2. 41) should be satisfied for all values of ψ from 0 to π inclusive. This, however, in general can be obtained only by taking an infinite number of terms in the series (2. 30). The method commonly used in searching for an approximate solution is to require that (2. 39) shall be satisfied at a limited number of points only. Then the number of coefficients can be limited to the same value as the number of points. Applying Eq. (2.39) to each of these points, a sufficient set of equations is obtained, from which the values of the coefficients A_n can be found without great difficulty. The degree of approximation obtained in this way naturally becomes greater with increase in the number of points. When the determination of the A's has been effected, the distribution of ℓ and of the angle ϕ can be calculated.

This technique will be applied below to the wing with an aileron. The method of solution which is usually applied to the wing (without an aileron) theory and in which usually only four terms are used, becomes less satisfactory in this case, and it is necessary to take a greater number of terms. Wieselsberger has remarked that as now the influence of the wing tips becomes rather important (in the circulation of the moments M_x and M_z) care must be taken that Eq. (2.29) is satisfied at the points $\psi = 0$ and $\psi = \pi$. This equation is fully equivalent to Eq. (2.41) at all points where $\sin\psi$ is different from zero. However, at the points $\psi = 0$ and $\psi = \pi$, Eq. (2.41) is satisfied automatically, while Eq. (2.39) still imposes a condition on the A's. Taking the first point, $\psi = 0$, it is seen that this condition assumes the form

$$\sum n^2 A_n = \alpha \quad . \tag{2.42}$$

At the point $\psi = \pi$, a similar equation is obtained where the terms of even index, however, have the minus sign.

In treating the aileron problem for the rectangular wing it is assumed that both c and m remain constant along the span, while the angle of incidence has the following values:

$$\begin{aligned} &-b < y < a \ (0 < \psi < \psi_a): \ \alpha + \epsilon \quad ; \\ &-a < y < +a (\psi_a < \psi < \pi - \psi_a): \ \alpha \quad ; \\ &+a < y + b \ (\pi - \psi_a < \psi < \pi): \ \alpha - \epsilon \quad . \end{aligned} \tag{2.43}$$

Here (b - a) denotes the length of the ailerons, while the angle ψ_a is defined by

$$a = b \cos\psi_a \quad . \tag{2.44}$$

As Eq. (2.41) is linear both in the A's and in the angle of incidence, it is possible to build up the solution as the sum of two special solutions, one relating to a constant angle of incidence of the magnitude α, the other to an angle of incidence having the values

$$0 < \psi < \psi_a : +\epsilon \quad ;$$
$$\psi_a < \psi < \pi - \psi_a : 0 \quad ;$$
$$\pi - \psi_a < \psi < \pi : -\epsilon \quad . \qquad (2.45)$$

The first solution is the symmetrical solution for the rectangular wing with constant angle of incidence, which has been considered in many numerical examples. Hence, it remains to consider the other solution, which has an antisymmetrical lift distribution to be represented by a series containing only the sines of even multiples of the angle ψ. One may take 8 terms in this series, with coefficients A_2, $A_4, \ldots, A_{16}$, determined by means of the conditions: (a) that Eq. (2.42) must be satisfied (relating to the point $\psi = 0^\circ$); (b) that Eq. (2.41) must be satisfied at the points $\psi = 20^\circ$, 35°, 45°, 55°, 65°, 75°, 85°, respectively. It is then automatically satisfied also for the other half of the airfoil.

One may consider four cases, in which the angle ψ_a respectively has the values 40°, 60°, 70°, 90°. As these points lie between the points where (2.41) must be satisfied, the problem treated does not actually represent the case of an abrupt change of the angle of incidence, but corresponds to a certain gradual change.

The results obtained by previous authors may be expressed in the following form:

$$M_x = \frac{1}{2} \rho V^2 (2b)^3 \zeta \epsilon \quad ; \qquad (2.46)$$

$$M_z = \frac{1}{2} \rho V^2 (2b)^3 \xi \alpha \epsilon \quad ; \qquad (2.47)$$

$$\delta D_i = \frac{1}{2} \rho V^2 (2b)^2 \eta \epsilon^2 \quad . \qquad (2.48)$$

The symbols used denote:

M_x, M_z = the values of the moments;

δD_i = the increase in induced drag.

For the case of aspect ratio $\lambda = (2b)^2/S$, S = the area of the wing, $\mu = 1/4$, Eq. (2.40), the numbers ζ, ξ, η are given in the table below. The ratio $(b-a)/b$ is the ratio of the length of an aileron to half span of the airfoil.

ψ_a	$\frac{b-a}{b}$	ζ	ξ	η
40°	0.234	0.047	0.0492	0.0462
60°	0.500	0.100	0.0895	0.1114
70°	0.658	0.114	0.0965	0.1440
90°	1.000	0.135	0.1089	0.1980

Another case which may be of interest is the case where both ailerons are moved in the same direction. In that case no moments are obtained; there is, however, an increase both of lift and of induced drag, which are expressed by equations of the form

$$\delta L = \frac{1}{2} \rho V^2 (2b)^2 \mathcal{K}_L \, \epsilon \quad ; \tag{2.49}$$

$$\delta D_i = \frac{1}{2} \rho V^2 (2b)^2 \mathcal{K}_D \, \epsilon \quad ; \tag{2.50}$$

The coefficients $\mathcal{K}_L$, $\mathcal{K}_D$ for the same case as mentioned above, are given in the following table.

ψ_a	$\frac{b-a}{b}$	$\mathcal{K}_L$	$\mathcal{K}_D$
40^o	0.234	0.130	0.056
60^o	0.500	0.326	0.116
70^0	0.658	0.442	0.137
80^o	0.826	0.587	0.163
90^o	1.000	0.729	0.178

Another set of calculations has been developed by Gates. It differs from the method described above by the way in which the coefficients of the Fourier series are determined. Instead of applying the condition that Eq. (2.41) must be satisfied at a finite number of points, equal to the number of terms retained in the series, it is required that the square of the error remaining in the fulfillment of this ecuation, integrated over the whole span, shall be a minimum. This condition is expressed by the set of equations

$$\frac{\partial}{\partial A_n} \int_0^{\pi} d\psi \left[\sum A_n \sin n\psi (n\mu + \sin\psi) - \mu\alpha \sin\psi \right]^2 = 0 \quad . \tag{2.51}$$

It is readily seen that the number of equations obtained in this way is equal to the number of coefficients to be calculated, and that all these equations are linear in the unknowns. It seems probable that this procedure with the same number of terms affords a better approximation than the original method of satisfying Eq. (2.41) at a set of isolated points.

A great advantage would be gained, if the calculations could be made in the form of a series of successive approximations, where each new step is based upon the results of the preceding steps, so that the degree of approximation can be steadily pushed farther along. We shall describe below a method proposed by Lotz. The starting point is again the Fourier

Series for ℓ which is written in a form slightly different from the previous form:

$$\ell = \frac{1}{2} \rho V^2 c_0 m \sum a_n \sin n\psi \quad , \tag{2.52}$$

where c_0 is the chord of the median section. The equation for ϕ then becomes

$$\phi = \frac{mc_0}{8b} \sum na_n \frac{\sin n\psi}{\sin\psi} \quad . \tag{2.53}$$

The new features of the process are that Fourier Series are introduced for the quantities $\alpha \sin\psi$ and $(c_0/c) \sin\psi$ (α being the geometrical angle of incidence, c the chord of a particular section) as follows:

$$\alpha \sin\psi = \sum \alpha_n \sin n\psi \quad , \tag{2.54}$$

$$\frac{c_0}{c} \sin\psi = \sum \beta_n \cos n\psi \quad . \tag{2.55}$$

By means of the ordinary method of Fourier analysis the coefficients α_n, β_n of these series can be calculated as soon as both α and c are known as functions of ψ. Moreover, each coefficient can be calculated separately, so that it is possible to increase the accuracy by taking more terms in the development without changing the values of the coefficients already obtained. When the planform of the airfoil is symmetric, the series (2.55) contains cosines of even multiples of ψ only. Similar simplifications may occur in the series for $\alpha \sin\psi$. In the case of the rectangular wing, the coefficients β_n have the following values:

$$\beta_\nu = 2\pi^{-1} \; ; \; \beta_{2n} = - \frac{4}{\pi(4n^2 - 1)} \; ; \; \beta_{2n+1} = 0 \quad . \tag{2.56}$$

Eq. (2.41) is now replaced by;

$$\left(\sum a_n \sin n\psi\right)\left(\sum \beta_n \cos n\psi\right) + \mu_0 \sum na_n \sin n\psi = \sum \alpha_n \sin n\psi \quad , \tag{2.57}$$

$$\mu_0 = \frac{mc_0}{8b} \quad . \tag{2.58}$$

In the product of two series occurring in the left hand member of Eq. (2.57) one may write provisionally, as indices, k and ℓ instead of n; the product can then be brought into the form of a double series

$$\sum_k \sum_\ell a_k \beta_\ell \sin k\psi \cos \ell\psi \quad , \tag{2.59}$$

which transforms into

$$\frac{1}{2}\sum_{k}\sum_{\ell} a_k\beta_\ell[\sin(k+\ell)\psi + \sin(k-\ell)\psi] \quad . \tag{2.60}$$

In this double series, which is found to be

$$a_n\beta_0 + \frac{1}{2}a_{n-1}\beta_1 + \frac{1}{2}a_{n-2}\beta_2 + \ldots + \frac{1}{2}a_1\beta_{n-1} + \frac{1}{2}a_{n+1}\beta_1 + \frac{1}{2}a_{n+2}\beta_2 + \ldots - \frac{1}{2}a_1\beta_{n+1} - \frac{1}{2}a_2\beta_{n+2} - \ldots \quad , \tag{2.61}$$

we select the coefficients of $\sin n\psi$. After some rearrangement one obtains

$$\frac{1}{2}a_1(\beta_{n-1} - \beta_{n+1}) + \frac{1}{2}a_2(\beta_{n-2} - \beta_{n+2}) + \ldots + \frac{1}{2}a_{n-1}(\beta_1 - \beta_{2n-1}) + a_n(\beta_0 - \frac{1}{2}\beta_{2n}) + \frac{1}{2}a_{n+1}(\beta_1 - \beta_{2n+1}) + \frac{1}{2}a_{n+2}(\beta_2 - \beta_{2n+2}) + \ldots \tag{2.62}$$

The coefficients of $\sin n\psi$ on both sides of Eq. (2. 57) must be the same; this condition furnishes the following system of equations:

$$\frac{1}{2}a_1(\beta_{n-1} - \beta_{n+1}) + \ldots + \frac{1}{2}a_{n-1}(\beta_1 - \beta_{2n-1}) + a_n(\beta_0 - \frac{1}{2}\beta_{2n} + n\mu_0) + \frac{1}{2}a_{n+1}(\beta_1 - \beta_{2n+1}) + \frac{1}{2}a_{n+2}(\beta_2 - \beta_{2n+2}) + \ldots = \alpha_n \tag{2.63}$$

In its exact form the system contains an infinite number of equations with an infinite number of unknowns, a_1, a_2, ... But in the n^{th} equation the unknown a_n has the greatest coefficient while the coefficients of the other terms are usually smaller and decrease rather rapidly. On account of this circumstance, the solution of the system can be approximated by successive steps as follows:

First, consider the system of equations

$$\frac{1}{2}a_1(\beta_{n-1} - \beta_{n+1}) + \ldots + \frac{1}{2}a_{n-1}(\beta_1 - \beta_{2n-1}) + a_n(\beta_0 - \frac{1}{2}\beta_{2n} + n\mu_0) = \alpha_n \quad , \tag{2.64}$$

which are obtained from Eq. (2. 63) by rejecting the terms with a_{n+1}, a_{n+2}, etc. The first equation of the system (2. 64) appears to be

$$a_1(\beta_0 - \frac{1}{2}\beta_2 + \mu_0) = \alpha_1 \quad , \tag{2.65}$$

and thus gives a value for a_1; then from the second one, which contains only a_1 and a_2, a value of a_2 is obtained; a_3 is obtained from the third, and so on. This procedure serves to calculate the first approximation. Let us write the original system (2. 63) in the form

$$\frac{1}{2} a_1(\beta_{n-1} - \beta_{n+1}) + \ldots + \frac{1}{2} a_{n-1}(\beta_1 - \beta_{2n-1}) + a_n(\beta_0 - \frac{1}{2} \beta_{2n} + n\mu_0)$$
$$= \alpha_n - \frac{1}{2} a_{n+1}(\beta_1 - \beta_{2n+1}) - \ldots \qquad (2.66)$$

On the right hand side of Eq. (2. 66) one should insert the values of the a's obtained from the first approximation. The system obtained in this way, can be solved in the same way as the system (2. 64) and so a second approximation is obtained. Then this second approximation can be introduced on the right hand side of the system (2. 66) and a third approximation can be found. In this way the process can be carried on until the desired degree of accuracy is obtained. In starting the work, as many equations are taken as may appear to give values of a_n of sufficient importance in the right hand member of Eq. (2. 66). If required, it is always possible to increase the number of equations afterward, so as to obtain further coefficients, using the values already calculated as a provisional approximation, and correcting them according to the procedure indicated.

If the planform of the airfoil is symmetric, so that β's of uneven order vanish, the system of Eq. (2. 63), as well as the system (2. 64) and (2. 65) can be separated into one set of equations for the a's of uneven order, and another set for the a's of even order. The method has been applied to the case of the rectangular airfoil with ailerons. The angle of incidence changes along the span in the manner indicated in Eq. (2. 43); the solution can be built up from two separate parts, one relating to the ordinary rectangular wing with constant angle of incidence, the other relating to the antisymmetrical distribution of the angle of incidence given in Eq. (2. 45). The coefficients of α_n, β_n, of the series (2. 54) and (2. 55) corresponding to the various cases must be prepared in advance and then the system (2. 62) can be attacked. The results may be given in the form of diagrams for the coefficients ζ, ξ, η, $\mathscr{K}_L$, $\mathscr{K}_D$, as functions of the ratio (b-a)/2b, i. e., the aileron length divided by the total span. The coefficient m can be taken equal to 5, λ to 5, 6, 7, or 8, so that the parameter $1/\mu$ may have the values of 3. 96, 6. 34, etc. There is another way of attacking the problem in question, i. e., the influence of the deflected flaps or ailerons upon the pressure distribution on the wing. This will be described below.

If a wing and an aileron or a flap are considered together, a combination of this kind should be regarded as a single airfoil of somewhat unusual profile like a bent flat plate. For experimental results of tests on this combination, reference may be made to some reports on the working of a flap on a profile. Some general results of such tests will be cited below.

The Reynolds number was of the order of 4, 000, 000. The flap ran along the entire span and its chord was 20 per cent of the combined chord. The experiments were carried out on three combinations with varying proportions of elevator to total area, but all combinations have the same overall form (contour and profile) for zero deflection of the aileron. The results are compared with the theoretical values. The comparison was made for the angle of incidence (α_0) at which the lift vanishes; the agreement is good for small deflections of the aileron but for large values additional deflection produces far less effect than theory predicts, a fact which must be ascribed to separation of the flow at the rear of the wing. Similar results are found for the theoretical and measured values of the moment; the agreement is good only for small angles of incidence and small deflections of the flap (aileron). In addition to the usual quantities, C_L, C_D, C_M, for the aileron structure as a whole, one has to measure the moment about the axis of the elevator or flap or aileron as well as the moment coefficient

$$C_E = \frac{M_E}{S_E c_E (\rho/2) V^2} \quad . \tag{2.67}$$

Here M_E is the moment about the axis of the flap, aileron or elevator, S_E and c_E the surface area and the chord of the flap, aileron or elevator, calculated from the axis to the trailing edge. This moment is important because it determines the force which must be exerted in moving the elevator.

For convenience of calculation in practical cases, one can arrange the results of the experiments in the following manner. The component of the force perpendicular to the plane of the wing, i. e., the so-called normal force N, and its non-dimensionl coefficient, C_n,

$$C_n = \frac{N}{[(\frac{1}{2})\rho v^2 S]} \quad , \tag{2.68}$$

can be expressed with good approximation by the equation

$$C_n = k(\alpha - \tau\beta) \quad , \tag{2.69}$$

where β is the angle between stabilizer and elevator. Since the normal force is almost equal to the lift, the coefficient k represents essentially the known connection between the coefficient of lift and angle of incidence of ordinary airfoils. The following equation is approximately true:

$$k = \frac{2\pi}{[1 + 2S/(2b)^2]} \quad . \tag{2.70}$$

The value of τ depends on the ratio of the surface of the elevator (aileron) area to the total area of the tail-plane structure. From the results of the experiments it is possible to derive a curve connecting τ and S_E (elevator or aileron)/S. For any given tail-plane (or aileron-wing) combination, the magnitude τ is a characteristic constant. The moment of the air force about the elevator (aileron) axis can be expressed approximately by the formula

$$M_E = k_1(\beta - \tau_1 \alpha) \quad , \tag{2. 71}$$

where $\tau_1 \alpha$ is the angular movement of the elevator (aileron) for which the moment vanishes. If the angle of incidence is not too large ($\alpha <$ about 12^o), $\tau_1 \alpha$ is approximately proportional to the angle of incidence, so that inside of this domain of values for α, τ_1 is a constant characteristic of the tailplane (aileron). The value of this constant depends on the ratio of S_E/S, and a very crude approximation is $\tau_1 \sim S_E/S$.

In the case a definite stability is required when the control surface is free, its location, in such cases, must be investigated. Stability results from the combined effect of the forces due to air and the forces otherwise acting on the elevator (aileron). Apart from acting forces due to the air, the control surface is chiefly under the influence of gravitational (and possibly also inertial) forces. These forces are due to the weight of the aileron (elevator) itself, and their moment about the axis depends on the position of the elevator with respect to the vertical or with respect to the direction of mass forces; this means that it depends on the angle $\beta - \theta$. Here β denotes the elevator deflection (angle between the aileron and wing or elevator and stabilizer) and θ the angle between the wing (or stabilizer) and the horizontal. When the elevator (aileron) and stabilizer are at zero position, i.e., $\theta = \beta = 0$, the control stick may have an inclination ϵ to the vertical; hence, the gravitational moments about the elevator (aileron) axis can be expressed in the following form:

$$M_G = M_1 \sin(\epsilon - \mathcal{K}\beta - \theta) + M_2 \cos(\beta - \theta) \quad . \tag{2. 72}$$

This moment due to the actual weights or masses must be balanced by the moment of the forces due to the air when the aileron (or rudder) is free. The latter moment is given in the formula

$$M_A = C_E \frac{1}{2} \rho V^2 S_E c_E \quad , \tag{2. 73}$$

and there must be

$$M_G + M_A = 0 \quad . \tag{2. 74}$$

If the angles occurring in the above formulae are small, so that the sine of an angle may be replaced by the angle and the cosine by 1, it follows that, in equilibrium, the aileron (elevator) deflection β_0 is such that

$$\beta_0 = \frac{[\tau_1 \alpha - m_1(\epsilon - \theta) - m_2]}{(1 - \mathcal{K} m_1)} \quad , \tag{2.75}$$

$$m_1 = \frac{M_1}{\frac{1}{2}\rho V^2 k_1 S_E c_E} \quad , \tag{2.76}$$

$$m^2 = \frac{M_2}{\frac{1}{2}\rho V^2 k_1 S_E c_E} \quad . \tag{2.77}$$

In general, an aileron is a special asymmetric arrangement of the wings with flaps. Each half of the wing has its own special flap which in most cases extends only along the outer part of the wing. Both flaps (ailerons) are manipulated in opposite directions so that the lift is increased on one side and decreased on the other, thus producing a rolling moment. The difficulty of obtaining a quantitative estimate of the effect of ailerons is increased by the fact that their efficiency falls away at their ends. At the outer parts, in fact, the effects of ailerons diminish approximately in proportion to the lift of the wing itself. In order to estimate the decrease at the inner ends, it is possible to consider an infinitely long wing having a discontinuity in the angle of incidence at one point. The theory of the lift distribution in the neighborhood of such a discontinuity is available. It has not been possible to deduce, however, from the knowledge of single end effects any sufficiently reliable rule for calculating the combined results of two such effects. For a theoretical discussion of this matter, consideration must be given to the effect of all irregularities in the form of the wing. The ailerons belong to this class when in action . This problem can be solved by a practical procedure of calculating the lift distribution of wings with arbitrary distribution of chord and angle of incidence.

One can calculate the effects of the aileron or flap deflection by using the method of vortex fields. Obviously, an S-shaped form must be included. In the simplest case this is given by the equation

$$y = \frac{c}{2}\mathcal{K}\left(\frac{\xi^3}{3} - \frac{\xi}{2}\right) \quad , \tag{2.78}$$

which corresponds to a distribution of lift over the airfoil chord in accordance with

$$\frac{dC_L}{d\xi} = 2\mathscr{K}\xi\sqrt{1-\xi^2} \quad . \tag{2.79}$$

Here $\xi = 2y/c$, y is the distance of a point from the middle of the plate, c is the chord length. The lift resulting from this component is zero and it only provides a pure moment, the coefficient of which is

$$C_M = -\frac{\mathscr{K}\pi}{8} \quad . \tag{2.80}$$

This moment, when in conjunction with a circular curvature, produces a shift of the lift due to the circular curvature ($C_{L_0} = (2\pi)(2f/c)$, f is the height of camber) away from the middle of the span; this shift has the value

$$\Delta s = c\,\frac{\mathscr{K}}{32}\,\frac{c}{f} \quad . \tag{2.81}$$

If the lift be shifted in this manner to a point c/4 from the front edge, it coincides in position with the component provided by an increasing angle of incidence, so that in this case, alteration of the angle of incidence produces no displacement of the point of application. The cross-section thus obtained is a so-called "fixed center of pressure" profile, the condition being

$$\Delta s = \frac{c}{4} \quad . \tag{2.82}$$

It follows that

$$\mathscr{K}_0 = \theta = \frac{8f}{c} \quad , \tag{2.83}$$

where θ is the angle at the center, and

$$y_0 = \frac{c}{2}\,\theta\left(\frac{\xi^3}{3} - \frac{\xi}{2}\right) \quad . \tag{2.84}$$

It should be observed that the S-shaped profile which has no resultant lift, but a pure moment, has, however, an angle of incidence of amount

$$\alpha_S = \frac{\mathscr{K}}{6} \quad . \tag{2.85}$$

Here $\mathscr{K}$ denotes a special coefficient, depending on the lift distribution, Eq. (2.79). The more general cross section obtained by superimposing this cross section on a circular arc profile of angle of incidence zero, will also have an angle of incidence α_S. In order to have the ordinates still measured from the chord, it is therefore necessary to subtract the ordinates

$z = -1/2\, c\alpha_S \xi$ of a flat plate with angle of incidence α_S. Similarly, in obtaining the values of the forces and moments for an arbitrary angle of incidence α (superposition of a flat plate) it is necessary to observe that only the difference $\alpha - \alpha_S \mathcal{K}/6$ is effective as an additional angle of incidence. For a cross section whose shape is composed of a circular arc of curvature $f/c = \theta/8$ and an S-section of constant $\mathcal{K}$, the calculation supplies the equation

$$y = \frac{c}{2}\left[\frac{\theta}{4}(1 - \xi^2) + \mathcal{K}\left(\frac{\xi^3}{3} - \frac{\xi}{2} + \frac{\xi}{6}\right)\right] = \frac{c}{2}\left[\frac{\theta}{4}(1 - \xi^2) + \frac{\mathcal{K}}{3}(\xi^3 - \xi)\right] , \qquad (2.86)$$

and the following coefficients of lift and moment for an angle of incidence α:

$$C_L = 2\pi \left(\sin\alpha + \frac{\theta}{4} - \frac{\mathcal{K}}{6}\right) , \qquad (2.87)$$

$$C_M = \frac{\pi}{2}\left(\sin\alpha + \frac{\theta}{2} - \frac{\mathcal{K}}{4} - \frac{\mathcal{K}}{6}\right) = \frac{\pi}{2}\left(\sin\alpha + \frac{\theta}{2} - \frac{5}{12}\right) , \qquad (2.88)$$

where

$$\theta = 8f/c \quad . \qquad (2.89)$$

The superposition of the S-shape on the circular arc displaces the position of greatest camber height and in the shapes used in practical applications, where it is desirable to make the movement of the center of pressure as small as possible, this displacement always takes place forward. The camber height at the middle of the cross section is not affected by the symmetrical S-shape and is simply a measure of the amount of the circular curvature, so that the camber height to be taken in the above formulae is not the maximum value, but the value at the middle of the cross section. The curvature of the cross section decreases continually from the front to the back, and eventually may even become negative (S-shape). The difference between the angles ψ and ϕ at the forward and after edges of the profile may be taken as a measure of the S component of the profile, while the sum $\psi + \phi$ is a measure of the circular curvature. The following equations apply here:

$$\psi + \phi = \mathcal{K} + 2\alpha_S = \frac{4}{3}\mathcal{K} \quad ; \qquad (2.90)$$

$$\psi + \phi = \theta = \frac{8f}{c} \quad . \qquad (2.91)$$

The condition that a cross section should have fixed center of pressure is $\mathcal{K} = \theta$, giving

$$3(\psi - \phi) = 4(\psi + \phi) \; ; \; \text{or } \psi = -7\phi \quad . \qquad (2.92)$$

A cross-section of this type and having fixed center of pressure has a point of inflection at $x = c/8$. The greatest camber height occurs at

$$x = \frac{c}{2}\left(\frac{1}{4} - \sqrt{\frac{19}{48}}\right) \approx \frac{c}{2}(0.38) \quad . \tag{2.93}$$

There is no difficulty in calculating properties of any arbitrarily given cross section by the method of vortex fields. In particular, there are the general expressions furnished by Munk's integrals

$$C_L = 2\pi\alpha + 2\int_{-1}^{+1} \frac{y}{c} \frac{d\xi}{(1-\xi)\sqrt{1-\xi^2}} \quad ; \tag{2.94}$$

$$C_M = \frac{\pi\alpha}{2} + 2\int_{-1}^{+1} \frac{y}{c} \frac{1-\xi+\xi^2}{(1-\xi)\sqrt{1-\xi^2}} \, d\xi \tag{2.95}$$

Munk's integral especially adapts itself to the case of a given cross section whose shape deviates considerably from the normal and whose properties are to be estimated. If, however, the problem to be solved consists of finding a cross section, or altering the shape of a given cross section in order to obtain certain desired properties, the previously described procedure of superposition of typical forms is more suitable.

Some remarks will be given below on the discontinuous flow around an airfoil with flap.

The perfect fluid theory of Kutta and Joukowski for calculating the reaction of the air on an airfoil with infinite span, engaged in a uniform rectilinear translation through a bulk of air at rest, gives satisfactory results so far as the lift is concerned. This theory fails to account for all details of the flow, however. In particular, it neglects the wake of deadwater which exists at the trailing edge. The effect of this wake is to make the lift slightly smaller than the calculated value and to reduce the negative pressures along the rear portion of the suction side. Since the effect is greatest near the trailing edge, the discrepancies between calculations and observation will be most pronounced for the total hinge moment of the pressures on a trailing edge flap.

The boundary layer theory has been used to calculate the size of the wake, i.e., the point where the wake detaches itself from the body. Basing his calculations on the observed distribution, Hiemenz in 1911 obtained from the boundary layer theory an angle of 82° from the forward point for the point of detachment in flow around an infinite circular cylinder, a value in good agreement with his experiments. However, his experiments were made at low Reynolds numbers; an airfoil would be stalled for such a flow. For the high Reynolds numbers corresponding to the normal, unstalled flight of an airfoil, the calculated point of detachment for flow around the cylinder is at least 20° smaller than the observed value, even though the calculations are based on experimental pressure distributions.

A definite advance was made by C. Schmieden in 1932 when he showed that for high Reynolds numbers the perfect fluid theory is adequate to explain the wake behind a cylinder if one assumes a discontinuous flow. According to this view, the wake is obtained as a special case of the classical theory of jets. The theory of jets, due to Helmholtz and Levi-Civita, assumes a wake of stationary fluid at uniform pressure, bounded by two streamlines along which the speed is constant and different from zero. In spite of the fact that such a discontinuity in velocities would be impossible in a real fluid, Schmieden's calculated values of the pressures around the cylinder agree remarkably well with experiment. The agreement is perfect up to the pressure minimum; beyond that there are some deviations, which can be attributed to turbulence in the boundary layer and the circulation of fluid in the wake. The point of detachment is approximately correct, but the observed point is somewhat masked by the turbulence, and the circulation of the fluid in the wake causes the constant pressure in the wake to be negative instead of zero, as predicted by the theory.

Schmieden found, however, that the equations of motion for a perfect fluid, plus the usual boundary condition that the velocity approach the stream velocity as the distance from the cylinder increases without bound, are insufficient to determine the discontinuous flow uniquely. Various sizes and types of wakes are possible. There exist symmetric discontinuous flows with wakes detaching from the cylinder at every angle from about 55° to 180°. For angles between 55° and about 124° the wake extends to infinity and is bounded by streamlines which are first concave toward the wake and then, after passing through a point of inflection, are convex; the drag on the cylinder is positive, and the constant pressure in the wake is zero. For angles between 124° and 180° the wake is finite in extent, the drag is zero, and the pressure in the wake is positive. For the critical angle of about 55° the wake boundaries are always convex (Helmholtz case). For the critical angle of about 124° the wake is infinite but has a width which tends asymptotically to zero, the boundaries of the wake are concave, the drag vanishes, and the pressure in the wake is zero; we shall refer to this as the Schmieden case.

Since a correctly set physical problem should have a unique answer even for a perfect fluid, an additional boundary condition is evidently required to determine the flow. Schmieden has chosen the auxiliary condition that the wake boundaries be concave and infinite in extent.

A possible reason for selecting the condition of concavity is the intuitive feeling that in a viscous fluid any portion of a streamline with a point of inflection would be swept away to infinity. However, for a perfect fluid there would be no such tendency; moreover, the condition of concavity is an "internal" condition, more in the nature of a law of motion than a boundary condition. The required boundary condition must be "external" in character—a condition which can be imposed arbitrarily as a constraint on the system. Such an external condition could only be imposed by specifying something about the nature of the impinging stream. In particular, we could require that this stream be as nearly uniform as possible, that is, the difference between the velocity and the undisturbed stream velocity shall approach zero as rapidly as possible as one recedes from the cylinder in the direction of the stream source. In the present paper we show that this assumption of "minimum disturbance at infinity" does in fact lead to the Schmieden case, at least for infinite wakes.

On the experimental side the justification for choosing the Schmieden case for an approximation to the flow of an actual fluid at high Reynolds numbers lies in the agreement previously mentioned between calculated and observed pressure distributions. Of the various discontinuous flows, the Schmieden case gives the best agreement for the pressure distribution as a whole, but more particularly for the forward part of the cylinder where turbulence is absent. As previously mentioned, the observed pressure in the wake is negative instead of zero, but this is still the best agreement possible since the theory predicts a positive pressure behind the cylinder for finite wakes. Quantitative technical applications involving pressures behind the cylinder are subject to the limitations imposed by this discrepancy. Further refinements of the theory to eliminate this discrepancy by taking into account the turbulence in the wakes have been suggested by Schmieden.

In 1940 Schmieden applied his theory of discontinuous flow to the case of an airfoil with infinite span whose profile is an inclined straight line segment. It was found that the pressure distributions so obtained, agree almost exactly with the pressure calculated from the Kutta-Joukowski theory, except near the trailing edge, where the wake would be expected to exert an appreciable influence. It should be observed that the Kutta-Joukowski theory also uses an additional assumption beyond those involved in the perfect fluid equations, namely, the Joukowski hypothesis that the circulation is such that the velocity at the trailing edge is finite. Schmieden makes no direct assumption about the circulation, but replaces the Joukowski hypothesis by the above assumption concerning the nature of the wake. From Schmieden's point of view the

Joukowski hypothesis is a special assumption concerning the nature of the wake in the limiting case when the wake is made to disappear.

An objection has been raised to Schmieden's theory of the airfoil with straight line profile in that the pressure is negatively infinite at the leading edge; it is one of the requirements of the classical theory of jets that separation of the fluid from the body occurs at such points. However, in an actual airfoil no separation occurs at the leading edge (unless the airfoil is not stalled) because the leading edge is rounded off. The infinite velocity is not a necessary feature of the Schmieden theory, but only results from the sharp leading edge which was assumed to render the mathematics feasible. Singularities of exactly the same order are obtained from the Kutta-Joukowski theory when applied to sharp leading edges.

One may apply the Schmieden theory to the case of two-dimensional flow around an airfoil with flap, the profile being a broken line.

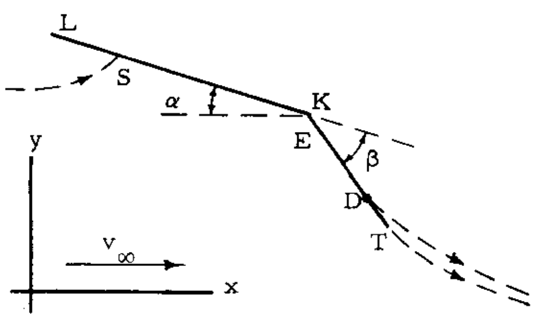

Figure 1

Consider a plate whose cross section is a broken straight line (Fig. 1). The angle of attack of the main wing may be denoted by α and the angle of attack of the flap by $\alpha + \beta$. Thus β is the angle of depression of the flap. We assume that α is positive and that β, if negative, is greater than $-\alpha$. The velocity of the undistributed stream (velocity of flight) is denoted by v_∞.

There will be a critical streamline which divides at the stagnation point S, follows both sides of the airfoil to the points of detachment, D and T, and then to infinity as boundaries of the wake. At the points of detachment the boundaries of the wake leave the plate tangentially.

Evidently the ratio of the lengths (chords) $\overline{KT}$ to $\overline{LK}$ must not be too small, or else the point of detachment D will not fall on the flap. We restrict attention to cases where the flap is long enough for D to lie on the flap—an assumption that appears to be justified in all cases of technical interest.

The method of Levi-Civita does not give the velocity distribution along the surface of the plate directly in terms of the position which the point under consideration has on the plate; but instead, both position and velocity are expressed parametrically in terms of an auxiliary variable ϕ, where ϕ is an angle ranging from 0 to π. The explicit expressions are as follows, where v is the speed of the fluid and s is the distance measured along the broken line from T:

$$v = v_\infty \frac{\sin\frac{1}{2}(\phi_L+\phi)\sin\frac{1}{2}|\phi_S-\phi|}{\sin\frac{1}{2}|\phi_L-\phi|\sin\frac{1}{2}(\phi_S+\phi)} \left[\frac{\sin\frac{1}{2}(\phi_K+\phi)\sin\frac{1}{2}|\phi_E-\phi|}{\sin\frac{1}{2}|\phi_K-\phi|\sin\frac{1}{2}(\phi_E+\phi)}\right]^{\beta/\pi} . \qquad (2.96)$$

$$s = 4c^2\int_0^\phi \frac{\sin\frac{1}{2}(\phi_L-\phi)\sin^2\frac{1}{2}(\phi_S+\phi)}{\sin\frac{1}{2}(\phi_L+\phi)} \left[\frac{\sin\frac{1}{2}|\phi_K-\phi|\sin\frac{1}{2}(\phi_E+\phi)}{\sin\frac{1}{2}(\phi_K+\phi)\sin\frac{1}{2}|\phi_E-\phi|}\right]^{\beta/\pi} \sin\phi\, d\phi \qquad (2.97)$$

Here the constants ϕ_E, ϕ_S, ϕ_L, ϕ_K and c^2 depend on the dimensions of the plate and on α and β. The number c^2 is a proportionality factor determining the scale of the figure. Values of ϕ between 0 and ϕ_L correspond to points on the under side of the plate while values between ϕ_L and π give points on the upper side. The determination of the numbers ϕ_E, ϕ_S, ϕ_L, and ϕ_K is the most difficult part of the whole procedure and will be discussed later. For the present we suppose that they are known. It will be sufficient now to observe that these four constants are angles between 0 and π, whose magnitudes are in the order written, which if used as the upper limit will yield the positions of the points E, S, L, and K respectively. Also, the angles ϕ_S and ϕ_L are near $\pi/2$ if α and β are small.

If the integration in Eq. (2.97) is performed there is obtained with (2.96) a complete parametric representation of the speed at the airfoil surface. From Bernoulli's theorem it is then a simple matter to calculate the pressure in terms of the parameter ϕ. If the pressure at infinity is p_∞, the pressure at any point will be

$$p = \frac{\rho}{2}(v_\infty^2 - v^2) + p_\infty , \qquad (2.98)$$

where ρ is the density of the fluid.

The total hydrodynamic forces acting on all or part of the airfoil may be found by integration of the pressure. In particular, the total moment of the forces acting on the flap taken with respect to the hinge will be

$$M_H = \int_0^{\phi_E} p(\ell_F - s)\frac{ds}{d\phi}\, d\phi - \int_{\phi_K}^{\pi} p(\ell_F - s)\frac{ds}{d\phi}\, d\phi , \qquad (2.99)$$

where ℓ_F is the length (chord) of the flap $\overline{ET}$ and moments in the counterclockwise direction are considered positive.

The resultant force on the airfoil is vertical; the drag vanishes and the total lift is

$$Y = -\frac{1}{2}\pi\rho v_\infty^2 c^2 \left[\sin 2\phi_L - \sin 2\phi_S + \frac{\beta}{\pi}(\sin 2\phi_K - \sin 2\phi_E)\right]$$

In addition to the distributed pressures there is a concentrated force (suction) at the leading edge which acts parallel to the plate LK. Its horizontal component must equal the horizontal component of the resultant pressure on the airfoil, since there is no concentrated force at the hinge K. The magnitude of the force at L is

$$F = 4\pi\rho v_\infty^2 c^2 \sin\phi_L \sin^2 \frac{1}{2}(\phi_L - \phi_S)\left[\frac{\sin\frac{1}{2}(\phi_L+\phi_K)\sin\frac{1}{2}(\phi_L-\phi_E)}{\sin\frac{1}{2}(\phi_K-\phi_L)\sin\frac{1}{2}(\phi_L+\phi_E)}\right]^{\beta/\pi} .$$

The integrations must in general be carried out numerically or graphically. The integral has been carried out in closed form only for the case of a straight plate, i. e., $\beta = 0$. The problem is much simplified in that case by the fact that of the four constants, ϕ_E and ϕ_K do not occur and $\phi_L = \frac{1}{2}(\pi + \alpha)$, $\phi_S = \frac{1}{2}(\pi - \alpha)$.

As ϕ varies from 0 to ϕ_E the corresponding point in Fig. 1 will move along the underside of the flap from T to E; as ϕ goes in succession from ϕ_E through ϕ_S, ϕ_L, ϕ_K to π, the corresponding point will move along the underside of the plate through S to L and then back along the upper side through K to D. Now the distance traversed on the underside between E and L must equal the distance on the upper side from L to K. Hence, if the integrand in equation (2.97) is $f(\phi, \phi_E, \phi_S, \phi_L, \phi_K)$, then

$$\int_{\phi_E}^{\phi_L} f(\phi, \phi_E, \phi_S, \phi_L, \phi_K)d\phi = \int_{\phi_K}^{\phi_L} f d\phi \quad . \tag{2.100}$$

If $\lambda = \overline{TK}/\overline{KL}$ is the ratio of the length of the flap to the length of the stationary part of the airfoil, we must have

$$\int_0^{\phi_E} f d\phi = \lambda \int_{\phi_E}^{\phi_L} f d\phi \quad . \tag{2.101}$$

Equations (2.100) and (2.101) are the two conditions on the constants imposed by the geometry of the airfoil. A third condition is obtained from the requirement that the velocity must approach the stream velocity as the distance from the airfoil tends to infinity. The following equation is the mathematical formulation of this condition:

$$\phi_L - \phi_S + \frac{\beta}{\pi}(\phi_K - \phi_E) = \alpha + \beta \quad . \tag{2.102}$$

For the fourth condition, we need the Schmieden hypothesis mentioned in the introduction, or some alternative. The hypothesis which we propose is a natural and direct extension of the physical assumption on the basis of which (2.102) was obtained. Whatever physical principle causes the velocity to approach the stream velocity as the distance from the airfoil becomes large might also be expected to cause it to approach the stream velocity as rapidly as possible. This is our basic hypothesis; it says that the disturbance at distant points shall be a minimum.

The general mathematical formulation of our hypothesis for our case of a broken straight line leads to the condition

$$\sin\phi_L - \phi_S + \frac{\beta}{\pi}(\sin\phi_K - \sin\phi_E) = 0 \quad . \tag{2.103}$$

For $\beta = 0$ this reduces to the condition which Schmieden has used for determining size of the wake, namely $\phi_L = \pi - \phi_S$. Putting $\beta = 0$ in (2.102) we get $\phi_L - \phi_S = \alpha$. Hence $\phi_L = \frac{1}{2}(\pi + \alpha)$ and $\phi_S = \frac{1}{2}(\pi - \alpha)$.

The four equations will determine the four constants involved. These equations can only be solved by successive approximation. Equations (2.100) and (2.101) can be solved by trial, the integrations being performed either graphically or numerically.

We consider Fig. 1 as a diagram in a complex z-plane, $z = x + iy$. We choose the complex potential

$$w = \psi_1 + i\psi_2 \quad ,$$

in such a way that the streamline $\psi_2 = 0$ will be the critical streamline which follows the surface of the airfoil and wake, with $\psi_1 = 0$ at S.

The w plane minus the positive half of the real axis is mapped onto the interior of the upper half of the unit circle in a τ plane by the transformation

$$w = a^2\left[\cos\phi_S - \frac{1}{2}\left(\tau + \frac{1}{\tau}\right)\right]^2 \quad . \tag{2.104}$$

The radii from -1 to 0 and from 0 to 1 in this τ-plane correspond to the free streamlines. The points on the unit circle with arguments ϕ_E, ϕ_S, ϕ_K correspond respectively to E, S, L, K. The number a is a constant.

Consider the complex velocity

$$\frac{dw}{dz} = ve^{-i\theta} \quad . \tag{2.105}$$

Along the real axis in the τ-plane between -1 and +1 the speed v must be constant and equal to v_∞, the undisturbed stream velocity. Along the successive segments of the unit circle between the points T', E', S', L', K', and D', the angle θ must have the respective constant values $-(\alpha+\beta)$, $-\alpha$, $\pi - \alpha$, $-\alpha$ and $-(\alpha+\beta)$. It will now be shown that the following expression for the complex velocity will satisfy these conditions:

$$\frac{dw}{dz} = v_\infty e^{i(\alpha+\beta)} \frac{(\tau - e^{-i\phi_L})e^{i\phi_L}(\tau - e^{i\phi_S})}{(\tau - e^{i\phi_L})(\tau - e^{-i\phi_S})e^{i\phi_S}} \left[\frac{(\tau - e^{-i\phi_K})e^{i\phi_K}(\tau - e^{i\phi_E})}{(\tau - e^{i\phi_K})(\tau - e^{i\phi_E})e^{i\phi_E}}\right]^{\beta/\pi} . \qquad (2.106)$$

We use that determination of the bracketed quantity to the β/π power whose argument vanishes for $\tau = 1$. The absolute value of this expression is obviously constant and equal to v_∞ if τ is real. For $\tau = e^{i\phi}$ on the unit circle we make use of the identity

$$e^{i\phi} - e^{i\phi'} = e^{\frac{1}{2} i(\phi+\phi')}\left[e^{\frac{1}{2} i(\phi - \phi')} - e^{-\frac{1}{2} i(\phi-\phi')}\right] = 2ie^{\frac{1}{2} i(\phi+\phi')} \sin \frac{1}{2}(\phi-\phi') ,$$

to rewrite our expression in the form

$$\frac{dw}{dz} = v_\infty e^{i(\alpha+\beta)} \frac{\sin\frac{1}{2}(\phi+\phi_L) \sin\frac{1}{2}(\phi'-\phi_S)}{\sin\frac{1}{2}(\phi-\phi_L) \sin\frac{1}{2}(\phi+\phi_S)} \left[\frac{\sin\frac{1}{2}(\phi+\phi_K) \sin\frac{1}{2}(\phi-\phi_E)}{\sin\frac{1}{2}(\phi-\phi_K) \sin\frac{1}{2}(\phi+\phi_E)}\right]^{\beta/\pi} , \qquad (2.107)$$

where the determination is chosen to agree with that in (2.106). If ϕ is between 0 and ϕ_E each factor involving the sine of a difference is negative, all the negative signs will cancel and the argument of the whole expression will be $\alpha+\beta$; hence $\theta = -(\alpha+\beta)$ as desired. If ϕ is between ϕ_E and ϕ_S, the quantity inside the brackets will be negative and have an argument $-\pi$; hence the entire expression will have an argument α. In this way all the prescribed values of θ may be verified. Since our expression for dw/dz is analytic and not zero inside the upper half of the unit circle in the τ-plane and satisfies the required conditions for v and θ on the boundary of that semicircle, it follows that the flow around our airfoil is thereby correctly determined. If we take absolute values of both sides of (2.107) we get the required formula (2.96). Also, from (2.104) for $\tau = e^{i\phi}$

$$\frac{dw}{dz} = -a^2[\cos\phi_S - \frac{1}{2}(\tau + 1/\tau)](1 - 1/\tau^2) = -2a^2 i(\cos\phi_S - \cos\phi)e^{-i\phi}\sin\phi$$

$$= 4a^2 ie^{-i\phi}\sin\frac{1}{2}(\phi_S+\phi)\sin\frac{1}{2}(\phi_S-\phi)\sin\phi . \qquad (2.108)$$

Since $dz = (dz/dw)(dw/d\tau)d\tau$, we have

$$|dz| = \frac{1}{v} \left|\frac{dw}{d\tau}\right| |d\phi| \quad . \tag{2.109}$$

Now ds will have the same sign as $d\phi$, if ϕ is less than ϕ_L and opposite signs if $\phi > \phi_L$. We can therefore get ds from $|dz|$ by removing the absolute value signs around $d\phi$ and around the quantity $\phi_L - \phi$ in the expression for v. Hence (2.97) follows immediately on substituting (2.96) and (2.108) into (2.109), integrating, and setting $c^2 = a^2/v_\infty$.

We need only observe that the complex velocity must approach v_∞ as $\tau \to 0$. Putting $\tau = 0$ in (2.106) we get

$$v_\infty = v_\infty e^{i(\alpha+\beta)} e^{-i\phi_L} e^{i\phi_S} [e^{-i\phi_K} e^{i\phi_E}]^{\beta/\pi} \quad ,$$

which reduces at once to (2.102).

Consider the function

$$\omega(\tau) = \ln\left(v_\infty \frac{dz}{dw}\right) = \ln \frac{v_\infty}{v} + i\theta \quad . \tag{2.110}$$

This function is regular within the upper half of the unit circle and continuous on the diameter formed by the segment of the real axis between -1 and +1. It is also purely imaginary on this diameter. Hence it can be continued into the lower half of the unit circle by reflection of $i\omega(\tau)$; and $\omega(\tau)$ will then be regular within the entire unit circle.

Expanding $\omega(\tau)$ in a power series we get

$$\frac{dw}{dz} = v_\infty e^{-\omega(\tau)} = v_\infty e^{-\omega(0) - \omega'(0)\tau - \omega''(0)\tau^2/2 - \dots}$$

$$= v_\infty \left\{1 - \omega'(0)\tau + [(\omega'(0))^2 - \omega''(0)] \frac{\tau^2}{2} - \dots\right\} \quad . \tag{2.111}$$

Here we have put $\omega(0) = 0$, which is the condition that the velocity equals v_∞ at infinity.

In all cases discussed in detail by Schmieden and in the present paper, the flow is uniquely determined by the condition

$$\omega'(0) = 0 \quad . \tag{2.112}$$

Hence, there is one and just one flow for which

$$\frac{d\omega}{dz} - v_{\infty} \sim \tau^{n} \text{ as } \tau \to 0 \ ,$$

for $n \geq 2$; for every other flow $n = 1$. Since $\tau \to 0$ as $z \to \infty$ (for points outside the wake), dw/dz will approach v_{∞} at a maximum rate as $z \to \infty$ if the flow satisfies (2.112). This is, for the cases under consideration, the desired mathematical formulation of our hypothesis that the disturbance of the main stream at infinity shall be a minimum.

Equation (2.112) would be insufficient to determine a unique flow if one of the two points of detachment of the wake had not been determined a priori. Thus, in the case of an airfoil with sharp trailing edge, one point of detachment is placed at the trailing edge; for the case of a circular cylinder, the two points of detachment are assumed to be symmetrically placed. Situations can be imagined, however, such as an airfoil with blunt trailing edge, where neither point of detachment could be determined in advance. In such a case one can have a still smaller disturbance of the main stream at infinity (i.e., $n \geq 3$ in the above asymptotic formula) by imposing in addition to (2.112) the condition

$$\omega''(0) = 0 \ . \qquad (2.113)$$

For symmetric flows this last condition is automatically satisfied whenever (2.112) holds.

The theory predicts the following sequence of events as one passes continuously from the case of a circular cylinder to an inclined plate by way of elliptic cylinders with increasing eccentricity but with major axis having a small constant inclination with the direction of the stream; for small eccentricities (and very high Reynolds numbers) both $\omega'(0)$ and $\omega''(0)$ vanish, both the drag and lift are zero and the disturbance of the main stream at distant points is the least possible. As the ellipse becomes flatter and the trailing edge less blunt, the local viscosity and pressure conditions at the trailing edge gain control over the lower point of detachment of the wake, the condition (2.113) is lost, and a corresponding lift is developed. The flow in this state corresponds to that in the normal flight of an airfoil. For still flatter ellipses, higher angles of attack or lower Reynolds numbers, the local conditions around the leading edge gain control of the upper point of detachment, the condition (2.112) is also lost, and there is a positive drag proportional to $\omega'(0)$ and a positive, although much smaller, lift. In this state the airfoil is clearly stalled. Thus the development of a lift and of a drag mark abrupt changes in the state of the flow associated with the loss of the conditions (2.113) and (2.112) respectively; and there is a critical range of Reynolds numbers marking the effect of local conditions which determine the transitions from one type of flow to another.

Consider the expression

$$\omega_1(\tau) = \ln(\tau - e^{i\phi_1}) - \ln(\tau - e^{-i\phi_1}) ,$$

where ϕ_1 is an arbitrary constant angle. Then

$$\omega_1'(\tau) = \frac{1}{\tau - e^{i\phi_1}} - \frac{1}{\tau' - e^{-i\phi_1}} ,$$

$$\omega_1''(\tau) = -\frac{1}{(\tau - e^{i\phi_1})^2} + \frac{1}{(\tau - e^{-i\phi_1})^2} ,$$

$$\omega_1'(0) = -e^{-i\phi_1} + e^{i\phi_1} = 2i \sin\phi_1 ,$$

$$\omega_1''(0) = -e^{-2i\phi_1} + e^{2i\phi_1} = 2i \sin 2\phi_1 .$$

Now, from (2.106) it follows that $\omega(\tau)$ is the sum of a constant and constant multiples of expressions of the form $\omega_1(\tau)$. Hence

$$\omega'(0) = 2i[\sin\phi_L - \sin\phi_S + \frac{\beta}{\pi}(\sin\phi_K - \sin\phi_E)] ,$$

$$\omega''(0) = 2i[\sin 2\phi_L - \sin 2\phi_S + \frac{\beta}{\pi}(\sin 2\phi_K - \sin 2\phi_E)] . \qquad (2.114)$$

Equation (2.103) is an immediate consequence of the first of these equations and our hypothesis (2.112).

According to the Levi-Civita formula, the total drag on the airfoil is proportional to $\omega'(0)$. From our hypothesis it follows that the drag is zero. In fact, in the case under consideration our hypothesis is equivalent to the condition that the drag vanishes. However, in other situations such as the case of a finite wake discussed by Kolscher, the two conditions differ.

The total lift may be calculated from the Levi-Civita formula

$$Y = \frac{1}{4}\pi\rho v_\infty^2 c^2 i\omega''(0) , \qquad c^2 = a^2/v_\infty ,$$

and (2.114) to be

$$Y = -\frac{1}{2}\pi\rho v_\infty^2 c^2 [\sin 2\phi_L - \sin 2\phi_S + \frac{\beta}{\pi}(\sin 2\phi_K - \sin 2\phi_E)] .$$

For $\beta = 0$ this reduces to the Schmieden expression

$$Y = \pi \rho v_\infty^2 c^2 \sin \alpha \quad .$$

Consider the flow around a corner K with arbitrary angle $\mu\pi$, $0 \leq \mu \leq 1$. Draw the small circle C of radius r about K. The finite force at K, if any, will be obtained by applying Euler's momentum theorem to the fluid inside C and taking the limit as r approaches zero. We assume the fluid as a free body, where $-\vec{F}$ is the reaction of the concentrated force $\vec{F}$ on K.

We have

$$\vec{F} - \int_{C+AKB} \vec{n}\, p\, ds = \rho \int_C \vec{n}\, \vec{v}\, \vec{v}\, ds \quad ,$$

where $\vec{n}$ is the inward unit normal.

It is assumed that the stagnation point S is not at the corner. Hence for small r, setting $\lambda = \mu/(1+\mu)$, $0 \leq \lambda \leq \frac{1}{2}$

$$\frac{dw}{dz} = k/(z-K)^\lambda + (r^{1-2\lambda}) \quad , \tag{2. 115}$$

where k is a constant and $0(r^{1-2\lambda})$ is a quantity such that $0(r^{1-2\lambda})/r^{1-2\lambda}$ is bounded as $r \to 0$. Hence, if we put $z - K = re^{i\psi}$,

$$v = |k|r^{-\lambda} + 0(r^{1-2\lambda}) \quad , \quad v^2 = |k|^2 r^{-2\lambda} + 0(r^{1-3\lambda}) \quad ,$$

$$e^{i\theta} = (|k|/k)e^{i\lambda\psi} + 0(r^{1-2\lambda}) \quad , \quad p = -\frac{1}{2}\, |k|^2 \rho r^{-2\lambda} + 0(r^\sigma) \quad ,$$

where $\sigma = 0$ if $\lambda \leq 1/3$, $= 1 - 3\lambda$ if $\lambda > 1/3$, and $0(r^{1-2\lambda})$ is a quantity such that $0(r^{1-2\lambda})/r^{1-2\lambda} \to 0$ as $r \to 0$.

Now

$$\int_A^K \vec{n}\, p\, ds = -\frac{1}{2}\, \vec{n}\, |k|^2 \rho \int_0^r r^{-2\lambda}\, dr + \vec{n} \int_0^r 0(r^\sigma)\, dr \quad .$$

Both these integrals tend to zero with r if $\mu < 1$. If $\mu = 1$, this integral and the corresponding integral along KB both diverge, but since, in this case, the pressures along AK and KB are directly opposing, it is permissible to use the principal value of the integral along AKB. With this understanding we may write

$$\int_{AKB} \vec{n}\, p\, ds = -\frac{1}{2}\, \vec{n}_1\, |k|^2 \rho \int_0^r (r^{-1} - r^{-1})\, dr + \int_0^r \vec{n}\, 0(r^\sigma)\, dr,$$

where $\vec{n}_1$ is the normal to AK. Both these integrals tend to zero. For the arc C

$$\int_C \vec{n}\, p\, ds = -\frac{1}{2}\,|k|^2\,\rho \int_0^{\pi(1+\mu)} r^{-2\lambda+1} e^{i(\psi-\pi)} d\psi + \int_C \vec{n}\, 0(r^{\sigma}) ds \quad . \quad (2.116)$$

These integrals also approach zero; the first integral is zero if $\mu = 1$.

The Euler momentum theorem thus reduces to

$$\vec{F} = \lim_{r\to 0} \rho \int_C \vec{n}\,\vec{v}\,\vec{v}\, ds \quad .$$

But $\cos(\vec{n}, \vec{v}) = \cos(\psi - \theta - \pi)$, $\vec{v} = ve^{i\theta}$,

$$\rho \int_C \vec{n}\,\vec{v}\,\vec{v}\, ds = -\frac{\rho}{2} \int_C v^2 e^{i\psi} ds - \frac{\rho}{2} \int_C v^2 e^{-i\psi} e^{2i\theta} ds \quad .$$

The first of these integrals is similar to (2.116) and will approach zero for the same reason. For the second integral

$$-\frac{\rho}{2} \int_C v^2 e^{-i\psi} e^{2i\theta} ds = \frac{-\rho}{2} \int_0^{\pi(1+\mu)} \frac{|k|^2}{r^{2\lambda}}\, e^{-i\psi}\, \frac{|k|^2}{k^2}\, e^{2i\lambda\psi} r\, d\psi - \frac{\rho}{2} \int_C 0(r^{1-4\lambda}) ds \, .$$

The last integral approaches zero. The first integral also approaches zero if $\mu < 1$. If $\mu = 1$, however, its value is not zero. Evaluating this integral we get finally

$$\vec{F} = -\pi\rho\, \frac{|k|^4}{k^2} \quad , \quad \text{if} \quad \mu = 1 \, ,$$

$$= 0 \quad , \quad \text{if} \quad \mu \neq 1 \quad . \qquad (2.117)$$

We have thus proved the general result that for a concentrated force to exist at a corner which is not a stagnation point the corner must be a cusp. In particular, there will be no concentrated force at the hinge K. The concentrated force at the leading edge may be found by evaluating k, giving

$$\vec{F} = -4\rho\pi v_\infty^2 c^2 e^{-i\alpha} \sin^2\phi_L \, \sin^2\frac{1}{2}(\phi_L - \phi_S) \left[\frac{\sin\frac{1}{2}(\phi_L+\phi_K)\sin\frac{1}{2}(\phi_L-\phi_E)}{\sin\frac{1}{2}(\phi_K-\phi_L)\sin\frac{1}{2}(\phi_L+\phi_E)} \right]^{\beta/\pi} \quad ,$$

where, as before, $c^2 = a^2/v_\infty$. The direction of the force is parallel to the plate LK and toward the left. In the case $\beta = 0$ this reduces to

$$\vec{F} = -\rho\pi v_\infty^2 c^2 e^{-i\alpha} \sin^2\alpha ,$$

which agrees with the expression given by Schmieden.

It will now be shown that under the minimum hypothesis the width of the wake tends to zero asymptotically as the distance from the airfoil becomes infinite.

We have as in (2.111)

$$\frac{dz}{dw} = \frac{1}{v_\infty} e^{\omega(\tau)} = \frac{1}{v_\infty} [1 + \omega''(0) \frac{\tau^2}{2} + \omega'''(0) \frac{\tau^3}{6} + \dots] .$$

Also

$$\frac{dw}{d\tau} = -a^2 (\frac{1}{2} \frac{1}{\tau^3} - \frac{1}{\tau^2} \cos\phi_S + \cos\phi_S - \frac{1}{2} \tau) .$$

Hence

$$dz = \frac{dz}{dw} \frac{dw}{d\tau} d\tau = -\frac{a^2}{v_\infty} \left[\frac{1}{2} \frac{1}{\tau^3} - \frac{1}{\tau^2} \cos\phi_S + \frac{\omega''(0)}{4} \frac{1}{\tau} + 0(1) \right] d\tau .$$

Integrating:

$$z = C_1 + iC_2 - \frac{a^2}{v_\infty} \left[-\frac{1}{4} \frac{1}{\tau^2} + \frac{1}{\tau} \cos\phi_S + \frac{\omega''(0)}{4} \ln\tau + 0(\tau) \right] ,$$

where C_1 and C_2 a are real constants. This expression is of the form

$$z = C_1 + iC_2 + \frac{A}{\tau^2} + \frac{B}{\tau} + iD \ln\tau + 0(\tau) ,$$

where A, B, and D are real constants and A is positive. For τ real and positive this will give the coordinates of a point (x_1, y_1) on the lower boundary of the wake

$$x_1 = C_1 + \frac{A}{\tau^2} + \frac{B}{\tau} + 0(\tau) ,$$

$$y_1 = C_2 + D \ln\tau + 0(\tau) . \tag{2.118}$$

If τ is negative we put $\tau = -\tau'$ where τ' is positive and obtain in like manner the coordinates (x_2, y_2) of a point on the upper boundary of the wake

$$x_2 = C_1 + \frac{A}{\tau'^2} - \frac{B}{\tau'} - \pi D + 0(\tau') , \tag{2.119}$$

$$y_2 = C_2 + D \ln\tau' + 0(\tau') .$$

Consider the particular values of τ and τ' defined by the equations

$$\frac{1}{\tau} = \frac{-B + \sqrt{B^2 - 4A(C_1 - t)}}{2A} \quad , \qquad \frac{1}{\tau'} = \frac{B + \sqrt{B^2 - 4A(C_1 - \pi D - \tau)}}{2A} \quad ,$$

where t is a larger real positive parameter. As t becomes infinite both τ and τ' tend to zero through positive values. Substituting these expressions into (2.118) and (2.119) we get

$$x_2 - x_1 = 0(\tau') - 0(\tau)\,, \quad y_2 - y_1 = D \ln \frac{-B + \sqrt{B^2 - 4A(C_1 - t)}}{B + \sqrt{B^2 - 4A(C_1 - \pi D - t)}} + 0(\tau') - 0(\tau)\,.$$

As $t \to \infty$ both these differences approach zero; hence the width of the wake tends to zero.

2.3 Correlation Between Wind-Tunnel and Flight-Test Data on Stability and Control

Below, we shall demonstrate the procedure of the correlation of wind-tunnel data and flight-test data referring to stability and control for an airplane. The following nomenclature will be used:

W = airplane weight, lbs.,

S = area of wing, sq. ft.,

S_a = area of aileron, sq. ft.,

S_e = area of elevator, sq. ft.,

S_r = area of rudder, sq. ft.,

c = wing mean aerodynamic chord (M. S. C.), in.,

a = center of gravity movement, in.,

c_a = aileron mean geometric chord aft aileron hinge line, in.,

c_e = elevator mean geometric chord aft elevator hinge line, in.,

c_r = rudder mean geometric chord aft rudder hinge line, in.,

β = angle of sideslip, positive when right wing is forward, deg.,

ψ = angle of yaw, positive when left wing is forward, deg. $(-\beta)$,

$V_{m.p.h.}$ = air speed, miles per hour,

ρ = mass air density, slugs per cu. ft.,

σ = density ratio,

q = dynamic pressure, lbs. per sq. ft. [$q = (1/2\rho)v^2$],

C_L = lift coefficient (lift/qS),

C_m = pitching moment coefficient about c. g. (pitching moment/qSc),

C_h = hinge moment coefficient. Subscript a, e, or r denotes aileron, elevator, or rudder. Based on mean geometric chord and control surface area,

F_s = stick force, lbs.,

F_p = pedal force, lbs.,

δ = control surface setting, deg. Subscript a, e, or r denotes aileron, elevator or rudder.,

$\Delta\delta$ = total angular range of control surface, deg. Subscript a, e, or r denotes aileron, elevator, or rudder,

$\Delta\theta$ = angular stick or pedal displacement corresponding to $\Delta\delta$, deg.,

ℓ_s = stick length, in.,

ℓ_p = pedal arm length, in.,

dC_m/di_t = change in pitching moment with change in stabilizer incidence,

dC_{he}/di_t = change in elevator hinge moment with change in stabilizer incidence,

$d\delta_r/d\psi$ = change in rudder deflection required for trim per degree change in yaw angle,

n = load factor,

g = acceleration of gravity, ft. per sec. per sec.,

ξ = tunnel wall correction factor, equal to 0.105 for Wright Brothers Wind Tunnel,

τ = downwash factor for tunnel wall correction to pitching moment,

A = tunnel cross-section area, 57.3 sq. ft.

The standard Glauert wall corrections to drag and angle of attack were applied to the wind-tunnel data.

Pitching moment corrections to the wind-tunnel data due to wall restraint on the flow at the tail were computed from

$$\Delta C_m = -57.3 \xi \tau \frac{S}{A} \frac{dC_m}{di_t} C_L \quad , \qquad (2.120)$$

where the factor τ is a function of the tail length and was derived by Lotz.

Tare and alignment corrections were incorporated in the wind-tunnel data. No corrections were applied to the wind-tunnel control surface hinge moments.

The flight-test instruments were calibrated on the ground, and the necessary corrections were applied to the flight-test data. Where necessary, position error corrections were also applied.

In analyzing the data, a gross weight of 12, 389 lbs. was used. The above gross weight is an average of the gross weight range of 12, 000 to 12, 672 lbs., with a corresponding c. g. range of 23. 3 to 32. 3 per cent M. A. C., used during the flight-test program. When referring to the data, indicated velocities will be used throughout the report. Some error, not serious, however, is introduced in this analysis, since the wind-tunnel power data were based on a gross weight of 13, 509 lbs. and sea-level altitude.

The flight-test and wind-tunnel control forces were trimmed to the velocities indicated in the following table:

Configuration	Velocity
Cruising, power off	300 m. p. h.
Cruising, rated power	300 m. p. h.
Landing, power-off	96 m. p. h.
Landing, rated power	100 m. p. h.
Diving, power-off	300 m. p. h.

The methods used in trimming the data will be explained later.

The indicated velocity corresponding to a given lift-coefficient was computed from

$$V_t = \sqrt{391 W/SC_L} \ . \qquad (2.121)$$

The control surface deflections were measured with respect to the stabilizer and fin chord line, respectively, during the text program.

The stick fixed neutral point variation throughout the flight range was computed from the stabilizer effectiveness data.

The wind-tunnel pitching moment curves were plotted directly from the tabulated data of a reference, from which it was necessary to transfer the data to the flight-test c. g. positions. This was done approximately by the following method. The equation for the moment transfer from $(c. g.)_1$ to $(c. g.)_2$ is

$$M_2 = M_1 + La \cos \alpha + Da \sin \alpha \ , \qquad (2.122)$$

or in coefficient form

$$C_{m_2} = C_{m_1} + \frac{a}{c} C_L \cos \alpha + \frac{a}{c} C_D \sin \alpha \ . \qquad (2.123)$$

By approximation, $\cos\alpha = 1$ and $\sin\alpha = 0$; therefore,

$$C_{m_2} = C_{m_1} + (a/c)C_L \quad . \tag{2.124}$$

Equation (2.124) was used for transferring the wind-tunnel pitching moment data to the flight-test c. g. positions .

The longitudinal control characteristics were obtained from the elevator effectiveness data in the reference.

The stick forces were computed from the wind-tunnel data using the following control force equation:

$$F_s = \frac{\Delta\delta_e}{\Delta\delta} \; \frac{1}{\ell_s} \; C_{h_e} q S_e c_e \quad . \tag{2.125}$$

Since there were no wind-tunnel tab effectiveness data, the flight-test tab effectiveness was used in determining the required elevator trim tab angle at the specified trim velocity.

The stick force and elevator deflection required for the accelerated flight condition were computed by the approximate method.

The directional control characteristics were determined from the wind-tunnel rudder effectiveness data. The pedal forces were calculated using the following equation:

$$F_p = \frac{\Delta\delta_r}{\Delta\theta} \; \frac{1}{\ell_p} \; C_{h_r} S_r c_r \quad . \tag{2.126}$$

The flight-test tab effectiveness was used in determining the required rudder trim tab angle at the specified trim velocity.

In the control force equations, the values of the mechanical advantage factor, $\Delta\delta/\Delta\theta$, were assumed to remain constant; irrespective of control surface deflection. This assumption is reasonable; the stick and rudder positions closely follow a linear relationship with the control surface deflections. The data were obtained by actual measurement on the ground.

The wind-tunnel directional control data were modified to include the flight-test angle of sideslip. This was done by determining a value for the parameter, $d\delta_r/d\psi$, from the wind-tunnel tests. The angle of yaw is equal in magnitude to the angle of sideslip but opposite in sign. Therefore,

$$d\delta_r/d\psi = -\,d\delta_r/d\beta \quad , \tag{2.127}$$

from which the incremental change in rudder angle required to trim when the airplane is flying at small sideslip angles is

$$\Delta\delta_r = -(d\delta_r/d\psi)\Delta\beta \quad . \qquad (2.128)$$

Applying this increment to the wind-tunnel data places the wind-tunnel directional control data on a comparable basis with the flight-test data.

The directional control data were not transferred to c. g. positions corresponding to those used during the flight tests, since at or near zero sideslip any such corrections would be small. Neither were the data corrected for the yawing moment induced by the deflected aileron required to hold the wings level. An examination of the data indicated this correction to be of negligible magnitude, since the aileron deflection required always remained small.

For the flight tests, the control position indicators were rigged so that the elevator angles were measured with respect to the thrust line and the rudder angles were measured with respect to the airplane centerline. The deflections for the elevator and rudder have been corrected to measure from the stabilizer and fin chord lines, respectively, for this analysis, since this is the normal production rigging.

The lift coefficient corresponding to a given velocity was computed from

$$C_L = 391W/SV_i 2 \quad . \qquad (2.129)$$

The stick fixed neutral point variations were computed from the flight-test data by the use of the elevator control data. The method used for determining the stick fixed neutral point variation is given in literature. To apply the method, a plot of elevator area, S_e, versus the airplane lift coefficient, C_L, for at least three center of gravity positions is required.

The airplane pitching moments are obtained from the flight-test longitudinal control data by the following method. The method consists of determining the C_L's for trim from the several c. g.'s tested (at least three c. g.'s are necessary) at a constant elevator angle. These points are spotted on the C_L scale for $C_m = 0$ of a C_m versus C_L graph. The change in C_m due to a change in c. g. from c. g.$_1$ to c. g.$_2$ is

$$\Delta C_m = C_{m_2} - C_{m_1} = -\frac{c.g._2 - c.g._1}{100} C_{L_2} \quad . \qquad (2.130)$$

When pitching moments are desired for elevator angles for which there are no trim lift coefficients at any of the several c. g.'s tested, it is necessary to obtain values for the parameters $dC_m/d\delta_e$ for the flight range.

For a constant C_L on the δ_e versus C_L plot, a change in c. g. causes a change in the elevator deflection required for trim. Therefore, a ΔC_m can be computed from

$$\Delta C_m = -(\Delta c.g. / 100) C_L \quad . \tag{2.131}$$

The corresponding $\Delta\delta_e$ can also be computed;

$$\Delta\delta_e = \delta_{e_1} - \delta_{e_2} \quad . \tag{2.132}$$

Dividing these equations gives the $dC_m/d\delta_e$ for the given C_L ;

$$\frac{dC_m}{d\delta_e} = \frac{\Delta c.g.}{100(\delta_{e_1} - \delta_{e_2})} C_L \quad . \tag{2.133}$$

This is done for several values of lift coefficient in order to determine the elevator effectiveness throughout the flight range. Having previously computed a pitching moment curve for one elevator setting, usually zero degrees, additional curves can be calculated for the desired elevator deflection. This parameter will be satisfactory for low elevator deflections, say = 10^{o}. For elevator deflections beyond this range, the value of the parameter may decrease because the elevator effectiveness tends to decrease.

The flight-test and wind-tunnel longitudinal control data were trimmed at the velocities indicated previously. This was accomplished by obtaining the elevator tab effectiveness at the required trim velocity. The amount of tab required was determined as follows:

At the required trim velocity, obtain $dF_s/d\delta_1$ from the diagram. Then,

$$\delta_t = (F_s)_{\text{zero tab}} / dF_s/d\delta_t \quad . \tag{2.134}$$

The stick force at the trim velocity will now be zero. A new force curve can then be obtained for for the fixed trim tab setting throughout the velocity range.

The maneuvering flight data were plotted directly from flight data. The major portions of the data were taken at an air speed of 200 m. p. h. However, there seemed to be a negligible change in the data between 200 and 280 m. p. h. It is estimated that there would be no appreciable difference between 200 and 240 m. p. h. An air speed of 240 m. p. h. is used because the wind-tunnel data were computed for this air speed.

The flight-test and wind-tunnel directional control data were trimmed by the same method as that used in trimming the longitudinal control data.

The similarity of the configuration as tested in the wind-tunnel and in flight must be compared before any attempt can be made to coordinate the results between the two types of tests.

The neutral point comparison indicates that the wind-tunnel data are generally conservative. For the cruising configuration with power-off, the flight-test data show a $3\frac{1}{2}$ percent stability margin over the wind-tunnel data in the V_{max} and V_{climb} range. In the V_{glide} range, the two curves converge, and the wind-tunnel data indicate better stability than the flight-test data.

The application of rated power for the cruising configuration is destabilizing in each case, but the flight-test data maintains a 1 percent margin of stability over the wind-tunnel data throughout most of the speed range. For high speed the flight-test and wind-tunnel neutral point locations are the same.

For the landing configuration with power-off, the flight-test data show a 3 per cent average stability margin over the wind-tunnel data throughout the flight range. Rated power tends to bring the flight-test and wind-tunnel data in close agreement, except for high approach velocities where the wind-tunnel data indicate better stability.

For the diving configuration the airplane shows a 3 per cent margin in stability over the model. However, the stability trend diverges sharply at lift coefficients greater than one. The reason for this is not readily apparent.

In connection with the neutral point data it was considered advisable to compare the pitching moments as obtained from the flight-test and wind-tunnel data. The pitching moment curves show the same degree of comparison as the neutral point analysis, which is to be expected since both were based on the same data. However, it is to be noted that the elevator effectiveness determined from the flight-test data is slightly greater than that shown by the wind-tunnel data.

The longitudinal control data show good agreement for all configurations. However, for the cruising configuration with power-off, the flight-test data show a slightly greater change in elevator deflection with velocity, indicating that the increased stability has a greater effect than the increased elevator effectiveness. With rated power the elevator deflection curves, though displaced, are nearly parallel, thereby indicating that the increased stability and elevator effectiveness of the flight-test data tend to cancel each other.

The stick forces likewise show fair agreement, although this is regarded as more or less coincidental because of the 5-lb. friction force present in the airplane control system, for which no allowance was made in the analysis of the wind-tunnel data. In many cases, the friction force was greater than the measured stick force. This may partially explain the difference in trim tab angles required.

There were no tab effectiveness data obtained during the wind-tunnel tests, and it was necessary to use the flight-test tab effectiveness data in determining the tab angle for trim for the wind-tunnel data. The use of the flight-test tab effectiveness in the analysis of the wind-tunnel data is questionable, since it is possible that the wind-tunnel tab effectiveness would be different from that measured in flight test. However, it is considered more desirable than the use of calculated tab effectiveness.

The data indicate that the correlation is well within satisfactory limits based on the magnitude of control system friction that was inherent in the flight airplane.

It may be of interest to compare the hinge moment parameters $dC_{h_e}/d\alpha_i$ and $dC_{h_e}/d\delta_e$ as obtained from the flight and wind-tunnel tests. The values of these parameters were determined to be

Parameters	Wind Tunnel	Flight Test
$dC_{h_e}/d\alpha_i$	0	-0.0012
$dC_{h_e}/d\delta_e$	-0.0024	-0.0033

The comparison is not, in general, considered completely satisfactory.

The comparison between directional control data for the cruising configuration is satisfactory. The cruising configuration, power-off, indicates a difference in rudder deflection required for trim of 1.3° throughout the speed range. However, the control gradient, $d\delta_r/dV$, is approximately the same. Rated power causes a steeper control gradient for the wind-tunnel data than for the flight-test data.

There is a discrepancy of considerable magnitude in the rudder required for trim for the landing configuration. With power off the difference varies from 2-1/2° at 100 m.p.h. to 5-1/2° at 160 m.p.h. The difference using rated power is approximately 5-1/2° throughout the flight range. If the flight-test data had not been available prior to the wind-tunnel tests, it is possible that considerable effort would have been expended in an attempt to improve the directional control in a waveoff, which is characterized by high powers at very low speed and is generally the most critical from a control standpoint. For this reason, the wind-tunnel data for this condition is not considered satisfactory.

The directional control forces do not agree in magnitude at various air speeds. However, the trends are similar for the wind-tunnel and flight-test data throughout the flight range of all configurations. Again this is regarded as coincidental because of the large friction forces found on the airplane.

The rudder tab angles required for trim are subject to the same discrepancies as the elevator tab angle, since the flight-test tab effectiveness was used to determine the tab angle for trim for the wind-tunnel data.

There were no comparable directional control data available from the wind-tunnel tests for the diving configuration. However, it is believed that a comparison of data for the diving configuration would agree as well as that for the cruising configuration, since the airplane flight characteristics are similar for these two configurations

The values of the rudder hinge moment parameters as determined from the wind-tunnel and flight-test data are:

Parameters	Wind Tunnel	Flight Test
$dC_{h_r}/d\alpha_t$	0	0
$dC_{h_r}/d\delta_r$	-0.0028	-0.0028

The comparison is in much better agreement than that for the elevator.

No data are shown for directional control at various angles of sideslip, since there are not sufficient wind-tunnel data available. What data were available did not represent the correct lift coefficients. Similarly, no comparison is shown for lateral control because of the incomplete wind-tunnel data.

The wind-tunnel and flight-test data are subject to various differences, some of which may be apparent in the data and some which are considered likely to exist but whose magnitudes are unknown. These differences can best be explained by listing and briefly discussing those applicable to each type of data.

Because the airplane velocity is greater than the velocity at which tunnel tests are made, the Reynolds Number of the airplane is greater; provided the altitude at which the airplane is flown is not excessive. The initial flow separation on the model wing, occurring at a lower angle of attack than on the airplane, should manifest itself as a progressive increase in longitudinal stability up to the model stall because of the breakdown in downwash angle at the tail. The divergence of the neutral point data for the diving configuration is unexplainable at this time because there were not sufficient data available to determine the cause. Principally, scale effects will cause the greatest differences in maximum lift coefficient and longitudinal stability near the stall, provided that the angle of attack of the tail surfaces is not large enough to result in a tail stall at lower lift coefficients.

The two types of corrections applied to the data consist of a mechanical correction due to flow misalignment and balance tares and an aerodynamic correction due to the effect of the tunnel walls on the model characteristics. The mechanical correction is generally determined for the propeller-off condition and is probably not correct for a power-on condition.

The classical wind-tunnel wall corrections are based on an ideal wing having an elliptical distribution and are not, therefore, strictly applicable to any other wing or to a complete model, although it can be shown that minor variations from an elliptical lift distribution will have a negligible effect on the magnitude of the correction. The application of power may cause abrupt changes in the lift distribution because of slipstream twist and velocity and should, therefore, require an additional correction of the type derived by Swanson.

No wall corrections are applied to rolling or yawing moments or control surface hinge moments, since such corrections are small and generally negligible.

The propeller on the model is a fixed-pitch unit and does not, therefore, duplicate completely the characteristics of a full-scale constant-speed propeller, the most important of which may be the propeller side forces. Some calculations made in conjunction with another model indicated that the side-force coefficients of the model propeller were nearly three times those of the full-scale propeller. However, a calculated correction for this difference cannot be justified.

Similarly, because the model and airplane torque coefficients are not equal, the slipstream twist angles are not equal, which will manifest itself in the yawing moment data. Interpretation of the data may then give misleading results.

It is customary to omit from the model numerous external drag items such as rivets, lap joints, radio masts, etc., since such items have been found to be extremely sensitive to changes in Reynolds number. This omission is satisfactory provided the items are not located on the wing where induced flow separation could be started which could affect stability characteristics; also, if the drag items are large, the stability may be changed because of the drag moment. The latter is particularly true in this analysis, since the landing gear and cowl flaps were omitted from the model.

Since all of the longitudinal data are critically affected by the c. g. position, it is necessary to determine as accurately as possible the flight-test c. g. position. Because of continuous consumption of the fuel load, this is sometimes difficult to do, and it is often necessary to use an average c. g. position. For planes whose c. g. is not affected by fuel consumption, this problem is of little importance.

The effects of c. g. movement due to fuel consumption on directional control data at or near zero yaw are small and need not be considered in this analysis.

To evaluate static stability correctly it is desirable that no acceleration other than that due to gravity be present in the data. Provided that a precise flying technique is carefully followed, this will normally be true, but gusts or other unusual weather conditions may prevent satisfactory data from being obtained. In addition, when steady state longitudinal data are obtained, it is desirable that the rate of change of velocity with time be not greater than approximately 1/2 m. p. h. per sec.

One of the most difficult items to evaluate is the variation in flying technique of different pilots or the day-to-day variation in an individual pilot, since the accuracy and usefulness of the data will depend almost entirely on the pilot. For this reason it is advisable, if possible, for one pilot to make all the tests or, failing this, to have pilots of at least equal abilities and temperament. It is not possible to state what influence this may have on the analysis in this report.

The airplane structure, particularly the wings and tail surfaces, is elastic enough to cause noticeable changes in all stability parameters because of deflections. Because the wind-tunnel model is much more rigid, the deflections are smaller and the effect on the stability parameters is less. These effects undoubtedly may cause some of the discrepancy shown between the wind-tunnel and the flight-test data.

The control surfaces provide a graphic example of the effect of air loads on surface deformation, since it has been demonstrated that the effects of fabric bulge under load may cause as much as 100 per cent variation in the hinge moment characteristics of closely balanced surfaces. The use of a solid control surface for the prediction of stick and pedal forces is therefore of doubtful value.

The changes in instrument calibrations or malfunctioning of an instrument during any flight is often unknown until the data are ready for reduction, at which time it is necessary to either neglect the data for that instrument or to repeat the flight. The wind-tunnel tests are more closely supervised, and a running check of the data as taken generally reveals any discrepancy.

There is also some doubt about the accuracy of the method for obtaining some of the flight-test data—for example, the measurement of the sideslip angles. The sideslip angles are determined by means of a vane attached to a mast projecting ahead of the leading edge of the wing at the tip, and it is assumed that the equilibrium angle of the vane is the sideslip angle. Such a method probably does not possess sufficient accuracy to be used for a close comparison with wind-tunnel data because of the influence of the field of flow ahead of the wing on the airflow direction around the vane.

The correlation of comparable wind-tunnel and flight-test data verifies the reliability and usefulness of powered wind-tunnel tests for predicting stability and control characteristics of airplanes. Several basic differences in the data have been briefly discussed, and the conclusion is reached that the degree of correlation for this airplane and model is satisfactory. The correlated data of several airplanes might well be examined statistically in order to determine to what degree wind-tunnel data may be trusted in the design of future airplanes.

2.4 List of References to Chapter 2

1. Adamson, D., and W. B. Boatright: Investigation of Downwash, Sidewash, and Mach Number Distribution Behind a Rectangular Wing at a Mach Number of 2.41. 14 Sept. 1950. NACA RM L50G12.

2. Alford, W. J., Jr., and K. P. Spreemann: Small-Scale Transonic Investigation of a 45° Sweptback Wing of Aspect-Ratio 4 with Combinations of Nose-Flap Deflections and Wing Twist. Jan. 1953. NACA RM L52K13.

3. Anderson, S. B., H. C. Quigley: Flight Measurements of the Low-Speed Characteristics of a 35° Sweptwing Airplane with Area-Suction Boundary-Layer Control on the Trailing-Edge Flaps. Oct. 1956. NACA RM A56G30.

4. Anderson, S. B., H. C. Quigley, and R. C. Innis: Flight Measurements of the Low-Speed Characteristics of a 35° Sweptwing Airplane with Blowing-Type Boundary-Layer Control on the Trailing-Edge Flaps. Oct. 1956. NACA RM A56G30.

5. Bandettini, A: An Investigation at Subsonic Speeds of the Rolling Effectiveness of a Small Perforated Spoiler on a Wing Having 45° of Sweepback. Sept. 1952. NACA RM A52G02.

6. Beavan, J. A., and G. A. M. Hyde: Examples of Pressure Distribution of Compressibility Speeds on E. C. 1250, Great Britain, ARC R & M No. 2056, 1942.

7. Beavan, J. A., and G. A. M. Hyde: Interim Report on the Rectangular High Speed Tunnel Including Some Pilot Traverse Measurements of Drag of the Aerofoil. E. C. 1250, Great Britain, ARC R & M No. 2067, 1942.

8. Beavan, J. A., G. A. M. Hyde, and R. G. Flower: Pressure and Wake Measurements Up to Mach Number 0.85 on an E. C. 1250, Section with 25% Control. Great Britain, ARC R & M No. 2065, 1945.

9. Berman, J. H: Lift and Moment Coefficients for an Oscillating Rectangular Wing -Aileron Configuration in Supersonic Flow. July 1956. NACA TN 3644.

10. Blackaby, J. R: Wind-Tunnel Investigation at Low Speed of a Wing Having 63° Sweepback and a Drooped Tip. Apr. 1955. NACA RM A55B14.

11. Bland, W. M. Jr., and E. T. Marley: Free Flight Investigation at Zero Lift in the Mach Number Range Between 0.7 and 1.4 to Determine the Effectiveness of an Inset Tab as a Means of Aerodynamically Relieving Aileron Hinge Moments. NACA RM L52K07, Jan. 1953.

12. Boatright, W. B., and R. W. Rainey: Hinge Moment Measurements of a Wing with Leading Edge and Trailing Edge Flaps at a Mach Number of 1.93. NACA RM L8K12a, Jan. 1949.

13. Boyd, J. W: A Comparison of the Experimental and Theoretical Loading Over Triangular Wings in Sideslip at Supersonic Speeds. 18 May 1951. NACA RM A51C13.

14. Boyd, J. W: Aerodynamic Characteristics of a Two 25-Percent Area Trailing-Edge Flaps on an Aspect-Ratio 2 Triangular Wings at Subsonic and Supersonic Speeds. July 1952. NACA RM A52D01c.

15. Boyd, J. W., and E. R. Phelps: A Comparison of the Experimental and Theoretical Loading Over Triangular Wings at Supersonic Speeds. 3 Jan. 1951. NACA RM A50J17.

16. Burrows, D. L: Large-Scale Low-Speed Wind-Tunnel Tests of a Model Having a 60° Delta Horizontal Canard Control Surface and Wing to Obtain Static Longitudinal Stability and Canard Surface Hinge Moment Data. June 1954. NACA RM L54D16a.

17. Cahill, J. F., Aerodynamic Load Measurements Over a Leading-Edge Slat on a 40° Sweptback Wing at Mach Numbers From 0.10 to 1.91. Sept. 1952. NACA RM L52G18a.

18. Campbell, J. P., and J. L. Johnson, Jr: Wind-Tunnel Investigation of an External-Flow Jet-Augmented Slotted Flap Suitable for Application to Airplanes with Pod-Mounted Jet Engines. Dec. 1956. NACA TN 3898.

19. Campbell, G. S., and W. D. Morrison, Jr: A Small-Scale Investigation of "M" and "W" Wings at Transonic Speeds. 2 Oct. 1950. NACA RM L50H25a.

20. Cancro, P. A: Low Speed Aileron Effectiveness as Determined by Force Tests and Visual Flow Observations on a 52° Sweptback Wing with an Without Chord Extensions. NACA RM L53B26, Apr. 1953.

21. Church, J. D: Flight Investigation of the Rolling Effectiveness of Fingered Semaphore Spoilers on a Tapered 45° Sweptback Wing Between Mach Numbers 0.6 and 1.3. Jan. 1954. NACA RM L53K20.

22. Church, J. D: Rocket-Powered-Model Investigation of the Hinge-Moment and Normal-Force Characteristics of a Half-Diamond Tip Control on a 60° Sweptback Diamond Wing Between Mach Numbers of 0.5 and 1.3. Apr. 1954. NACA RM L54C10.

23. Cleary, J. W., and L. E. Boddy: Wind-Tunnel Investigation of a 45° Sweptback Wing Having a Symmetrical Root and a Highly Cambered Tip, Including the Effects of Fences and Lateral Controls. Nov. 1953. NACA RM A53I21.

24. Conner, D. W., and E. B. May, Jr: Control Effectiveness Load and Hinge-Moment Characteristics of a Tip Control Surface on a Delta Wing at a Mach Number of 1.9. 7 Oct. 1949. NACA RM L9H05.

25. Conner, D. W., and E. B. May, Jr: Control Effectiveness and Hinge-Moment Characteristics of a Tip Control Surface on a Low-Aspect-Ratio Pointed Wing at a Mach Number of 1.9. 5 Oct. 1949. NACA RM L9H26.

26. Conner, D. W., and M. H. Mitchell, Jr: Control Effectiveness and Hinge Moment Measurements at a Mach Number of 1.9 of a Nose-Flap and Trailing Edge Flap on a Highly Tapered Low-Aspect-Ratio Wing. NACA RM L8K17a, Jan. 1949.

27. Conner, D. W., and M. H. Mitchell, Jr. Effects of Spoiler on Airfoil Pressure Distribution and Effects of Size and Location of Spoilers on the Aerodynamic Characteristics of a Tapered Unswept Wing of Aspect-Ratio 2.5 at a Mach Number of 1.90. 24 Jan. 1951. NACA RM L50L20.

28. Cook, W. L., R. N. Griffin, Jr., and D. H. Mickey: A Preliminary Investigation of the Use of Circulation Control to Increase the List of a 45° Sweptback Wing by Suction Through Trailing-Edge Slots. Dec. 1954. NACA RM A54I21.

29. Cook, W. L., R. N. Griffin, Jr., and G. M. McCormack: The Use of Area Suction for the Purpose of Delaying Separation of Air Flow at the Leading Edge of a 63° Sweptback Wing. 22 Nov. 1950. NACA RM A50H09.

30. Cook, W. L., C. A. Holzhauser, and M. W. Kelly: The Use of Area Suction for the Purpose of Improving Trailing-Edge Flap Effectiveness on a 35° Sweptback July 1953. NACA RM A53E06.

31. Cook, W. L., and M. W. Kelly: The Use of Area Suction for the Purpose of Delaying Separation of Air Flow at the Leading Edge of a 63° Sweptback Wing-Effects of Controlling the Chordwise Distribution of Suction-Air Velocities. Jan. 1952. NACA RM A51J24.

32. Cooper, G. E., and R. C. Innis: Effect of Area-Suction-Type Boundary-Layer Control on the Landing-Approach Characteristics of a 35° Sweptwing Fighter. Feb. 1956. NACA RM A55K14.

33. Crane, H. L., G. J. Hurt, Jr., and J. M. Elliott: Subsonic Flight Investigation of Methods to Improve the Damping Lateral Oscillations by Means of a Vicous Damper in the Rudder System in Conjunction with Adjusted Hinge-Moment Parameters. June 1954. NACA RM L54D09.

34. Crigler, J. L: Comparison of Calculated and Experimental Load Distribution on Thin Wings at High Subsonic and Sonic Speeds. Jan. 1957. NACA TN 3941.

35. Croom, D. R: A Low-Speed Investigation of a Thin 60° Delta Wing Equipped with a Double Slotted Flap to Determine the Chordwise Pressure Distribution and the Effect of Vane Size. Mar. 1955. NACA TM L54L03a.

36. Croom, D. R., and J. K. Huffman: Investigation at Transonic Speeds of Deflectors and Spoilers as Gust Alleviators on a 35° Sweptwing Transonic-Bump Method. June 1957. NACA TN 4006.

37. Croom, D. R., and J. K. Huffman: Investigation at Low Speeds of Deflectors and Spoilers as Gust Alleviators on a Model of the Bell X-5 Airplane with 35° Sweptwings and on a High-Aspect-Ratio 35° Sweptwing-Fuselage Model. June 1957. NACA TN 4057.

38. Czarnecki, D. R., and R. L. Douglas: Simplified Procedures for Estimating Flap-Control Loads at Supersonic Speeds. May 1955. NACA RM L55E12.

39. Czarnecki, D. R., and D. R. Lord: Simplified Procedures for Estimating Flap-Control Loads at Supersonic Speeds. May 1955. NACA RM L55E12.

40. Dannenberg, R. E., J. A. Weiberg, and B. J. Gambucci: Perforated Sheets as the Porous Material for a Suction-Flap Application. May 1957. NACA TN 4038.

41. Donlan, C. J., and J. Weil: Characteristics of Sweptwings at High Speeds. Jan. 1952. NACA RM L52A15.

42. Drake, H. M., Aileron and Elevator Hinge Moments of the Bell X-1 Airplane Measured in Transonic Flight. NACA RM L53E04, June 1953.

43. Dugan, D. W: Effects of Three Types of Blunt Trailing Edges on the Aerodynamic Characteristics of a Plane Tapered Wing of Aspect-Ratio 3.1 with a 3-Percent-Thick Biconvex Section. July 1952. NACA RM A52E01.

44. Dunning, R. W., and E. F. Ulmann: Aerodynamic Characteristics at Mach Number 4.04 of a Rectangular Wing of Aspect-Ratio 1.33 Having a 6-Percent-Thick Circular-Arc Profile and a 30-Percent-Chord Full-Span Trailing-Edge Flap. May 1953. NACA RM L53D03.

45. Eggleston, J. M., and F. W. Diederich: Theoretical Calculation of the Power Spectra of the Rolling and Yawing Moments on a Wing in Random Turbulence. Dec. 1956. NACA TN 3864.

46. Eisner, F: Widerstnadsmessungen an Umstroemten Zylindern. Mitteilungen der Preussischen Versuchsanstalt fuer Wasserbau und Schiffbau, Heft 4, Berlin, 1929.

47. Ellenberger, G: "Bestimmung der Luftkraefte auf Einen Abenen Tragfluegel mil Querruder." Zeitschr. f. Angew. Math. u. Mech. 16, 199-266, 1936.

48. Emerson, H. F., and B. M. Gale: Aerodynamic Characteristics of Two Plane, Unswept Tapered Wings of Aspect-Ratio 3 and 3-Percent Thickness From Tests on Transonic Bump. May 1952. NACA RM A52C07.

49. Emerson, H. F., and B. M. Gale: Transonic Aerodynamic Characteristics of Three Thin Triangular Wings and a Trapezoidal Wing, all of Low Aspect-Ratio. July 1952. NACA RM A52D21.

50. English, R. D: Some Effects of Leading-Edge Roughness on the Aileron Effectiveness and Drag of a Thin Rectangular Wing Employing a Full-Span Plain Aileron at Mach Numbers From 0.6 to 1.5. Nov. 1953. NACA RM L53I25.

51. English, R. D: Flight Investigation of an Aileron and a Spoiler on a Wing of the X-3 Airplane Plan Form at Mach Numbers From 0.5 to 1.6. NACA RM L54D26a.

52. English, R. D: Some Effects of External Wing Tip Stores on the Rolling Effectiveness and Drag of Plain and Half-Delta Tip Ailerons on A 4-Percent-Thick Tapered, Unswept Wing. NACA RM L54F29a, Aug. 1954.

53. Fields, E. M: Some Effects of Spoiler Height, Wing Flexibility, and Wing Thickness on Rolling Effectiveness and Drag of Unswept Wings at Mach Numbers Between 0.4 and 1.7. Oct. 1952. NACA RM L52H18.

54. Fink, M. P., and B. W. Cocke: A Low-Speed Investigation of the Aerodynamic, Control, and Hinge-Moment Characteristics of Two Types of Controls and Balancing Tabs on a Large-Scale Thin Delta-Wing-Fuselage Model. Mar. 1954. NACA RM L54B03.

55. Fitzpatrick, J. E., and R. L. Woods: Low-Speed Lateral Control Characteristics of an Unswept Wing with Hexagonal Airfoil Sections and Aspect-Ratio 2.5 Equipped with Spoilers and with Sharp and Thickened-Trailing-Edge Flap-Type Ailerons at a Reynolds Number of 7.6×10^6. NACA RM L52B15. Apr. 1952.

56. Foster, G. V., and W. C. Schneider: Effects of Leading-Edge Radius on the Longitudinal Stability of Two 45° Sweptback Wings as Influenced by Reynolds Numbers Up to 8.20×10^6 and Mach Numbers Up to 0.303. July 1955. NACA RM L55F06.

57. Fradenburgh, E. A., L. J. Obery, and J. F. Mello: Influenced of Fuselage and Canard-Type Control Surface on the Flow Field Adjacent to a Rearward Fuselage Station at a Mach Number of 2.0-Data Presentation. Jan. 1952. NACA RM E51L05.

58. Franks, R. W: Tests in the Ames 40-by-80 Foot Wind-Tunnel of an Airplane Model with anAspect-Ratio 4 Triangular Wing and All-Movable Horizontal Tail-High-Lift Devices and Lateral Controls. NACA RM A52K13, Feb. 1953.

59. Franks, R. W: Tests in the Ames 40-by-80 Foot Wind-Tunnel of the Aerodynamic Characteristics of Airplane Models with Plain Spoiler Ailerons. Dec. 1954. NACA RM A54H26.

60. Franks, R. W: The Application of a Simplified Lifting-Surface Theory to the Prediction of the Rolling Effectiveness of Plain Spoiler Ailerons at Subsonic Speeds. Dec. 1954. NACA RM A54G26a.

61. Furlong, G. C., and J. G. McHugh: A Summary and Analysis of the Low-Speed Longitudinal Characteristics of Sweptwings at High Reynolds Number. Aug. 1952. NACA RM L52D16.

62. Gardner, W. N: Aerodynamic Characteristics of a Canard-Balanced, Free-Floating, All-Movable Stabilizer as Obtained From Rocket-Powered-Model Flight Tests and Low-Speed Wind-Tunnel Tests. Dec. 1953. NACA RM L53I28a.

63. Gardner, W. N., and H. J. Curfman, Jr: Flight Investigation to Determine the Hinge Moments of Beveled-Edge Aileron on a 45° Sweptback Wing at Transonic and Low Supersonic Speeds. 12 Nov. 1947. NACA RM L7H26.

64. Gault, D. E: A correlation of Low-Speed, Airfoil-Section Stalling Characteristics with Reynolds Number and Airfoil Geometry. Mar. 1957. NACA TN 3963.

65. Goin, K. L: Investigation at a Mach of 1.9 and a Reynolds Number of 22×10^6 of Several Flap Type Lateral-Control Devices on a Wing Having 42.7° Sweepback of the Leading Edge. NACA RM L9A18a, Mar. 1949.

66. Goin, K. L: Theoretical Analysis to Determine Unbalanced Trailing Edge Controls Having Minimum Hinge Moments Due to Deflection at Supersonic Speeds. NACA RM L51F19, and TN 3471, Aug. 1955.

67. Graham, R. R., and W. A. Jacques: Wind-Tunnel Investigation of Stall Control by Suction Through a Porous Leading Edge on a 37° Sweptback Wing of Aspect-Ratio 6 at Reynolds Numbers From 2.50×10^6 to 8.10×10^6. Mar. 1953. NACA RM L52L05.

68. Graham, D., and D. G. Koenig: Tests in the Ames 40- by 80-Foot Wind-Tunnel of an Airplane Configuration with an Aspect-Ratio 2 Triangular Wing and an All-Movable Horizontal Tail-Lateral Characteristics. NACA RM A51L03, Feb. 1952.

69. Griner, R. F., and G. V. Foster: Low-Speed Longitudinal and Wake Airflow Characteristics at a Reynolds Number of 6.0×10^6 of a 52° Sweptback Wing Equipped with Various Spans of Leading-Edge and Trailing-Edge Flaps, a Fuselage, and a Horizontal Tail at Various Vertical Positions. 28 Feb. 1951. NACA RM L50K29.

70. Guy, L. D: Some Effects of Chordwise Fences on the Aerodynamic Characteristics of Four Moderately Sweptback Wings in the Low-Lift Range at Transonic Mach Numbers and at Mach Number 1.9. 21 July 1950. NACA RM L50E16.

71. Guy, L. D: Control Hinge-Moment and Effectiveness Characteristics of a 60° Half-Delta Tip Control on a 60° Delta Wing at Mach Numbers of 1.41 and 1.96. Oct. 1952. NACA RM L52H13.

72. Guy, L. D: Control Hinge-Moment and Effectiveness Characteristics of a Horn-Balanced, Flap-Type Control on a 55° Sweptback Triangular Wing of Aspect-Ratio 3.5 at Mach Numbers of 1.41, 1.62, and 1.96. Jan. 1953. NACA RM L52L15.

73. Hammond, A. D., and J. C. Graven, Jr: The Twisting Effect at Transonic Speeds of Spoiler Ailerons on a 45° Sweptback, Aspect-Ratio 4, Tapered Wing. Jan. 1954. NACA RM L53K03a.

74. Hammond, A. D., and W. C. Hayes, Jr: Pressure Distributions on Plug-and Semaphore-Type Spoiler Ailerons on a 35° Sweptback Wing of Aspect-Ratio 4, Taper-Ratio 0.6, and NACA 65A006 Airfoil Section at High Subsonic Speeds. Aug. 1954. NACA RM L54F08.

75. Hammond, A. D., and B. M. Keffer: The Effect of High Subsonic Speeds of a Flap Aileron on the Chordwise Pressure Distribution Near Mid-Semispan of a Tapered 35° Sweptback Wing of Aspect-Ratio 4 Having NACA 65A006 Airfoil Section. NACA RM L53C23, May 1953.

76. Hammond, A. D., and B. M. Keffer: Chordwise Pressures and Section Force and Moment Coefficients at High Subsonic Speeds Near Midspan of a Tapered 35° Sweptback Wing with a Flap-Type Control and an Attached Tab. NACA RM L54A22, Mar. 1954.

77. Hammond, A. D., and B. M. McMullan: Chordwise Pressure Distribution at High Subsonic Speeds Near Mid-Semispan of a Tapered 35° Sweptback Wing of Aspect-Ratio 4 Having NACA 65A006 Airfoil Sections and Equipped with various Spoiler Ailerons. NACA RM L52C28, June 1952.

78. Hatch, J. E. Jr: and J. J. Gallagher: Aerodynamic Characteristics of a 68.4° Delta Wing at Mach Numbers of 1.6 and 1.9 Over a Wide Reynolds Number Range. Nov. 1953. NACA RM L53I08.

79. Hatch, J. E. Jr., and L. K. Hargrave: Effects of Reynolds Number on the Aerodynamic Characteristics of a Delta Wing at Mach Number of 2.41. Oct. 1951. NACA RM L51H06.

80. Hedgepeth, J. M., and R. J. Kell: Comparison Between Theoretical and Experimental Rates of Roll of Two Models with Flexible Rectangular Wings at Supersonic Speeds. NACA RM L54F23. Aug. 1954.

81. Heitmeyer, J. C: Lift, Drag, and Pitching Moment of Low-Aspect-Ratio Wings at Subsonic and Supersonic Speeds-Plane Triangular Wing of Aspect-Ratio 4 with 3-Percent-Thick, Biconvex Section. 8 June 1951. NACA RM A51D30.

82. Heitmeyer, J. C: Lift, Drag, and Pitching Moment of Low-Aspect-Ratio Wings at Subsonic and Supersonic Speeds-Plane Triangular Wing of Aspect-Ratio 3 with NACA 0003-63 Section. Sept. 1951. NACA RM A51H02.

83. Heitmeyer, J. C: Lift, Drag, and Pitching Moment of Low-Aspect-Ratio Wings at Subsonic and Supersonic Speeds-Plane 45° Sweptback Wing of Aspect-Ratio 3, Taper-Ratio 0.4 with 3-Percent-Thick, Biconvex Section. Sept. 1951. NACA RM A51H10.

84. Heitmeyer, J. C: Lift, Drag, and Pitching Moment of Low-Aspect-Ratio Wings at Subsonic and Supersonic Speeds-Plane Tapered Wing of Aspect-Ratio 3.1 with 3-Percent-Thick Rounded-Nose Section. July 1952. NACA RM A52D23.

85. Heitmeyer, J. C., and R. C. Hightower: Lift, Drag, and Pitching Moment of Low-Aspect-Ratio Wings at Subsonic and Supersonic Speeds-Plane Triangular Wing of Aspect-Ratio 4 with 3-Percent-Thick Rounded-Nose Section. Aug. 1951. NACA RM A51F21.

86. Heitmeyer, J. C., and W. G. Smith: Lift, Drag, and Pitching Moment of Low-Aspect-Ratio Wings at Subsonic and Supersonic Speeds-Plane Triangular Wing of Aspect-Ratio 2 with NACA RM A50K24a.

87. Heitmeyer, J. C., and J. D. Stephenson: Lift, Drag, and Pitching Moment of Low-Aspect-Ratio Wings at Subsonic and Supersonic Speeds-Plane Triangular Wing of Aspect-Ratio 4 with NACA 0005-63 Section.

88. Henderson, J. H: Effect at Transonic Speeds of Inboard Spoilers on the Static Longitudinal Stability Characteristics of a 45° Sweptback Wing-Body Combination Having a Leading Edge Chord Extension. NACA RM L54D13, June 1954.

89. Henning, A. B., — Results of a Rocket-Model Investigation of Control-Surface Buzz and Flutter on a 4-Percent-Thick Unswept Wing and on 6, 9, and 12-Percent-Thick Sweptwings at Transonic Speeds. Nov. 1953. NACA RM L53I29.

90. Higgins, G. J., and E. N. Jacobs: — The Effects of Flap and Ailerons on the NACA M6 Airfoil Section. NACA Tech. Rep. 260, 1927.

91. Hightower, R. C: — Lift, Drag, and Pitching Moment of Low-Aspect-Ratio Wings at Subsonic and Supersonic Speeds. Comparisons of Three Wings of Aspect-Ratio 2 of Rectangular, Sweptback, and Triangular Planform, Including Effects of Thickness Distribution. Feb. 1953. NACA RM A52L02.

92. Hobzhauser, C. A., and R. S. Bray: — Wind-Tunnel and Flight Investigations of the Use of Leading-Edge Area Suction for the Purpose of Increasing the Maximum Lift Coefficient of a 35° Sweptwing Airplane. 1956. NACA Rep. 1276, Supersedes RM A52G17, RM A55C07.

93. Hobzhauser, C. A., and R. K. Martin: — The Use of a Leading-Edge Area-Suction Flap to Delay Separation of Air Flow From the Leading Edge of a 35° Sweptback Wing. Dec. 1953. NACA RM A53J26.

94. Hopkins, E. J: — Aerodynamic Study of a Wing-Fuselage Combination Employing a Wing Sweptback 63°. Effects of Split Flaps, Elevons, and Leading-Edge Devices at Low Speed. 19 May 1949. NACA RM A9C21.

95. Hopko, R. N., and C. A. Sandahl: — Free-Flight Investigation of the Zero-Lift Drag of Several Wings at Supersonic Mach Numbers Extending to 2.6. Dec. 1952. NACA RM L52D29.

96. Hunton, L. W: — A Study of the Application of Airfoil Section Data to the Estimation of the High Subsonic Speed Characteristics of Sweptwings. June 1955. NACA RM A55C23.

97. Jacobsen, C. R: — Effects on Control Effectiveness of Systematically Varying the Size and Location of Trailing-Edge Flaps on a 45° Sweptback Wing at a Mach Number of 1.9. Dec. 1951. NACA RM L51I26.

98. Jacobsen, C. R: Control Characteristics of Trailing-Edge Spoilers on Untapered Blunt Trailing-Edge Wings of Aspect-Ratio 2.7 with 0° and 45° Sweepback at Mach Numbers of 1.41 and 1.96. Dec. 1952. NACA RM L52J28.

99. James, H. A., and L. W. Hunton: Estimation of Incremental Pitching Moments Due to Trailing-Edge Flaps on Swept and Triangular Wings. June 1955. NACA RM A55D07.

100. Jaquet, B. M: Effects on Chord-Extension and Droop Combined Leading-Edge Flap and Chord-Extension on Low-Speed Static Longitudinal Stability Characteristics of an Airplane Model Having a 35° Sweptback Wing with Plain Flaps Neutral or Deflected. Jan. 1953. NACA RM L52K21a.

101. Jaquet, B. M: Some Low-Speed Wind-Tunnel Experiments Pertaining to the Longitudinal Stability Characteristics of a 35° Swept-wing Model and an Unswept-Wing Model. Oct. 1953. NACA RM L53H31.

102. Johnson, H. S: Wind-Tunnel Investigation at Subsonic and Low Transonic Speeds of the Effects of Aileron Span and Spanwise Location on the Rolling Characteristics of a Test Vehicle with Three Untapered 45° Sweptback Wings. NACA RM L51B16, Apr. 1951.

103. Johnson, H. S: Wind-Tunnel Investigation at Subsonic and Low Transonic Speeds of the Effects of Aileron Span and Spanwise Location on the Rolling Characteristics of a Test Vehicle with Three Untapered 45° Sweptback Wings. 6 Apr. 1951. NACA RM L51B16.

104. Johnson, B. H. Jr: and F. A. Demele: Investigation of a Thin Wing of Aspect-Ratio 4 in the Ames 12-Foot Pressure Wind-Tunnel. III. The Effectiveness of Constant-Chord Aileron. NACA RM A8I17, Nov. 1948.

105. Johnson, C. T., and A. E. Kuhl: Flight Measurements of Elevon Hinge Moments on the XF-92A Delta-Wing Airplane. Jan. 1955. NACA RM H54J25, H54J25a.

106. Katzen, E. D., D. M. Kuehn, and W. A. Hill, Jr: Investigation of the Effects of Profile Shape on the Aerodynamic and Structural Characteristics of Thin, Two-Dimensional Airfoils at Supersonic Speeds. May 1954. NACA RM A54B08a.

107. Kelly, M. W., and W. H. Tolhurst, Jr: The Use of Area Suction to Increase the Effectiveness of a Trailing-Edge Flap on a Triangular Wing of Aspect-Ratio 2. Apr. 1954. NACA RM A54A25.

108. Kelly. M. W., and W. H. Tolhurst, Jr: Full-Scale Wind-Tunnel Tests of a 35° Sweptback Wing Airplane with High-Velocity Blowing Over the Trailing-Edge Flaps. Nov. 1955. NACA RM A55I09.

109. Kemp, W. B. Jr: Aerodynamic Characteristics at Small Scale and a Mach Number of 1.38 of Untapered Wings Having "M" and "W" Planforms. June 1954. NACA RM L54D15a.

110. Kemp, W. B. Jr: and R. E. Becht: Damping-in-Pitch Characteristics at High Subsonic and Transonic Speeds of Four 35° Sweptback Wings. Oct. 1953. NACA RM L53G29a.

111. Kirby, R. H: Exploratory Investigation of the Effectiveness of Biplane Wings with Large-Chord Double Slotted Flaps in Redirecting a Propeller Slipstream Downward for Vertical Take-Off. Oct. 1956. NACA TN 3800.

112. Koenig, D. G: Tests in the Ames 40-by-80 Foot Wind-Tunnel of an Airplane Configuration with an Aspect-Ratio 3 Triangular Wing and an All-Movable Horizontal Tail-Longitudinal and Lateral Characteristics. Apr. 1953. NACA RM A52L15.

113. Koenig, D. G: Tests in the Ames 40by-80 Foot Wind-Tunnel of an Airplane Configuration with a Variable-Incidence Triangular Wing and an All-Movable Horizontal Tail. June 1953. NACA RM A53D21.

114. Kolscher, M: "Unstetige Stroemungen mit Endlichen Totwasser." Luftfahntforschung, 17, 154-160. 1940.

115. Kuhn, R. E: Investigation of Effectiveness of a Wing Equipped with a 50-Percent-Chord Sliding Flap, a 30-Percent-Chord Slotted Flap, and a 30-Percent-Chord Slat in Deflecting Propeller Slipstreams Downward for Vertical Take-Off. Jan. 1957. NACA TN 3919.

116. Kuhn, R. E., and A. L. Byrnes, Jr: Aerodynamic Loading Characteristics in Sideslip of a 45° Sweptback Wing with and Without a Fence at High Subsonic Speeds. Jan. 1955. NACA RM L54K15.

117. Kuhn, R. E., and W. C. Hayes, Jr: Wind-Tunnel Investigation of Effect of Propeller Slipstreams on Aerodynamic Characteristics of a Wing Equipped with a 50-Percent-Chord Sliding Flap and a 30-Percent-Chord Slotted Flap. Feb. 1957. NACA TN 3918.

118. Kuhn, R. E., J. W. Wiggins, and A. L. Byrnes, Jr: Wind-Tunnel Investigation of the Effects of a Fence and a Leading-Edge Notch on the Aerodynamic Loading Characteristics in Pitch of a 45° Sweptback Wing at High Subsonic Speeds. Oct. 1953. NACA RM L53H24.

119. Lockwood, V. E., J. W. Wiggins, and A. L. Byrnes, Jr: Wind-Tunnel Investigation of the Effects of a Fence and a Leading-Edge Notch on the Aerodynamic Loading Characteristics in Pitch of a 45° Sweptback Wing at High Subsonic Speeds. Dec. 1956. NACA TN 3865.

120. Lord, D. R., and C. Driver: Investigation of theEffect of Balancing Tabs on the Hinge-Moment Characteristics of a Trailing-Edge Flap-Type Control on a Trapezoidal Wing at a Mach Number of 1.61. Aug. 1954. NACA RM L54F22.

121. Lowry, J. G., J. A. Axelson, and H. I. Johnson: Effects of Sweep on Controls. June 1948. NACA RM L8A28c.

122. Lowry, J. G., and E. C. Polhamus: A Method for Predicting Lift Increments Due to Flap Deflection at Low Angles of Attack in Incompressible Flow. Jan. 1957. NACA TN 3911.

123. Lowry, J. G., and R. D. Vogler: Wind-Tunnel Investigation at Low Speeds to Determine the Effect of Aspect-Ratio and End Plates on a Rectangular Wing with Jet Flaps. Deflected. 85°. Dec. 1956. NACA TN 3863.

124. McCormack, G. M., and W. H. Tolhurst, Jr: The Effects of Boundary-Layer Control on the Longitudinal Characteristics of a Sweptback Wing Using Suction Through Streamwise Slots in the Outboard Portion of the Wing. 5 Jan. 1951. NACA RM A50K06.

125. MacLeod, R. G: Wind-Tunnel Investigation at Transonic Speeds of a Leading-Edge Slat on a Modified-Double-Wedge Wing. Dec. 1951. NACA RM L51J22a.

126. Maki, R. L., and L. W. Hunton: An Investigation at Subsonic Speeds of Several Modifications to the Leading-Edge Region of the NACA 64A010 Airfoil Section Designed to Increase Maximum Lift. Dec. 1956. NACA TN 3871.

127. Marley, E. T., and R. D. English: Some Effects of Aeroelasticity at Mach Numbers From 0.7 to 1.6 on the Rolling Effectiveness of Thin Flat-Plate Delta Wings Having 45° Swept Leading Edges and Full-Span Constant-Chord Ailerons. Feb. 1952. NACA RM L51L05.

128. Martz, C. W., and J. D. Church: Flight Investigation at Subsonic, Transonic, and Supersonic Velocities of the Hinge-Moment Characteristics, Lateral-Control Effectiveness, and Wing Damping in Roll of a 60° Sweptback Delta Wing with Half-Delta Tip Ailerons. (Revised). Sept. 1951. NACA RM L51G18.

129. Martz, C. W., J. D. Church, Free-Flight Investigation to Determine Force and Hinge-Moment Characteristics at Zero Angle of Attack of a 60° Sweptback Half-Delta Tip Control on a 60° Sweptback Delta Wing at Mach Numbers Between 0.68 and 1.44. Dec. 1951. NACA RM L51I14.

130. Martz, C. W., J. D. Church, and J. W. Gosiec: Rocket-Model Investigation to Determine the Force and Hinge-Moment Characteristics of a Half-Delta Tip Control on a 59° Sweptback Delta Wing Between Mach Numbers of o. 55 and 1. 43. Oct. 1952. NACA RM L52H06.

131. Mastrocola, N., and A. Assadourian: Low-Speed Wind-Tunnel Tests of a Pilotless Aircraft Having Horizontal and Vertical Wings and a Cruciform Tail. NACA RM L6J18a, Aug. 1947.

132. Matteson, F. H., and R. D. Van Dyke, Jr: Flight Investigation of the Effects of a Partial-Span Leading-Edge Chord-Extension of the Aerodynamic Characteristics of a 35° Sweptwing Fighter Airplane. Apr. 1954. NACA RM A54B26.

133. May, E. B. Jr: Investigation of the Effects of Leading-Edge Chord-Extensions on the Aerodynamic and Control Characteristics of Two Sweptback Wings at Mach Numbers of 1.41, 1.62, and 1.96. 16 Jan. 1951. NACA RM L50L06a.

134. Mitchell, M. H. Jr: Effects of Varying The Size and Location of Trailing Edge Flap-Type Controls on the Aerodynamic Characteristics of an Unswept Wing at a Mach Number of 1.9. NACA RM L50F08, Aug. 1950.

135. Morrill, C. P. Jr., and L. E. Boddy: High-Speed Stability and Control Characteristics of a Fighter Airplane Model with a Sweptback Wing and Tail. 14 Apr. 1948. NACA RM A7K28.

136. Morrison, W. D. Jr: Transonic Aerodynamic Characteristics of Three W-Planform Wings Having Aspect-Ratio 8, Taper-Ratio 0.45, and NACA 63A Series Airfoil Sections. July 1952. NACA RM L52E14a.

137. Morrison, W. D. Jr: Transonic Aerodynamic Characteristics in Pitch of a W-Wing Having 60°48' Panel Sweep, Aspect-Ratio 3.5, and Taper-Ratio 0.25. Aug. 1953. NACA RM L53F22.

138. Morrison, W. D. Jr., and W. J. Alford, Jr: Effects of Horizontal-Tail Height and a Wing Leading-Edge Modification Consisting of a Full-Span Flap and a Partial-Span Chord-Extension on the Aerodynamic Characteristics in Pitch at High Subsonic Speeds of a Model with a 45° Sweptback Wing. June 1953. NACA RM L53E06.

139. Naeseth, R. L: Low-Speed Longitudinal Aerodynamic Characteristics of a 45° Sweptback Wing with Double Slotted Flaps. Apr. 1956. NACA RM L56A10.

140. Naeseth, R. L., D. R. Croom, and J. W. McKee: Lateral Control Characteristics of Two Structurally Similar Flexible Wings with 45° Sweep: A Sweptback Wing and a Wing with M Planform. Apr. 1954. NACA RM L54C19.

141. Nelson, W. H., and J. L. Frank: The Effect of Wing Profile on the Transonic Characteristics of Rectangular and Triangular Wings Having Aspect-Ratios of 3-Transonic Bump Technique. Oct. 1954. NACA RM A54H12a.

142. Newsom, W. A. Jr: Effect of Propeller Location and Flap Deflection on the Aerodynamic Characteristics of a Wing-Propeller Combination for Angles of Attack From 0° to 80°. Jan. 1957. NACA TN 3917.

143. Obery, L. J., and H. S. Krasnow: Influence of a Canard-Type Control Surface on the Internal and External Performance Characteristics of Nacelle-Mounted Supersonic Diffusers (Conical Centerbody) at a Rearward Body Station for a Mach Number of 2.0. Aug. 1952. NACA RM E52F16.

144. Olson, R. N., and M. H. Mead: Aerodynamic Study of a Wing-Fuselage Combination Employing a Wing Sweptback 63°. Effectiveness of an Elevon as a Longitudinal Control and the Effects of Camber and Twist on the Maximum Lift-Drag Ratio at Supersonic Speeds. 8 May 1950. NACA RM A50A31a.

145. Page, W. A: Experimental Determination of the Range of Applicability of the Transonic Area Rule for Wings of Triangular Plan Form. Dec. 1956. NACA TN 3872.

146. Pearcey, H. H., and J. A. Beavan: Force and Pressure Coefficients Up to Mach No. 0.87 on the Goldstein Roof-Top Section 1442/1547. Great Britain; ARC RM 2346, 1946.

147. Petersen, R. B: The Effects of Circular End Plates on the Lift, Drag, and Pitching Moment at Subsonic and Supersonic Speeds on a Modified Triangular Wing Having an Aspect-Ratio of 2, a Taper-Ratio of 0.33, and a 45° Swept Leading Edge. Mar. 1954. NACA RM A53J14.

148. Pfyl, F. A: Aerodynamic Study of a Wing-Fuselage Combination Employing a Wing Sweptback 63° Effectiveness of an Inboard Elevon as a Longitudinal-and Lateral-Control Device at Subsonic and Supersonic Speeds. Dec. 1951. NACA RM A51I18.

149. Phelps, E. R., and W. G. Smith: Lift, Drag, and Pitching Moment of Low-Aspect-Ratio Wings at Subsonic and Supersonic Speeds-Triangular Wing of Aspect-Ratio 4 with NACA 0005-63 Thickness Distribution, Cambered and Twisted for Trapezoidal Span Load Distribution. 2 Feb. 1951. NACA RM A50K24b.

150. Phillips, W. H., and R. F. Thompson: Investigation by the Transonic Bump Method of a 35° Sweptback Semispan Model Equipped with a Flap Operated by a Series of Servo-Vanes Located Ahead of and Geared to the Flap. Apr. 1956. NACA RM L51J10; Also, NACA TN 3689.

151. Polhamus, E. C: Some Factors Affecting the Variation of Pitching Moment with Sideslip of Aircraft Configurations. July 1955. NACA RM L55E20b.

152. Queijo, M. J: Theoretical Span Load Distributions and Rolling Moments for Sideslipping Wings of Arbitrary Plan From in Incompressible Flow. 1956. NACA Rep. 1269, Supersedes TN 3605.

153. Rathert, G. A. Jr., L. S. Rolls, and C. M. Hanson: The Transonic Characteristics of a Low-Aspect-Ratio Triangular Wing with a Constant-Chort Flap as Determined by Wing-Flow Tests, Including Correlation with Large-Scale Tests. July 1950. NACA RM A50E10.

154. Reed, V. D., and D. W. Smith: The Lateral Control Characteristics of Constant Percent Chord Trailing Edge Elevons on a Pointed Wing of Aspect-Ratio 2 at Mach Numbers Up to 0.96. Aug. 1953. NACA RM A53F03.

155. Reese, D. E., and E. R. Phelps: Lift, Drag, and Pitching Moment of Low-Aspect-Ratio Wings at Subsonic and Supersonic Speeds-Plane Tapered Wing of Aspect-Ratio 3.1 with 3-Percent-Thick, Biconvex Section. 30. Jan. 1951. NACA RM A50K28.

156. Riebe, J. M: A Correlation of Two-Dimensional Data on Lift Coefficient Available with Blowing-, Suction-, Slotted-, and Plain-Flap High-Lift Devices. Oct. 1955. NACA RM L55D29a.

157. Riebe, J. M., and J. C. Graven, Jr: Low-Speed Investigation of the Effects of Location of a Delta Horizontal Tail on the Longitudinal Stability and Control of a Fuselage and Thin Delta Wing with Double Slotted Flaps Including the Effects of a Ground Board. Oct. 1953. NACA RM L53H19a.

158. Riebe, J. M., and J. C. Graven, Jr: Low-Speed Investigation of the Effects of Location of a Delta and a Straight Tail on the Longitudinal Stability and Control of a Thin Delta Wing with Extended Double Slotted Flaps. Jan. 1954. NACA TM L53J26.

159. Riebe, J. M., and R. G. MacLeod: Low-Speed Wind-Tunnel Investigation of a Thin 60° Delta Wing with Double Slotted, Single Slotted, Plain, and Split Flaps. Jan. 1953. NACA RM L52J29.

160. Riley, D. R., J. D. Bird, and L. R. Fisher: Experimental Determination of the Aerodynamic Derivatives Arising From Acceleration in Sideslip for a Triangular, a Swept, and an Unswept Wing. Mar. 1955. NACA RM L55A07.

161. Rossow, V. J: A Theoretical Study of the Lifting Efficiency at Supersonic Speeds of Wings Utilizing Indirect Lift Induced by Vertical Surfaces. Mar. 1956. NACA RM A55L08.

162. Runckel, J. F., and W. H. Gray: An Investigation of Loads on Ailerons at Transonic Speeds. May 1955. NACA RM L55E13.

163. Sandahl, D. A: Free-Flight Investigation of Control Effectiveness of Full-Span, 0.2 Chord Plain Ailerons at High Subsonic, Transonic, and Supersonic Speeds to Determine Some Effects of Wing Sweepback, Taper, Aspect-Ratio, and Section Thickness Ratio. Aug. 1947. NACA RM L7F30.

164. Sandahl, C. A: Free-Flight Investigation at Transonic and Supersonic Speeds of a Wing-Aileron Configuration Simulating the D-558-2 Airplane. 21 July 1948. NACA RM L8E28.

165. Sandahl, C. A: Free-Flight Investigation of the Rolling Effectiveness of Several Delta Wing-Aileron Configurations at Transonic Speeds. 27 Aug. 1948. NACA RM L8D16.

166. Sandahl, C. A: Free-Flight Investigation at Transonic and Supersonic Speeds of the Rolling Effectiveness of a 42.7° Sweptback Wing Having Partial-Span Ailerons. 25 Oct. 1948. NACA RM L8E25.

167. Sandahl, C. A: Free-Flight Investigation at Transonic and Supersonic Speeds of the Rolling Effectivenessof a Thin, Unswept Wing Having Partial-Span Ailerons. Oct. 1948. NACA RM L8G20a.

168. Sandahl, C. A: Free-Flight Investigation at Transonic and Supersonic Speeds of the Rolling Effectiveness of Several Aileron Configurations on a Tapered Wing Having 42.7° Sweepback. Jan. 1949. NACA RM L8K23.

169. Sandahl, C. A., W. M. Bland, Jr., and H. K. Strass: Effects of Some Airfoil Section Variations on Wing-Aileron Rolling Effectiveness and Drag as Determined in Free Flight at Transonic andSupersonic Speeds. July 1949. NACA RM L9D12.

170. Sandahl, C. A., and H. K. Strass: Additional Results in a Free-Flight Investigation of Control Effectiveness of Full-Span, 0.2 Chord Plain Ailerons at High Subsonic, Transonic and Supersonic Speeds to Determine Some Effects of Wing Sweepback, Aspect-Ratio, Taper, and Section Thickness Ratio. Apr. 1948. NACA RM L7L01.

171. Sandahl, C. A., and H. K. Strass: Comparative Tests of the Rolling Effectiveness of Constant-Chord, Full-Delta, and Half-Delta Ailerons on Delta Wings at Transonic and Supersonic Speeds. 12 Dec. 1949. NACA RM L9J26.

172. Sandahl, C. A., H. K. Strass, and R. O. Piland: The Rolling Effectiveness of Wing-Tip Ailerons as Determined by Rocket-Powered Test Vehicles and Linear Supersonic Theory. Appendix: Determination of the Theoretical Rolling Effectiveness of Wing-Tip Ailerons. Robert O. Piland. 29 Aug. 1950. NACA RM L50F21.

173. Sanders, E. C. Jr: and J. L. Edmondson: Damping in Roll of Rocket-Powered Test Vehicles Having Swept, Tapered Wings of Low-Aspect-Ratio. Oct. 1951. NACA RM L51G06.

174. Scallion, W. I: Low-Speed Investigation of the Aerodynamic Control, and Hinge-Moment Characteristics of Two Types of Controls on a Delta-Wing-Fuselage Model with and Without Nacelles. May 1953. NACA RM L53C18

175. Scallion, W. I: Low-Speed Investigation of the Aerodynamic, Control, and Hinge-Moment Characteristics in Sideslip of a Delta-Wing-Fuselage Model with Horn-Balance-Type Ailerons and with and Without Nacelles. Aug. 1953. NACA RM L53G09b.

176. Scallion, W. I: The Effect of Ground on the Low-Speed Aerodynamic Control, and Control Hinge-Moment Characteristics of a Delta-Wing-Fuselage Model with Trailing-Edge Controls. Sept. 1954. NACA RM L54H03.

177. Schmieden, C: "Ueber die Eindeutigkeit der Loesungen in der Theorie der Unstetigen Stroemungen." Ingenieur-Arch. 3, 356-370, 1932; 5, 373-375, 1934.

178. Schmieden, C: "Die Stroemung um Einen Ehenen Tragfluegel mit Querruder." Zamm, 16, 194-198, 1936.

179. Schmieden, C: "Ueber Tragfluegel Stroemungen mit Wirbelabloesung." 17, 37-44, 1940.

180. Schult, E. D., andE. M. Fields: Free-Flight Measurements of the Rolling Effectiveness and Drag of Trailing-Edge Spoilers on a Tapered Swept-back Wing at Mach Numbers Between 0.6 and 1.4. Feb. 1954. NACA RM L53L14a.

181. Schult, E. D., H. K. Strass, and E. M. Fields: Free-Flight Measurements of Some Effects of Aileron Span, Chord, and Deflection and of Wing Flexibility on Sweptback Wings at Mach Numbers Between 0.8 and 1.6. Jan. 1952. NACA RM L51K16.

182. Shaw, R. A: Changes in Control Characteristics with Changes in Flow Pattern at High Subsonic Speeds. Tests on an E. C. Airfoil with 25% Concave Control Flap. Great Britain, ARC RM No. 2436, 1948.

183. Sivells, J. C., and K. L. Goin: Experimental and Calculated Hinge Moments of Two Ailerons on a 42.7° Sweptback Wing at a Mach Number of 1.9. Jan. 1959. NACA RM L8K24a.

184. Smith, D. W., and J. C. Heitmeyer: Lift, Drag, and Pitching Moment of Low-Aspect-Ratio Wings at Subsonic and Supersonic Speeds-Plane Triangular Wing of Aspect-Ratio 2 with NACA 0008-63 Section. 1 Feb. 1951. NACA RM A50K20.

185. Smith, D. W., and J. C. Heitmeyer: Lift, Drag, and Pitching Moment of Low-Aspect-Ratio at Subsonic and Supersonic Speeds-Plane Triangular Wing of Aspect-Ratio 2 with NACA 0005-63 Section. 1 Feb. 1951. NACA RM A50K21.

186. Smith, W. G., and E. R. Phelps: Lift, Drag, and Pitching Moment of Low-Aspect-Ratio Wings at Subsonic and Supersonic Speeds. Triangular Wing of Aspect-Ratio 2 with NACA 0005-63 Thickness Distribution, Cambered and Twisted for a Trapezoidal Span Load Distribution. 5 Feb. 1951. NACA RM A50K27a.

187. Smith, D. W., and V. D. Reed: A Comparison of the Chordwise Pressure Distribution of Loading at Subsonic Speeds on Two Triangular Wings of Aspect-Ratio 2 Having NACA 0005 and 0008 Sections. May 1952. NACA RM A51L21.

188. Smith, D. W., and V. D. Reed: Subsonic Static Longitudinal Stability and Control Characteristics of a Wing-Body Combination Having a Pointed Wing of Aspect-Ratio 2 with Constant-Percent-Chord Trailing-Edge Elevons. May 1953. NACA RM A53C20.

189. Smith, D. W., and V. D. Reed: A Comparison of the Chordwise Pressure Distribution and Spanwise Distribution of Loading at Subsonic Speeds. on Two Triangular Wings of Aspect-Ratio 2 Having NACA 0005 and 0008 Sections. May 1952. NACA RM A51L21.

190. Spearman, M. L., and R. B. Robinson: Wind-Tunnel Investigation of a Ram-Jet Canard Missile Model Having a Wing and Canard Surfaces of Delta Plan Form with 70° Swept Leading Edges. Longitudinal and Lateral Stability and Control Characteristics at a Mach Number of 1.60. Aug. 1952. NACA RM L52E15.

191. Spreemann, K. P: Experimental Investigation at High Subsonic Speeds of the Effects of Leading-Edge Radius on the Aerodynamic Characteristics of a Sweptback Wing-Fuselage Combination with Leading-Edge Flaps and Chord-Extensions. July 1955. NACA RM L55E25a.

192. Spreemann, K. P., and W. J. Alford, Jr: Investigation of the Effects of Leading-Edge Flaps on the Aerodynamic Characteristics in Pitch at Mach Numbers From 0.40 to 0.93 of a Wing-Fuselage Configuration with a 45° Sweptback Wing of Aspect-Ratio 4. Aug. 1953. NACA RM L53G13.

193. Spreemann, K. P., and W. J. Alford, Jr: Investigation of the Effects of Leading-Edge Chord-Extensions and Fences in Combination with Leading-Edge Flaps on the Aerodynamic Characteristics at Mach Numbers From 0.40 to 0.93 of a 45° Sweptback Wing of Aspect-Ratio 4. Apr. 1957. NACA TN 3845. Supersedes RM L53A09a.

194. Spreemann, K. P., and R. E. Kuhn: Investigation of the Effectiveness of Boundary-Layer Control by Blowing Over a Combination of Sliding and Plain Flaps in Deflecting a Propeller Slipstream Downward for Vertical Take-Off. Dec. 1956. NACA TN 3904.

195. Stephenson, J. D., and R. Selan: The Static Longitudinal Characteristics at Mach Numbers Up to 0.95 of a Triangular Wing Canard Model Having a Triangular Control. Dec. 1951. NACA RM A51I07.

196. Stevens, V. I: and J. W. Boyd: A Comparison of Theoretical and Experimental Loading of a 63° Sweptback Wing at Supersonic Speeds. 14 Sept. 1949. NACA RM A9C16.

197. Stone, D. G: Flight-Test Evaluation of the Longitudinal Stability and Control Characteristics of 0.5-Scale Models of the Lark Pilotless-Aircraft Configuration. 6 Feb. 1948. NACA RM L7I26.

198. Stone, D. G: Comparisons of the Effectiveness and Hinge Moment of All-Movable Delta and Flap-Type Controls on Various Wings. Apr. 1951. NACA RM L51C22.

199. Stone, D. G: Recent Data on Controls. Jan. 1952. NACA RM L52A10.

200. Strass, H. K: Free-Flight Investigation of the RollingEffectiveness at High Subsonic, Transonic, and Supersonic Speeds of Leading-Edge and Trailing Edge Ailerons in Conjunction with Tapered and Untapered Plan Forms. July 1948. NACA RM L8E10.

201. Strass, K: The Effect of Spanwise Aileron Location on the Rolling Effectiveness of Wings with 0° and 45° Sweep at Subsonic, Transonic, and Supersonic Speeds. Apr. 1950. NACA RM L50A27.

202. Strass, H. K., E. M. Fields, and P. E. Purser: Experimental Determination of Effect of Structural Rigidity on Rolling Effectiveness of Some Straight and Swept Wings at Mach Numbers From 0.7 to 1.7. 4 Oct. 1950. NACA RM L50G14b.

203. Strass, H. K: Summary of Some Rocket-Model Investigations of Effects of Wing Aspect-Ratio and Thickness on Aileron Rolling Effectiveness Including Some Effects of Spanwise Aileron Location for Sweptback Wings with Aspect-Ratio of 8.0. Feb. 1954. NACA RM L53L11.

204. Strass, H. K., E. M. Fields, and E. D. Schult: Free-Flight Investigation at Transonic and Supersonic Speeds of the Rolling Effectiveness of a Partial-Span Aileron on an Inversely Tapered Sweptback Wing. May 1950. NACA RM L50B08.

205. Strass, H. K., E. M. Fields, and E. D. Schult: Some Effects of Spanwise Aileron Location and Wing Structural Rigidity on the Rolling Effectiveness of 0.3-Chord Flap Type Ailerons on a Tapered Wing Having 63° Sweepback at the Leading Edge and NACA 64A005 Airfoil Sections. June 1951. NACA RM L51D18a.

206. Strass, H. K., and E. T. Marley: Rolling Effectiveness of All-Movable Wings at Small Angles of Incidence at Mach Numbers From 0.6 to 1.6. Oct. 1951. NACA RM L51H03.

207. Strass, H. K., and C. A. Sandahl: Additional Results in a Free-Flight Investigation of Control Effectiveness of Full-Span, 0.2-Chord Plain Ailerons at High Subsonic, Transonic, and Supersonic Speeds to Determine Some Effects of Wing Sweepback, Aspect-Ratio, Taper, and Section Thickness Ratio. 23 Apr. 1948. NACA RM L7L01.

208. Sutton, F. B., and J. K. Dickson: A Comparison of the Longitudinal Aerodynamic Characteristics at Mach Numbers Up to 0.94 of Sweptback Wings Having NACA 4-Digit or NACA 64A Thickness Distributions. Aug. 1954. NACA RM A54F18.

209. Thompson, R. F: Hinge-Moment, Lift, and Pitching Moment Characteristics of a Flap-Type Control Surface Having Various Hinge-Line Locations on a 4-Percent Thick 60° Delta Wing. Transonic Bump Method. Mar. 1954. NACA RM L54B08.

210. Thompson, R. F., and R. T. Taylor: Effect of a Wing Leading-Edge Flap andChord-Extension on the High Subsonic Control Characteristics of a Spoiler-Slot-Deflector Control Located at Two Spanwise Positions. Nov. 1954. NACA RM L54I09.

211. Tingling, B. E., and A. V. Karpen: The Effects of Trailing-Edge Flaps on the Subsonic Aerodynamic Characteristics of an Airplane Model Having a Triangular Wing of Aspect-Ratio 3. Jan. 1955. NACA RM A54L07.

212. Ulmann, E. F., and D. R. Lord: An Investigation of Flow Characteristics at Mach Number 4.04 Over 6- and 9-Percent Thick Symmetrical Circular-Arc Airfoils Having 30-Percent Chord Trailing-Edge Flaps. July 1951. NACA RM L51D30.

213. Vogler, R. D: Wind-Tunnel Investigation at High Subsonic Speeds of Spoilers of Large Projection on an NACA 65A006 Wing with Quarter-Chord Line Sweptback 32.6° Jan. 1952. NACA RM L51L10.

214. Vogler, R. D: Wind-Tunnel Investigation at High Subsonic Speeds of a Spoiler-Slot-Deflector Combination on a NACA 65A006 Wing with Quarter Chord Line Sweptback 32.6°. May 1953. NACA RM 53D17.

215. Vogler, R. D: Wind-Tunnel Investigation at Transonic Speeds of a Spoiler-Slot-Deflector Combination on an Unswept NACA 65A006 Wing. Dec. 1953. 27 p. Diagrs., 3 Tabs. NACA RM L53J21.

216. Vogler, R. D: Wind-Tunnel Investigation at Transonic Speeds of the Lift and Hinge-Moment Characteristics of a Flap with Attached Balancing Tab on a 45° Sweptback Wing. Dec. 1954. NACA RM L54J28a.

217. Weiberg, J. A., and H. C. Carel: Wind-Tunnel Investigation at Low Speed of a Wing Sweptback 63° and Twisted and Cambered for a Uniform Load at a Lift Coefficient of 0.5. 9 May 1950. NACA RM A50A23.

218. Weiberg, J. A., and H. C. Carel: Wind-Tunnel Investigation at Low Speed of a Wing Sweptback 63° and Twisted and Cambered for Uniform Load at a Lift Coefficient of 0.5 and with a Thickened Tip Section. 21 Nov. 1950. NACA RM A50I14.

219. Weil, J., and E. C. Polhamus: Aerodynamic Characteristics of Wings Designed for Structural Improvements. 28 May 1951. NACA RM L51E10a.

220. White, M. D: Effect of Camber and Twist on the Stability Characteristics of Models Having a 45° Sweptwing as Determined by the Free-Fall Method at Transonic Speeds. Aug. 1952. NACA RM A52F16.

221. Whittle, E. F. Jr., and H. Clyde McLemore: Aerodynamic Characteristics and Pressure Distributions of a 6-Percent-Thick 49° Sweptback Wing with Blowing Over Half-Span and Full-Span Flaps. Sept. 1955. NACA RM L55F02.

222. Whittle, E. F. Jr., and S. Lipson: Effect on the Low-Speed Aerodynamic Characteristics of a 49° Sweptback Wing Having an Aspect-Ratio of 3.78 of Blowing Air Over the Trailing-Edge Flap and Aileron. April. 1954. NACA RM L54C05.

223. Whittle, E. F. Jr., and H. C. McLemore: Aerodynamic Characteristics and Pressure Distributions of a 6-Percent-Thick 49° Sweptback Wing with Blowing Over Half-Span and Full-Span Flaps. Sept. 1955. NACA RM L55F02.

224. Wiggins, J. W: Wind-Tunnel Investigation at High Subsonic Speeds of the Static Longitudinal and Static Stability Characteristics of a Wing-Fuselage Combination Having a Triangular Wing of Aspect-Ratio 2.31 and an NACA 65A003 Airfoil. Aug. 1953. NACA RM L53G09a.

225. Wiggins, J. W: Wind-Tunnel Investigation at High Subsonic Speeds to Determine the Rolling Derivatives of Two Wing-Fuselage Combinations Having Triangular Wings, Including a Semi-Empirical Method of Estimating the Rolling Derivatives. Feb. 1954. NACA RM L53L18a.

226. Wiggins, J. W: Wind-Tunnel Investigation of Effect of Sweep on Rolling Derivatives at Angles of Attack Up to 13° and at High Subsonic Mach Numbers, Including a Semi-Empirical Method of Estimating the Rolling Derivatives. Apr. 1954. NACA RM L54C26.

227. Wiley, H. G: A Wind-Tunnel Investigation at High Subsonic Speeds of the Lateral Control Characteristics of Various Plain Spoiler Configurations on a 3-Percent-Thick 60° Delta Wing. May 1954. NACA RM L54D01.

228. Wiley, H. G., and D. R. Riley: An Experimental and Theoretical Investigation at High Subsonic Speeds of the Effects of Horizontal-Tail Height on the Aerodynamic Characteristics in Sideslip of an Unswept, Untapered Tail Assembly. Dec. 1953. NACA RM L53J19.

229. Wiley, H. G., and R. T. Taylor: Investigation at Transonic Speeds of the Lateral-Control and Hinge-Moment Characteristics of a Flap Type Spoiler Aileron on a 60° Delta Wing. Jan. 1954. NACA RM L53J05.

230. Wilson, H. B. Jr: Investigation at a Mach Number of 1.2 of Two 45° Swept-back Wings Utilizing NACA 2-006 and NACA 65A006 Air-foil Sections. Sept. 1952. NACA RM L52G17.

231. Wise, G. A: Influence of End Plates on Lift and Flow Field of a Can-ard-Type Control Surface at a Mach Number of 2.00. Mar. 1953. NACA RM E53A02.

232. Woods, R. L., and S. H. Spooner: Effects of High-Lift and Stall-Control Devices, Fuselage, and Horizontal Tail on a Wing Sweptback 42° at the Lead-ing-Edge and Having Symmetrical Circular-Arc Airfoil Sections at a Reynolds Number of 6.9×10^6. 20 Apr. 1949. NACA RM L9B11.

233. Yates, E. C. Jr: Low-Speed Wind-Tunnel Investigation of Leading-Edge Porous Suction on a 4-Percent-Thick 60° Delta Wing. Mar. 1955. NACA RM L54L21.

234. Yates, E. C. Jr: Theoretical Analysis of Linked Leading-Edge and Trail-ing-Edge Flap-Type Controls at Supersonic Speeds. Mar. 1956. NACA TN 3617.

Chapter 3

CHARACTERISTIC PROPERTIES OF NONSTEADY COMPOSITE ELEMENTS, AERODYNAMICS, FLUTTER, BUFFETING, AND TAIL SURFACES

3.1 Fundamental Notions and Equations

This chapter refers to a nonsteady flow of an inviscid, non-heat conducting compressible fluid along bodies and lifting surfaces. In this section, some fundamental notions and equations will be given, pertinent to the problem in question.

The condition for the irrotational flow is

$$\operatorname{curl} \vec{q} = 0 \quad , \tag{3.1}$$

and this implies that a scalar velocity potential, Φ, exists such that

$$\vec{q} = \operatorname{grad} \Phi \quad . \tag{3.2}$$

The equation of continuity has the form

$$\frac{\partial \rho}{\partial t} + \operatorname{div}(\rho \vec{q}) = 0 \quad , \tag{3.3}$$

and this may be written in the form

$$\frac{\partial \rho}{\partial t} + \vec{q} \operatorname{grad} \rho + \rho \operatorname{div} \operatorname{grad} \Phi = 0 \quad . \tag{3.4}$$

The generalized Bernoulli equation is

$$\frac{\partial \Phi}{\partial t} + \frac{1}{2} q^2 + \int \frac{dp}{\rho} = 0 \quad . \tag{3.5}$$

with

$$a^2 = \frac{\partial p}{\partial \rho} \quad , \tag{3.6}$$

denoting the local variable speed of sound, the equation of continuity can be expressed by means of the form

$$\frac{1}{a^2} \left(\frac{\partial}{\partial t} + \vec{q}_c \cdot \nabla \right)^2 \Phi = \nabla^2 \Phi \quad , \tag{3.7}$$

where the subscript c indicates that the designated variable is to be treated as constant with respect to the operations ∇ and $\partial/\partial t$. With the corresponding operator

$$\frac{Dc}{Dt} = \frac{\partial}{\partial t} + \vec{q}_c \nabla \quad , \tag{3.8}$$

Eq. (3.7) takes the form

$$\frac{1}{a^2} \frac{Dc^2 \Phi}{Dt^2} = \nabla^2 \Phi \quad . \tag{3.9}$$

This is an invariant form, i.e., it permits an easy conversion to any coordinate system whether fixed or moving. In a space-fixed Cartesian coordinate system it is

$$\left(1 - \frac{u^2}{a^2}\right)\frac{\partial^2 \Phi}{\partial x^2} + \left(1 - \frac{v^2}{a^2}\right)\frac{\partial^2 \Phi}{\partial y^2} + \left(1 - \frac{w^2}{a^2}\right)\frac{\partial^2 \Phi}{\partial z^2} - 2\frac{uv}{a^2}\frac{\partial^2 \Phi}{\partial x \partial y} - 2\frac{vw}{a^2}\frac{\partial^2 \Phi}{\partial y \partial z}$$

$$- 2\frac{wu}{a^2}\frac{\partial^2 \Phi}{\partial z \partial x} - 2\frac{u}{a^2}\frac{\partial^2 \Phi}{\partial x \partial t} - 2\frac{v}{a^2}\frac{\partial^2 \Phi}{\partial y \partial t} - 2\frac{w}{a^2}\frac{\partial^2 \Phi}{\partial z \partial t} - \frac{1}{a^2}\frac{\partial^2 \Phi}{\partial t^2} = 0 \quad . \tag{3.10}$$

One method of solving this equation is to apply a linearization. This consists of regarding all velocity disturbances small in comparison with U, a and (U-a), of expanding a^2 around its value for the undisturbed stream, and of retaining first order terms only; the result is

$$\frac{1}{a_\infty^2}\left(\frac{\partial}{\partial t} + \vec{U}\cdot\nabla\right)^2 \phi = \nabla^2 \phi \quad , \tag{3.11}$$

where a_∞ is now the constant value of the sound speed in the uniform stream and grad ϕ now represents the disturbance velocity vector $\vec{q}-\vec{U}$.

In Cartesian coordinates Eq. (3.11) becomes

$$\left(1 - \frac{U^2}{a_\infty^2}\right)\frac{\partial^2 \phi}{\partial x^2} + \frac{\partial^2 \phi}{\partial y^2} + \frac{\partial^2 \phi}{\partial z^2} - 2\frac{U}{a_\infty^2}\frac{\partial^2 \phi}{\partial x \partial t} - \frac{1}{a_\infty^2}\frac{\partial^2 \phi}{\partial t^2} = 0 \quad . \tag{3.12}$$

Applying the transformations

$$x = \xi + Ut \quad ; \quad y = \eta \quad ; \quad z = \zeta \quad ; \quad t = t \quad , \tag{3.13}$$

transforms Eq. (3.12) into the form

$$\Box^2 \phi = \frac{\partial^2 \phi}{\partial \xi^2} + \frac{\partial^2 \phi}{\partial \eta^2} + \frac{\partial^2 \phi}{\partial \zeta^2} - \frac{1}{a_0^2}\frac{\partial^2 \phi}{\partial t^2} = 0 \quad . \tag{3.14}$$

Let

$$\phi = \phi^{*} \exp(i\,\omega\, t) \quad , \tag{3.15}$$

then the equation for ϕ^{*} has the form

$$\frac{\partial^2 \phi^*}{\partial \xi^2} + \frac{\partial^2 \phi^*}{\partial \eta^2} + \frac{\partial^2 \phi^*}{\partial \zeta^2} + \mathcal{K}^2 \phi^* = 0 \quad , \tag{3.16}$$

where

$$\mathcal{K} = \frac{\omega}{a_{\infty}} \quad . \tag{3.17}$$

Another method of solution consists of the application of the acceleration potential. From Euler's equation,

$$\frac{D\vec{q}}{Dt} = -\,\mathrm{grad} \int \frac{dp}{\rho} \quad , \tag{3.18}$$

it follows that the acceleration vector $D\vec{q}/Dt$ may be expressed as the gradient of a scalar

$$\Psi = -\int \frac{dp}{\rho} \quad . \tag{3.19}$$

Let

$$\vec{q} = \mathrm{grad}\, \phi \quad , \tag{3.20}$$

then

$$\frac{D_c \Phi}{Dt} = \Psi = -\int \frac{dp}{\rho} \quad . \tag{3.21}$$

The relation between the disturbance potential ϕ and the pressure p can be inverted to yield the relation

$$\phi(x, y, z, t) = -\frac{1}{\rho_{\infty} U} \int_{-\infty}^{x} p(x', y, z, t - \frac{x - x'}{U})\, dx' \quad , \tag{3.22}$$

where far ahead of the disturbance at $x = -\infty$ the potential has been assumed to be 0. With

$$\phi(x, y, z, t) = \phi^{*}(x, y, z) \exp(i\,\omega\, t) \quad ,$$

Eq. (3.22) transforms into the form

$$\phi^{*}(x, y, z) = -\frac{1}{\rho_{\infty} U} \exp\left[-i\,\omega\,(xU^{-1})\right] \int_{-\infty}^{x} p^{*}(x', y, z) \exp\left[i\omega x' U^{-1}\right] dx' \quad . \tag{3.23}$$

Let the mean camber surface be designated by

$$z = Z(x, y, t) \quad . \tag{3.24}$$

Then assuming that the profile in a nonsteady flow is represented by its mean camber surface, the boundary condition is

$$w(x, y, 0, t) = \frac{\partial Z}{\partial t} + U \frac{\partial Z}{\partial x} \quad . \tag{3.25}$$

Obviously, its value is given by

$$w = \left(\frac{\partial \phi}{\partial z}\right)_{z=0} \quad . \tag{3.26}$$

The disturbance pressure is an odd function of z, and therefore is zero on the $\{x, y\}$ - plane, except at the lifting surface where the pressure difference $P = p_u - p_\ell$ (between the top and the bottom surface), positive downward (i. e., the lift is negative), is given by

$$P(x, y, t) = p(x, y, +0, t) - p(x, y, -0, t) = 2p(x, y, 0, t) = 2\rho_\infty\left(\frac{\partial \phi}{\partial t} + U \frac{\partial \phi}{\partial x}\right) . \tag{3.27}$$

The mathematical problem then consists in determination of ϕ, (for the velocity and pressure fields) in the upper half space $z \geq 0$ from a knowledge of the differential equations, the conditions at the boundary surface $z = 0$, and conditions at infinity. On the plane $z = 0$ ahead of the location of the wing, the perturbation potential ϕ is zero, i. e., $\partial\phi/\partial t$ and $\partial\phi/\partial x$ also are zero; aft of the wing location, P given by Eq. (3. 27) is zero. The trailing edge conditions or other edge conditions are regarded as part of the boundary conditions.

Below, we may briefly discuss some fundamental methods of solution of the differential equation, given above.

Consider Green's theorem. For any two functions ϕ and ψ, which with their first derivatives are finite, continuous and single-valued, the theorem states that

$$\int_V (\psi \nabla^2\varphi - \phi \nabla^2\psi) dV = \int_S \left(\psi \frac{\partial \phi}{\partial n} - \phi \frac{\partial \psi}{\partial n}\right) dS \quad . \tag{3.28}$$

This represents a reduction of a volume integral into a surface integral, with $(\partial/\partial n)$ denoting differentiation along the outward normal to the surface S. A classical application of it to the case where ϕ is a regular solution of Laplace equation in the space region V, and ψ is chosen to be equal to $1/r$, gives

$$\phi_P = \frac{1}{4\pi}\int_S \left[\frac{\partial\phi}{\partial n}\frac{1}{r} - \phi\frac{\partial}{\partial n}\left(\frac{1}{r}\right)\right] dS \ , \tag{3.29}$$

where ϕ_P is the potential at a field point P expressed in terms of the boundary surface values of ϕ and $\partial\phi/\partial n$. One may notice that solutions are here built up by integration of surface distributions of the elementary unit source solution

$$\phi_1 = -\frac{1}{4\pi r} \ , \tag{3.30}$$

and of the doublet or dipole solution with axis in the direction n:

$$\phi_2 = -\frac{1}{4\pi}\frac{\partial}{\partial n}\left(\frac{1}{r}\right) \ , \tag{3.31}$$

where r is the geometric distance $\sqrt{(x-\xi)^2 + (y-\eta)^2 + (z-\zeta)^2}$ from the field point (x, y, z) to the source of disturbance at $\{\xi, \eta, \zeta\}$. For the wave equation, the Kirchhoff formula appears as the basic solution:

$$\phi_P = \frac{1}{4\pi}\int_S \left[\frac{1}{r}\left(\frac{\partial\phi}{\partial n}\right)_{t-\frac{r}{a_\infty}} - \frac{\partial}{\partial n}\,\frac{\phi\left(t - \frac{r}{a_\infty}\right)}{r}\right] dS \ , \tag{3.32}$$

or also,

$$\phi_P = \frac{1}{4\pi}\int_S G\left(t - \frac{r}{a_\infty}\right) dS \ , \tag{3.33}$$

with

$$G(t) = \frac{1}{r}\frac{\partial\phi}{\partial n} - \phi\frac{\partial}{\partial n}\left(\frac{1}{r}\right) + \frac{1}{a_\infty r}\frac{\partial\phi}{\partial t}\frac{\partial r}{\partial n} \ . \tag{3.34}$$

The argument $t-(r/a_\infty)$ corresponds to the time of action of the disturbancees whose influences reach the field point at time t; sometimes the name of the retarded potential is used for this sort of potential. The fundamental solutions appearing in Eq. (3.32) which correspond to the source and doublet are

$$\phi_1 = -\frac{1}{4\pi r}\, f\left(t - \frac{r}{a_\infty}\right) ; \tag{3.35}$$

$$\phi_2 = -\frac{1}{4\pi}\frac{\partial}{\partial n}\left[\frac{1}{r}\, f\left(t - \frac{r}{a_\infty}\right)\right] \ . \tag{3.36}$$

For the harmonic wave equation, Kirchhoff's formula appears as the equation of Helmholtz; the source and doublet relations become

$$\phi_1^* = -\frac{1}{4\pi r}\exp(-i\mathcal{K}r) \quad , \tag{3.37}$$

$$\phi_2^* = -\frac{1}{4\pi}\frac{\partial}{\partial n}\left[\frac{1}{r}\exp(-i\mathcal{K}r)\right] \quad , \tag{3.38}$$

with

$$\mathcal{K} = \frac{\omega}{a_\infty} \quad . \tag{3.39}$$

In two dimensions the familar solutions are

$$\phi_1 = \frac{1}{2\pi}\ln r \quad ; \tag{3.40}$$

$$\phi_2 = \frac{1}{2\pi}\frac{\partial}{\partial n}\ln r = \frac{1}{2\pi r}\frac{\partial r}{\partial n} \quad , \tag{3.41}$$

with

$$r = \sqrt{(x-\xi)^2 + (y-\eta)^2} \quad . \tag{3.42}$$

For cyclindrical wave disturbances corresponding to the plane case of Eq. (3. 35), the results are

$$\phi_1 = -\frac{1}{2\pi}\int_0^\infty f(t - \frac{r}{a_\infty}\cosh u)du \quad ; \tag{3.43}$$

$$= -\frac{1}{2\pi}\int_{-\infty}^{t-r/a_\infty}\frac{a_\infty f(\theta)d\theta}{\sqrt{a_\infty^2(t-\theta)^2 - r^2}} \quad . \tag{3.44}$$

A simpler form can be obtained as a source-pulse or temporary source solution by considering the source act only during a brief interval at time $\theta=\tau$. If instead of $f(\theta)$ there is introduced $f(\tau)\delta(\theta-\tau)$, where $\delta(\theta)$ is a singular impulse function or Dirac δ function defined as zero everywhere, except at $\theta=0$, where it is characterized by having unit area, one obtains as the source-pulse solution:

$$\phi_0 = -\frac{1}{2\pi}\frac{a_\infty f(\tau)}{\sqrt{a_\infty^2(t-\tau)^2 - r^2}} \quad . \tag{3.45}$$

The cylindrical harmonic solution corresponding to Eq. (3. 37) is

$$\phi_1^* = -\frac{1}{2\pi}\frac{\pi}{2i} H_0^{(2)}(\mathcal{K} r) = \frac{i}{4} H_0^{(2)}(\mathcal{K} r) \quad , \tag{3.46}$$

where use has been made of the following integral relations:

$$\int_0^\infty \exp(-i\mathcal{K} r \cosh u)\, du = \int_1^\infty \exp(-i\mathcal{K} ru)\frac{du}{\sqrt{u^2-1}} = \frac{\pi}{2i} H_0^{(2)}(\mathcal{K} r) \quad , \tag{3.47}$$

and where the Hankel function is defined as a combination of Bessel functions of the first and second (Neumann) kind:

$$H_0^{(2)}(k) = J_0(k) - iY_0(k) \quad . \tag{3.48}$$

The function $H_0^{(2)}$ has the following expansion:

$$H_0^{(2)}(k) = \frac{2}{i\pi} \ln k + \ldots \text{ for } k \to 0, \quad = \sqrt{\frac{2}{\pi k}} \exp[-i(k - \frac{\pi}{4})] + \ldots \text{ for } k \to \infty. \tag{3.49}$$

If one defines

$$H_1^{(2)}(k) = J_1(k) - iY_1(k) \quad , \tag{3.50}$$

and

$$H_1^{(2)}(k) = -\frac{d}{dk} H_0^{(2)}(k) \quad , \tag{3.51}$$

then the doublet solution (3.38) takes the form

$$\phi_2^* = \frac{i}{4}\frac{\partial}{\partial n} H_0^{(2)}(kr) = \frac{ik}{4} H_1^{(2)}(kr) \frac{\partial r}{\partial n} \quad . \tag{3.52}$$

Consider Eq. (3.12); the fundamental solutions of it may be called moving sources and doublets. Let the arbitrary function f(t) in Eq. (3.35) be defined as an impulse occurring at time $t=\tau$, i.e.,

$$f(\tau)\delta(t-\tau) \quad , \tag{3.53}$$

where $\delta(\tau) = 0$ for $\tau \neq 0$ and for $\tau = 0$ it has unit area with respect to τ. The function (3.53) possesses the property

$$\int_{-\infty}^{+\infty} f(t-\sigma)\delta(\sigma)d\sigma = f(s) \quad . \tag{3.54}$$

Consider a series of impulses, one following the other in a path, whose points are given in the space-fixed coordinate system by

$$\xi = \xi(\tau) \; ; \quad \eta = \eta(\tau) \; ; \quad \zeta = \zeta(\tau) \quad . \tag{3.55}$$

The effect of all such impulses which act before the time t, up to the time t, is given by

$$\phi = -\frac{1}{4\pi}\int_{-\infty}^{t-r/a_\infty} \frac{f(\tau)}{r}\,\delta\left(t-\tau\,\frac{r}{a_\infty}\right)d\tau \quad ; \tag{3.56}$$

the non-zero contribution to the integral is only for values of τ defined by the relation

$$t - \tau = \frac{r}{a_\infty} = \frac{1}{a_\infty}\sqrt{[x-\xi(\tau)]^2 + [y-\eta(\tau)]^2 + [z-\zeta(\tau)]^2} \quad . \tag{3.57}$$

To find a solution in the case of a uniform motion with velocity U in the negative x-direction, let the sources be located on the ξ-axis and let them flow one after another at the positions

$$\xi = -U\tau \; ; \quad \eta = 0 \; , \quad \zeta = 0 \quad . \tag{3.58}$$

Thus for $\tau = -\infty$ the source is located at $\xi = \infty$, and for $\tau = 0$ the source is located at the origin. The distance between the source point and the point in the field is

$$r = \sqrt{(x + U\tau)^2 + y^2 + z^2} \quad . \tag{3.59}$$

Introduce a transformation of coordinates

$$\tau \rightarrow \theta \; , \quad t - \tau - \frac{r}{a_\infty} = -\theta \quad , \tag{3.60}$$

then the integral ϕ will have a value only for $\theta = 0$, equal to

$$\phi = -\frac{1}{4\pi}\left[\frac{f(\tau)}{r}\,\frac{d\tau}{d\theta}\right]_{\theta=0} \quad . \tag{3.61}$$

Eqs. (3.59) and (3.60) give the value of τ:

$$\tau = \frac{1}{\beta^2}\left(t + \frac{Ux}{a_\infty^2} - \frac{\mathscr{R}}{a_\infty}\right) \quad ; \tag{3.62}$$

$$\mathscr{R} = \sqrt{(x + Ut)^2 + \beta^2(y^2 + z^2)} \quad ; \tag{3.63}$$

$$M_\infty = \frac{U}{a_\infty} \quad . \tag{3.64}$$

Also

$$\frac{1}{r}\frac{d\tau}{d\theta} = \frac{a_\infty}{a_\infty r + U(x + U\tau)} \quad . \tag{3.65}$$

The equation for ϕ takes the form

$$\phi = -\frac{1}{4\pi}\frac{1}{R} f\left[\left(t + \frac{Ux}{a_\infty^2}\frac{\mathscr{R}}{a_\infty}\right)\frac{1}{\beta^2}\right] \quad , \tag{3.66}$$

which may be transferred from a space-fixed coordinate to a coordinate system (x_0, y_0, z_0) moving uniformly along with the source located at (ξ_0, η_0, ζ_0):

$$x + Ut = x_0 - \xi_0 \ ; \quad y = y_0 - \eta_0 \ ; \quad z = z_0 - \xi_0 \quad . \tag{3.67}$$

The result of all the manipulations is:

(a) Subsonic point source:

$$\phi_1 = -\frac{1}{4\pi} f(t - \frac{D}{a_\infty}) = -\frac{1}{4\pi R} f(t - \tau_1) \ ; \tag{3.68}$$

$$\mathscr{R} = \sqrt{(x - \xi)^2 + \beta^2[(y - \eta)^2 + (z - \zeta)^2]} \ ; \tag{3.69}$$

$$\tau_1 = \frac{D}{a_\infty} = \frac{- M_\infty(x - \xi) + \mathscr{R}}{a_\infty \beta^2} \ ; \tag{3.70}$$

$$\beta^2 = 1 - M_\infty^2 \quad . \tag{3.71}$$

One may call the quantities $\mathscr{R}$ and D as amplitude radius and phase radius. The harmonically oscillating moving source is given by

$$\phi_1^* = -\frac{1}{4\pi\mathscr{R}} \exp(-i\omega\tau_1) \quad , \tag{3.72}$$

or

$$\phi_1^* = -\frac{1}{4\pi\mathscr{R}} \exp[-i\mu(x - \xi) - i\mathscr{K}\mathscr{R}] \ , \tag{3.73}$$

$$\mathscr{K} = \omega(a_\infty\beta^2)^{-1} \ ; \quad \mu = \omega M_\infty(a_\infty\beta^2)^{-1} \quad . \tag{3.74}$$

(b) Subsonic line source:

$$\phi_1 = -\frac{1}{2\pi\beta}\int_0^\infty f\left[t + \frac{M_\infty(x-\xi)}{a_\infty\beta^2} - \frac{\cosh U}{a_\infty\beta^2}\right] du \quad , \tag{3.75}$$

$$\mathcal{R} = \sqrt{(x-\xi)^2 + \beta^2(y-\eta)^2} \quad ; \quad \beta = |1 - M_\infty^2|^{1/2} \quad . \tag{3.76}$$

To the equation (3. 45) there corresponds the equation

$$\phi_0 = -\frac{1}{2\pi}\frac{a_\infty f(T)}{\sqrt{a_\infty^2(t-T)^2 - [x - \xi - U(t-T)]^2 - (y-\eta)^2}} \quad , \tag{3.77}$$

and to Eq. (3. 47),

$$\phi_1^* = -\frac{1}{2\pi\beta}\exp[i\mu(x-\xi)]\int_0^\infty \exp(-i\mathcal{K}\cosh\mu)\, du \quad , \tag{3.78}$$

or

$$\phi_1^* = \frac{i}{4\beta}\exp[-i\mu(x-\xi)]\, H_0^{(2)}\left[\mathcal{K}\sqrt{(x-\xi)^2 + \beta^2(y-\eta)^2}\right] \quad . \tag{3.79}$$

(c) Supersonic point source:

$$\phi_1 = -\frac{1}{4\pi\mathcal{R}}[f(t-\tau_1) + f(t-\tau_2)] \quad , \tag{3.80}$$

$$\mathcal{R} = \sqrt{(x-\xi)^2 - (M_\infty^2 - 1)[(y-\eta)^2 + (z-\zeta)^2]} \quad , \tag{3.81}$$

$$\tau_1 = \frac{D}{a_\infty} = \frac{1}{a_\infty}\left[\frac{M_\infty(x-\xi) - \mathcal{R}}{M_\infty^2 - 1}\right] \tag{3.82}$$

$$\tau_2 = \frac{D'}{a_\infty} = \frac{1}{a_\infty}\left[\frac{M_\infty(x-\xi) + \mathcal{R}}{M_\infty^2 - 1}\right] \tag{3.83}$$

For harmonic oscillations, the source moving at a supersonic speed has the potential

$$\phi_1^* = -\frac{1}{4\pi\mathcal{R}}[\exp(-i\omega\tau_1) + \exp(-i\omega\tau_2)] \quad , \tag{3.84}$$

or

$$\phi_1^* = -\frac{1}{2\pi\mathscr{R}} \exp[-i\mu(x-\xi)] \cos \mathscr{K}\mathscr{R} , \tag{3.85}$$

$$= \frac{\omega}{a_\infty} \frac{1}{M_\infty^2 - 1} , \quad \mu = \frac{\omega}{a_\infty} \frac{M_\infty}{M_\infty^2 - 1} . \tag{3.86}$$

(d) Supersonic line source:

$$\phi_1 = -\frac{1}{2\pi\beta} \int_0^\pi f\left[t - \frac{M_\infty(x-\xi)}{a_\infty\beta^2} + \frac{\mathscr{R}\cos\theta}{a_\infty\beta^2}\right] d\theta \quad ; \tag{3.87}$$

the source-pulse solution with $t - T = \tau$ is

$$\phi_0 = -\frac{1}{2\pi\beta} \frac{f(t-\tau)}{\sqrt{(\tau - \tau_1)(\tau_2 - \tau)}} d\tau , \tag{3.88}$$

$$\tau_{1,2} = \frac{M_\infty(x-\xi)}{a_\infty\beta^2} \pm \frac{\mathscr{R}}{a_\infty\beta^2} , \tag{3.89}$$

$$\mathscr{R} = \sqrt{(x-\xi)^2 - \beta^2(y-\eta)^2} , \tag{3.90}$$

$$\beta = |M_\infty^2 - 1|^{1/2} , \tag{3.91}$$

and the harmonically oscillating source

$$\phi_1^* = -\frac{1}{2\pi\beta} \int_{\tau_1}^{\tau_2} \frac{\exp(-i\omega\tau)}{(\tau-\tau_1)(\tau_2-\tau)} d\tau , \tag{3.92}$$

or

$$\phi_1^* = -\frac{1}{2\pi\beta} \exp[-i\mu(x-\xi)] \int_0^\pi \exp(i\mathscr{K}\mathscr{R}\cos\theta)d\theta , \tag{3.93}$$

$$\mathscr{K} = \frac{\omega}{a_\infty\beta^2} , \quad \mu = \frac{\omega M_\infty}{a_\infty\beta^2} , \tag{3.94}$$

and

$$\phi_1^* = -\frac{1}{2\beta} \exp[-i\mu(x-\xi)] J_0\left[\mathscr{K}\sqrt{(x-\xi)^2 - \beta^2(y-\eta)^2}\right]. \tag{3.95}$$

(e) Sonic point source:

For a source moving uniformly in the negative x-direction one gets

$$\phi_1 = -\frac{1}{4\pi(x-\xi)} f(t-\tau_1) \quad , \tag{3.96}$$

where

$$\tau_1 = \frac{1}{2a_\infty}\left[x-\xi+\frac{(y-\eta)^2+(z-\zeta)^2}{(x-\xi)}\right] = \frac{D}{a_\infty} \quad . \tag{3.97}$$

For the harmonically oscillating source the result is

$$\phi_1^* = -\frac{1}{4\pi(x-\xi)} \exp(-i\omega\tau_1) \quad . \tag{3.98}$$

(f) Sonic line source:

$$\phi_1 = -\frac{1}{4\pi(x-\xi)}\int_{-\infty}^{+\infty} f\left[t-\frac{(x-\xi)^2+(y-\eta)^2}{2a_\infty(x-\xi)}-\frac{z^2}{2a_\infty(x-\xi)}\right]dz \; ; \tag{3.99}$$

$$\phi_1^* = -\frac{\exp(-i\omega\tau_0)}{2\pi(x-\xi)}\int_0^\infty \exp(-\lambda^2 z^2)dz \quad , \tag{3.100}$$

$$\tau_0 = \frac{1}{2a_\infty}\left[x-\xi+\frac{(y-\eta)^2}{(x-\xi)}\right] \; ; \tag{3.101}$$

$$\lambda^2 = \frac{i\omega}{2a_\infty(x-\xi)} \quad . \tag{3.102}$$

The integral in Eq. (3.100) can be evaluated, (it is equal to $\sqrt{\pi}/2\lambda$) and thus

$$\phi_1^* = \frac{1}{B\sqrt{x-\xi}} \exp(-i\omega\tau_0) \quad , \tag{3.103}$$

$$B = -2\sqrt{2\pi}\sqrt{i}\,(\omega a_\infty^{-1})^{1/2} \; ; \quad i^{1/2} = \exp\left(i\frac{\pi}{4}\right) \quad . \tag{3.104}$$

3.2 Applications to Airfoil

Consider an airfoil in a two-dimensional flow of incompressible fluid. Suppose an airfoil of chord $c = 2b$ moves uniformly with velocity U and creates small disturbances. Let the normal velocity of an element located at $x = x_1$ be $w(x_1, t)$. The primary pattern of the flow arising from the disturbances created by this element is the so-called noncirculatory one. The upper surface velocity potential at any point x due to the normal velocity w at x_1 is

$$\Delta\phi_1 = \frac{1}{2\pi} w(x_1, t) b \; \Delta x_1 L(x, x_1) \qquad (3.105)$$

$$L(x, x_1) = 2\ln\left|\frac{1 - xx_1 - \sqrt{1 - x^2}\sqrt{1 - x_1^2}}{x - x_1}\right| . \qquad (3.106)$$

The distribution of surface pressure difference associated with the noncirculatory potential is

$$\Delta P_1 = -2\rho_\infty\left(\frac{U}{b}\frac{\partial}{\partial x} + \frac{\partial}{\partial t}\right)\Delta\phi_1 = -\frac{2\rho_\infty}{\pi}\left(\frac{U}{b}\;\frac{1}{x - x_1}\frac{\sqrt{1 - x_1^2}}{\sqrt{1 - x^2}}\right) bw\Delta x_1$$

$$-\frac{\rho_\infty}{\pi} L(x, x_1) b \;\frac{\partial\omega}{\partial t}\;\Delta x_1 \quad . \qquad (3.107)$$

The flow pattern given by Eq. (3.105) furnishes an infinite velocity and pressure at $x = x_1$ and at the edges. The singularity at $x = x_1$ vanishes by making use of continuous distributions w and Cauchy's principal part in the integrations. A circulatory flow pattern must now be superimposed of such a magnitude as to cancel the infinity at the trailing edge at each instant. As a consequence of that, a surface discontinuity of velocity appears at the trailing edge and a free vorticity left behind in the wake. Consider an element of this surface at $x = x_0 > 1$ (behind the airfoil), of a magnitude $E(x_0, t)$ per unit length, that is $\Delta\Gamma = Eb\Delta x_0$. The surface velocity potential induced by this element at the airfoil can also be found by a conformal mapping method and is

$$\Delta\phi_2' = \frac{Eb\,\Delta x_0}{2\pi}\tan^{-1}\frac{\sqrt{1 - x^2}\sqrt{x_0^2 - 1}}{1 - x\,x_0} \quad . \qquad (3.108)$$

If the wake extends from $x_0 = 1$ to $x_0 = s$, i.e., the airfoil motion starts at $t = (s - 1)b/U$ earlier, then the velocity potential of all elements is

$$\Delta\phi_2 = \int_1^s \frac{\Delta\phi_2'}{\Delta x_0}\, dx_0 \quad . \qquad (3.109)$$

The trailing edge condition for smooth flow must give the finiteness of the expression

$$\frac{\partial}{\partial x}\left(\Delta\phi_1 + \Delta\phi_2\right)_{x=1} \quad . \qquad (3.110)$$

Using Eqs. (3.105) and (3.109) this condition becomes

$$\frac{1}{\pi}\ w(x_1, t)\ \Delta x_1 \sqrt{\frac{1 + x_1}{1 - x_1}} = -\frac{1}{2\pi}\int_1^s E(x_0, t)\sqrt{\frac{1 + x_0}{x_0 - 1}}\ dx_0 \quad . \tag{3.111}$$

This may be regarded as an integral equation for determining the wake vorticity in terms of the normal velocity w for any element Δx_1.

The pressure due to circulatory potential is

$$\Delta P_2 = -2\rho_\infty \frac{U}{b}\left(\frac{\partial}{\partial x} + \frac{\partial}{\partial x_0}\right)\Delta\phi_2 = -\frac{2\rho_\infty U}{\sqrt{1 - x^2}}\int_1^s \frac{E}{2\pi}\frac{x_0 + x}{\sqrt{x_0^2 - 1}}\ dx_0 \quad , \tag{3.112}$$

or

$$\Delta P_2 = \frac{2\rho_\infty U}{\sqrt{1 - x^2}}\ \frac{\displaystyle\int_1^s E\,\frac{x_0 + x}{\sqrt{x_0^2 - 1}}\ dx_0}{\displaystyle\int_1^s E\sqrt{\frac{x_0 + 1}{x_0 - 1}}\ dx_0}\ \Delta Q(r_1, t) \quad , \tag{3.113}$$

$$\Delta Q(x_1, t) = \frac{1}{\pi}\ w(x_1, t)\ \Delta x_1\sqrt{\frac{1 + x_1}{1 - x_1}} \quad . \tag{3.114}$$

Consider an example: let

$$w(x_1, t) = w^*(x_1)\exp(i\omega t) \quad , \tag{3.115}$$

$$E(x_0, t) = E_0 \exp\left\{i\omega\left[t - (x_0 - 1)\frac{b}{U}\right]\right\} \quad , \tag{3.116}$$

$$= E_0 \exp\left\{i\left[\omega t - k(x_0 - 1)\right]\right\} \quad , \tag{3.117}$$

where w^* and E_0 are complex amplitudes; the coefficient k is

$$k = \frac{\omega b}{U} = \frac{\omega c}{2U} \quad . \tag{3.118}$$

Then the equation for ΔP_2 can be rewritten in the form

$$\Delta P_2 = \frac{2\rho_\infty U}{\sqrt{1 - x^2}}\ \frac{\displaystyle\int_1^s \frac{x_0 + x}{\sqrt{x_0^2 - 1}}\exp(-ikx_0)\ dx_0}{\displaystyle\int_1^s \frac{x_0 + 1}{\sqrt{x_0^2 - 1}}\exp(-ikx_0)\ dx_0}\ \Delta Q \quad , \tag{3.119}$$

$$\Delta Q = \frac{1}{\pi}\, w(x_1, t)\, \Delta x_1 \sqrt{\frac{1 + x_1}{1 - x_1}} \quad , \tag{3.120}$$

The evaluation of the integrals for $s \to \infty$ requires a special effort. To this end, let us consider the expression

$$\frac{\int_1^s \frac{x_0}{\sqrt{x_0^2 - 1}} \exp(-ikx_0)\, dx_0}{\int_1^s \frac{x_0 + 1}{\sqrt{x_0^2 - 1}} \exp(-ikx_0)\, dx_0} = 1 - \frac{\int_1^s \frac{\exp(-ikx_0)}{\sqrt{x_0^2 - 1}}\, dx_0}{\int_1^s \frac{\exp(-ikx_0)}{\sqrt{x_0^2 - 1}}\, dx_0 + \int_1^s \frac{x_0 \exp(-ikx_0)}{\sqrt{x_0^2 - 1}}\, dx_0} \quad . \tag{3.121}$$

On the right hand side of this equation the integral

$$I(k) = \int_1^s \frac{x_0 \exp(-ikx_0)}{\sqrt{x_0^2 - 1}}\, dx_0 \quad , \tag{3.122}$$

may represent some difficulty for $s \to \infty$. It is possible to evaluate it with the result that

$$I(k) = -\frac{1}{2}\, \pi\, H_1^{(2)}(k) \quad . \tag{3.123}$$

The expression (3.121) for $s \to \infty$ takes the form

$$C(k) = \frac{H_1^{(2)}(k)}{H_1^{(2)}(k) + iH_0^{(2)}(k)} \quad . \tag{3.124}$$

Equation (3.119) takes the form

$$\Delta P_2 = \frac{2\rho_\infty U}{\pi} \sqrt{\frac{1 - x}{1 + x}} \sqrt{\frac{1 + x_1}{1 - x_1}} \left[C(k) - 1 + \frac{1}{(1 - x)} \right] w \Delta x_1 \quad . \tag{3.125}$$

The function C(k), proposed by Theodorsen, is often written in the form

$$C(k) = F(k) + iG(k) \quad , \tag{3.126}$$

and is tabulated. The total pressure is the sum of ΔP_1 and ΔP_2, or

$$\frac{dP}{dx_1} = -\frac{\rho_\infty}{\pi} L(x, x_1) b \frac{\partial w}{\partial t} + 2\rho_\infty \frac{U}{\pi} \sqrt{\frac{1 - x}{1 + x}} \sqrt{\frac{1 + x_1}{1 - x_1}} \left(\frac{1}{x_1 - x} + C(k) - 1 \right) w \quad , \tag{3.127}$$

and the total loading at x is given by

$$P(x) = \int_{-1}^{+1} \frac{dP}{dx_1} dx_1 \quad . \tag{3.128}$$

There exist a few other formulas for the pressure difference P(x, t), such as:

$$\Pi(\theta, t) = \rho_\infty U^2 \exp(i\omega t)\left(2a_0 \cot\frac{\theta}{2} + 4 \sum_1^\infty a_n \frac{\sin n\theta}{n}\right) \quad , \tag{3.129}$$

where

$$a_0 = C(k)(A_0 - A_1) + A_1 \quad ; \tag{3.130}$$

$$a_n = \frac{ik}{2} A_{n-1} - nA_n - \frac{ik}{2} A_{n+1}, \quad (n \geq 1) \quad , \tag{3.131}$$

and where the coefficients A_n are supposed to be known from the expansion of the normal velocity

$$w = U \exp(i\omega t)(A_0 + 2 \sum_1^\infty A_n \cos n\eta) \quad . \tag{3.132}$$

Another function used is

$$T(k) = 2C(k) - 1 = \frac{H_0^{(2)}(k) + iH_1^{(2)}(k)}{-H_0^{(2)}(k) + iH_1^{(2)}(k)} \quad , \tag{3.133}$$

and

$$\Pi(\theta, t) = \frac{2}{\pi} \rho_\infty U \int_0^\pi w(-\cos\eta, t) F(\theta, \eta, k)\, d\eta \quad , \tag{3.134}$$

with

$$F(\theta, \eta, k) = -ik\mathscr{L}(\theta, \eta)\sin\eta + \frac{\sin\theta}{\cos\theta - \cos\eta} + \cot\frac{\theta}{2}[(1 - \cos\eta)C(k) + \cos\eta] \tag{3.135}$$

The total value of dP/dx_1 in an incompressible fluid may be separated into two parts; the non-circulatory terms, arising from $\Delta\phi_1$, which act instantaneously, and the circulatory terms (potential), which are in general a function of the wake (i. e., of the past history of the motion). The part due to the wake may be given in form of the expression

$$(P')_c = nC(k)w^*(x_1)\exp(i\omega t) \quad , \tag{3.136}$$

$$n = n(x, x_1) = \frac{2\rho_\infty U}{\pi}\sqrt{\frac{1 - x}{1 + x}}\sqrt{\frac{1 + x_1}{1 - x_1}} \quad . \tag{3.137}$$

Another representation for the total pressure difference is

$$P = P_H + P_I \quad ; \tag{3.138}$$

$$P_H = \pi \rho_\infty U w_0 \sqrt{\frac{1 + x}{1 - x}}\, k_1(s) \quad , \tag{3.139}$$

where the symbols used denote:

$w_0 = w_0(x_1)$ = constant, which implies that the entire airfoil suddenly acquires a uniform normal velocity;

$k_1(s)$ — this function is related to the function $C(k)$ by means of the equation

$$\frac{C(k) - 1}{ik} = \int_0^\infty [k_1(s) - 1] \exp(-iks)ds \quad ; \tag{3.140}$$

$$P_I = \pi\rho_\infty b w_0 \sqrt{1 - x^2}\, \delta(s) \quad ; \tag{3.141}$$

the delta function $\delta(s)$ represents

$$\delta(s) = \frac{\partial H(s)}{\partial s} \quad ; \quad H(s) = \exp(iks) \quad . \tag{3.142}$$

The total lift per unit span may be expressed as

$$L = 2\pi\rho_\infty b U w_0 [k_1(s) + \frac{1}{2} b\delta(s)] \quad . \tag{3.143}$$

The application of the principle of superposition for the general transient distribution of normal velocity leads to the contribution of the non-instantaneous wake terms, to the pressure term dP/dx_1. One form for this result is:

$$(P')_w = n(x, x_1)\left[w(x_1, 0)k_1(s) + \int_0^s k_1(s - \sigma) \frac{\partial}{\partial\sigma} w(x_1, \sigma)ds \right] . \tag{3.144}$$

The result (3.144), together with the instantaneous terms remaining in Eq.(3.127) when the term containing the factor $C(k)$ is omitted, is the complete result for the density of pressure difference or loading dP/dx_1, for the arbitrary normal velocity function $w(x_1, s)$.

Sometimes, the normal velocity function is separated into two parts; one part, w_1, is associated with the motion of the airfoil, the other, w_2, is associated with a penetration of the airfoil into a nonuniform air stream or gust. In developing the analysis for the complete pressure distribution, there appears another pair of functions to be derived. One function, $k_2(s)$, corresponds to an indicial response to a unit traveling wave $[HI(U/b)t - x_1]$ or $H(s - x_1)$, that is, to the penetration effect into a sharp normal gust. The other function corresponds to the sinusoidal velocity wave $w = \exp[i(\omega t - kx_1)]$ traveling down from the leading edge toward the trailing edge. Below, one will find the lift distribution corresponding to the harmonic traveling wave. With $x_1 = -\cos\eta$, one has

$$w = w_0 \exp(i\omega t)\exp(ik\cos\eta) \quad . \tag{3.145}$$

The trigonometric representation

$$\exp(ik\cos\eta) = B_0 + 2\sum_1^\infty B_n \cos(n\eta) \quad , \tag{3.146}$$

furnishes the coefficients

$$B_n = i^n J_n(k) \quad . \tag{3.147}$$

From Eq. (3.132) one gets

$$A_n = \frac{w_0}{U} i^n J_n(k) \quad . \tag{3.148}$$

With the use of the coefficients (3.131) the total lift per unit span length is given by the formula

$$L = 2\pi\rho b U^2 (a_0 + a_1)\exp(i\omega t) \quad , \tag{3.149}$$

where

$$a_0 = \left\{ C(k)[J_0(k) - iJ_1(k)] + iJ_1(k) \right\} \frac{w_0}{U} \quad . \tag{3.150}$$

In particular, one may use the formula

$$L = 2\pi\rho b U w_0 \exp(i\omega t) \left\{ C(k)[J_0(k) - iJ_1(k)] + J_1(k) \right\} \quad . \tag{3.151}$$

The moment about the quarter chord per unit span is given by

$$M = \pi\rho b^2 U^2 \exp(i\omega t)(a_1 - \frac{1}{2}a_2) \quad . \tag{3.152}$$

In the present case, this gives, $M = 0$. Consider now the lift after penetration into the normal sharp gust $w = w_0 H(s - x_1)$. Then one gets

$$L = 2\pi\rho b U w_0 k_2(s) \quad . \tag{3.153}$$

The pair of functions

$$k_2(s) \quad \text{and} \quad C(k)[J_0(k) - iJ_1(k)] + iJ_1(k) \quad ,$$

are related by means of a Laplace transformation. Similarly, the function $k_2(s)$ can be expressed in terms of the function $k_1(s)$ as:

$$k_2(s) = k_3(s) + k_4(s) \quad , \tag{3.154}$$

$$k_3(s) = \frac{1}{\pi}\int_{-1}^{+1} k_1(s-\sigma)\sqrt{\frac{1+\sigma}{1-\sigma}}\, d\sigma \quad , \tag{3.155}$$

$$k_4(s) = \frac{1}{\pi}\sqrt{1-s^2} \quad \text{for} \quad |s| < 1 \quad ,$$
$$= 0 \qquad \text{for} \quad s > 1 \quad ; \tag{3.156}$$

moreover, one has $k_1(s) = 0$ for $s < 0$. By inspection, one may notice that $k_2(s)$ corresponds to the wake (including the quasi-steady) effects, and $k_4(s)$ to the apparent mass effect. The variable s is measured in half chords and corresponds to the distance of penetration of the midchord into the gust, so that $s = -1$ corresponds to penetration by the leading edge.

Let the normal velocity distribution be given by

$$w(-\cos\eta, s) = w_1 + w_2 \quad , \tag{3.157}$$

where w_1 is due to the motion of the airfoil and w_2 due to the penetration into the disturbed atmosphere or medium. The pressure difference, as given by Kuessner, is of the form

$$\Pi(\theta, s) = \frac{2\rho_\infty U}{\pi}\int_0^\pi [F_1(\theta,\eta,s) + F_2(\theta,\eta,s) + F_3(\theta,\eta,s)]\, d\eta \quad , \tag{3.158}$$

where

$$F_1 = \left[\cos\eta\cot\frac{\theta}{2} + \frac{\sin\theta}{\cos\theta - \cos\eta} + \frac{1}{2}\sin\eta\ \ln\frac{1-\cos(\theta-\eta)}{1-\cos(\theta+\eta)}\frac{\partial}{\partial s}\right] w_1 \quad ; \tag{3.159}$$

$$F_2 = (1-\cos\eta)\cot\frac{\theta}{2}\int_0^s k_1(s-\sigma)\frac{\partial w_1}{\partial\sigma}\, d\sigma \quad ; \tag{3.160}$$

$$F_3 = (1-\cos\eta)\cot\frac{\theta}{2}\int_0^{s+1} k_2(s-\sigma)\frac{\partial w_2}{\partial\sigma}\, d\sigma \quad . \tag{3.161}$$

The functions $k_1(s)$ and $k_2(s)$ correspond to those defined earlier. Thus, F_1 corresponds to the apparent mass effect, F_2 to the wake, including the quasi-steady effects for the part w_1 and F_3 to the entire effect of penetration into the gust w_3.

3.3 Airfoil – Aileron - Tab Combination

Assume a dynamic system consisting of a wing, aileron, and tab. Let us consider the harmonic oscillations of this system including aerodynamic balance. Assume that a wing section possesses two hinges; an aileron hinge (or elevator, or rudder hinge) at $x = x_e$, and a tab hinge at $x = x_f$. The leading edge of the wing section is at $x = -1$, the trailing edge at $x = +1$. The half-chord $b = c/2$ is used as the reference length. The leading edge of the aileron is located at $x = x_c$ and the distance from $(x_e - x_c)$ is denoted by ℓ. Similarly, the leading edge of the tab is at $x = x_d$ and the distance from the tab hinge to the tab leading edge $(x_f - x_d)$ is denoted by m. Let us assume that the wing undergoes the harmonic oscillatory motions with amplitudes:

(i) a displacement h (or the velocity h) in the vertical direction downward;

(ii) a turning about the axis $x = x_a$, the instantaneous angle of attack being α;

(iii) a rotation of the aileron about $x = x_e$, the angle of the aileron, β, being measured with respect to the wing, i. e., with respect to the angle α;

(iv) a rotation of the tab about $x = x_f$, the angle of the tab, γ, being again measured with respect to the aileron.

Similarly, we have to discuss the types of the normal velocity distributions involved in this representation. These are:

(i) for the magnitudes of h and α, the velocity is uniform and proportional to x over the entire chord, namely,

$$w(x) = -[h + U\alpha + (x - x_a)\alpha] \quad ; \tag{3.162}$$

(ii) for β and for γ, the velocity is assumed to be zero for $x < x_c$, uniform and proportional to x over the aileron chord, namely

$$w(x) = -[U\beta + (x - x_c)\beta] \quad . \tag{3.163}$$

One may consider some additional terms associated with the leading edge of the aileron and with the distance ℓ; this may be treated as the step-shape limit $\Delta x_c \rightarrow 0$ of a distribution

$$w = 0 \text{ for } x < x_c \text{ and for } x > x_c + \Delta x_c \quad ; \tag{3.164}$$

$$w = \frac{U\beta\ell}{\Delta x_c} \text{ for } x_c < x < x_c + \Delta x_c \quad . \tag{3.165}$$

The total velocity potential can be considered as a sum of terms, one associated with each term in w. This means that

$$\phi = \sum_n \phi_n \quad , \tag{3.166}$$

with

$$n = \dot{h},\ \alpha,\ \dot{\alpha},\ \beta,\ \dot{\beta},\ \gamma,\ \dot{\gamma}\ .$$

In the relations for the pressure difference there also appear terms containing $\ddot{h}$, $\ddot{\alpha}$, $\ddot{\beta}$, $\ddot{\gamma}$.

The total force positive downward, the total moment about $x = x_a$, and the aileron and tab hinge moments (the sign convention is as follows: positive moments tend to raise the leading edge and correspond to the clockwise direction) taken per unit span length are expressed by the formulas

$$F = b\int_{-1}^{+1} P dx \quad ; \tag{3.167}$$

$$M_\alpha = b^2\int_{-1}^{+1} P(x - x_a)\, dx \quad ; \tag{3.168}$$

$$M_\beta = b^2\int_{x_c}^{1} P(x - x_e)\, dx \quad ; \tag{3.169}$$

$$M_\gamma = b^2\int_{x_d}^{1} P(x - x_f)\, dx \quad , \tag{3.170}$$

where P is the pressure difference. Below, we quote some results for the h and α degrees of freedom. These are

$$F = -\rho_\infty b^2(\pi h + U\pi\dot{\alpha} - \pi b x_a \ddot{\alpha}) - 2\pi\rho_\infty U b C(k) Q \quad ; \tag{3.171}$$

$$M_a = -\rho_\infty b^2[-\pi b x_a \ddot{h} + \pi(\tfrac{1}{2} - x_a)Ub\dot{\alpha} + \pi b^2(\tfrac{1}{8} + x_a^2)\ddot{\alpha}] + 2\pi\rho_\infty U b^2(\tfrac{1}{2} + x_a)C(k)Q; \tag{3.172}$$

$$Q = U\alpha + \dot{h} + b(\tfrac{1}{2} - x_a)\dot{\alpha} \quad . \tag{3.173}$$

The following terms may be associated with the corresponding physical interpretations:

(i) the apparent mass term per unit length associated with vertical acceleration of a plate, $\pi\rho b^2$;

(ii) the apparent moment of inertia term, $\rho_\infty b^4\pi(\frac{1}{8} + x_a^2)$;

(iii) the damping terms associated with the angular velocity $\dot{\alpha}$;

(iv) the velocity term Q associated with C(k), which corresponds to the resultant velocity at the three-quarter position ($x_a = \frac{1}{2}$), and one may note the fact that the part of the moment involving C(k) vanishes at $x_a = -\frac{1}{2}$. One may introduce various short notations:

$$-F = \frac{1}{2} \rho_\infty U^2 c c_\ell \quad ; \tag{3.174}$$

$$M_a = \frac{1}{2} \rho_\infty U^2 c^2 c_m \quad ; \tag{3.175}$$

$$c_\ell = (c_{\ell, h}) \frac{h}{b} + (c_{\ell, \alpha}) \alpha \quad ; \tag{3.176}$$

$$c_m = (c_{m, h}) \frac{h}{b} + (c_{m, \alpha}) \alpha \quad . \tag{3.177}$$

One may introduce certain coefficients:

$$A_{11} = \frac{1}{\pi} c_{\ell, h} \quad ; \quad A_{12} = \frac{1}{\pi} c_{\ell, \alpha} \quad ; \tag{3.178}$$

$$A_{21} = -\frac{2}{\pi} c_{m, h} \quad ; \quad A_{22} = -\frac{2}{\pi} c_{m, \alpha} \quad ; \tag{3.179}$$

Since these coefficients are complex, they may be separated into real and imaginary parts:

$$A_{11} = R_{11} + iI_{11} = \frac{1}{\pi} [(c_{\ell, h})r + i(c_{\ell, h})i] \quad ; \tag{3.180}$$

$$A_{12} = R_{12} + iI_{12} = \frac{1}{\pi} [(c_{\ell, \alpha})r + i(c_{\ell, \alpha})i] \quad ; \tag{3.181}$$

$$A_{21} = R_{21} + iI_{21} = -\frac{2}{\pi} [(c_{m, h})r + i(c_{m, h})i] \quad ; \tag{3.182}$$

$$A_{22} = R_{22} + iI_{22} = -\frac{2}{\pi} [(c_{m, \alpha})r + i(c_{m, \alpha})i] \quad . \tag{3.183}$$

It is clear that the aerodynamic coefficients A can be conveniently represented in the form of a matrix; the rank of the matrix is equal to the number of degrees of freedom in the system in question. In each term A_{ij} of the matrix, the aerodynamic inertia and restoring terms can be grouped into real parts R and the damping terms into the imaginary parts I. The various coefficients are often referred to as aerodynamic derivatives. One may notice that the moment is taken variously about spanwise axes through the quarter chord, midchord, or leading edge positions, so that a conversion formula of the type

$$M_\alpha = M_0 + nbF \quad , \tag{3.184}$$

is valid.

With the inclusion of aileron and tab-control surface degrees of freedom, there appear numerous parameters in the aerodynamic results.

Obviously, the whole problem of what simplified substitutions to employ for the velocity distribution normal to the wing surface, in order to properly represent the actual physical behavior of the airfoil or its control surface, is an important one. The theoretical results, in particular for control surfaces, may need some modifications. This is due to physical reasons, like the large influence of the boundary layer on hinge moments, etc. There are some ideas of using, in addition to rectilinear segments, parabolic arc segments to represent the effective camber lines. It has been proposed to use empirical or semi-empirical factors to modify various coefficients. Thus, based on some experimental information, the inertia, damping, and elastic aerodynamic terms may in certain cases be multiplied by factors which are less than unity. Such propositions, although useful, are not too satisfactory in many general cases, because of the quite different behavior of the boundary layer and of the flow pattern for low and high oscillation frequencies. Similarly, the dynamics of the boundary layer and of flow separation is important in the effect of varying mean angle of attack, both for unstalled and stalled conditions.

One may discuss a solution of the equations, derived above, in a particular case of a subsonic oscillating flow in two dimensions. The differential equation satisfied by the acceleration potential or by the pressure p is given in Eq. (3.12), where for the present case, the variable z has to be omitted and the coordinate y takes the role of the coordinate z in the boundary conditions. The normal velocity can be written in the form

$$w(x,0,t) = -\frac{1}{\rho_\infty U} \int_{-\infty} \frac{\partial}{\partial y}\, p(x', y, t - \frac{x-x'}{U})dx' \quad ; \tag{3.185}$$

for the harmonic oscillations

$$w = w^*(x) \exp(i\omega t) \quad , \tag{3.186}$$

Eq. (3.185) takes the form

$$w^*(x) = -\frac{1}{\rho_\infty U} \exp(-i\omega \frac{x}{U}) \int_{-\infty}^{x} \frac{\partial}{\partial y}\, p^*(x', y) \exp(i\omega \frac{x'}{U})dx' \quad , \tag{3.187}$$

where y is supposed to be made to approach zero in the integrals.

Satisfying the conditions of a given distribution of the velocity w requires a proper distribution over the chord of fundamental solutions involving pressure jump across the wing surface. This usually leads to an integral equation involving the known function w^*, an unknown distribution function and a kernel function is determined from Eq. (3.187). The fundamental doublet solution, obtained from the oscillating moving source solution, Eq. (3.79), by differentiation in the present case with respect to the position variable η, results in the following form:

$$\frac{-p^*(x', y)}{\rho_\infty} = -\frac{i}{4\beta}\frac{\partial}{\partial y}\{\exp[-i\mu(x'-\xi)]\, H_0^{(2)}(\mathscr{K} R')\exp(i\omega t)\}, \qquad (3.188)$$

where

$$\mathscr{K} = \frac{\omega M_\infty}{U\beta^2}\ ; \quad \mu = \frac{\omega}{U}\frac{M_\infty^2}{\beta^2}\ ; \qquad (3.189)$$

$$R' = \sqrt{(x'-\xi)^2 + \beta^2(y-\eta)^2}\ ; \qquad (3.190)$$

$$\beta = |1 - M_\infty^2|^{1/2}. \qquad (3.191)$$

The doublet expression (3.188) has been normalized to represent a total jump in the pressure potential across the surface which is harmonic and of magnitude unity. That is, the total pressure difference is

$$P = -\rho_\infty \exp(i\omega t). \qquad (3.192)$$

Substitution of Eq. (3.188) into Eq. (3.187) gives a particular distribution of normal velocity w, associated with the normalized doublet and which is used to define the kernel function. Thus the kernel function has the property of giving the normal velocity at any field point induced by unit harmonic loading at the loading point. The substitution yields

$$K_1(x, \xi; M_\infty\omega) = \lim_{y\to 0} \frac{-i\exp[-i(x/U) - i\mu\xi]}{4\beta U}\int_{-\infty}^{x}\exp\left(\frac{i\omega x'}{U\beta^2}\right)\frac{\partial^2}{\partial y^2}H_0^{(2)}(\mathscr{K}R')\,dx'. \qquad (3.193)$$

The result (3.193) is presented in a simple form, but it is a divergent one for $y \to 0$. One may replace the operation $\partial^2/\partial y^2$ by the operation

$$\frac{\partial^2}{\partial y^2} = - \left[(1 - M_\infty^2) \frac{\partial^2}{\partial x^2} + \left(\frac{\omega}{U}\right)^2 \frac{M_\infty^2}{1 - M_\infty^2} \right] . \tag{3.194}$$

Integrating twice by parts, letting η and y approach 0, and using the expression

$$\int_{-\infty}^{0} \exp(i\lambda) H_0^{(2)} (M_\infty |\lambda|) d\lambda = \frac{2}{\pi\beta} \ln \frac{1+\beta}{M_\infty} , \tag{3.195}$$

gives the following result for K_1 :

$$K_1 = \frac{\omega}{U^2} K\left(\frac{\omega}{U}(x-\xi), M_\infty\right) , \tag{3.196}$$

and

$$K\left(\frac{\omega}{U} x, M_\infty\right) = - \frac{1}{4\beta} \exp(i\mu x) \left\{ H_0^{(2)}(\mathscr{K}|x|) - iM_\infty \frac{x}{|x|} H_1^{(2)}(\mathscr{K}|x|) - i\beta^2 \exp\left(\frac{-i\omega x}{U\beta^2}\right) \left(\frac{2}{\pi\beta} \ln \frac{1+b}{M_\infty} + \int_0^{\omega x/U\beta^2} \exp(i\lambda) H_0^{(2)}(M_\infty|\lambda|) d\lambda \right) \right\} \tag{3.197}$$

Let the line airfoil be represented by its distribution of normal velocity extending from the leading edge x = - 1 to the trailing edge x = 1, the actual chord being 2b. Let the normal velocity distribution be harmonic of the form $w^*(x)\exp(i\omega t)$. Then the following expression relates the known function $w^*(x)$, the normalized influence function K_1 and the unknown loading function $l(\xi)$ where $l(\xi)$ represents the local intensity of the surface jump in ψ or $(-P/\rho_\infty)$:

$$w^*(x) = b \int_{-1}^{+1} K_1 \, l(\xi) d\xi . \tag{3.198}$$

This integral can be written in the form

$$w^*(x) = k \int_{-1}^{+1} \gamma^*(\xi) K(s, M_\infty) d\xi ; \tag{3.199}$$

in this equation, the intensity of loading, γ^*, is defined by the equation

$$P = -\rho_\infty U \gamma^*(\xi) \exp(i\omega t) ; \tag{3.200}$$

$$k = \frac{\omega b}{U} ; \quad s = k(x - \xi) ; \tag{3.201}$$

$$\mathscr{K} = \frac{\omega b}{U} \frac{M_\infty}{\beta^2} = \frac{kM_\infty}{\beta^2} ; \tag{3.202}$$

$$\mu = \frac{\omega b}{U} \frac{M_\infty^2}{\beta^2} = \frac{kM_\infty^2}{\beta^2} \quad . \tag{3.203}$$

From the boundary condition it is required that $\gamma^*(1) = 0$. The function γ^* may be expressed in terms of

$$\gamma^*(x) = U\left[2a_0 \cot\frac{\theta}{2} + 4\sum_{i}^{\infty} a_n \frac{\sin n\theta}{n}\right] , \tag{3.204}$$

where $x = -\cos\theta$ and the a's are complex coefficients to be determined. The kernel function $K(s, 0)$ for the incompressible flow is given by

$$K(s, 0) = \frac{1}{2\pi s} - \frac{i \exp(-is)}{2\pi}\left[Ci(s) + i\left(Si(s) + \frac{\pi}{2}\right)\right] \tag{3.205}$$

with

$$s = \frac{\omega b}{U}(x - \xi) = k(x - \xi) \quad , \tag{3.206}$$

$$Ci(s) = -\int_{-s}^{\infty} \frac{\cos u}{u} du = \ln \exp(\gamma s) - \int_0^s \frac{1 - \cos u}{u} du \quad ; \tag{3.207}$$

$$Si(s) = \int_0^s \frac{\sin u}{u} du \quad . \tag{3.208}$$

To calculate the coefficients a_n, one has to apply the method of successive approximations which will be described below. This method has been applied mainly to the wing without aileron undergoing vertical translation (h) and pitching motion (α). Let

$$w(x,t) = \exp(i\omega t)\, w^*(x) = -[\dot{h} + U\alpha + b(x - x_a)\dot{\alpha}] \quad , \tag{3.209}$$

be expressed in the form

$$w^* = U\left[A_0 + 2\sum_{1}^{\infty} A_n \cos n\theta\right] . \tag{3.210}$$

Comparison of Eq. (3.210) with (3.209) with $x = -\cos\theta$ shows that the coefficients a_n are zero for $n \geq 2$. The collocation method consists in setting up and solving a system of n linear equations for the first complex coefficients $a_0, \ldots, a_{n-1}$, so that the Posio integral equation is effectively satisfied at n points of the chord $\theta_1, \ldots, \theta_n$. The coefficients of the a's in this system of equations are given by definite integrals, involving the product of the known kernel K and one of the chosen aerodynamic mode shapes appearing in the relation (3. 204). These integrals are obtained by numerical integrations and are functions of frequency, Mach number, and of the distance between downwash and loading points. The numerical methods of solving Eq. (3. 199) are based on the tables of the numerical values of the kernel function $K(s, M_\infty)$. The kernel function may be expressed in the form

$$K(s, M_\infty) = \frac{F(M_\infty)}{s} + iG(M_\infty) \ln s + K_r(s, M_\infty) \quad , \tag{3. 211}$$

$$F(M_\infty) = \frac{\sqrt{1 - M_\infty^2}}{2\pi} \quad , \tag{3. 212}$$

$$G(M_\infty) = \frac{1}{2\pi \sqrt{1 - M_\infty^2}} \quad , \tag{3. 213}$$

$$K_r(0, M_\infty) = - \frac{1}{4\sqrt{1 - M_\infty^2}} + i\left[- \frac{M_\infty^2}{2\pi\sqrt{1 - M_\infty^2}} + \frac{1}{2\pi \sqrt{1 - M_\infty^2}} \ln \frac{e^\gamma M_\infty}{2(1 - M_\infty^2)} + \frac{1}{2\pi} \ln \frac{1 + \sqrt{1 - M_\infty^2}}{M_\infty}\right], \tag{3. 214}$$

where $\gamma = 0.5772 \ldots$ is Euler's constant. Another iterative procedure, which will be described below, may be applied to include effects of aileron motion. For a given normal velocity function $w(x, t)$ the value of γ^* (or P) for the incompressible flow may be represented by subscript zero as γ_0^*. The required distribution γ may be written as

$$\gamma^* = \gamma_0^* + \Delta\gamma_0^* \quad , \tag{3. 215}$$

or

$$w^*(x) = k \int_{-1}^{+1} [\gamma_0^*(x) + \Delta\gamma_0^* (\xi)] K(s, M_\infty) d\xi \quad . \tag{3. 216}$$

By the definition of γ_0^*

$$w^*(x) = k \int_{-1}^{+1} \gamma_0^*(\xi) K(s, 0) d\xi \quad , \tag{3. 217}$$

so that

$$k \int_{-1}^{+1} \Delta\gamma_0^*(\xi) K(s, M_\infty) d\xi = k \int \gamma_0^*(\xi) [K(s, 0) - K(s, M_\infty)] d\xi = w_1^*(x) \quad , \tag{3. 218}$$

where $w_1^*(\xi)$ is a known function defined by γ_0^* and by the difference in the kernel functions.

Then one can apply the iterative process in the form

$$\gamma^* = \gamma_0^* + \gamma_1^* + \gamma_2^* + \dots + \gamma_n^* + \Delta\gamma_n^* \quad , \tag{3.219}$$

where the remainder term satisfied an equation of the original type but the other terms can be obtained as exactly as desired from the simpler equations utilizing $K(s, 0)$. In the steady case the convergence of γ^* to its value $\gamma_0^* / \sqrt{1 - M_\infty^2}$ is reached in the manner of the sequence

$$\gamma_0^*(1 + \mu + \mu^2 + \dots) \quad , \tag{3.220}$$

with

$$\mu = 1 - \sqrt{1 - M_\infty^2} \quad . \tag{3.221}$$

This method was applied to the calculation of the force and moments for a wing undergoing vertical translation and pitching, and the aileron coefficients were included for the value 0.15 of the aileron chord ratio.

3.4 General Remarks

According to the results in the past, the control surface derivatives have exhibited wider deviations from theory than the wing derivatives. This is because the controls usually operate in the boundary layer (often separated) of the main wing; there appears flow leakage and sharp variation in the pressure distributions near leading edges of the control. Some data on controls are given in works by van de Vooren, Erickson, and Robinson, Andreopoulos, Cheilek and Donovan, and Drescher.

3.5 List of References to Chapter 3

1. Acum, W. E. A., and H. C. Garner: Approximate Wall Corrections for an Oscillating Swept Wing in a Wing Tunnel of Closed Circular Section. Brit. Ministry of Supply, CP 184, 1935.

2. Alford, W. J. Jr., and T. B. Pasteur, Jr.: The Effects of Changes in Aspect Ratio and Tail Height on the Longitudinal Stability Characteristics at High Subsonic Speeds of a Model with a Wing Having 32.6° Sweepback. Feb. 1954. NACA RM L53L09.

3. Andreopoulos, T. C., H. A. Cheilek, A. F. Donovan: Measurements of the Aerodynamic Hinge Moments of an Oscillating Flap and Tab. Air Material Command, U.S. Air Force Tech. Rep. 5784, 1949.

4. Ashley, H.: Some Unsteady Aerodynamic Problems Affecting the Dynamic Stability of Aircraft. Sc. D. Thesis, MIT, 1951.

5. Ashley, H., G. Zartarian, and D. O. Neilson: Investigation of Certain Unsteady Aerodynamic Effects in Longitudinal Dynamic Stability. Wright Air Devel. Center, U.S. Air Force Tech. Rep. 5986, 1951.

6. Axelson, J. A.: Downwash Behind a Triangular Wing of Aspect Ratio 3-Transonic Bump Method. Dec. 1953. NACA RM A53I23.

7. Baird, E. F., and H. J. Kelly: "Formulation of the Flutter Problem for Solution on an Electronic Analog Computer." J. Aer. Sci. 17, 189-190, 1950.

8. Baker, B. B., and E. T. Copson.: The Mathematical Theory of Huygen's Principle. Oxford Univ. Press, 1939.

9. Baker, J. E.: The Effects of Various Parameters, Including Mach Number, on Propeller Blade Flutter with Emphasis on Stall Flutter. NACA TN 3357, 1955.

10. Baker, T. F.: Results of Measurements of Maximum Lift and Buffeting Intensities Obtained During Flight Investigation of the Northrop X-4 Research Airplane. Aug. 1953. NACA RM L53G06.

11. Baker, T. F., and W. E. Johnson: Flight Measurements at Transonic Speeds of the Buffeting Characteristics of the XF-92A Delta-Wing Research Airplane. Apr. 1955. NACA RM H54L03.

12. Barmby, J. G., H. J. Cunningham, and I. E. Garrick: Study of Effects of Sweep on the Flutter of Cantilever Wings. NACA Rep. 1014, 1951.

13. Barton, M. V.: "Stability of an Oscillating Airfoil in Supersonic Airflow." J. Aer. Sci. 15, 371-376, 1948.

14. Behrbohm, H.: The Flat Triangular Wing with Subsonic Leading Edges in Steady Pitch. Svenska Aeroplan Aktiebolaget, Linkoping, TN 9, 1952.

15. Bergh, H.: Experimental Determination of the Aerodynamic Coefficients of an Oscillating Wing in Incompressible, Two-Dimensional Flow. Part III: Experiments at Zero Speed. Natl. Aer. Res. Inst. Amsterdam, NLL Rep. F 103, 1952.

16. Bergh, H., and A. I. van de Vooren: Experimental Determination of the Aerodynamic Coefficients of an Oscillating Wing in Incompressible Two-Dimensional Flow. Part IV: Calculation of the Coefficients. Natl. Aer. Res. Inst. Amsterdam, NLL Rep. F 104, 1952.

17. Berndt, S. B.: On the Theory of Slowly Oscillating Delta Wings at Supersonic Speeds Medd. Flytekniska Forsoksanstalten, Stockholm, 43, 1952.

18. Billing, H., K. Katterbach, and H. G. Kuessner: Untersuchung der Bewegung Einer Platte Bein Eintritt in Eine Strahlgrenze. Zent. Wissensch. Berichtsw. Ueber Luftfahrtforsch., Berlin, FB 1640, 1942.

19. Billington, A. E.: Harmonic Oscillations of an Aerofoil in Subsonic Flow. Australian Aer. Res. Lab. Rep. A 65, 1949.

20. Biot, M. A.: Aerodynamic Theory Applied to Flutter Analysis. Guggenheim Aer. Lab. CALTECH, Rep. 6, U.S. Army Air Force, 1942.

21. Biot, M. A.: "Loads on Supersonic Wing Striking Sharp-Edged Gust." J. Aer. Sci. 16, p. 296, 1949.

22. Biot, M. A.: "Transonic Drag of an Accelerated Body." Quarterly Appl. Math. 7, 101-105, 1949.

23. Biot, M. A., and L. Arnold: Investigation of Aileron Compressibility Flutter. Air Force TR 6341, 1950.

24. Biot, M. A., and L. Arnold: Unsteady Supersonic Generalized Aerodynamic Forces on a Delta Wing with Arbitrary Deflection Mode Shape. Air Force Contract 113583, SD Rep. 13, 1953.

25. Biot, M. A., and C. T. Boehnlein: Aerodynamic Theory of Oscillating Wing of Finite Span. Guggenheim Aer. Lab. Calif. Inst. Tech. Rep. 5 U. S. Army Air Force, 1942.

26. Birnbaum, W.: "Das Ebene Problem des Schlagenden Fluegels." Z. ang. Math. u. Mech. 4, 277-292, 1924. Also: NACA TM 1364, 1954.

27. Bisplinghoff, R. L., H. Ashley, and R. L. Halfman: Aeroelasticity. Addison-Wesley, 1955.

28. Bleich, F., C. B. McCullough, R. Rosecrans, and G. S. Vincent: The Mathematical Theory of Vibration in Supension Bridges. U. S. Govt. Printing Office, 1950.

29. Bollay, W., and C. D. Brown: "Some Experimental Results on Wing Flutter." J. Aer. Sci. 8, 313-318, 1941.

30. Borbely, von S.: "Aerodynamic Forces on a Harmonically Oscillating Wing at Supersonic Speed. (Two-Dimensional Case)." Z. ang. Math. u. Mech. 22, 190-205, 1942.

31. Borbely, von S.: "Ueber Einen Grenzfall der Insttationaeren Vaumlichen Tragfluegelstrommung." Zamm 18, 319, 1938. Also: Brit. ARC RM 4090, 1939.

32. Bratt, J. B., and C. T. Davis: The Influence of Aspect Ratio and Taper on the Fundamental Damping Derivative Coefficient for Flexural Motion. Brit. ARC RM 2032, 1945.

33. Bratt, J. B., and C. Scruton: Measurements of Pitching Moment Derivatives for an Aerofoil Oscillating About the Half-Chord Axis. Brit. ARC RM 1921, 1938.

34. Bratt, J. B., and K. C. Wight: The Effect of Mean Incidence, Amplitude of Oscillation, Profile and Aspect Ratio on Pitching Moment Derivatives. Brit. ARC RM 2064, 1945.

35. Briggs, D. W.: Flight Determination of the Buffeting Characteristics of the Bell X-5 Research Airplane at 58.7° Sweepback. May 1954. NACA RM L54C17.

36. Brown, C. E., and H. S. Heinke, Jr: Preliminary Wind-Tunnel Tests of Triangular and Rectangular Wings in Steady Roll at Mach Numbers of 1.62 and 1.93. June 1956, NACA TN 3740. Supersedes RM L8L30.

37. Buchan, A. L., K. D. Harris, and P. M. Somervail: The Measurement of the Derivative Z_w for an Oscillating Aerofoil. Brit. ARC RM 40, 1950.

38. Bursnall, W. J.: Initial Flutter Tests in the Langley Transonic Blowdown Tunnel and Comparison with Free-Flight Flutter Results. Jan. 1953. NACA RM L52K14.

39. Campbell, J. P., J. L. Johnson, Jr., Low-Speed Study of the Effect of Frequency on the Stability Derivatives of Wings Oscillating in Yaw with Particular Reference to High Angle-of-Attack Conditions. Nov. 1955. NACA RM L55H05.

40. Carrier, G. F.: "The Oscillating Wedge in a Supersonic Stream." J. Aer. Sci. 16, 150-152, 1949.

41. Carrier, G. F., and R. M. Ring: The Lift and Moment on an Oscillating Wedge. Office of Air Research, Rep. AF 33 (038) 13279, Brown Univ. 1951.

42. Chang, C. C.: "The Transient Reaction of an Airfoil Due to Change in Angle of Attack at Supersonic Speeds." J. Aer. Sci. 15, 635-655, 1948.

43. Chang, C. C.: Transient Aerodynamic Behavior of an Airfoil Due to Different Arbitrary Modes of Nonstationary Motions in a Supersonic Flow. NACA TN 2333, 1951.

44. Chang, C. C.: The Aerodynamic Behavior of a Harmonically Oscillating Finite Sweptback Wing in Supersonic Flow. NACA TN 2567, 1951.

45. Chiarulli, P.: Oscillating Wings of Finite Aspect Ratio. Air Material Command, U.S. Air Force Tech. Rep. 102, AC 49/9-100, 1949.

46. Chuan, R. L., and R. J. Magnus: Study of Vortex Shedding as Related to Self Excited Torsional Oscillations of an Airfoil. NACA TN 2429, 1951.

47. Cicala, P.: "Aerodynamic Forces on an Oscillating Profile in a Uniform Stream." Mem. reale acad. Sci. Torino, 68, 2, 73-98, 1934, 1935.

48. Cicala, P.: "Sul Moto Non-Stazionario di un'ala di Allungamento Finito." Rendiconti Acad. Nazl. Lincei, Rome. 25, Series 6a, 3-4, 97-102, 1937.

49. Cicala, P.: Comparison of Theory with Experiment in Phenomena of Wing Flutter. NACA TM 887, 1939.

50. Cicala, P.: "Present State of Research on the Non-Steady Motion of a Lifting Wing." Aerotecnica, 19, p. 341-347, 1941. Also: Brit. RTP Transl. 1867, 1947.

51. Clevenson, S. A., and E. Widmayer, Jr: Preliminary Experiments on Forces and Moments of an Oscillating Wing at High Subsonic Speeds. NACA Research Mem. L9K28a, 1950.

52. Clevenson, S. A., E. Widmayer, Jr., and F. W. Diederich: An Exploratory Investigation of Some Types of Aeroelastic Instability of Open and Closed Bodies of Revolution Mounted on Slender Struts. NACA TN 3308, 1954.

53. Coe, C. G., Buffeting Forces on Two-Dimensional Airfoils as Affected by Thickness and Thickness Distribution. Feb. 1954. NACA RM A53K24.

54. Collar, A. R.: Resistance Derivatives of Flutter Theory. Part II. Brit. ARC RM 2139, 1944.

55. Couchet, G.: Les Mouvements Plans Non Stationnaires a Circulation Constante et les Mouvements Infiniment Voisins. Office Natl. Etudes et Recherches Aeronaut. 31, 1949; 56, 1952.

56. Cunningham, H. J.: Total Lift and Pitching Moment on Thin Arrowhead Wings Oscillating in Supersonic Potential Flow. NACA TN 3433, 1955.

57. Dietze, F.: I. The Air Forces of the Harmonically Vibrating Wing in a Compressible Medium at Subsonic Velocity. II. Numerical Tables and Curves. ZWB FB 1733, 1943. Translation: Air Material Command, U.S. Air Force, F TS 506 RE and F TS 948 RE, 1947.

58. Dingel, M., Beitraege zur Instationaeren Tragflaechen Theorie. Part VIII: Die Schwingende Tragflaeche Grosser Streckung. ZWB FB 1774, 1943. Also: Air Material Command, U. S. Air Force, Tran. F TS 935 RE, 1947.

59. Doerr, J.: "Influence de l'Allongement Dans les Calculs de Flutter. Calculs Comparatifs sur un Empennage Circulaive." Recherche Aer. 37, 57-63, 1949.

60. Doerr, J.: "Les Forces Aerodynamiques sur une Aile Vibrant Harmoniquement Dans un c'Colement Supersonique." Office Natl. Etudes et Recherches Aeroaut. 37, 63-78, 1949.

61. Drescher, H.: Unsteady Processes. G2 Experimental Determination of Unsteady Lift. AVA Monographs, Rep. and Tran. 1011, 1948.

62. Drescher, H.: Untersuchungen an Einem Symmetrischen Tragfluegel mit Spaltlos Angeschlossenem Ruder bei Raschen Aenderugen des Ruder-Auschlugs (Ebene Stroemung). Max Planck Institute Fuer Stroemungsforschung, Goettingen, Mitt. 6, 1948.

63. Drischler, J. A.: Calculation and Compilation of the Unsteady-Lift Functions for a Rigid Wing Subjected to Sinusoidal Gusts and to Sinusoidal Sinking Oscillations. Oct. 1956. NACA TN 3748.

64. Drischler, J. A., and F. W. Diederich: Lift and Moment Responses to Penetration of Sharp-Edged Traveling Gusts, with Application to Penetration of Weak Blast Waves. May 1957. NACA TN 3956.

65. Duncan, W. J.: The Principles of the Control and Stability of Aircraft. Cambridge Univ. Press, 1952.

66. Duncan, W. J., and A. R. Collar: Resistance Derivatives of Flutter Theory. Brit. ARC RM 1500, 1932.

67. Eckhaus, W.: On the Theory of Oscillating Airfoils of Finite Span in Subsonic Flow. Natl. Aer. Res. Inst. Amsterdam, NLL Rep. F 153, 1954.

68. Eichler, M.: Aufloesung der Integralgleichung von Possio Fuer den Harmonisch Schwingenden Tragfluegel in Kompressiblen Medium Durch Zurechfuehrung auf ein Linearesgleichung System. Deutsche Lufthahrtforschung. FB 1681, 1942.

69. Ellenberger, G.: "Luftkraefte bei Beliebiger Instationaeren Bewegung Eines Tragfluegels mit Querruder und bei Vorhandensein von Boen." Zamm, 18, 173-176, 1938.

70. Epstein, M.: The Two-Dimensional Supersonic Aerodynamic Coefficients for Oscillatory Parabolic Bending of an Airfoil Mean Chord Line. Wright Air Dev. Center, Tech. Note WCLS 53-55, 1953.

71. Epstein, M.: The Effect of an Axially Symmetric Fuselage on the Non-Stationary Supersonic Airloads Acting on a Wing with Supersonic Edges. Wright Air Dev. Center, Tech. Rep. 54-196, 1954.

72. Erickson, A. L., and R. C. Robinson: Some Preliminary Results in the Determination of Aerodynamic Derivatives of Control Surfaces in the Transonic Speed Range by Means of a Flush-Type Electrical Pressure Cell. NACA Res. Mem. A8 H03, 1948.

73. Evvand, J. C.: Use of Source Distributions for Evaluating Theoretical Aerodynamics of Thin Finite Wings at Supersonic Speeds. NACA Rep. 951, 1950.

74. Falkner, V. M.: The Calculation of Aerodynamic Loading Surfaces of any Shape. Brit. ARC RM 1910, 1943.

75. Farren, W. S.: The Reaction on a Wing Whose Angle of Incidence is Changing Rapidly. Wind Tunnel Experiments with a Short Period Recorded Balance. Brit. ARC RM 1648, 1935.

76. Fettis, H. E.: Tables of Lift and Moment Coefficients for an Oscillating Wing-Aileron Combination in Two-Dimensional Subsonic Flow. U.S. Air Force Tech. Rep. 6688, 1951. Supplement 1, 1953.

77. Fettis, H. E.: An Approximate Method for the Calculation of Non-Stationary Air Forces at Subsonic Speeds. Wright Air Dev. Center, Tech. Rep. 52-56, 1952.

78. Few, A. G., Effects of Sweep and Thickness on the Static Longitudinal Aerodynamic Characteristics of a Series of Thin, Low-Aspect-Ratio, Highly Tapered Wings at Transonic Speeds. Transonic-Bump Method. Apr. 1954. NACA RM L54B25.

79. Few, A. G. Jr., and T. J. King: Some Effects of Tail Height and Wing Plan Form on the Static Longitudinal Stability Characteristics of a Small-Scale Model at High Subsonic Speeds. May 1957. NACA TN 3957, Supersedes RM L54G12.

80. Fisher, L. R.: Experimental Determination of the Effects of Frequency and Amplitude on the Lateral Stability Derivatives for a Delta, a Swept, and an Unswept Wing Oscillating in Yaw. Apr. 1956. NACA RM L56A19.

81. Fisher, L. R., and H. S. Fletcher: Effect of Lag of Sidewash on the Vertical-Tail Contribution to Oscillatory Damping in Jaw of Airplane Models. NACA TN 3356, 1955.

82. Fisher, L. R., W. D. Wolhart: Some Effects of Amplitude and Frequency on the Aerodynamic Damping of a Model Oscillating Continuously in Yaw. NACA TN 2766, 1952.

83. Fitzpatrick, J. L. G.: Natural Flight and Related Aeronautics. Inst. Aeronaut. Sic. SMF Fund Paper FF-7, 1952. Also: Supplement, 1954.

84. Flax, A. H.: "The Reverse-Flow Theorem for Nonstationary Flows." J. Aer. Sci. 19, 352-353, 1952; 20, 120-126, 1953.

85. Foster, G. V., and W. C. Schneider: Effects of Leading-Edge Radius on the Longitudinal Stability of Two 45° Sweptback Wings as Influenced by Reynolds Numbers Up to 8.20×10^6 and Mach Numbers Up to 0.303. July 1955. NACA RM L55F08.

86. Frankl, F. I.: Effect of the Acceleration of Elongated Bodies of Revolution Upon the Resistance in a Compressible Flow. NACA TM 1230, 1949.

87. Frazer, R. A.: Flexure-Torsion Flutter-Derivatives for Semi-Rigid Wing. Brit. ARC RM 1942, 1941.

88. Frazer, R. A.: The Flutter and Airplane Wings. Brit. ARC RM 1155, 1928; 1255, 1931.

89. Froehlich, J. E.: "Non-Stationary Motion of Purely Supersonic Wings." J. Aer. Sci. 18, 298-310, 1951.

90. Fung, Y. C.: Introduction to the Theory of Aeroelasticity. J. Wiley, New York, 1955.

91. Furlong, G., and J. G. McHugh: A Summary and Analysis of the Low-Speed Longitudinal Characteristics of Swept Wings at High Reynolds Number. Aug. 1952. NACA RM L52D16.

92. Gardner, C. S., and H. F. Lundloff: "Influence of Acceleration on the Aerodynamic Characteristics of Thin Wings in Supersonic and Transonic Flight." J. Aer. Sci. 17, 47-59, 1950.

93. Garrick, I. E.: Propulsion of a Flapping and Oscillating Airfoil. NACA Rep. 567, 1936.

94. Garrick, I. E.: On Some Fourier Transforms in the Theory of Non-stationary Flows. Proc. Fifth Inter. Con. Appl. Mech. 590-593, 1938. Also: NACA Rep. 629, 1938.

95. Garrick, I. E.: A Survey of Flutter. NACA Univ. Conference on Aerodynamics, June 1948. Durand Reprinting Committee, p. 38-47.

96. Garrick, I. E.: Some Research on High-Speed Flutter. Proc. Third Anglo-Amer. Aer. Con. 419-446, 1951.

97. Garrick, I. E.: Moving Sources in Nonsteady Aerodynamics and in Kirchhoff's Formula. Proc. First U.S. Natl. Con. Appl. Mech. Chicago, 1951. Also. Tran. Amer. Soc. Mech. Eng. 74, 733-739, 1952.

98. Garrick, I. E.: "A Review of Unsteady Aerodynamics of Potential Flows." Appl. Mech. Rev. 3, 89-91 1952.

99. Garrick, I. E.: and S. I. Rubinow: Flutter and Oscillating Air Force Calculations for an Airfoil in a Two-Dimensional Supersonic Flow. NACA Rep. 846, 1946.

100. Garrick, I. E., and S. I. Rubinow: Theoretical Study of Air Forces on an Oscillating or Steady Thin Wing in a Supersonic Main Stream. NACA Tech. Rep. 872, 1947.

101. Garrick, I. E., and C. E. Watkins: Some Recent Developments in the Aerodynamic Theory of Oscillating Wings. NACA Univ. Conference on Aerodynamics, Construction and Propulsion, Oct. 1954.

102. George, M. B. T: A Theoretical Approach to the Problem of Stall Flutter. Cornell Univ. Grad. School of Aer. Eng. Contract AF 33 (038) 21406, 1953.

103. Germain, P., and R. Bader: "Quelques Remarques sur les Mouvements Vibratoires d'une Aile en Regime Supersonique." Recherche Acronautique, 11, 1949.

104. Gills, C. L.: Buffeting Information Obtained From Rocket-Propelled Airplane Models Having Thin Unswept Wings. 18 Oct. 1950. NACA RM L50H22a.

105. Gillis, C. L., R. F. Peck, and A. J. Vitale: Preliminary Results From a Free-Flight Investigation at Transonic and Supersonic Speeds of the Longitudinal Stability and Control Characteristics of an Airplane Configuration with a Thin Straight Wing of Aspect Ratio 3. 14 Feb. 1950. NACA RM L9K25a.

106. Glauert, H.: The Force and Moment on an Oscillating Airfoil. Brit. Aer. Research Council Reps. and Mem. 1242, 1929.

107. Goland, M.: "The Flutter Steady Air Forces for Use in Low Frequency Stability Calculations." J. Aer. Sci. 17, 601-608, 1950.

108. Goland, M., Y. L. Luke, and M. A. Dengler: Theoretical Studies of the Effects of Aspect Ratio on Flutter. Wright Air Dev. Center, Tech. Rep. 54-29, 1954.

109. Goodman, T. R.: "Aerodynamics of a Supersonic Rectangular Wing Striking a Sharp Edged Gust." J. Aer. Sci. 18, 519-526, 1951.

110. Goodman, T. R.: The Quarter-Infinite Wing at Supersonic Speeds. Cornell Aer. Lab. Rep. 36, 1951.

111. Goodman, T. R.: "The Upwash Corrections for an Oscillating Wing in a Wind Tunnel." J. Aer. Sci. 20, 383-406, 1953.

112. Goodson, K. W., and R. E. Becht: Wind-Tunnel Investigation at High Subsonic Speeds of the Stability Characteristics of a Complete Model Having Sweptback, M, W, and Cranked-Wing Plan Forms and Several Horizontal-Tail Locations. May 1954. NACA RM L54C29.

113. Greenberg, J. M.: Airfoil in Sinusoidal Motion in a Pulsating Stream. NACA TN 1326, 1947.

114. Greenberg, J. M.: Some Considerations on an Airfoil in an Oscillating Stream. NACA TN 1372, 1947.

115. Greidanus, J. H.: Mathematical Methods of Flutter Analysis. Natl. Aer. Res. Inst. Amsterdam, NLL Rep. V 1384, 1947.

116. Greidanus, J. H., and A. van Heemert: Theory of the Oscillating Aerofoil in a Two-Dimensional Incompressible Flow. Parts I, II. Natl. Aer. Res. Inst. Amsterdam, NLL F 41, 1948.

117. Greidanus, J. H., A. E. van de Vorren, and H. Bergh: Experimental Determination of the Aerodynamic Coefficients of an Oscillating Wing in Incompressible, Two-Dimensional Flow. Part I: Wing with Fixed Axis of Rotation. Natl. Aer. Res. Inst. Amsterdam, NLL Rep. F 101, 1952.

118. Halfman, R. L.: Experimental Aerodynamic Derivatives of a Sinusoidally Oscillating Airfoil in Two-Dimensional Flow. NACA Rep. 1108, 1952.

119. Halfman, R. L., H. C. Johnson, Evaluation of High Angle of Attack Aerodynamic Derivative Data and Stall Flutter Prediction Techniques. NACA TN 2533, 1951.

120. Hanel, D.: Determination Theorique des Coefficients Aerodynamiques d'une Structure Quelconque en Mouvement Vibratoire Harmonique. Office Natl. Etudes et Recherches Aer. TN 6, 1951.

121. Harvard, Comp. Lab.: Tables of the Complete Cicala Function. Harvard Computation Lab. Problem Rep. 58, (Air Force Problem 77), 1952.

122. Haskind, M. D.: Oscillations of a Wing in a Subsonic Gas Flow. Prikl. Mat. i. Mekh. 11, 120-146, 1947. Also: Air Material Command, U.S. Air Force, Tran. A 9, T 22, 1948.

123. Heaslet, M. A., and H. Lomax: Two-Dimensional Unsteady Lift Problems in Supersonic Flight. NACA Rep. 945, 1949.

124. Heaslet, M. A., H. Lomax, and J. R. Spreiter: Linearized Compressible Flow Theory for Sonic Flight Speeds. NACA TN 1767, 1949. Also: NACA Rep. 956, 1950.

125. Heaslet, M. A., and J. R. Spreiter: Reciprocity Relations in Aerodynamic. NACA TN 2700, 1952.

126. Heitmeyer, J. C.: Lift, Drag, and Pitching Moment of Low-Aspect-Ratio Wings at Subsonic and Supersonic Speeds-Plane Triangular Wing of Aspect Ratio 4 with 3-Percent-Thick, Biconvex Section. 8 June 1951. NACA RM A51D30.

127. Heitmeyer, J. C.: Lift, Drag, and Pitching Moment of Low-Aspect-Ratio Wings at Subsonic and Supersonic Speeds-Plane Triangular Wing of Aspect Ratio 3 with NACA 0003-63 Section. Sept. 1951. NACA RM A51H02.

128. Heitmeyer, J. C.: Lift, Drag, and Pitching Moment of Low-Aspect-Ratio Wings at Subsonic and Supersonic Speeds-Plane 45° Swept-Back Wing of Aspect Ratio 3, Taper Ratio 0.4 with 3-Percent-Thick, Biconvex Section. Sept. 1951. NACA RM A51H10.

129. Helfer, A.: Electrical Pressure Integrator. NACA TN 2607, 1952.

130. Hoenl, H.: Two-Dimensional Wing Theory in the Supersonic Range. NACA TM 1238, 1949.

131. Hoenl, H.: On the Sound Field of a Point-Shaped Sound Source in Uniform Translatory Motion. NACA TM 1362, 1954.

132. Hofsommer, D. J.: Systematic Representation of Aerodynamic Coefficients of an Oscillating Aerofoil in Two-Dimensional Incompressible Flow. Natl. Aer. Res. Inst. Amsterdam, NLL Rep. F 61, 1950.

133. Houbolt, J. C.: A Recurrence Matrix Solution for the Dynamic Response of Aircraft in Gusts. NACA TR 1010, 1951.

134. Houbolt, J. C., and E. E. Kordes: Gust-Response Analysis of an Airplane Including Wing Bending Flexibility. NACA TN 2763, 1952.

135. Huckel, V.: Tabulation of the f_λ-Functions Which Occur in Unsteady Aerodynamic Theory for Supersonic Flow. NACA TN 3606, 1955.

136. Huckel, V., and B. Durling: Tables of Wing-Aileron Coefficients of Oscillating Air Forces for Two-Dimensional Supersonic Flow. NACA TN 2055, 1950.

137. Huston, W. B., and T. H. Skopinski: Measurement and Analysis of Wing and Tail Buffeting Loads on a Fighter Air-Plane. 1955. NACA Rep. 1219, Supersedes TN 3080.

138. Isaacs, R.: "Airfoil Theory for Flows of Variable Velocity." J. Aer. Sci. 12, 218-220, 1946.

139. Issaacs, R.: "Airfoil Theory for Flows of Variable Velocity." J. Aer. Sci. 13, 218-220, 1946.

140. Jaeckel, K.: "Forces on an Oscillating Airfoil in Accelerated Flow." Ing. Arch. 9, 371-395, 1938.
"Ueber die Bestimmung der Zirkulationsverteilung Fuer den Zwei-Dimensionalen Tragfluegel bew Beliebigen Periodischen Bewegungen. Luftfahrtforschung 16, 135-138, 1939.

141. Jager. de E. M.: The Aerodynamic Forces and Moments on an Oscillating Aerofoil with Control-Surface Between Two Parallel Walls. Natl. Aer. Res. Inst. Amsterdam, NLL Rep. F 140, 1953.

142. Jaquet, B. M.: Effects of Chord Discontinuities and Chordwise Fences on Low-Speed Static Longitudinal Stability of an Airplane. Model Having a 35° Sweptback Wing. June 1952. NACA RM L52C25.

143. Johnson, D. F., Preliminary Investigation of the Effects of Cascading on the Oscillating Lift Force of an Airfoil Vibrating in Bending. NACA RM E 53, F 29, 1953.

144. Jones, R. T.: The Unsteady Lift of a Wing of Finite Aspect Ratio NACA Rep. 681, 1940.

145. Jones, R. T.: The Unsteady Lift of a Finite Wing. NACA TN 682, 1939.

146. Jones, R. T.: Properties of Low Aspect Ratio Pointed Wings at Speeds Below and Above the Speed of Sound. NACA Rep. 853, 1946.

147. Jones, W. P.: Summary of Formula and Notations in Two-Dimensional Derivative Theory. Brit. ARC RM 1942, 1958.

148. Jones, W. P.: Wind Tunnel Interference Effect on the Values of Experimentally Determined Derivative Coefficients for Oscillating Airfoils. Brit. ARC RN 1912, 1943.

149. Jones, W. P.: Theoretical Air-Load and Derivative Coefficients for Rectangular Wings. Brit. ARC RM 2142, 1943.

150. Jones, W. P.: Aerodynamic Forces on Wings in Simple Harmonic Motion. Brit. ARC RM 2026, 1945.

151. Jones, W. P.: Aerodynamic Forces on Wings in Non-Uniform Motion Brit. ARC RM 2117, 1945.

152. Jones, W. P.: The Calculation of Aerodynamic Derivative Coefficients for Wings of any Planform in Non-Uniform Motion. Brit. ARC RM 2470, 1952.

153. Jones, W. P.: Airfoil Oscillations at High Mean Incidences. Brit. Aer. RC RM 2654, 1953.

154. Jones, W. P.: Supersonic Theory for Oscillating Wings of Any Plan Form. Brit. ARC RM 2655, 1953.

155. Jones, W. P.: The Influence of Thickness Chord Ratio and Supersonic Derivatives for Oscillating Aerofoils. Brit. ARC RM 2679, ARC 10,871, 1947; Pub. 1954.

156. Jones, W. P.: and S. W. Skan: Calculation of Derivatives for Rectangular Wings of Finite Span by Cicala's Method. Brit. ARC RM 1920, 1940.

157. Jones, W. P. Aerodynamic Forces on Biconvex Aerofoils Oscillating in a Supersonic Airstream. Brit. ARC RM 2749, 1953.

158. Jordan, P.: Unsteady Aerodynamic Coefficients for Supersonic Flow. Part I: Analytical. Brit. ARC RM 10,052, 1946. Part II: Numerical Tables. Ibid., 11,400, 1946.

159. Jordan, P.: Semi-Experimental Determination of Aerodynamic Derivatives for an Oscillating Wing-Aileron System. Roy Airc. Est., TN Structures 28, 1948.

160. Karman, V. Th., and W. R. Sears: "Airfoil Theory for Non-Uniform Motion." J. Aer. Sci., 5, 379-390, 1938.

161. Karp, S. N., S. S. Shu, and H. Weil: Aerodynamics of the Oscillating Airfoil in Compressible Flow. Monograph III. Part I: Air Material Command, Air Force Tech. Rep. F TR 116 ND, 1947.

162. Karp, S. N., and H. Weil: The Oscillating Airfoil in Compressible Flow. A Review of Graphical and Numerical Data. Air Material Command, Air Force Tech. Rep. F TR 1195 ND, 1948.

163. Katterbach, K.: Contributions to the Nonstationary Wing Theory. IX, Number Comparisons of Various Approximations Theories on the Oscillating Wing of Large Aspect Ratio ZWB FB 1789, 1943. Also: Translation, Air Material Command,, U. S. Air Force F TS 943 RE, 1947.

164. Kochin, N. E.: "Steady Vibrations of Wing of Circular Plan Form and Theory of Wing of Circular Plan Form." Prikl. Mat. Mekh. 4, 3-32, 1940; 6, 287-316, 1942. Also: NACA TM 1324, 1953.

165. Koenig, D. G.: Tests in the Ames 40- by 80-Foot Wind Tunnel of the Effects of Various Wing Modifications on the Longitudinal Characteristics of Two Triangular-Wing Airplane Models with and Without Horizontal Tails. Apr. 1954. NACA RM A54B09.

166. Krasilshchikova, E. A.: Supersonic Flows Over Slender Bodies. Scientific Record of Moscow State Univ. V. 154, Mechanics, 181-239, 1951. Also: NACA TM 1383, 1956.

167. Kuessner, H. G.: "Augenblicklicher Entwicklungsstand der Frage des Fluegelflatterns." Luftfartforschung, 6, 193-209, 1935. Also: NACA TM 782, 1936.

168. Kuessner, H. G.: "Zusammenfassender Bericht ueber den instatisnaeren Auftrieb von Tragfluegeln." Luftfahrtforschung 13, 410-424, 1936.

169. Kuessner, H. G.: "Allgemeine Tragflaechen theorie." Luftfahrtforschung, 17, 370-378, 1940. Also: NACA TM 979, 1941.

170. Kuessner, H. G.: "Das Zweidimensionale Problem der beliebig bewegten Tragflaeche unter Beruecksichtigung von Partialbewegungen der Flussigkeit." Luftfahrtforschung 17, 335-361, 1940. Also: Brit. RTP Tran. 1541, 1943.

171. Kuessner, H. G.: Unsteady Processes. AVA Monographs, Sec. G. (A. Betz, Editor), Great Brit. Minister of Aircraft Prod., Rep. and Tran., MAP (Volkenrode), 1009-1014, 1945-1946.

172. Kuessner, H. G.: A Review of the Two-Dimensional Problem of Unsteady Lifting Surface Theory During the Last Thirty Years. Univ. Maryland Lecture Series, 23, Apr. 1953.

173. Kuessner, H. G.: The Oscillating Lifting Surface in the Range of Subsonic Flow. Mitteil. Max-Planck-Inst. Stroemungsforsch, Goettingen, 53/F/2, 1953.

174. Kuessner, H. G.: "A General Method for Solving Problems of the Unsteady Lifting Surface Theory in the Subsonic Range." J. Aer. Sci. 21, 17-27, 1954.

175. Kuessner, H. G.: "Aeroelastische Probleme des Flugzeugbaus." Z. Flugwiss. 3, 1-18, 1955.

176. Kuessner, H. G.: "The Difference Property of the Kernel of the Unsteady Lifting Surface Theory." J. Aer. Sci. 22, 227-230, 1955.

177. Kuessner, H. G., and H. Billing: Unsteady Flow. Hydro-and Aero-Dynamics. Chap. XI, (A. Betz, Editor), Central Air Document Office, ATI, 72854, 1950.

178. Kuessner, H. G., and L. Schwarz: "Der schwingende Fluegel mit aerodynamisch ausgeglichenen Ruder." Luftfahrtforschung, 17, 377-354, 1940. NACA TM 991, 1941.

179. Laidlaw, W. R.: Theoretical and Experimental Pressure Distributions on Low Aspect Ratio Wings Oscillating in an Incompressible Flow. MIT, Aeroelastic and Structures Res. Lab., Tech. Rep. 51-2, 1954.

180. Laidlaw, W. R., and R. L. Halfman: Experimental Pressure Distributions on Oscillating Low Aspect Ratio Wings. Inst. Aer. Sci. Preprint 499, 1955.

181. Lance, G. N.: "The Kernel Function of the Integral Equation Relating the Lift and Downwash Distributions of Oscillating Finite Wings in Subsonic Flow." J. Aer. Sci. 21, 635-636, 1954.

182. Landahl, M. T.: The Flow Around Oscillating Low Aspect Ratio Wings at Transonic Speeds. Roy. Inst. Tech. Stockholm, KTH Aer. Tech. Note 40, 1954.

183. Landahl, M. T.: Unsteady Flow Around Thin Wings at High Mach Numbers. Office Sci. Res. Tech. Note 55-245, MIT Group Rep. 55-3, 1955.

184. Landahl, M. T., and V. J. E. Stark: An Electrical Analogy for Solving the Oscillating-Surface Problem for Incompressible Nonviscid Flow. Roy. Inst. Tech., Stockholm, KTH Aer. TN 34, 1953.

185. Lapin, E., R. Crookshanks, and H. F. Hunter: "Downwash Behind a Two-Dimensional Wing Oscillating in Plunging Motion." J. Aer. Sci., 19, 447-450, 1952.

186. Lauten, W. J. Jr., and B. R. O'Kelly: Results of Two Experiments on Flutter of High-Aspect-Ratio Swept Wings in the Transonic Speed Range. July 1952. NACA RM L52D24b.

187. Lawrence, H. R., and E. H. Gerber: "The Aerodynamic Forces on Low Aspect Ratio Wings Oscillating in an Incompressible Flow." J. Aer. Sci. 19, 769-781, 1952.

188. Lessing, H. C., T. B. Fryer, and M. H. Mead: A System for Measuring the Dynamic Lateral Stability Derivatives in High Speed Wind Tunnels. NACA TN 3348, 1954.

189. Li, Ta: Aerodynamic Influence Coefficients for an Oscillating Finite Thin Wing in Supersonic Flow. Inst. Aer. Sci., Preprint 500, 1955.

190. Li, T. Y., and H. J. Stewart: "On an Integral Equation in the Supersonic Oscillating Wing Theory." J. Aer. Sci. 20, 724-726, 1953.

191. Liban, E., J. Neuringer, and S. Rabinowitz: Flutter Analysis of an Elastic Wing with Supersonic Edges. Republic Aviation Corp. Rep. E-SAF-1, 1953.

192. Lighthill, M. J.: "Oscillating Airfoils at High Mach Number." J. Aer. Sci. 20, 402-406, 1953.

193. Lilienthal, Gesellschaft: Conference. Lilienthal Gesellschaft fuer Luftfahrtforschung. Bericht No. 135, Mar. 6-8, 1941.

194. Lin, C. C., E. Reissner, and H. S. Tsien: "On Two-Dimensional Nonsteady Motion of a Slender Body in a Compressible Fluid." J. Math. and Phys. 27, 220-231, 1948.

195. Lomax, H.: Lift Developed on Unrestrained Rectangular Wings Entering Gusts at Subsonic and Supersonic Speeds. NACA Rep. 1162, 1954.

196. Lomax, H., F. B. Fuller, and L. Sluder: Generalized Indicial Forces on Deforming Rectangular Wings in Supersonic Flight. NACA TN 3286, 1954.

197. Lomax, H., M. A. Heaslet, and F. B. Fuller: Two-and Three-Dimensional Unsteady Lift Problems in High-Speed Flight. NACA Rep. 1077, 1952.

198. Lomax, H., M. A. Heaslet, and L. Sluder: The Indicial Lift and Moment for a Sinking or Pitching Two-Dimensional Wing Flying at Subsonic or Supersonic Speeds. NACA TN 2403, 1951.

199. Lorell, J.: The Aerodynamic Forces on an Oscillating Airfoil in Supersonic Flow: A Comparison Between Two-and Three Dimensional Theories: CALTECH, Jet Prop. Labor, Rep. 20-64, 1952.

200. Luke, Y. L.: Tables of Coefficients for Compressible Flutter Calculations. Air Material Command, Air Force Tech. Rep. 6200, 1950.

201. Lyon, H. M.: Aerodynamical Derivatives of Flexural-Torsional Flutter of a Wing of Finite Span. Brit. ARC RM 1900, 1939.

202. Marini, M.: "Aerodynamic Effects on Swept Wings in Oscillatory Motion." Aerotecnica, 4, 275-287, 1953.

203. Martin, J. C., and N. Gerber: "The Effect of Thickness on Airfoils with Constant Vertical Acceleration at Supersonic Speeds." J. Aer. Sci. 22, 179-188, 1955.

204. Mason, H. P.: Low-Lift Buffet Characteristics Obtained from Flight Tests of Unswept Thin Intersecting Surfaces and of Thick 35° Sweptback Surfaces. January 1953, NACA RM L52H12.

205. Mayer, J. P., and G. M. Valentine: Flight Measurements with the Douglas D-558-II (Buaero No. 37974) Research Airplane. Measurements of the Buffet Boundary and Peak Airplane Normal-Force Coefficients at Mach Numbers up to 0.90. 28 August 1950, NACA RM L50E31.

206. Mazelsky, B.: Numerical Determination of Indicial Lift. NACA TN 2562, 1951; and TN 2613, 1952.

207. Mazelsky, B.: "On the Noncirculatory Flow About a Two-Dimensional Airfoil at Subsonic Speeds." J. Aer. Sci., 19, 848-849, 1952.

208. Mazelsky, B., and J. A. Drischler: Numerical Determination of Indicial Lift and Moment Functions for a Two-Dimensional Sinking and Pitching Airfoil. NACA TN 2739, 1952.

209. Mazet, R., and J. Doerr: Determination par le calcul et par essais en sufflerie des vitesses critiques de vibrations d'une maguette rigid de profil constant, montee sur ressorts. Office Natl. Etudes et Recherches Aer. 39, 1950.

210. Meller, M. G.: Etude Preliminaire Sur le Flutter des Aubes de Compresseur. Office Natl. Etudes et Recherches Aer. TN 18, 1953.

211. Mendelson, A.: "Aerodynamic Hysteresis as a Factor in Critical Flutter Speed of Compressor Blades at Stalling Conditions." J. Aer. Sci. 16, 645-652, 1949.

212. Merbt, H., and M. Landahl: Aerodynamic Forces on Oscillating Low Aspect Ratio Wings in Compressible Flow. Roy. Inst. Tech., Stockholm, KTH Aer. TN 30, 1953.

213. Merbt, H., and M. Landahl: The Oscillating Wing of Low Aspect Ratio--Results and Tables of Auxiliary Functions. Roy. Inst. Tech., Stockholm, KTH Aer. TN 31, 1954.

214. Mickleboro, H. C., and J. Funk: A Flight Study of Compressibility Effects on the Gust Loads of a 35° Sweptback-Wing Airplane. Aug. 1954. NACA RM L54G09a.

215. Migotsky, E.: Some Considerations on Two-Dimensional Thin Airfoils Deforming in Supersonic Flow. NACA TN 3386, 1955.

216. Miles, J. W.: "Harmonic and Transient Motion of a Swept Wing in Supersonic Flow." J. Aer. Sci. 15, 343-346, 1948.

217. Miles, J. W.: "Transient Loading of Airfoils at Supersonic Speeds." J. Aer. Sci., 15, 592-598, 1948.

218. Miles, J. W.: "The Oscillating Rectangular Airfoil at Supersonic Speeds." J. Aer. Sci., 16, 381, 1949. Also: U. S. Nav. Ord. Rep. 1170, NOTS 226, 1949. Also: Quart. Appl. Math. 9, 47-65, 1951.

219. Miles, J. W.: "On the Compressibility Correction for Subsonic Unsteady Flow." J. Aer. Sci., 7, 181-182, 1950.

220. Miles, J. W.: "On Nonsteady Motion of Slender Bodies." Aer. Quart. 2, 183-194, 1950.

221. Miles, J. W.: The Application of Unsteady Flow Theory to the Calculation of Dynamic Stability Derivatives. North Amer. Aviation Rep. AL-957, 1950.

222. Miles, J. W.: On Harmonic Motion of Wide Delta Airfoils at Supersonic Speeds. U. S. Nav. Ord. Test Station, RR B-36, 1950.

223. Miles, J. W.: Linearized Theory of Nonstationary Flow at Supersonic Speeds. U. S. Nav. Ord. Test Station, Rep. 1930, 1951.

224. Miles, J. W.: "Quasi-Stationary Airfoil Theory in Subsonic Compressible Flow." Quart. Appl. Math. 8, 351-358, 1951.

225. Miles, J. W.: Transient Loading of Thin Wings. U. S. Nav. Ord. Test Station, Rep. 2077, 1953.

226. Miles, J. W.: "A Note on Subsonic Edges in Unsteady Supersonic Flow." Quart. Appl. Math. 3, 363-367, 1953.

227. Miles, J. W.: "A General Solution for the Rectangular Airfoil in Supersonic Flow." Quart. Appl. Math., 1, 1-8, 1953.

228. Miles, J. W.: "On the Low Aspect Ratio Oscillating Rectangular Wing in Supersonic Flow." Aer. Quart. 4, 231-244, 1953.

229. Miles, J. W.: "On the Nonlinear Thickness Effect for a Supersonic Oscillating Airfoil." J. Aer. Sci. 21, 714-715, 1954.

230. Miles, J. W.: "Linearization of the Equations of Nonsteady Flow in a Compressible Fluid. J. Math. and Phys." 33, 135-143, 1954.

231. Miles, J. W.: "On Solving Subsonic Unsteady Flow Lifting Surface Problems by Separating Variables." J. Aer. Sci. 6, 427-728, 1954.

232. Miles, J. W.: Unsteady Supersonic Flow. Air Research and Devel. Command, Contract AF 18 (600) 432, 1955.

233. Miles, J. W., I. Naiman, G. M. Schroedter: Aerodynamic Derivatives for an Oscillating Rectangular Airfoil at Supersonic Speeds. Nav. Ord. Test Station NAVORD, Rep. 1292, 1951.

234. Minhinnicki, I. T.: Tables of Functions for a Valuation of Wing and Control Surface Flutter Derivatives for Incompressible Flow. Brit. ARC 13730, Rep. Structures 86, 1950.

235. Minhinnicki, I. T.: Subsonic Aerodynamic Flutter Derivatives for Wings and Control Surfaces. Brit. ARC 14228, 1950.

236. Mollo-Christensen, E. L.: An Exploratory Investigation of Unsteady Transonic Flow. I. Theoretic Discussion. Mass. Inst. Tech. TACP Rep. 5 June 1954.

237. Molyneus, W. G.: Techniques for the Measurement of the Aerodynamic Forces on Oscillating Aerofoils. Roy. Airc. Inst. Est. TN Structures 161, 1955.

238. Morris, R. M.: "The Two-Dimensional Hydrodynamical Theory of Moving Aerofoils." Proc. Roy. Soc. London, A 188, 439-463, 1947.

239. Morrison, W. D. Jr.: Transonic Aerodynamic Characteristics in Pitch of a W-Wing Having 60° 48' Panel Sweep, Aspect Ratio 3.5, and Taper Ratio 0.25. Aug. 1953. NACA RM L53F22.

240. Moskowitz, B., and W. E. Moeckel: First Order Theory for Unsteady Motion of Thin Wing at Supersonic Speeds. NACA TN 2043, 1950.

241. Nav. Ord. Test Station.: Handbook of Supersonic Aerodynamics. Aeroelastic Phenomenon. Nav. Ord. Test Station, Rep. Vol. 4, Secting 12, 1952.

242. Nekrasov, A. I.: "Wing Theory for Nonstationary Flow." Doklady Akad. Nauk. SSSR (NS) 95, 6, 1010-1016, 1947.

243. Nelson, H. C.: Lift and Moment on Oscillating Triangular and Related Wings with Supersonic Edges. NACA TN 2494, 1951.

244. Nelson, H. C., and J. H. Berman: Calculations on the Forces and Moments for an Oscillating Wing-Aileron Combination in Two-Dimensional Potential Flow at Sonic Speed. NACA Rep. 1128, 1953.

245. Nelson, H. C., and H. J. Cunningham: Theoretical Investigation of Flutter of Two-Dimensional Flat Panels with One Surface Exposed to Supersonic Potential Flow. NACA TN 3465, 1955.

246. Nelson, H. C., R. A. Rainey, and C. E. Watkins: Lift and Moment Coefficients Expanded to the Seventh Power of Frequency for Oscillating Rectangular Wings in Supersonic Flow and Applied to a Specific Flutter Problem. NACA TN 3076, 1954.

247. Neumark, S.: "Pressure Distribution on an Airfoil in Nonuniform Motion." J. Aer. Sci. 19, 214-215, 1952.

248. Patterson, J. L.: A Miniature Electrical Pressure Gage Utilizing a Stretched Flat Diaphragm. NACA TN 2659, 1952.

249. Phillips, W. H.: Loads Implication of Gust-Alleviation Systems. June 1957. NACA TN 4056.

250. Pines, S., and J. Dugundji: Application of Aerodynamic Flutter Derivatives to Flexible Wings with Supersonic and Subsonic Edges. Republic Aviation Corp. Rep. E-SAF-2, 1954.

251. Possio, C.: "Aerodynamic Forces on an Oscillating Profile at Supersonic Speeds." Pontif. Acad. Sci. Acta I, 11, 93-106, 1937.

252. Possio, G.: "Aerodynamic Action on a Wing in Oscillating Motion." Atti acad. nazl. Linzei, Rome, Rendiconti, (V, I), 28, 194-200, 1938.

253. Possio, C.: "Nonstationary Motion of a Compressible Fluid." Proc. acad. nazl. Lincei, Rome, 29, Series 62, 9, 1939.

254. Possio, C.: "Aerodynamic Forces on an Oscillating Profile in a Compressible Fluid at Subsonic Speeds." Aerotecnica 18, 441-458, 1938. Also: Brit. Air Ministry, Tran. 830, 1941.

255. Postel, E. E., and E. L. Leppert: "Theoretical Pressure Distributions for a Thin Airfoil Oscillating in Incompressible Flow." J. Aer. Sci. 15, 486-492, 1948.

256. Prandtl, L.: "Theorie des Flugzeugtragfluegelsin Zusammendrueckbaren Medium." Luftfahrtforschung, 13, 313-319, 1936.

257. Pratt, G. L.: Experimental Flutter Investigation of a Thin Unswept Wing at Transonic Speeds. Apr. 1955. NACA RM L55A18.

258. Purser, P. E., and J. A. Wyse: Review of Some Recent Data on Buffet Boundaries. May 23, 1951. NACA RM L51E02a.

259. Queijo, M. J., H. S. Fletcher, C. G. Marple, and F. M. Hughes: Preliminary Measurements of the Aerodynamic Yawing Derivatives of a Triangular, a Swept, and an Unswept Wing Performing Pure Yawing Oscillations, with a Description of the Instrument Employed. Apr. 1956. NACA RM L55L14.

260. Radok, J. R. M.: Gust Loads on Two-Dimensional Aerofoils in Supersonic Flow. Australian Aer. Res. Lab. Rep. A66 and SM142, 1949.

261. Radok, J. R. M.: An Approximate Theory of the Oscillating Wing in a Compressible Subsonic Flow for Low Frequencies. Natl. Aer. Res. Inst., Amsterdam, NLL Rep. F97, 1951.

262. Radok, J. R. M.: "The Theory of Aerofoils in Unsteady Motion." Aer. Quart. 4, 297-320, 1952.

263. Rainey, A. G.: Preliminary Study of Some Factors Which Affect the Stall-Flutter Characteristics of Thin Wings. Mar. 1956. NACA TN 3622. Supersedes RM L52D08.

264. Rathert, G. A., Jr., H. L. Ziff, and G. E. Cooper: Preliminary Flight Investigation of the Maneuvering Accelerations and Buffet Boundary of a 35° Swept-Wing Airplane at High Altitude and Transonic Speeds. 21 Feb. 1951. NACA RM A50L04.

265. Reissner, E.: On the General Theory of Thin Airfoils for Nonuniform Motion. NACA TN 946, 1944.

266. Reissner, E.: Effect of Finite Span on Airload Distributions for Oscillating Wings. I. NACA TN 1194, 1947.

267. Reissner, E.: Wind Tunnel Correction for the Two-Dimensional Theory of Oscillating Airfoils. Cornell Aer. Lab. Rep. SB-318-S-3, 1947.

268. Reissner, E.: "Boundary Value Problems in Aerodynamics of Lifting Surfaces in Nonuniform Motion." Bull. Am. Math. Soc. 55, 825-850, 1949.

269. Reissner, E.: On the Theory of Oscillating Airfoils of Finite Span in Subsonic Compressible Flow. NACA Rep. 1002, 1950.

270. Reissner, E.: A Problem of the Theory of Oscillating Airfoils. Proc. First U. S. Natl. Congress Appl. Mech. 923-925, 1951.

271. Reissner, E.: Investigation of Oscillating Lifting Surfaces of Finite Span in Incompressible Flow. Tech. Rep. for Air Res. and Dev. Command, No. 383, Oct. 1951.

272. Reissner, E.: Extension of the Theory of Finite Span in Subsonic Compressible Flow. NACA TN 2274, 1951.

273. Reissner, E.: On the Application of Mathieu Functions in the Theory of Subsonic Compressible Flow Past Oscillating Airfoils. NACA TN 2363, 1951.

274. Reissner, E., and S. Sherman: Compressibility Effects in Flutter. Curtiss-Wright Research Lab. Rep. SB-240-S-1, 1944.

275. Reissner, E., and J. E. Stevens: Effect of Finite Span on Airload Distributions for Oscillating Wings. II. NACA TN 1195, 1947.

276. Ritter, A.: Determination of the Unsteady Lift Coefficients in Wind Tunnel Tests by Means of Light Interference Methods. Air Material Command, U. S. Air Force, F-TR-1158-ND, 1948.

277. Robinson, A.: On Some Problems of Unsteady Supersonic Aerofoil Theory. College of Aeronautics, Cranfield, Rep. 16, 1948.

278. Rott, N.: "Oscillating Airfoils at Mach Number 1." J. Aer. Sci. 16, 380, 1949.

279. Rott, N.: "Fluegelschwingengsformen in ebener kompressibler Potentialstroemung." ZAMP, 1, 380-410, 1950.

280. Rott, N.: "On the Unsteady Motion of a Thin Rectangular Wing in Supersonic Flow." J. Aer. Sci. 18, 775-776, 1951.

281. Rott, N., and M. B. T. George: An Approach to the Flutter Problem in Real Fluids. Inst. Aer. Sci. Preprint 509, 1955.

282. Roumieu, C.: "Etude des regimes transitoires en aerodynamique supersonique a deux dimensions, apercu theorique sur le domaine transsonique." Recherche Aer. 9, 1949.

283. Runyan, H. L.: Single-Degree-of Freedom Flutter Calculations for a Wing in Subsonic Potential Flow and a Comparison with an Experiment. NACA Rep. 1089, 1952.

284. Runyan, H. L., H. J. Cunningham, and C. E. Watkins: "Theoretical Investigation of Several Types of Single-Degree-of-Freedom Flutter." J. Aer. Sci. 19, 101-110, 1952.

285. Runyan, H. L., and C. E. Watkins: Consideration on the Effect of Wind Tunnel Walls on Oscillating Air Forces for Two-Dimensional Subsonic Compressible Flow. NACA TN 2552, 1951.

286. Runyan, H. L., and D. S. Woolston: Method for Calculating the Aerodynamic Loading on an Oscillating Finite Wing in Subsonic and Sonic Flow. Aug. 1956. NACA TN 3694.

287. Runyan, H. L., D. S. Woolston, and A. G. Rainey: A Theoretical and Experimental Investigation of the Effect of Tunnel Walls on the Forces on an Oscillating Airfoil in Two-Dimensional Subsonic Compressible Flow. NACA TN 3416, 1955.

288. Sauer, R.: "Elementare Theorie des langsam schwingenden Ueberschallfluegels." ZAMP, 1, 248-253, 1950.

289. Scanlan, R. M.: "Correction for Aspect Ratio of the Indicial Lift Functions of Wagner and Kuessner." J. Aer. Sci. 19, 357-358, 1952.

290. Scanlan, R. H., and R. Rosenbaum: Introduction to Study of Aircraft Vibration and Flutter. Macmillan Pub. Comp. 1951.

291. Schade, T.: Beitrag zu Zahlentafeln zur Luftkraftberechnung der Schwingenden Tragflaeche in Ebener Unterschall stroemung. ZWB UM 3211, 1944.

292. Schade, T., "The Oscillating Circular Airfoil on the Basis of Potential Theory." Luftfahrtforschung 17, 387-400, 1940; 19, 282-291, 1943. Also: NACA TM 1098, 1947.

293. Scherer, M.: "Mesure en Soufflerie de la Resultante Aerodynamique sur un Profil de Courant Plan a Incidence Variable in Regime Harmonique. CR Acad Sci. Paris, 230, 2071-2073, 1950.

294. Schmeidler, W.: "Thrust and Drag." Zamm, 19, 65-86, 1939.

295. Schnittger, J. R.: "Single Degree of Freedom Flutter of Compressor Blades in Separated Flow." J. Aer. Sci. 21, 27-36, 1954.

296. Schwarz, L.: "Benechnung der Druckverteilung Einer Harmonisch Sich Verformenden Tragflaeche in Ebener Stroemung." Luftfahrtforschung 17, 379-386, 1940. Also: Brit. RTP Tran. 1543, 1943.

297. Schwarz, L.: Numerical Tables for Air Forces Calculated for Oscillating Wings in Two-Dimensional Compressible Flow at Subsonic Velocity. ZWB FB 1838, 1943. Tran. Air Material Command, U.S. Air Force, F TS 599 RE, 1946.

298. Schwarz, L.: "Untersuchung Einigre mit den Zylinderfunktionen Nullter Ordnung Verwandter Funktionen." Fuftfahrtforschung. 20, 341-372, 1944.

299. Schwarz, L.: A Semi-Experimental Method for Determining Unsteady Pressure Distributions. Brit. ARC RM 10387, 1947.

300. Sears, W. R.: A Contribution to the Airfoil Theory for Nonuniform Motion. Proc. Fifth Inter. Con. Appl. Mech., 483-487, 1938.

301. Sears, W. R.: "Operational Methods in the Theory of Airfoils in Non-uniform Motion." J. Franklin Inst. 130, 95-111, 1940.

302. Sears, W. R.: "Some Aspects of Non-Stationary Airfoil Theory and Its Practical Application." J. Aer. Sci. 8, 104-108, 1941.

303. Sears, W. R., and A. M. Kuethe: "The Growth of the Circulation of an Airfoil Flying Through a Gust." J. Aer. Sci. 6, 376-378, 1939.

304. Sears, W. R., and B. O. Sparks: "On the Reaction of an Elastic Wing to Vertical Gusts." J. Aer. Sci. 8, 64-67, 1941.

305. Sedov, L. I.: On the Theory of Unsteady Planning and the Motion of a Wing with Vortex Separation. NACA TM 942, 1940.

306. Sedov, L. I.: On the Theory of the Unsteady Motion of an Airfoil. NACA TM 1156, 1947.

307. Sewell, G. L.: "Theory of an Oscillating Supersonic Aerofoil." Aer. Quart. 2, 34-38, 1950.

308. Sewell, G. L.: "A Theory of Uniform Supersonic Flow Past a Thin Oscillating Aerofoil at Appreciable Incidence to the Main Stream." Aer. Quart. 5, 185-194, 1954.

309. Shen, S. F.: Flutter of a Two-Dimensional Simply Supported Uniform Panel in a Supersonic Stream. Office of Naval Res., MIT Aer. Eng. Dept., Contract N5 ori-07833, 1952.

310. Shen, S. F.: Effect of Structural Flexibility on Aircraft Loading. Part X. A New Lifting Line Theory for the Unsteady Lift of a Swept or Unswept Wing in an Incompressible Fluid. Wright Air Dev. Center, Tech. Rep. 6358, 1953.

311. Silverstein, A., and U. T. Joyner: Experimental Verification of the Theory of Oscillating Airfoils. NACA Rep. 673, 1939.

312. Sisto, F.: "Stall Flutter in Cascades." J. Aer. Sci. 20, 598-605, 1953.

313. Sisto, F.: "Unsteady Aerodynamic Reactions on Airfoils in Cascade." J. Aer. Sci. 22, 297-302, 1955.

314. Smilg, B.: The Prevention of Aileron Oscillating at Transonic Air Speeds. Air Material Command, U.S. Air Force Tech. Rep. 5530, 1946.

315. Smilg, B., and L. S. Wassermon: Application of Three-Dimensional Flutter Theory to Aircraft Structures. Air Material Command, U.S. Air Force TR 4798, 1942.

316. Soehngen, H.: "Bestimmung der Auftriebsverteilung Fuer Beliebige Instationaere Bewegungen (Ebenes Problem)." Luftfahrtforschung 17, 401-419, 1940. Also: Brit. RTP Tran. 1446, 1943.

317. Spence, D. A.: The Characteristic Frequency of Small Oscillatings in the Flow Past Bluff Bodies. Royal Aircraft Establishment. Rep. Aer. 2532, 1955.

318. Spiegel, van E., and A. I. van de Vooren: On the Theory of the Oscillating Wing in Two-Dimensional Subsonic Flow. Natl. Aer. Res. Inst. Amsterdam, NLL Rep. F 142, 1953.

319. Spielberg, I. N.: "The Two-Dimensional Incompressible Aerodynamic Coefficients for Oscillatory Changes in Airfoil Camber." J. Aer. Sci. 20, 432-434, 1953.

320. Spielberg, I. N., H. E. Fettis, and H. S Toney: Methods for Calculating the Flutter and Vibration Characteristics of Swept Wings. Air Material Command, U.S. Air Force MR MC RE XA5, 4595, 8-4, 1948.

321. Statler, I. C.: "Dynamic Stability at High Speeds from Unsteady Flow Theory." J. Aer. Sci. 17, 232-242, 1950.

322. Statler, I. C., and M. Easterbrook: Handbook for Computing Non-Stationary Flow Effects on Subsonic Dynamic Longitudinal Response Characteristics of an Airplane. Cornell Aer. Lab. Rep. TB 495, F 12, 1950.

323. Stewartson, K.: "On the Linearized Potential Theory of Unsteady Supersonic Motion." Quart. J. Mech. and Appl. Math. 3, 182-199, 1950.

324. Stewartson, K.: "On the Linearized Potential Theory of Unsteady Supersonic Motion. II." Quart. J. Mech. and Appl. Math. 5, 137-154, 1952.

325. Strang, W. J.: "A Physical Theory of Supersonic Aerofoils in Unsteady Flow." Proc. Roy. Soc. London, A195, 245-264, 1948.

326. Strang, W. J.: Gust Loading of Rectangular Supersonic Wings. Council for Sci. and Ind. Research, Div. of Aer., A57, 1949.

327. Strang, W. J.: Transient Source Doublet and Vortex Solutions of Linearized Equations of Supersonic Flow. Dept. of Supply and Dev., Div. of Aer. A60, 1949.

328. Strang, W. J.: "Transient Lift of Three-Dimensional Purely Supersonic Wings." Proc. Roy. Soc. London, A202, 54-80, 1950.

329. Studer, H. L.: Experimentalle Untersuchungen ueber Fluegelschwingen. Inst. Aer. Tech. HS Aachen, Mitt. 4, 1936.

330. Sutton, F. B., and J. K. Dickson: A Comparison of the Longitudinal Aerodynamic Characteristics at Mach Numbers Up to 0.94 of Sweptback Wings Having NACA 4-Digit or NACA 64A Thickness Distributions. Aug. 1954. NACA RM A54F18.

331. Teitelbaum, J. M.: Flight Investigation of Flutter Models with 1/10-Scale Douglas D-558-2 Wing Panels. 16 Feb. 1949. NACA RM L9A06.

332. Temple, G.: Unsteady Compressible Flow in Two-Dimensions. Brit. ARC FM 1089, 1947.

333. Temple, G., and H. A. John: Flutter at Supersonic Speeds. Brit. Aer. R. C., RM 2140, 1945.

334. Templeton, H.: Mass Balancing of Aircraft Control Surfaces. Chapman and Hall, 1954.

335. Theodorsen, T.: General Theory of Aerodynamic Instability and the Mechanism of Flutter. NACA Rep. 496, 1935.

336. Theodorsen, T., and I. E. Garrick: Non-Stationary Flow About a Wing-Aileron Tab Combination Including Aerodynamic Balance. NACA Rep. 736, 1942.

337. Theodorsen, T., and A. A. Regier: Effect of the Lift Coefficient on Propeller Flutter. NACA Wartime Rep. ACR L5F30, 1945.

338. Thompson, F. L.: Flight Research at Transonic and Supersonic Speeds with Free-Falling and Rocket-Propelled Models. Second Inter. Aer. Conference, Inst. Aer. Sci., New York, 1949, Paper No. 38.

339. Timman, R.: Beschouwingen over de luchkrachten op trillende vliegtuigvlengels. Dissertation, Tech. Hogeschoot, Delft, 1946.

340. Timman, R.: "The Aerodynamic Forces on an Oscillating Aerofoil Between Two Parallel Walls." Appl. Sci. Res. A3, 1, 31-57, 1951.

341. Timman, R.: Approximate Theory of the Oscillating Wing in Compressible Subsonic Flow for High Frequencies. Natl. Aer. Res. Inst., Amsterdam, NLL Rep. F99, 1951.

342. Timman, R.: "Linearized Theory of the Oscillating Airfoil in Compressible Subsonic Flow." J. Aer. Sci. 21, 230-236, 1954.

343. Timman, R.: Report on Methods and Results of Nonstationary Airfoil Theory. AGARD, Rep. AG5/P6, 50-55, 1954.

344. Timman, R., and A. I. Van de Vooren: Theory of the Oscillating Wing with Aerodynamically Balanced Control Surface in a Two-Dimensional Subsonic Compressible Flow. Natl. Aer. Res. Inst., Amsterdam, NLL Rep. F54, 1949.

345. Timman, R., A. I. Van de Vooren, and J. H. Greidanus: "Aerodynamic Coefficients of an Oscillating Airfoil in Two-Dimensional Subsonic Flow." J. Aer. Sci. 18, 717-802, 1951. Also: J. Aer. Sci. 21, 499, 1954.

346. Timman, R., A. I. van de Vooren, and J. H. Greidanus: Tables of Aerodynamic Coefficients for an Oscillating Wing-Flap System in a Subsonic Compressible Flow. Natl. Aer. Res. Inst. Amsterdam, NLL Rep. F 151, 1954.

347. Tobak, M.: On the Use of the Indicial Function Concept in the Analysis of Unsteady Motions of Wings and Wing-Tail Combinations. NACA Rep. 1188, 1954.

348. Tood (Taussky), O.: On Some Boundary Value Problems in the Theory of the Non-Uniform Supersonic Motion of an Aerofoil. Brit. ARC RM 2141, 1945.

349. Turner, M. J.: "Aerodynamic Theory of Oscillating Sweptback Wings." ZAMP 28, 280-293, 1950.

350. Turner, M. J., and S. Rabinowitz: Aerodynamic Coefficients for an Oscillating Airfoil with Hinged Flap, with Tables for a Mach Number of 0.7. NACA TN 2213, 1950.

351. Valensi, J.: A Review of Techniques of Measuring Oscillatory Aerodynamic Forces and Moments on Models Oscillating in Wind Tunnels in Use on the Continent. AGARD, Paper AG 15/P6, 14-49, 1954.

352. Van de Vooren, A. I.: "Generalization of the Theodorsen Function to Stable Oscillations." J. Aer. Sci. 19, 209-213, 1952.

353. Van de Vooren, A. I.: Measurement of Aerodynamic Forces on Oscillating Aerofoils. Natl. Aer. Res. Inst. Amsterdam, NLL Rep. MP 100, 1954. Also: Agard Rep. AG 15/P6, 7-13, 1954.

354. Van de Vooren, A. I., and H. Bergh: Spontaneous Oscillations of an Aerofoil Due to Instability of the Laminar Boundary Layer. Natl. Aer. Res. Inst. Amsterdam, NLL Rep. F.96, 1951.

355. Van de Vooren, A. I., and H. Bergh: Experimental Determination of the Aerodynamic Coefficients of an Oscillating Wing in Incompressible, Two-Dimensional Flow. Part II: Wing with Oscillating Axis of Rotation. Natl. Aer. Res. Inst. Amsterdam, NLL Rep. F 102, 1952.

356. Van de Vooren, A. I., and D. J. Hofsommer: Binary Aileron-Tab Flutter. Natl. Aer. Res. Inst., Amsterdam, NLL Rep. F52, 1949.

357. Van de Vooren, A. I., and J. Yff: Aerodynamic Coefficients of an Oscillating Aerofoil with a Pressure-Seal Balanced Aileron. Natl. Aer. Res. Inst., Amsterdam, NLL, Rep. F115, 1952.

358. Van Dyke, M. D.: Supersonic Flow Past Oscillating Airfoils Including Nonlinear Thickness Effects. NACA TN 2982, 1953.

259. Veubeke, de, B. F.: Aerodynamique instationnaire des profils mince deformables. Bulletin du Service Tech. Aer. Brussels, Office Natl. Etudes et Recherches Aer. 25, 1953.

360. Victory, M.: Flutter at High Incidence. Brit. ARC RM 2048, 1943.

361. Voigt, H.: "Further Experiments on Wing Vibrations." Jahrbuch deut. Luftfahrtforschung, 1, 249-258, 1938. Also: RTP Tran. 874, 1943.

362. Voss, H. M.: Flutter of Low-Aspect Ratio Lifting Surfaces. MS Thesis MIT, 1951.

363. Voss, H. M., and H. J. Hassig: Introducing Study of Flutter of Low Aspect Ratio Wings at Subsonic Speeds. Mass. I. Tech. Aeroelastic and Structures Res. Rep. for Bur. of Aer., Navy Dept., 1952.

364. Voss, H. M., Zartarian, G., and P. T. Hsu: Theoretical and Experimental Investigation of the Aeroelastic Behavior of Low-Aspect-Ratio Wings. MIT Aer. and Structures Res., Contract NOa(s), 51-109-c, 1953.

365. Wagner, H.: "Ueber die Entstehung des dynamischen Auftriebs von Tragfluegeln." ZAMM, 5, 17-35, 1925. Also: Brit. RTP. Tran. 2315, 1936.

366. Walker, P. B.: Experiments on the Growth of Circulation About a Wing with a Description of the Apparatus for Measuring the Fluid Motion. Brit. Aer. RC RM 1402, 1931.

367. Walsh, J., G. Zartarian, and H. M. Voss: "Generalized Aerodynamic Forces on the Delta Wing with Supersonic Leading Edges." J. Aer. Sci. 21, 739-748, 1954.

368. Wang, C. T., Vaccaro, R. J, and De Santo D. F: A Practical Approach to the Problem of Stall Flutter. Office of Sci. Res. TN 55-98, New York Univ., 1955.

369. Wasserman, L. S.: Aspect Ratio Corrections in Flutter Calculations. Air Material Command, U.S. Air Force, MC RE XA5 4595, 8-5, 1948.

370. Watkins, C. E.: "On Transient Two-Dimensional Flows at Supersonic Speeds." J. Aer. Sci. 16, 569-570, 1949.

371. Watkins, C. E.: Effect of Aspect Ratio on Undamped Torsional Oscillations of a Thin Rectangular Wing in Supersonic Flow. NACA TN 1895, 1949.

372. Watkins, C. E.: Effect of Aspect Ratio on the Air Forces and Moments of Harmonically Oscillating Thin Rectangular Wings in Supersonic Potential Flow. NACA TN 2064, 1950.

373. Watkins, C. E., and J. H. Berman: Air Forces and Moments on Triangular and Related Wings with Subsonic Leading Edges Oscillating in Supersonic Potential Flow. NACA Rep. 1099, 1952.

374. Watkins, C. E., and J. H. Berman: Velocity Potential and Air Forces Associated with a Triangular Wing in Supersonic Flow, with Subsonic Leading Edges, and Deforming Harmonically According to a General Quadratic Equation. NACA TN 3009, 1953.

375. Watkins, C. E., and J. H. Berman: On the Kernel Function of the Integral Equation Relating Lift and Downwash Distributions of Oscillating Wings in Supersonic Flow. 1956, NACA Rep. 1257. Supersedes TN 3438.

376. Watkins, C. E., H. L. Runyan, and D. S. Woolston: On the Kernel Function of the Integral Equation Relating the Lift and Downwash Distributions of Oscillating Finite Wings in Subsonic Flow. 1955, NACA Rep. 1234. Supersedes Tn 3131.

377. Weber, R.: Tables des Coefficients Aerodynamiques Instationnaires Regime Plan Supersonique. Premiere Partie. Expose Sommaire de la Methode de L. Schwartz et Introduction aux Tables. Office Natl. Etudes et Recherches Aer. 41, 1950.

378. Widmayer, E. Jr., S. A. Clevenson, and S. A. Leadbetter: Some Measurements of Aerodynamic Forces and Moments at Subsonic Speeds on a Rectangular Wing of Aspect Ratio 2 Oscillating About the Midchord. Aug. 1953. NACA RM L53F19.

379. Wiley, H. G., and W. C. Moseley, Jr: An Investigation at High Subsonic Speeds of the Presure Distributions on a 45° Sweptback Vertical Tail in Sideslip with and Without a 45° Sweptback Horizontal Tail Located on the Fuselage Center Line. Nov. 1954. NACA RM L54H23.

380. Wiley, H. G., and W. C. Moseley, Jr: Investigation at High Subsonic Speeds of the Pressure Distribution on a 45° Sweptback Vertical Tail in Sideslip with a 45° Sweptback Horizontal Tail Mounted at 50-Percent and 100-Percent Vertical-Tail Span. Nov. 1954. NACA RM L54I08.

381. Williams, D. E.: On the Integral Equations of Two Dimensional Subsonic Flutter Derivative Theory. Roy. Airc. Est. TN Structures 181, 1955.

382. Williams, J.: An Examination of Experimental Data Relating to Flexural-Torsional Wing Derivatives. Brit. ARC RM 1943, 1944.

383. Williams, J.: Aircraft Flutter. Brit. ARC RM 2492, 1951.

384. Woods, L. C.: "The Lift and Moment Acting on a Thick Aerofoil in Unsteady Motion." Phil. Tran. Roy. Soc. London A 247, 925, 131-162, 1954.

385. Woods, L. C.: "Unsteady Plane Flow Past Curved Obstacles with Infinite Wakes." Proc. Roy. Soc. London, A 229, 152-180, 1955.

386. Woods, L. C.: "The Aerodynamic Forces on an Oscillating Aerofoil in Free Jet." Proc. Roy. Soc. London, A 229, 235-250, 1955.

387. Woolston, D. S., and H. L. Runyan: "Some Considerations on the Air Forces on a Wing Oscillating Between Two Tunnel Walls for Subsonic Compressible Flows." J. Aer. Sci. 22, 41-50, 1955.

388. Zartarian, G., G. Fotieo, and H. Ashley: Theoretical and Experimental Methods of Flutter Analysis. Vol. VII and VIII, Mass. Inst. Tech. Press, 1949.

389. Zartarian, G., P. T. Hsu, and H. M. Voss: Comparative Flutter Calculations on Low-Aspect Wings in Incompressible and Supersonic Flows. Mass. Inst. Tech. Aeroelastic and Structures Research Lab., Tech. Rep. 52-2, 1954.

390. Zartarian, G., P. T. Hsu, and H. M. Voss: Application of Numerical Integration Techniques to the Low-Aspect-Ratio Flutter Problem in Subsonic and Supersonic Flows. MIT, Aeroelastic and Structures Research Lab., Tech. Rep. 52-3, 1954.